

Friday, December 06, 2013

- 08:30-10:00 AM • **RC801** • Room: N230 • Waiting to Exhale: What's the Latest with Inhalation Lung Diseases?  
08:30-10:00 AM • **RC802** • Room: E353B • How to Be the Speaker Everyone Wants You to Be (An Interactive Session)  
08:30-10:00 AM • **RC803** • Room: E353A • Interactive Game: Read with the Experts (Cardiac Radiology)  
08:30-10:00 AM • **RC804** • • No Course RC804. See Series VSMK61 Musculoskeletal Radiology Series: Elbow, Hand and Wrist Imaging  
08:30-10:00 AM • **RC805** • Room: N227 • Brain Aneurysms  
08:30-10:00 AM • **RC806** • Room: S406B • Sinonasal Imaging  
08:30-10:00 AM • **RC807** • Room: N226 • Imaging and Treating Gynecologic Cancer 2013: What Really Works and What Is Most Cost Effective
- 08:30-10:00 AM • **RC808** • Room: E353C • Emergency Radiology Case-based Countdown (An Interactive Session)  
08:30-10:00 AM • **RC809** • Room: S402AB • Gastrointestinal: Imaging the Obese Patient (An Interactive Session)  
08:30-10:00 AM • **RC810** • Room: E351 • Right Upper Quadrant Ultrasound  
08:30-10:00 AM • **RC811** • Room: S504CD • Advances and Updates in SPECT/CT  
08:30-10:00 AM • **RC812** • • No Course RC812. See Series VSVA61 Vascular Imaging Series: MR Angiography-Principles and Technique Optimization...  
08:30-10:00 AM • **RC813** • Room: N229 • Chest/Cardiovascular Imaging II  
08:30-10:00 AM • **RC814** • • No Course RC814. See Series VSIR61 Interventional Radiology Series: Top 5 Complications in Interventional Oncology...  
08:30-10:00 AM • **RC815** • Room: E450A • Clinical Breast MR Imaging (An Interactive Session)  
08:30-10:00 AM • **RC816** • Room: S404AB • Radiology in the Developing World: Mistakes Made, Lessons Learned, What's Next? (Sponsored by the RSNA Committ...  
08:30-10:00 AM • **RC817** • Room: S505AB • Essentials of Molecular Imaging  
08:30-10:00 AM • **RC818** • Room: S404CD • Techniques for Quantitative Cancer Imaging: Current Status  
08:30-10:00 AM • **RC821** • Room: S405AB • Medical Physics 2.0: Magnetic Resonance Imaging  
08:30-10:00 AM • **RC823** • Room: S403B • Minicourse: Recording and Reporting Radiation Dose: Nuclear Medicine  
08:30-10:00 AM • **RC825** • Room: E263 • Quantitative Imaging: Quantitative Imaging in Ultrasound  
08:30-10:00 AM • **RC826** • Room: E350 • The Use of Business Analytics for Improving Radiology Operations, Quality, and Clinical Performance (In Associ...  
08:30-10:00 AM • **RC827** • Room: S504AB • Consumerism and Radiology  
08:30-10:00 AM • **RC829** • Room: E451B • Interactive Game: Clinical Problems in Body MRI - Case-based Instruction  
08:30-10:00 AM • **RC830** • Room: S403A • Current and Next Generation Health IT Tools To Enable Radiation Exposure Reduction - A Practical Guide  
08:30-10:00 AM • **RC831** • Room: E450B • US for Thyroid Cancer: Diagnosis, Surveillance, and Treatment (How-to Workshop)  
08:30-10:00 AM • **RC832** • Room: S502AB • Develop Your Radiology Financial Insight: Fundamental Principles You Should Know About Business  
08:30-10:00 AM • **RC850** • Room: E260 • Targeted Treatment and Imaging of Liver Cancers: Basic to Advanced Techniques in Minimally-Invasive Therapies ...  
08:30-10:00 AM • **RC851** • Room: E261 • Pediatric Neurosonography Update: Head, Spine, and Transcranial Doppler Ultrasound (How-to Workshop)  
08:30-10:00 AM • **RC852** • Room: E264 • US-guided Interventional Breast Procedures (Hands-on Workshop)  
08:30-10:00 AM • **RC853** • Room: S401CD • Advanced Image Analysis, including Applications such as Automated Stent Planning and Multimodality Image Fusio...  
08:30-10:00 AM • **RC854** • Room: S401AB • Basic Tools and Tricks for Data Collection and Organization for Practice Quality Improvement Projects and for ...  
08:30-12:00 PM • **VSIR61** • Room: E451A • Interventional Radiology Series: Top 5 Complications in Interventional Oncology - Avoidance, Recognition and M...  
08:30-12:00 PM • **VSMK61** • Room: N228 • Musculoskeletal Radiology Series: Elbow, Hand and Wrist Imaging  
08:30-12:00 PM • **VSVA61** • Room: E352 • Vascular Imaging Series: MR Angiography-Principles and Technique Optimization  
10:30-12:00 PM • **ICIW61** • Room: S401AB • National Library of Medicine PubMed: Find Articles You Need: Searching PubMed/MEDLINE Efficiently  
10:30-12:00 PM • **SST01** • Room: E450B • Breast Imaging (Issues in Screening)  
10:30-12:00 PM • **SST02** • Room: S502AB • Cardiac (Coronary CT/MR V)  
10:30-12:00 PM • **SST03** • Room: S504AB • Cardiac (Anatomy and Function II)  
10:30-12:00 PM • **SST04** • Room: E451B • Chest (Airways, Emphysema)  
10:30-12:00 PM • **SST05** • Room: E353B • Gastrointestinal (Small and Large Bowel Imaging)  
10:30-12:00 PM • **SST06** • Room: E353C • Gastrointestinal (MR Technique)  
10:30-12:00 PM • **SST07** • Room: E351 • Genitourinary (Anatomy and Dysfunction of the Female Pelvic Floor)  
10:30-12:00 PM • **SST08** • Room: E353A • Informatics (Segmentation, Measurement and CAD)  
10:30-12:00 PM • **SST09** • Room: N226 • Neuroradiology/Head and Neck (Advanced Head and Neck Imaging)  
10:30-12:00 PM • **SST10** • Room: N227 • Neuroradiology (Cerebral Ischemia, Hemorrhage and Vessel Wall Imaging)  
10:30-12:00 PM • **SST11** • Room: N230 • Neuroradiology (Quantitative Neuroimaging)  
10:30-12:00 PM • **SST12** • Room: S505AB • ISP: Nuclear Medicine (Cardiovascular Imaging)  
10:30-12:00 PM • **SST13** • Room: N229 • Pediatrics (Interventional)  
10:30-12:00 PM • **SST14** • Room: S403B • Physics (CT-Dose Optimization)  
10:30-12:00 PM • **SST15** • Room: S403A • Physics (Image-guided Radiation Therapy II)  
10:30-12:00 PM • **SST16** • Room: E350 • Vascular/Interventional (MR Guidance/Topics of Interest)  
12:30-03:00 PM • **SPMK61** • Room: E350 • Friday Imaging Symposium: MR Imaging of Common Musculoskeletal Injuries (An Interactive Session)

Waiting to Exhale: What's the Latest with Inhalation Lung Diseases?

Friday, 08:30 AM - 10:00 AM • N230



RC801 • AMA PRA Category 1 Credit™:1.5 • ARRT Category A+ Credit:1.5

RC801A • Smoking Related Lung Disease

Jeffrey P Kanne MD (Presenter) \*

LEARNING OBJECTIVES

- 1) Identify immunologic reactions to cigarette smoke in the lungs.
- 2) Describe the histopathologic features of smoking-related lung disease.
- 3) Illustrate the high-resolution CT findings of smoking-related lung disease.

[Back to Top](#)

## RC801B • Hypersensitivity Pneumonitis

**Justus E Roos** MD (Presenter)

### LEARNING OBJECTIVES

1) To review the most common clinical manifestations of hypersensitivity pneumonitis. 2) To demonstrate the range of histologic features of hypersensitivity pneumonitis and correlate them with radiologic findings. 3) To illustrate abnormalities indicative of hypersensitivity pneumonitis and their differential considerations at chest radiographs and CT.

ABSTRACT

## RC801C • Occupational Lung Disease

**Jonathan H Chung** MD (Presenter) \*

### LEARNING OBJECTIVES

1) List at least 3 common and 3 uncommon occupational lung diseases. 2) Briefly describe the prevalence and background of occupational lung diseases. 3) Describe and recognize the imaging manifestations of occupational lung diseases. 4) Describe the thoracic complications of occupational inhalational exposure.

ABSTRACT

## RC801D • Aspiration

**Santiago E Rossi** MD (Presenter) \*

### LEARNING OBJECTIVES

1) Discuss the most common risk factors, clinical manifestations and implications of aspiration. 2) Review the radiographic and both common and atypical CT findings of aspiration pneumonia including aspiration of solid foreign bodies and aspiration of liquids such as infectious material, gastric acid, partially digested food, lipid aspiration and chronic.

ABSTRACT

## How to Be the Speaker Everyone Wants You to Be (An Interactive Session)

Friday, 08:30 AM - 10:00 AM • E353B

PR ED

[Back to Top](#)

**RC802** • AMA PRA Category 1 Credit™:1.5 • ARRT Category A+ Credit:1.5

**Jannette Collins**, MD, MEd

### LEARNING OBJECTIVES

1) Apply adult learning principles. 2) Demonstrate effective presentations skills.

### ABSTRACT

Effectiveness of an oral presentation depends on the ability of the speaker to communicate with the audience. An important part of this communication is focusing on two to five key points and emphasizing those points during the presentation. Every aspect of the presentation should be purposeful and directed at facilitating learners' achievement of the objectives. This necessitates that the speaker has carefully developed the objectives and built the presentation around attainment of the objectives. A presentation should be designed to include as much audience participation as possible, no matter the size of the audience. Techniques to encourage audience participation include questioning, brainstorming, small-group activities, role-playing, case-based examples, directed listening, and use of an audience response system. It is first necessary to motivate and gain attention of the learner for learning to take place. This can be accomplished through appropriate use of humor, anecdotes, and quotations. This course will review adult learning principles and effective presentation skills.

©RSNA, 2004

URL's

<http://med.uc.edu/radiology/facstaff/collj4/index.html>

## Interactive Game: Read with the Experts (Cardiac Radiology)

Friday, 08:30 AM - 10:00 AM • E353A

CA

[Back to Top](#)

**RC803** • AMA PRA Category 1 Credit™:1.5 • ARRT Category A+ Credit:1.5

### Moderator

**Jill E Jacobs**, MD

**Frank J Rybicki**, MD, PhD \*

**Satinder P Singh**, MD

**Sanjeev Bhalla**, MD

**Jacobo Kirsch**, MD

### LEARNING OBJECTIVES

1) To illustrate common cardiac pathologies encountered in noninvasive imaging. 2) To review imaging protocols designed to best depict cardiac pathology. 3) To review image post-processing tools to render cardiac imaging findings for interpretation and communication with referring clinicians. This interactive session will use RSNA Diagnosis Live™. Please bring your charged mobile wireless device (phone, tablet or laptop) to participate.

### ABSTRACT

This session will include live reads with experts in cardiac radiology to meet the learning objectives. Specific cases and clinical scenarios will be presented to best demonstrate the pathology and the strategies for imaging and image interpretation.

## No Course RC804. See Series VSMK61 Musculoskeletal Radiology Series: Elbow, Hand and Wrist Imaging

Friday, 08:30 AM - 10:00 AM

RC804

**Brain Aneurysms****Friday, 08:30 AM - 10:00 AM • N227**

ER NR

[Back to Top](#)**RC805 • AMA PRA Category 1 Credit™:1.5 • ARRT Category A+ Credit:1.5****RC805A • Diagnostic Evaluation of Brain Aneurysms****Juan P Villablanca** MD (Presenter)**LEARNING OBJECTIVES**

The course will review the relative strengths and limitations of current imaging techniques for the detection and follow-up of patients with symptomatic and asymptomatic cerebral aneurysms. A practical strategy for image review and analysis will be provided that ensures complete lesion characterization and minimizes operator error. A rubric for the analysis of the pre- and post-operative aneurysm patients will also be presented with an emphasis on a practical clinical approach. A brief natural history and modality based literature review will also be provided.

ABSTRACT

**RC805B • Intervention for Brain Aneurysms****Steven W Hetts** MD (Presenter) \***LEARNING OBJECTIVES**

1) Discuss the current endovascular interventional approaches to both ruptured and unruptured brain aneurysm treatment. 2) Critically evaluate recent clinical trial results regarding interventional brain aneurysm treatment. 3) Appreciate the limitations to endovascular brain aneurysm treatment using current technologies. 4) Understand that cerebral vasospasm is the leading cause of mortality and morbidity for hospitalized patients with aneurysmal subarachnoid hemorrhage, and appreciate current approaches to treating vasospasm.

ABSTRACT

**RC805C • The Neurointerventional Suite of the Future****Charles M Strother** MD (Presenter) \***LEARNING OBJECTIVES**

1) To understand the basic concepts behind selection of patients for revascularization based on physiologic criteria. 2) To understand the capabilities of measuring brain perfusion using C-arm CT. 3) To appreciate the potential value of using a single modality environment for the diagnosis, triage and treatment of patients with an acute ischemic stroke.

**Sinonasal Imaging****Friday, 08:30 AM - 10:00 AM • S406B**

NR HN

[Back to Top](#)**RC806 • AMA PRA Category 1 Credit™:1.5 • ARRT Category A+ Credit:1.5**

LEARNING OBJECTIVES

**RC806A • Anatomy and Developmental Problems****C. Douglas Phillips** MD (Presenter) \***LEARNING OBJECTIVES**

1) Understand the normal embryology of the sinonasal cavity. 2) Recognize the appearance of developmental lesions of the sinonasal cavity. 3) Understand the strengths and weaknesses of CT and MR in evaluation of common developmental abnormalities of the sinonasal region.

ABSTRACT

There is a wide spectrum of maldevelopmental lesions of the midface and sinonasal cavity. Understanding the normal embryology of the face and sinuses help clarify the pathology visualized, and allows them to be segmented and characterized. The complex interplay of the sinonasal cavity and anterior fossa during development of the fetus must be understood. Imaging of the sinuses and anterior fossa are required on discovery of these complex midfacial lesions to give the surgeon clear understanding of the repair required. This talk will discuss the range of anterior fossa and sinonasal maldevelopmental lesions from choanal stenosis to encephaloceles.

**RC806B • Sinonasal Infections and Inflammation****Patricia A Hudgins** MD (Presenter) \***LEARNING OBJECTIVES**

1) Understand the pathophysiology of sinus inflammatory diseases and the rationale for FESS. 2) Learn and understand the surgical anatomy and anatomic variants of the sinonasal cavity, and be able to apply this knowledge such that an organized sinus dictation can be developed. 3) Know the CT and MR Imaging findings of sinonasal bacterial and fungal, both invasive and non-invasive infections.

ABSTRACT

The most important goal of sinus CT imaging in the patient with sinusitis or a history of repeat or prolonged sinus infections is to analyze each sinus outflow tract to determine whether there is an anatomic and surgically correctable cause for sinus cavity obstruction. While the description 'ostioameatal complex' has been popularized, the term oversimplifies CT analysis, and instead each sinus cavity should be individually assessed. This session will review the normal anatomy of each sinus outflow tract in coronal, axial and sagittal planes, and present the common correctable causes of ostial stenosis. Imaging findings of bacterial sinusitis will be presented, with a description of potential complications of severe infection. Invasive and non-invasive fungal sinonasal infection will be contrasted and compared, as the imaging findings are markedly different.

**RC806C • Sinonasal Masses****Michelle A Michel** MD (Presenter) \*

LEARNING OBJECTIVES

1) Discuss the role of imaging in evaluating sinonasal neoplasms. 2) Describe the risk factors and histologic classification of sinonasal malignancies. 3) Demonstrate the imaging features of a variety of sinonasal neoplasms. 4) Review staging, treatment, and prognosis of sinonasal neoplasms.

#### ABSTRACT

Although sinonasal malignancies are rare and they account for less than 1% of cancer deaths in western countries, these tumors arise in a complex anatomic location and are histologically diverse. In addition to new histologic and clinical classifications, the last decade has brought new insights into the etiological risk factors, tumor biology, and therapeutic options of these lesions. Sinonasal malignancies have a relatively poor prognosis and many present at an advanced stage due to delay in diagnosis. Diagnosis may be delayed because the presenting symptoms often mimic those of chronic rhinosinusitis, they generally present with little pain, and there is space for tumor growth within the sinus lumen. Epithelial tumors account for the majority of sinonasal malignancies and squamous cell carcinoma is the most common. Additional epithelial neoplasms include adenocarcinoma and adenoid cystic carcinomas. Soft tissue tumors of the nasal cavity and paranasal sinuses are uncommon and include rhabdomyosarcoma, hemangiopericytoma, and other very rare forms. Malignancies of bone and cartilage include osteosarcoma, chondrosarcoma, malignant giant cell tumor, and Ewing sarcoma. Additional neoplasms such as esthesioneuroblastoma, mucosal melanoma, and lymphomas are uncommon, but may have characteristic features that help to distinguish them from other lesions. CT and MR are the modalities of choice for imaging neoplasms of the sinonasal cavities and their roles are often complementary. CT demonstrates bony remodeling or destruction, identifies intratumoral calcification, demonstrates the matrix of cartilaginous and osseous neoplasms, and delineates obstruction of sinus drainage pathways. MR imaging is superior for distinguishing tumor margins from obstructed secretions; for delineating extension of tumor into the infratemporal fossa, orbit, and intracranial cavities; for detecting perineural tumor spread; and for demonstrating the vascularity of neoplasms.

## Imaging and Treating Gynecologic Cancer 2013: What Really Works and What Is Most Cost Effective

Friday, 08:30 AM - 10:00 AM • N226

[OI](#) [OB](#) [GU](#)

[Back to Top](#)

**RC807** • AMA PRA Category 1 Credit™:1.5 • ARRT Category A+ Credit:1.5

#### LEARNING OBJECTIVES

### RC807A • What Really Works: Overview of Imaging Procedures and Algorithm for Staging Gynecology

**Julia R Fielding** MD (Presenter)

#### LEARNING OBJECTIVES

1) To review the appearance of gynecologic cancer on CT, PET and MR images. 2) To determine when and why radiologic staging is necessary. 3) To show an algorithm that meets the needs of surgical and radiation oncology colleagues.

#### ABSTRACT

Staging gynecologic malignancies has evolved over the years to include multi-modality imaging. Although the official international standards (FIGO) allow for cross sectional imaging in some cases, examination under anesthesia remains the mainstay of diagnosis. In experienced hands and with the addition of biopsy results, manual staging of cervical cancer is excellent, while endometrial cancers are often understaged. It is now routine to stage advanced ovarian cancer with CT scans. The goal of this course is to impart 1) best imaging practices based on ACR guidelines, 2) review cost effectiveness of current staging algorithms and new imaging techniques and 3) show the important interactions required between radiology and radiation oncology to provide state of the art care.

### RC807B • Radiology Findings: Impact on Radiation Therapy

**Nina A Mayr** MD (Presenter)

#### LEARNING OBJECTIVES

1) To review current types of radiation therapy in use for gynecologic cancer. 2) To show the essential anatomic information required from imaging tests. 3) To demonstrate the value of functional and/or fused imaging in radiation therapy.

### RC807C • What Does It Cost? Appropriate Use of Imaging Technology

**Katarzyna J Macura** MD, PhD (Presenter) \*

#### LEARNING OBJECTIVES

1) To assess the appropriateness of utilization of imaging modalities in the work-up of women with gynecologic malignancies. 2) To discuss the cost of imaging technologies and oncologic outcome optimization.

## Emergency Radiology Case-based Countdown (An Interactive Session)

Friday, 08:30 AM - 10:00 AM • E353C

[ER](#) [MK](#) [GI](#) [CH](#)

[Back to Top](#)

**RC808** • AMA PRA Category 1 Credit™:1.5 • ARRT Category A+ Credit:1.5

### RC808A • Thoracic Top 10 Countdown

**Faisal Khosa** FFRRCSI, FRCPC (Presenter)

#### LEARNING OBJECTIVES

The audience will be shown cases with acute presentations in the ER, the format will be interactive utilizing audience response system. At the end of the session the participants will be able to efficiently deal with complex situations presenting as acute emergency in the ER with resultant improved patient care.

2.

#### ABSTRACT

The Top 10 countdown will comprise of interactive audience response system in which 10 unknown Thoracic emergencies will be presented. The salient features of the cases would be illustrated along with more complex imaging modalities and possible differential diagnoses where appropriate.

### RC808B • Abdominal Top 10 Countdown

**Joel A Gross** MD, MS (Presenter)

#### LEARNING OBJECTIVES

1) Select among varying imaging techniques to optimize the appropriate study for the patient. 2) Recognize classic and subtle signs of radiologic pathology, and avoid some common pitfalls and errors.

#### ABSTRACT

The Abdominal Top 10 Countdown is an interactive audience response based presentation in which 10 unknown abdominal cases from the emergency department will be presented. The participants are encouraged to interact with the cases. The salient features of the cases are then illustrated along with more complex imaging modalities, if appropriate. The interactive nature will challenge the learners' skill and knowledge applications.

### RC808C • Musculoskeletal Top 10 Countdown

**Manickam Kumaravel MD, FRCR** (Presenter)

#### LEARNING OBJECTIVES

1) Analyze varying imaging techniques and will be able to apply this knowledge to improve effective patient care. 2) Be proficient in scrutinizing subtle radiographic signs in musculoskeletal presentations in the emergency department and in understanding the use of more complex imaging techniques to ascertain the underlying pathology.

#### ABSTRACT

The Top 10 countdown is an interactive audience response based system in which 10 unknown Musculoskeletal cases from the emergency room will be presented. The participants are encouraged to interact with the cases. The salient features of the cases are then illustrated along with more complex imaging modalities, if appropriate. The interactive nature will challenge the learners' skill and knowledge applications.

## Gastrointestinal: Imaging the Obese Patient (An Interactive Session)

Friday, 08:30 AM - 10:00 AM • S402AB



[Back to Top](#)

RC809 • AMA PRA Category 1 Credit™:1.5 • ARRT Category A+ Credit:1.5

### RC809A • Challenges and Solutions in Imaging the Obese Patient

**Rajan T Gupta MD** (Presenter) \*

#### LEARNING OBJECTIVES

1) Identify and understand the challenges in imaging the obese patient. 2) Determine how to alter CT parameters in order to optimize imaging in this patient population. 3) Explore the other imaging modalities that can be used to detect and characterize disease processes in the obese patient.

#### ABSTRACT

### RC809B • Bariatric Surgery I: Overview and Roux-En-Y Gastric Bypass

**Courtney A Coursey MD** (Presenter) \*

#### LEARNING OBJECTIVES

1) Describe indications for bariatric surgery. 2) Identify expected post-operative changes following bariatric surgical procedures. 3) Identify complications following bariatric surgical procedures.

### RC809C • Bariatric Surgery II: Laparoscopic Gastric Banding

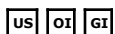
**Christine O Menias MD** (Presenter)

#### LEARNING OBJECTIVES

1) Familiarize the Radiologist with the Laparoscopic Gastric Band Apparatus. 2) Understand normal post procedure imaging of Laparoscopic Gastric Band. 3) Recognize potential complications with imaging.

## Right Upper Quadrant Ultrasound

Friday, 08:30 AM - 10:00 AM • E351



[Back to Top](#)

RC810 • AMA PRA Category 1 Credit™:1.5 • ARRT Category A+ Credit:1.5

### RC810A • Sonography of Focal Liver Lesions

**Mitchell E Tublin MD** (Presenter)

#### LEARNING OBJECTIVES

1) Describe a practical approach for the characterization of liver lesions at ultrasound. 2) Illustrate useful imaging features of typical and atypical hemangiomas. 3) Demonstrate the potential use of ultrasound contrast agents for liver mass characterization.

#### ABSTRACT

Despite improvements in ultrasound technology, the approach to characterization of liver lesions at ultrasound has changed little over the past thirty years. A recommendation for further evaluation by either MRI or CECT is typically given, though in many cases, the ultrasound features (in combination with clinical history) are sufficient for diagnosis. Microbubble contrast agents may improve ultrasound diagnostic specificity in the near future.

### RC810B • Liver Elastography

**Thomas H Grant DO** (Presenter)

#### LEARNING OBJECTIVES

1) What are these techniques. 2) When should they be used. 3) How effective are they. 4) Future innovations.

#### ABSTRACT

Noninvasive assessment of liver fibrosis is challenging given that chronic liver disease affects hundreds of million patients worldwide. Fibrosis is reversible with effective intervention. Therefore an effective, relatively fast method to detect fibrosis is essential.

## RC810C • Gallbladder and Biliary Disease

**Anthony E Hanbidge** MBBCh (Presenter)

### LEARNING OBJECTIVES

1) Discuss the value of ultrasound when evaluating the gallbladder and bile ducts. 2) Identify the imaging features of acute conditions of these structures and complications. 3) Recognize common pitfalls to avoid misinterpretation. 4) Describe other conditions of the gallbladder and bile ducts including adenomyomatosis, sclerosing cholangitis, gallbladder cancer and cholangiocarcinoma.

## Advances and Updates in SPECT/CT

Friday, 08:30 AM - 10:00 AM • S504CD



[Back to Top](#)

**RC811** • AMA PRA Category 1 Credit™:1.5 • ARRT Category A+ Credit:1.5

## RC811A • SPECT/CT in Musculoskeletal Diseases

**Christopher J Palestro** MD (Presenter)

### LEARNING OBJECTIVES

1) Describe the role of SPECT/CT in the workup of patients with malignancy. 2) Describe the role of SPECT/CT in musculoskeletal infection. 3) Use SPECT/CT to improve the accuracy of radionuclide studies for diagnosing musculoskeletal diseases.

### ABSTRACT

## RC811B • SPECT/CT in Endocrine Disorders and Others

**Don C Yoo** MD (Presenter)

### LEARNING OBJECTIVES

1) Discuss the advantages of SPECT/CT for the evaluation of endocrine disorders. 2) Discuss the limitations of SPECT/CT for the evaluation of endocrine disorders. 3) Discuss the impact of SPECT/CT on management in patients with endocrine disorders.

## No Course RC812. See Series VSVA61 Vascular Imaging Series: MR Angiography-Principles and Technique Optimization

Friday, 08:30 AM - 10:00 AM

RC812

[Back to Top](#)

## Chest/Cardiovascular Imaging II

Friday, 08:30 AM - 10:00 AM • N229



[Back to Top](#)

**RC813** • AMA PRA Category 1 Credit™:1.5 • ARRT Category A+ Credit:1.5

## RC813A • Pitfalls and Errors in Pediatric Thoracic Imaging

**George A Taylor** MD (Presenter)

### LEARNING OBJECTIVES

1) Understand the common sources of error in pediatric thoracic imaging. 2) Demonstrate understanding of the influence of biases on the diagnostic process. 3) Analyze image viewing techniques and apply them to strategies for improving image interpretation.

### ABSTRACT

The goal of this presentation is to describe common patterns and potential etiologies of diagnostic error in pediatric thoracic imaging identified over a 13-year experience at a large academic children's hospital. Errors are defined as a diagnosis that was delayed, wrong or missed; they are classified as perceptual, cognitive, system-related or unavoidable. Perceptual errors were the most common type of error, defined as a diagnostic finding that is noticeable but missed. Cognitive contributors to perceptual errors will be discussed, including the role of search satisfaction, visual distractors, and visual isolation. Cognitive errors were defined as faulty information processing, related to overinterpretation of an imaging finding, misinterpretation of a finding or failure to consider a different diagnosis for a given finding [premature closure]; faulty data gathering (poorly performed imaging examination, inadequate review of patient history or lack of consideration of a patient's underlying condition), or insufficient knowledge base. The presentation will also discuss a number of cognitive biases that subconsciously affect our ability to effectively reach the right diagnosis. These will include examples of availability heuristics (memory of a similar case), framing effect (how data are presented), the anchoring heuristic (premature closure), the reluctance to confront authority (blind obedience), and reader overconfidence. Finally, we will review organizational errors in which systems issues such as faulty medical history and inefficient processes contribute to diagnostic errors in the chest. The presentation will suggest strategies for systematic and individual improvement.

## RC813B • Back to Basics: Radiography of the Pediatric Chest

**Robert H Cleveland** MD (Presenter) \*

### LEARNING OBJECTIVES

1) Review strategies to improve diagnostic accuracy in interpreting chest radiographs. 2) Enhance confidence for NOT obtaining follow-up CT. 3) Increase appreciation of when follow-up CT is needed.

### ABSTRACT

In this session, we will review the role of the chest x-ray (CXR) in the era of high tech imaging. Specifically the need to re-establish a sense of confidence in interpreting CXR will be addressed. Situations where a confident interpretation of the CXR obviates the need for CT will be stressed as well as those where the CXR clearly requires CT follow-up. The need to "image gently", following ALARA, guidelines is now widely accepted in pediatric radiology and is growing in acceptance in adult imaging. In our department (Boston Children's Hospital) this has led to a 24% decrease in CT volume between 2006 and 2010. This in turn, means that a need for an increased nuanced approach to interpreting CXR is required. Specific recommendations to increase the accuracy in interpreting CXR will be discussed. As the indications for a high percentage of CXR in pediatrics are nonspecific, the need to constantly be vigilant regarding unexpected and uncommon conditions will be stressed. Particular attention will be paid to the broad range of conditions related to wheezing (or noisy breathing) and dyspnea including airway obstruction and interstitial lung disease. The increasing incidence of complications in pediatric community acquired pneumonia and the appropriate role of CXR in that situation will also be discussed.

## RC813C • Advanced Imaging of the Pediatric Chest

**Mantosh S Rattan MD** (Presenter)

### LEARNING OBJECTIVES

1) Introduce the ChILD (Children's Interstitial Lung Disease) Research Cooperative classification for pediatric diffuse lung disease. 2) Discuss imaging techniques in children with diffuse lung disease. 3) Review imaging features of specific disorders in the ChILD spectrum.

## No Course RC814. See Series VSIR61 Interventional Radiology Series: Top 5 Complications in Interventional Oncology - Avoidance, Recognition and Management

Friday, 08:30 AM - 10:00 AM

[Back to Top](#)

## RC814

## Clinical Breast MR Imaging (An Interactive Session)

Friday, 08:30 AM - 10:00 AM • E450A

[Back to Top](#)

**MR** **BR**

**RC815** • AMA PRA Category 1 Credit™:1.5 • ARRT Category A+ Credit:1.5

## RC815A • Breast MRI: Suspicious Lesions

**Christiane K Kuhl MD** (Presenter) \*

### LEARNING OBJECTIVES

1) To review breast MR imaging features used to distinguish suspicious from benign lesions. 2) To understand the appropriate use of the ACR Breast MR lexicon. 3) To review the management of suspicious breast MR findings.

### ABSTRACT

..

## RC815B • Breast MRI: BI-RADS 3

**Christopher E Comstock MD** (Presenter)

### LEARNING OBJECTIVES

1) Understand appropriate use of the ACR BI-RADS in MR Interpretation. 2) Review interesting cases using BI-RADS lexicon.

## RC815C • MR-guided Biopsy

**Carol H Lee MD** (Presenter)

### LEARNING OBJECTIVES

1) To review technical considerations in MR guided biopsy. 2) To discuss potential pitfalls associated with MR biopsy and how to handle them. 3) To understand appropriate post-biopsy management and follow-up.

### ABSTRACT

## Radiology in the Developing World: Mistakes Made, Lessons Learned, What's Next? (Sponsored by the RSNA Committee on International Radiology Education)

Friday, 08:30 AM - 10:00 AM • S404AB

[Back to Top](#)

**PR** **GN**

**RC816** • AMA PRA Category 1 Credit™:1.5 • ARRT Category A+ Credit:1.5

### Coordinator

**William W Mayo-Smith**, MD \*

## RC816A • RSNA Committee on International Radiology Education: How We Can Help

**Teresita L Angtuaco MD** (Presenter) ; **William W Mayo-Smith MD** (Presenter) \*

### LEARNING OBJECTIVES

1) Improved ability to participate in or develop global radiology projects. 2) Understand available resources and types of organizations involved in global radiology. 3) Create a viable framework for global radiology incorporating the multifactorial implementation challenges. 4) Develop global radiology strategies that maximize sustainability and scalability.

### ABSTRACT

## RC816B • Political Challenges and Ethical Practices

**Kristen K DeStigter MD** (Presenter) \*

### LEARNING OBJECTIVES

1) Describe the ethical considerations associated with setting up a global imaging project. 2) Discuss the political challenges that may be encountered when designing and implementing a global imaging endeavor. 3) Understand the cultural factors that play into the political and ethical challenges.

## RC816C • Involving Radiologists on the Ground: Dealing with Competing Incentives

**Marc D Kohli MD** (Presenter) \*

### LEARNING OBJECTIVES

1) Identify challenges particular to providing radiology service in a resource-constrained setting. 2) Explain how partnerships and bi-directional exchange can be used to address these challenges.

### ABSTRACT

## RC816D • Creating a Remote Digital Department: Funding Is the Easy Part

**Jeffrey B Mendel MD (Presenter) \***

### LEARNING OBJECTIVES

1) Improve ability to participate in or develop global radiology projects. 2) Understand available resources and types of organizations involved in global radiology. 3) Create a viable framework for global radiology incorporating the multifactorial implementation challenges. 4) Develop global radiology strategies that maximize sustainability and scalability.

### ABSTRACT

## RC816E • Strategies For Sustainability and Scalability of Radiology in Developing Countries: Lessons Learned from RAD-AID's Radiology-Readiness Model

**Daniel J Mollura MD (Presenter)**

### LEARNING OBJECTIVES

1) Describe evidence of radiology needs in limited-resource regions. 2) Describe how data collection and analysis can help radiology planning in developing world. 3) Provide examples showing that projects planned from data analysis can increase long term effectiveness of radiology services in the developing world.

### ABSTRACT

The World Health Organization (WHO) reports that 50-70% of the world's population has inadequate or no access to medical imaging, such as radiography, ultrasound and mammography. This disparity has contributed to inadequate health care among poor populations, such as for women's health (breast cancer screening and maternal infant health), HIV-related disease, Tuberculosis, cancer, heart disease, and trauma, because these diseases often require radiology for diagnosis and care. To address this worldwide problem, multidisciplinary approaches should be optimized to include economic development, health care system evaluation, technology innovation, clinical education, and technical training. Projects developed on this model can increase targeted effectiveness for long term radiology services by implementing programs that specifically meet measured needs and can be monitored for outcomes. Moreover, data collection and analysis of radiology needs should ideally encompass these multidisciplinary areas in order to clearly target the highest yield areas for intervention given the infrastructure, economic context, referral pathways, and epidemiological disease patterns. By scaling this model for diverse regions based on interdisciplinary teams and methods, radiology services in the developing world can address shortages and decrease global health care disparities.

## Essentials of Molecular Imaging

**Friday, 08:30 AM - 10:00 AM • S505AB**



[Back to Top](#)

**RC817 • AMA PRA Category 1 Credit™:1.5 • ARRT Category A+ Credit:1.5**

**Moderator**

**Steven M Larson, MD \***

## RC817A • Molecular Imaging as a Guide for Better Cancer Therapies

**Steven M Larson MD (Presenter) \***

### LEARNING OBJECTIVES

1) The participants will learn the definition of "theranostic" radiotracer. 2) The participants will learn the role of MEK in non-avid thyroid cancer. 3) The participants will learn why expression of Prostate Specific Membrane antigen (PSMA) offers potential for improved diagnosis and therapy of prostate cancer. 4) The participants will learn the contribution of radioactive nanoparticles both now and in the future for staging and drug delivery.

## RC817B • Pediatric Molecular Imaging

**Heike E Daldrop-Link MD (Presenter)**

### LEARNING OBJECTIVES

1) To understand advantages and limitations of radiation-free whole body diffusion MRI techniques for tumor staging in children. 2) To recognize the value of immediately clinically applicable iron oxide nanoparticles for tumor staging and tumor characterization in pediatric patients. 3) To learn about clinically relevant PET/MR applications in pediatric patients.

### ABSTRACT

#### Pediatric Molecular Imaging

How much does Molecular Imaging matter in our clinical environment? Molecular Imaging spurs the discovery of fundamentally new targets for imaging diagnoses, thereby leading to new knowledge and new concepts that substantially advance our approach to detecting, characterizing and treating disease. Translational molecular imaging approaches are increasingly integrated into the clinical care of adult patients, but applications in pediatric patients are still limited due to safety considerations and regulatory and administrative hurdles. The clinical need for more specific information along with the success of molecular imaging techniques in adult patients will ultimately penetrate into pediatric applications. New, child-adapted molecular imaging approaches are currently utilized to improve our knowledge of the biology of pediatric diseases, and to support personalized diagnostic and therapeutic approaches. This presentation will show three immediately clinically applicable molecular imaging applications for pediatric patients: (1) Novel approaches for radiation-free whole body staging, (2) Improved tumor characterization with clinically approved iron oxide nanoparticles and (3) clinically relevant MR/PET applications in pediatric patients. Further developments aim to integrate the advantages of multi-modality molecular imaging tools towards more comprehensive and quantitative diagnoses that can direct early decision making, guide individualized clinical care procedures, and ultimately, accelerate and improve positive treatment outcomes.

## RC817C • Molecular Imaging of Breast Cancer: Clinical and Biologic Insights

**David A Mankoff MD, PhD (Presenter)**

### LEARNING OBJECTIVES

1) Review breast cancer clinical and biologic concepts relevant to treatment. 2) Discuss how molecular imaging may be used to guide targeted breast cancer therapy. 3) Describe future directions in breast cancer biomarker imaging.

### ABSTRACT

This talk will review molecular imaging in the context of current knowledge of breast cancer biology and the increasing trend towards individualized and targeted breast cancer therapy. The discussion will emphasize molecular imaging, especially PET, and biomarker applications to guide treatment selection. Insights gained into the in vivo biology of breast cancer from quantitative molecular imaging will also be discussed.

## RC817D • New Tools and Targets for Molecular Imaging



**Martin G Pomper MD, PhD (Presenter) \***

**LEARNING OBJECTIVES**

1) Discuss emerging molecular imaging agents. 2) Discuss new targets for molecular imaging. 3) Focus on translation of molecular imaging agents to the clinic.

**ABSTRACT**

We will discuss how one goes about identifying a suitable target for molecular imaging and then actually generates the imaging agent - for a variety of modalities, whichever is appropriate to answer the question at hand. There will be a focus on clinical translation and discussion of combined diagnostic/therapeutic (theranostic) agents.

---

**Techniques for Quantitative Cancer Imaging: Current Status**

---

**Friday, 08:30 AM - 10:00 AM • S404CD**

---

**RO** **OI** **BQ**

[Back to Top](#)

**RC818 • AMA PRA Category 1 Credit™:1.5 • ARRT Category A+ Credit:1.5**

**RC818A • Computed Tomography**

**Binsheng Zhao DSc (Presenter)**

**LEARNING OBJECTIVES**

1) Familiarize the audience with conventional CT response assessment methods and their limitations, especially in the era of new drug development. 2) Provide examples of modified RECIST methods in several types of cancers. 3) Raise awareness of the need to re-evaluate RECIST guidelines and establish new response assessment criteria based on tumor volume and density changes. 4) Discuss the effects of CT imaging parameters on tumor measurement and the importance of standardizing an imaging acquisition protocol in response assessment.

**ABSTRACT**

Computed tomography (CT) has been widely used in assessing tumor response to therapy. This refresher course will familiarize the audience with conventional response assessment methods and their limitations, especially at a time of target drug development. Potential improvements will be discussed, including re-evaluating the RECIST (Response Assessment Criteria in Solid Tumors) guidelines and establishing new response assessment criteria based on tumor volume and density changes on CT. Several examples of modified RECISTs for lymphoma, mesothelioma, hepatocellular carcinoma (HCC) and gastrointestinal stromal tumor (GIST) will be provided. Last but not least, measurement variability will be addressed and the importance of standardizing an imaging acquisition protocol in oncologic response assessment will be discussed.

**RC818B • Magnetic Resonance Imaging**

**Gregory S Karczmar PhD (Presenter) \***

**LEARNING OBJECTIVES**

1) Gain familiarity with methods used for accurate measurements of tumor volumes with MRI, advantages of MRI, challenges, and sources of error. 2) Understand basic principles and clinical applications of dynamic contrast enhanced MRI; possibilities for standardized measurements of perfusion and capillary permeability, and sources of error. 3) Understand basic principles and clinical applications of diffusion-weighted imaging, measurements of the 'apparent coefficient of diffusion' (ADC), and sources of error.

**ABSTRACT**

Anatomic and functional MRI is increasingly used for diagnosis and staging of cancer, and for detection of response to therapy. However, standardized, quantitative measurements remain challenging. We will review use of MRI to reliably measure tumor volume, and two widely used functional MRI methods – dynamic contrast enhanced MRI (DCEMRI) and diffusion-weighted imaging (DWI). We will discuss methods used to standardize DCEMRI measurements, including quantitative measurements of contrast media as a function of time, measurement of the arterial input function, and use of an appropriate model for calculation of perfusion/capillary permeability, as well as 'model-free' approaches. We will discuss methods used to measure the apparent diffusion constant (ADC) and the relationship between the ADC and underlying physiology/anatomy at the microscopic level.

**RC818C • Positron Emission Tomography**

**Paul E Kinahan PhD (Presenter) \***

**LEARNING OBJECTIVES**

1) Understand the advantages and disadvantages of PET/CT as a quantitative imaging technique. 2) Understand sources of bias and variance in quantitative PET/CT imaging, both in data acquisition and analysis. 3) Learn techniques for limiting variability in quantitative PET/CT imaging.

**ABSTRACT**

Dual-mode positron emission tomography / x-ray computed tomography (PET/CT) imaging has become a standard tool in cancer imaging for detection, diagnosis and staging over the last decade, and is increasingly being used in therapy planning and assessing response to therapy. This refresher course will familiarize the audience with response assessment methods used in PET/CT imaging and their limitations. Recently proposed criteria will be discussed, including the PERCIST (PET Response Criteria in Solid Tumors) guidelines. Measurement variability will be addressed and the importance of standardizing an imaging acquisition protocol in oncologic response assessment with PET/CT will be discussed.

---

**Medical Physics 2.0: Magnetic Resonance Imaging**

---

**Friday, 08:30 AM - 10:00 AM • S405AB**

---

**PH** **MR**

[Back to Top](#)

**RC821 • AMA PRA Category 1 Credit™:1.5 • ARRT Category A+ Credit:1.5**

**Co-Director**

**Ehsan Samei** , PhD \*

**Co-Director**

**Douglas E Pfeiffer** , MS \*

**RC821A • Magnetic Resonance Imaging Perspective**

**Douglas E Pfeiffer MS (Presenter) \***

**LEARNING OBJECTIVES**

1) Understand the history and development of magnetic resonance imaging equipment. 2) Understand the impact of equipment development on testing protocols. 3) Understand the requirements for medical physics support in image quality and safety.

## ABSTRACT

Magnetic resonance imaging equipment has developed significantly since its inception. Field strength increases and technology development increase the complexity of the equipment and the need for medical physics and MRI scientist support. This talk will briefly introduce the developments that have taken place and discuss the impact that this development has had on testing and support.

### RC821B • Magnetic Resonance Imaging 1.0

**Ronald R Price** PhD (Presenter)

#### LEARNING OBJECTIVES

1) Review the image quality metrics that are currently used as part of an MRI system performance report. 2) Discuss how the medical physicist can assist in the development and evaluation of imaging sequences used as part of clinical protocols. 3) To review items that should be included as part of an MRI safety survey. 4) Discuss the steps necessary for establishing and maintaining a routine quality assurance program. 5) Review aspects of AAPM Report No. 100 regarding acceptance testing of new MRI systems. 6) Review modality and system specific requirements for MRI accreditation.

#### ABSTRACT

MRI 1.0: Magnetic Resonance Imaging Ronald R. Price The purpose of this presentation is to review the current role of the medical physicist in clinical Magnetic Resonance Imaging (MRI). The discussion will first discuss MRI acceptance testing with reference to the recommendations of AAPM Report No. 100 and will specifically include items that should be part of both the initial and annual MRI safety survey. This discussion will be followed by a review of the image quality metrics that are currently used as part of an MRI system performance report as well as how the medical physicist may go about assisting in the development and evaluation of imaging sequences used as part of clinical protocols. The presentation will also discuss the steps necessary for establishing and maintaining a routine quality assurance program with emphasis on the necessity of establishing a strong working relationship with the MRI quality assurance technologist. There will also be a review of the system specific requirements for MRI accreditation.

### RC821C • Magnetic Resonance Imaging 2.0

**David R Pickens** PhD (Presenter) \*

#### LEARNING OBJECTIVES

1) Identify requirements for ongoing quality assurance of ultra-high field MRI systems and hybrid MR/PET systems. 2) Identify the need for new quality assurance tools and testing procedures for advanced systems with many parallel imaging channels. 3) Identify site safety issues for ultra-high field and hybrid MR systems and expanded concerns for patient and staff safety. 4) Understand increased requirements from oversight and accreditation organizations. 5) Identify the need for improved continuing education for medical physicists/MRI scientists.

#### ABSTRACT

This talk will look into the future of clinical MR imaging and the role of the physicist as the technology of MR imaging evolves. Many of the quality assurance techniques used today will need to be extended to address the advent of higher field imaging systems and dedicated imagers for specialty applications. Included will be the need to address quality assurance and testing for hybrid devices such as MR/PET systems. Many new coil systems will be routinely provided in systems with large numbers of parallel receive channels along with parallel transmit channels. New pulse sequences and acquisition methods, increasing use of MR spectroscopy, and real-time guidance procedures will place the burden on the medical physicist to develop and use new phantoms and test procedures to evaluate clinical imagers. Many of these systems will have different potential side effects including potential problems associated with patient and staff safety. New software tools will be available for testing, but these must be understood by the physicist in order that they be used correctly for quality assurance purposes. Finally, new rules, requirements, and regulations undoubtedly will mean that the medical physicist must work closely with staff technologists to keep her/his sites compliant with the latest requirements and must actively keep abreast of these developments.

## Minicourse: Recording and Reporting Radiation Dose: Nuclear Medicine

Friday, 08:30 AM - 10:00 AM • S403B

QA PH NM

[Back to Top](#)

RC823 • AMA PRA Category 1 Credit™:1.5 • ARRT Category A+ Credit:1.5

#### Director

**J. Anthony Seibert**, PhD

### RC823A • Nuclear Medicine Dose Indices

**Wesley E Bolch** PhD (Presenter)

#### LEARNING OBJECTIVES

1) Identify the more common radiopharmaceuticals used in functional imaging of normal and diseased tissues. 2) Demonstrate understanding of the parameters needed to estimate tissue dose during nuclear medicine imaging and therapy. 3) Identify fundamental data sources for organ and effective dose per unit administered activity. 4) Demonstrate understanding of the physiological and anatomic sources of individual variability in organ and effective dose per unit administered activity. 5) Identify key features of new generation anatomical models that can reduce dose uncertainties through improved matching of patient body morphometry.

#### ABSTRACT

A main clinical application of nuclear medicine is that of functional imaging of normal and diseased tissue, and the localization of malignant tissue and its potential metastatic spread. In these applications, the amount of administered activity is such that the absorbed dose to both imaged and non-imaged tissues are typically very low and thus stochastic risks of cancer induction are greatly outweighed by the diagnostic benefit of the imaging procedure. Nevertheless, these tissues doses and their stochastic risks should be quantified for each patient, and placed in context of both their cumulative values received over multiple imaging sessions, and of doses and risks received by other diagnostic imaging procedures they may have (fluoroscopy and computed tomography, for example). The role of internal dosimetry in diagnostic nuclear medicine is thus to provide the basis for stochastic risk quantification. Once this risk is quantified, it may be used to optimize the amount of administered activity in order to maximize image quality while minimizing patient risk. This optimization process is of particular importance for pediatric patients owing to their enhanced organ radiosensitivities and years over which any stochastic effects may become manifest. This optimization should consider, as much as possible, patient age, gender, and body morphometry, and pharmacokinetics, along with all available image acquisition and processing techniques. Unlike other forms of diagnostic imaging, for which dose indices are readily measured, only the administered radioactivity is typically available for "dose tracking". In this course, we will review data sources for organ and effective dose per unit administered activity for the more common molecular imaging radiopharmaceuticals. Particular attention will be given to sources of individual variability in both organ and effective dose attributed to both physiological and anatomical variations among patients. Advances in computat

### RC823B • Tracking Doses in the Pediatric Population

**Frederic H Fahey** DSc (Presenter)

#### LEARNING OBJECTIVES

1) List three considerations in estimating the radiation dose from pediatric nuclear medicine. 2) Discuss three factors that affect the radiation dose from the CT component of hybrid imaging. 3) Describe three factors that can affect the appropriate choice of administered activity for a nuclear medicine study. 4) List 2 advances that may lead to further reduction in the administered activity in pediatric nuclear medicine.

## Quantitative Imaging: Quantitative Imaging in Ultrasound

Friday, 08:30 AM - 10:00 AM • E263

[Back to Top](#)

PH US BQ

RC825 • AMA PRA Category 1 Credit™:1.5 • ARRT Category A+ Credit:1.5

Director

Michael F McNitt-Gray, PhD \*

### RC825A • Elasticity and Backscatter Related Measures

Timothy J Hall PhD (Presenter) \*

#### LEARNING OBJECTIVES

1) Describe the various approaches and history of Quantitative Ultrasound. 2) Understand the difference in system-dependent and system-independent backscatter parameters. 3) Understand the benefits of system-independent backscatter parameters. 4) Describe the state of the art in elasticity imaging and quantitative ultrasound from backscattered echoes.

#### ABSTRACT

There is a long history of attempts to use the backscattered echo signals from medical ultrasound to describe disease conditions of various tissue types. For example, from the initial application of ultrasound in breasts, the investigators attempted to differentiate benign from malignant disease based on characteristics of the echo signals. Along the way, there have been substantial successes. For example, it was only 30yrs ago that we debated how to estimate blood flow based on ultrasound echo signals and how to interpret that data. Just over 20yrs ago we began to display flow dynamics with color flow imaging. More recently, elasticity imaging methods, which also began in the "tissue characterization" or "quantitative ultrasound" community, have become commercially viable products with clear diagnostic potential. These were "tissue characterization" methods in their early days. Now they are recognized as specific procedures with quantifiable diagnostic merit. Numerous other "quantitative ultrasound" (QUS) methods have been proposed, developed, tested and have demonstrated varying degrees of success. Many of these methods are still under development.

This presentation will discuss "quantitative ultrasound" methods based on backscattered echo signals focusing on the most recent techniques that are either commercially available or that show the greatest potential as diagnostic tools.

### RC825B • Volume Flow and Measures From Contrast Agents

Oliver D Kripfgans (Presenter) \*

#### LEARNING OBJECTIVES

1) Understand the pitfalls of ultrasound based blood flow acquisition, analysis, and interpretation. 2) Become familiar with current approaches of quantitative estimation of blood flow and learn how to minimize associated errors. 3) Obtain an overview of current commercial ultrasound contrast agents as well as their availability in the US. 4) Learn about contrast agent enhanced measurements in a clinical setting.

#### ABSTRACT

Clinical ultrasound scanners typically offer three methods of blood flow acquisition, namely pulse wave, color flow and power Doppler. While real-time blood flow visualization is one of the perks of ultrasound, standardized quantitative methods are still unavailable to the radiologist. Pulse wave offers volumetric flow computation based on assumptions that are often violated. Color flow has never been directly quantitative as no angle correction can be dialed-in. The advent of 2D ultrasound arrays (electronic or mechanically swept) has enabled color flow and power Doppler acquisition in the coronal plane thus yielding Doppler angle as well as geometry independent flow information for direct quantification of in situ real-time volumetric flow. Ultrasound contrast agents have been approved for many clinical applications in Europe, Asia and Canada. The FDA has limited the use of ultrasound contrast agents in the US and essentially only cleared ultrasound contrast agents for cardiac applications. However, off-label application is practiced in the US. Its extend and benefits will be discussed in this course along with current approaches for ultrasound contrast agents based clinical measurements.

#### URL's

www.ultrasound.med.umich.edu/ODK/RSNA2012

### RC825C • Ultrasound Measurements and FDA Criteria for Display of New Quantitative Measures

Brian S Garra MD (Presenter)

#### LEARNING OBJECTIVES

1) Review the main types of quantification of Ultrasound images. 2) Review some recent examples exploring sources of error in ultrasound morphometric quantification. 3) Summarize new ultrasound based parameters that might be displayed. 4) Discuss the formation of the Ultrasound QIBA Technical Committee and its objectives. 5) Review recent changes in FDA policy regarding display of quantitative features on ultrasound images.

#### ABSTRACT

Ultrasound images are probably the most frequently measured images and extensive literature on a wide variety of ultrasound image measurements exists going back to the 1960's. Most morphometric and Doppler measurements are well documented and are at a mature stage. Automated measurements of volume and structures such as arterial intimal medial thickness are also finding increasing clinical application but each method of image segmentation and quantification has its own characteristic problems and sources of error. Some newer measurements including measurement of tissue strain (elastography) and strain rate and one of the newest, shear wave speed, are the subject of considerable research activity and the sources of error and bias are just now being identified and quantified. The RSNA Quantitative Imaging Biomarker Alliance (QIBA) has recently undertaken the task of developing standardized protocols for measurement of ultrasound related parameters. The first project of the US QIBA technical committee is to develop a profile for measurement of shear wave speed in tissue using ultrasound. The FDA has long allowed many types of measurements to be displayed as part of the ultrasound image. A demonstration of reasonable accuracy and precision important for obtaining clearance to display a new measurement. Display of measurement accuracy may also be required and users should be informed of situations where the measurement may be inaccurate. The efforts of the QIBA may provide data that in the future will help to speed up FDA clearance for display of new types of measurements.

## The Use of Business Analytics for Improving Radiology Operations, Quality, and Clinical Performance (In Association with the Society for Imaging Informatics in Medicine)

Friday, 08:30 AM - 10:00 AM • E350

[Back to Top](#)

LM IN

RC826 • AMA PRA Category 1 Credit™:1.5 • ARRT Category A+ Credit:1.5

**Moderator**  
**Katherine P Andriole**, PhD

**LEARNING OBJECTIVES**

1) Understand what is meant by business analytics in the context of a radiology practice. 2) Be able to describe the basic steps involved in implementing a business analytics tool. 3) Learn how business analytics tools can be used for quality assurance in radiology, for maintenance of certification (MOC), and for practice quality improvement. 4) Be introduced to the capabilities of current and potential future business analytics technologies.

**ABSTRACT**

This course will provide an overview of the use of business analytics (BA) in radiology. How a practice manages information is becoming a differentiator in the competitive radiology market. Leveraging informatics tools such as business analytics can help a practice transform its service delivery to improve performance, productivity and quality. An introduction to the basic steps involved in implementing business analytics will be given, followed by example uses of BA tools for quality assurance, maintenance of certification (MOC) and practice quality improvement. The power of current business analytics technologies will be described, along with a look at potential future capabilities of business analytics tools.

**RC826A • An Introduction to Business Analytics Demonstrating Use of an Open-Source Tool for Application to Radiology**

**Katherine P Andriole** PhD (Presenter)

**LEARNING OBJECTIVES**

1) Gain an overview of business analytics tools and understand how they might be used in radiology. 2) Be able to describe the general steps involved in business analytics, including extract, transform, load (ETL) and key performance indicators (KPI). 3) See a demonstration implementation of an open-source business analytics tool using a radiology use case.

**ABSTRACT**

This session will provide a general overview of business analytics concepts and how they can be used in radiology. A walk through of the basic steps involved in implementation including identifying, collecting, transforming, and dynamically presenting key performance indicators (KPI) will be demonstrated. The extract, transform, load (ETL) steps will be shown using an example use case, and multiple database sources taken from a radiology practice.

**RC826B • Business Analytic Tools for Quality Assurance, MOC and PQI**

**Paul G Nagy** PhD (Presenter)

**LEARNING OBJECTIVES**

1) Discuss the importance of informatics tools for ABR MOC PQI and ACGME SBP quality efforts. 2) Identify the role of informatics in capturing, extracting, analyzing, and communication quality projects. 3) Illustrate graphical dashboarding examples to support quality efforts.

**RC826C • Capabilities of Current and Future Business Analytics Technologies**

**Tessa S Cook** MD, PhD (Presenter)

**LEARNING OBJECTIVES**

1) To gain familiarity with currently available business technologies and their relevance to radiology practice. 2) To consider how existing business technologies can support quality assurance in radiology. 3) To learn about business analytics features that may be available/desirable in the future to augment and support both the practice of radiology.

**ABSTRACT**

---

**Consumerism and Radiology**

**Friday, 08:30 AM - 10:00 AM • S504AB**



[Back to Top](#)

**RC827 • AMA PRA Category 1 Credit™:1.5 • ARRT Category A+ Credit:1.5**

**Richard Duszak**, MD  
**Christine Hughes** \*  
**Debra Richman**  
**Nancy Davenport-Ennis**, MD  
**Cherrill Farnsworth** \*  
**Steve Bonner**

**LEARNING OBJECTIVES**

1) Identify the present and future ramifications of the rise of consumerism on radiology. 2) Characterize strategies radiology practices and departments can use to prepare for these changes. 3) Define what consumers need to know about imaging and how is it best communicated to consumers. 4) Illustrate how to create a bond with consumers in a commodity market.

**ABSTRACT**

The rise of consumerism has impacted the relationships patients have with payors and providers. Because of the insular nature of radiology the full impact of consumerism has not yet been felt. Historically, radiologists have managed a Physician to Physician (P2P) relationship. Radiologists have been the invisible heroes in the patient care cycle. Ripples of Radiologist to Consumer (R2C) relationships are emerging in pockets of the US. This session will address the following questions: What are the present/ future ramifications of the rise of consumerism on radiology? How can radiology practices and departments prepare for these changes? What do consumers need to know about imaging and how is it best communicated to consumers? How is a bond created with consumers in a commodity market?

---

**Interactive Game: Clinical Problems in Body MRI - Case-based Instruction**

**Friday, 08:30 AM - 10:00 AM • E451B**



[Back to Top](#)

**RC829 • AMA PRA Category 1 Credit™:1.5 • ARRT Category A+ Credit:1.5**

**LEARNING OBJECTIVES**

This interactive session will use RSNA Diagnosis Live™. Please bring your charged mobile wireless device (phone, tablet or laptop) to participate.

**RC829A • Liver Lesion Differential Diagnosis**

**Christopher G Roth** MD (Presenter) \*

**LEARNING OBJECTIVES**

1) To appreciate and understand the typical imaging appearances of common liver lesions. 2) To understand the algorithmic approach to liver lesion differential diagnosis. 3) To understand how information from the various pulse sequences and contrast agents contribute to liver lesion assessment.

#### ABSTRACT

Given the ubiquitousness of liver lesions on imaging studies, it is incumbent upon radiologists to accurately characterize these lesions and differentiate benign from malignant. While the vast majority of liver lesions are benign incurring no further treatment or management and their features need to be recognized, the management of indeterminate and malignant lesions ranges from percutaneous biopsy to surgery to chemotherapy and a confident diagnosis or differential diagnosis should be pursued before these invasive measures are undertaken. While many lesions are adequately characterized on other imaging modalities, many require further analysis with MRI and some may initially present at MR imaging. Given the wide array of pulse sequences and protocols and proliferation of MR contrast agents, assimilating all of the necessary imaging information to generate an accurate diagnosis or differential diagnosis can be challenging. MRI is considered the most comprehensive and accurate modality for noninvasive assessment of liver lesions and in the majority of cases, a confident lesion diagnosis is possible based on the composite information from multiple pulse sequences. While many lesions exhibit classic features rendering diagnosis straightforward, lesions occasionally demonstrate unusual or atypical features that may complicate accurate diagnosis and familiarity with these infrequent appearances is important for accurate characterization and discrimination between benign and malignant etiology. The utility of the various MRI pulse sequences and contrast agents will be discussed and a diagnostic algorithm will be presented to help classify and accurately diagnose liver lesions.

### RC829B • Pancreatic Cysts - Achieving Consistency and Common Sense

**Masoom A Haider MD (Presenter) \***

#### LEARNING OBJECTIVES

1) To be able to perform an MRI protocol for evaluation of pancreatic cystic lesions. 2) To recognize the classic MRI findings for cystic pathologies of the pancreas. 3) To have a pragmatic approach to management recommendations of cystic lesions of the pancreas.

#### ABSTRACT

With the widespread use of cross sectional imaging cystic pancreatic lesions are being detected with increasing frequency. The dominance of pseudocyst as the commonest type of pancreatic cyst may no longer hold. Radiologists must be familiar with the features of cystic neoplasms. MRI offers excellent tissue contrast for characterization of pancreatic cysts as well as for assessment of relationship to the pancreatic duct which can be helpful for differential diagnosis. A number of MRI features can be used to help guide management and offer likely differential diagnosis and will be presented. At the same time MRI has resulted in increased detection of tiny incidental simple pancreatic cysts for which limited or no followup may be necessary. It is important to recognize that in some cases MRI and other non-invasive imaging methods cannot provide reliable diagnosis as there is substantial overlap in imaging findings between some benign and pre-malignant or malignant cystic neoplasm. These scenarios will be reviewed.

### RC829C • Cholangiocarcinoma - Addressing a Difficult Challenge

**Kartik S Jhaveri MD (Presenter) \***

#### LEARNING OBJECTIVES

1) To emphasize an optimal MR imaging protocol. 2) To highlight role of MRI in the diagnosis and classification. 3) To demonstrate the role of MRI in staging. 4) To understand limitations of MRI and review "mimics" of cholangiocarcinoma.

#### ABSTRACT

Although Cholangiocarcinoma is a rare tumour (

---

## Current and Next Generation Health IT Tools To Enable Radiation Exposure Reduction - A Practical Guide

---

Friday, 08:30 AM - 10:00 AM • S403A



[Back to Top](#)

**RC830 • AMA PRA Category 1 Credit™:1.5 • ARRT Category A+ Credit:1.5**

#### Moderator

**Ramin Khorasani, MD \***

### RC830A • Before the Scan: Optimizing Dose Before the Patient Is On the Table

**Rasu B Shrestha MD, MBA (Presenter) \***

#### LEARNING OBJECTIVES

1) Number of CT scans is increasing annually. 2) Wider adoption/ availability of CT scanners. 3) Indications for CT use are increasing (without possible consideration for risks). 4) Rapid increase in number of protocols: Varying equipment leading to protocol variance. Children are at greater risk from a given dose of radiation compared with adults. A thorough look at the issues around radiation dose in children will also be provided.

#### ABSTRACT

The acceptance of the risks associated with radiation is conditional on the benefits to be gained from the use of radiation. The risks must be restricted and protected against by the application of radiation safety standards. A significant part of the challenge of patient dose management in CT arises from the fact that over-exposure in CT is frequently not detected. In contrast to film based radiography where overexposure results in a dark image, increasing dose in CT and in other digital imaging techniques results in images with: (1) less noise (improved visual appearance) and (2) fewer streak artifacts, (3) although not necessarily with greater diagnostic information. Image quality in CT often exceeds the clinical requirements for diagnosis. It is critical to have a thorough understanding of the basics of radiation dose in CT before we explore the multiple issues around opportunities to reduce these dose parameters. Furthermore, it is also critical to comprehend the role of newer technologies, innovations and developments that are rapidly taking place to address radiation dose reduction in CT - both on the vendor as well as on the private and academic communities. A thorough and comprehensive understanding of the quality and patient safety issues around this is also critical to making sound decisions around imaging on multiple levels. Different organs have different sensitivities to radiation. Tissue Weighted Factor, WT takes into account the risk to the person exposed to radiation that is not uniform over the entire body. As an example, if 1 mSv is received only by the lungs, this results in an effective dose to that person of 0.12 mSv. This means that 1 mSv received by the lungs poses approximately the same risk as 0.12 mSv to the entire body. Fundamentals such as these will be presented in easily digestible chunks in the refresher course. Also covered will be Protocol Optimization, Scanner Interfacing, Data Connectivity and Interoperability.

### RC830B • During the Scan: Patient-Centric Imaging

**William W Boonn MD (Presenter) \***

#### LEARNING OBJECTIVES

1) Learn how modifications in CT scan protocol can affect image quality and radiation dose. 2) Understand how to optimize scanning protocols based on clinical indication and patient specific factors. 3) Learn how to measure and monitor protocols and dose to track and optimize performance.

### RC830C • After the Scan: Data-Mining Dose Data for Improved Quality, Safety, and Outcomes

**Aaron D Sodickson MD, PhD (Presenter)**

**LEARNING OBJECTIVES**

1) Understand available metrics of CT radiation exposure, and how they relate to patient dose. 2) Demonstrate methods to extract exposure data on a large scale. 3) Highlight quality improvement and patient safety applications of large radiation exposure databases.

**US for Thyroid Cancer: Diagnosis, Surveillance, and Treatment (How-to Workshop)**

**Friday, 08:30 AM - 10:00 AM • E450B**

[Back to Top](#)

**US** **OI** **NR** **HN**

**RC831 • AMA PRA Category 1 Credit™:1.5 • ARRT Category A+ Credit:1.5**

**Jill E Langer**, MD \*  
**Kathryn A Robinson**, MD  
**Sheila Sheth**, MD \*

**LEARNING OBJECTIVES**

1) Describe the sonographic characteristics of thyroid nodules that are suspicious for malignancy. 2) a. Discuss the Bethesda Cytology Classification of Thyroid FNA results and the risk of malignancy associated with each category. b. Describe the indications for two new genetic tests that may be performed on FNAs obtained from thyroid nodules with indeterminate cytology. 3) a. Describe the technique of US-guided biopsy of thyroid nodules and cervical lymph nodes in patients who have undergone thyroidectomy for thyroid cancer. b. Discuss the rationale and method of performance of US-guided ethanol ablation of malignant cervical adenopathy in post thyroidectomy patients.

**ABSTRACT**

This presentation will consist of a three individual presentations. The first will review the sonographic characteristics of thyroid nodules that are suggestive of malignancy. Recommendations for selecting which thyroid nodules require ultrasound-guided biopsies which have been provided by both Radiology consensus conferences and published Endocrinology guidelines will be discussed. The second presentation will review with the Bethesda Cytology Classification of Thyroid FNA results and the risk of malignancy associated with each category. Additionally this presentation describes the indications for two new genetic tests that may be performed on FNAs obtained from thyroid nodules with indeterminate cytology. The last presentation will provide a detailed description of the technique for performing ultrasound guided biopsy of thyroid nodules and cervical lymph nodes. Various methods will be discussed and required equipment outlined. Possible complications, though rare, will be described. A comparison of the typical sonographic features of normal versus abnormal lymph nodes will be presented in an effort to identify those patients in whom sonographic follow up can be used instead of biopsy. A discussion of the possible advantages of adding thyroglobulin assay to cytologic evaluation will be provided. The rationale for and technique of performing ultrasound guided ethanol ablation of malignant cervical lymph nodes in patients with thyroid cancer will be undertaken.

**Develop Your Radiology Financial Insight: Fundamental Principles You Should Know About Business**

**Friday, 08:30 AM - 10:00 AM • S502AB**

[Back to Top](#)

**LM**

**RC832 • AMA PRA Category 1 Credit™:1.5 • ARRT Category A+ Credit:1.5**

**RC832A • How Much Is It Worth: Valuing Assets and Investments**

**Kenneth A Buckwalter MD (Presenter)**

**LEARNING OBJECTIVES**

1) Understand the time value of money. 2) Review interest rate terminology such as Interest rate, Discount rate, and Hurdle rate. 3) Describe standard ways to value an investment for Payback time, Internal rate of return, and Net present value. 4) Use net present value to understand the loss of Tiger Woods's Brand Value in 2009.

**RC832B • Follow the Money: Everything You Ever Wanted to Know About the Revenue Cycle**

**Mark S Frank MD (Presenter)**

**LEARNING OBJECTIVES**

1) Know the definition of 'revenue cycle'. Be aware of how the revenue cycle revenue applies to a 'typical' diagnostic radiology practice. 2) Know the definition of accounts receivable (AR), and the important role that AR plays in radiology practices. 3) Understand the concept of 'charge lag' and the factors contributing to it. 4) Know the major factors that effect timeliness and amount of payment received once a bill is submitted. 5) Know the relationships between net income, accounts receivable, and cash flow. 6) Be aware of the Radiology Business Managers Association (RBMA) recommended factors for tracking AR. 7) Know the definition of Adjusted Collections Percentage (ACP). 8) Know some techniques for reducing AR and optimizing the revenue cycle. 9) Know the definition of RBRVS (Resource Based Relative Value Scale) and its relationship to the Current Procedural Terminology (CPT) coding model. 10) Know the concept and structure (components) of an RBRVS global payment. 11) Understand how work performed (as perceived by the radiologist) maps onto the RBRVS scale and the role of the RBRVS scale in financial payment mechanisms.

**Targeted Treatment and Imaging of Liver Cancers: Basic to Advanced Techniques in Minimally-Invasive Therapies and Imaging (How-to Workshop)**

**Friday, 08:30 AM - 10:00 AM • E260**

[Back to Top](#)

**OI** **IR** **GI**

**RC850 • AMA PRA Category 1 Credit™:1.5 • ARRT Category A+ Credit:1.5**

**John J Park**, MD, PhD  
**Jinha Park**, MD, PhD  
**Jonathan M Kessler**, MD  
**Steven S Raman**, MD  
**Marcelo Guimaraes** \*

**LEARNING OBJECTIVES**

1) Discuss the role of the interventional radiologist in the treatment and management of patients with primary and metastatic liver cancer as part of the multidisciplinary team. 2) Learn best practice techniques in the treatment of liver cancers, with emphasis on both locoregional and focal therapeutic approaches, and indications for treatment. 3) Explore various tips and tricks for each treatment modality and learn how to avoid complications through good patient selection, choosing the appropriate techniques, and knowing what common mistakes to avoid. 4) Learn about newer and developing techniques and devices, their potential roles and indications, and potential pitfalls. 5) Explore advanced imaging modalities in the detection of tumors and for monitoring treatment response.

**ABSTRACT**

## Pediatric Neurosonography Update: Head, Spine, and Transcranial Doppler Ultrasound (How-to Workshop)

Friday, 08:30 AM - 10:00 AM • E261

[Back to Top](#)

PD US NR

**RC851** • AMA PRA Category 1 Credit™:1.5 • ARRT Category A+ Credit:1.5

**M. Beth McCarville**, MD \*  
**Geetika Khanna**, MD,MS  
**Kristin A Fickensch**, MD

### LEARNING OBJECTIVES

1) Describe advances in neurosonography that can be applied on a local level to improve daily practice of neonatal neurosonography. 2) Review indications for neonatal spine sonography, identify normal variants/pitfalls that can simulate disease, and recognise the sonographic features of spinal anomalies. 3) Review the role of transcranial Doppler ultrasound with imaging (duplex) and without imaging (non-duplex), in assigning stroke risk to children with sickle cell disease.

### ABSTRACT

URL's

<http://www.umkcradres.org/education/peds/neuro/index.htm>

## US-guided Interventional Breast Procedures (Hands-on Workshop)

Friday, 08:30 AM - 10:00 AM • E264

[Back to Top](#)

US BR

**RC852** • AMA PRA Category 1 Credit™:1.5 • ARRT Category A+ Credit:1.5

**Jocelyn A Rapelyea**, MD  
**Priscilla J Slanetz**, MD, MPH \*  
**Shambhavi Venkataraman**, MD  
**Liane E Philpotts**, MD \*  
**Ermelinda Bonaccio**, MD  
**Stephen J Seiler**, MD  
**Bruno D Fornage**, MD  
**Rachel F Brem**, MD \*  
**William R Poller**, MD \*  
**Margaret M Szabunio**, MD

### LEARNING OBJECTIVES

1) Describe the equipment needed for ultrasound guided interventional breast procedures. 2) Review the basic principles of ultrasound guidance and performance of minimally invasive breast procedures. 3) Practice hands-on technique for ultrasound guided breast interventional procedures.

### ABSTRACT

This course is intended to familiarize the participant with equipment and techniques in the application of US guided breast biopsy and needle localization. Participants will have both basic didactic instruction and hands-on opportunity to practice biopsy techniques on tissue models with sonographic guidance. The course will focus on the understanding and identification of: 1) optimal positioning for biopsy 2) imaging of adequate sampling confirmation 3) various biopsy technologies and techniques 4) potential problems and pitfalls

## Advanced Image Analysis, including Applications such as Automated Stent Planning and Multimodality Image Fusion and Treatment Planning (Hands-on Workshop)

Friday, 08:30 AM - 10:00 AM • S401CD

[Back to Top](#)

IN IR

**RC853** • AMA PRA Category 1 Credit™:1.5 • ARRT Category A+ Credit:1.5

**Gary J Wendt**, MD,MBA \*

### LEARNING OBJECTIVES

1) To get hands-on experience using 3D / 4D tools to process huge data sets, specifically multislice CT and MR using data sets. 2) How to effectively deal with the following data: CT and MR angiograms, perfusion, and bone. 3) Getting hands on experience using 3D / 4D tools to process data in near realtime. 4) Introduce the basic 3D tools that are available and how they can be used both within radiology as well as how they apply to referring clinicians.

### ABSTRACT

This course will focus on how to get hands-on experience using 3D / 4D tools to process huge data sets, specifically multislice CT and MR using data sets. How to effectively deal with the following data: CT and MR angiograms, perfusion, and bone. It will also focus on providing hands on experience using 3D / 4D tools to process data in near realtime for emergencies like stroke work-up. It will also introduce the basic 3D tools that are available and how they can be used both within radiology as well as how they apply to referring clinicians

## Basic Tools and Tricks for Data Collection and Organization for Practice Quality Improvement Projects and for Research Data Management - A Step by Step Approach with Excel (Hands-on Workshop)

Friday, 08:30 AM - 10:00 AM • S401AB

[Back to Top](#)

RS IN

**RC854** • AMA PRA Category 1 Credit™:1.5 • ARRT Category A+ Credit:1.5

**Andrea J Frangos**, MPH  
**Jaydev K Dave**, PhD, MS

### LEARNING OBJECTIVES

1) Define the basic structure and functions of a spreadsheet. 2) Learn efficient techniques for data collection in a spreadsheet. 3) Demonstrate key data management skills. 4) Recognize differences between a spreadsheet and a database.

### LEARNING OBJECTIVES

1. Learn efficient techniques for manipulating data and performing data analysis with a spreadsheet program.
2. Define the basic structure and functions of a database.
3. Learn how to create a simple database for data collection and analysis.
4. Recognize tasks that are more easily accomplished with a database than a spreadsheet.

### ABSTRACT

A spreadsheet program is commonly employed to collect and organize data for practicing quality improvement, for research, and for other purposes. In this refresher course, we will demonstrate how to format and use a spreadsheet properly for data collection and analysis. We

will define the essential structure and function of a spreadsheet and elaborate on the process to create a basic spreadsheet. We will review common errors during data acquisition that may be avoided for streamlining the acquisition process. We will then consider several functionalities of a spreadsheet program that facilitate data management. We will also highlight the differences between a spreadsheet and a database, so that the participants may be able to identify best applications for their tasks. This course will accomplish its learning objective through hands-on tutorial demonstrations with Microsoft Excel – a spreadsheet program. Familiarity with Microsoft Windows environment will be assumed, but no experience with Microsoft Excel spreadsheet program or formula is necessary.

## Interventional Radiology Series: Top 5 Complications in Interventional Oncology - Avoidance, Recognition and Management

Friday, 08:30 AM - 12:00 PM • E451A

[Back to Top](#)



**VSIR61** • AMA PRA Category 1 Credit™:3.25 • ARRT Category A+ Credit:3.75

**Moderator**  
**Charles E Ray**, MD, PhD \*

### LEARNING OBJECTIVES

- 1) List 2 important recent publications in interventional oncology.
- 2) Explain the mechanism of one complication related to thermal ablation.
- 3) Describe pros and cons of chemoembolization versus radioembolization of hepatocellular carcinoma with portal vein thrombosis.
- 4) Outline 3 complications in combination therapy for hepatocellular carcinoma.
- 5) List three complications of chemo-embolization.
- 6) Describe rationale for and against interventional oncology as a distinct specialty.

### VSIR61-02 • Chemo-Embolization Cxs

**Charles E Ray** MD, PhD (Presenter) \*

#### LEARNING OBJECTIVES

View learning objectives under main course title.

### VSIR61-03 • Tc-99m Macroaggregated Albumine Lung Shunt Calculation Overestimates the Lung Dose in Radioembolization

**Mattijs Elschot** MSc ; **Jip F Prince** MSc (Presenter) ; **Maarten L Smits** ; **Marnix G Lam** MD ; **Johannes F Nijsen** PhD ; **Bernard A Zonnenberg** MD ; **Max A Viergever** \* ; **Maurice A Van Den Bosch** MD, PhD ; **Hugo W De Jong** PhD

#### PURPOSE

Hepatic radioembolization is preceded by a safety procedure in which a scout dose of  $^{99m}\text{Tc}$ -MAA is infused in the hepatic artery for assessment of lung shunting. If the lung shunt is substantial, the treatment dose is reduced to minimize the risk of radiation pneumonitis, which may lead to inadequate absorbed doses to tumors. The purpose of this study was to assess the accuracy of  $^{99m}\text{Tc}$ -MAA lung shunt calculations

#### METHOD AND MATERIALS

Fourteen patients were treated with radioembolization using holmium-166-loaded microspheres ( $^{166}\text{Ho}$ ). These particles can be quantified with SPECT and can be used for scout dose and treatment. During preparatory angiography,  $^{99m}\text{Tc}$ -MAA (150 MBq) was injected, followed by (planar) scintigraphy and SPECT-CT. At the day of treatment, a scout dose of  $^{166}\text{Ho}$ -microspheres (250 MBq) was first injected, followed by SPECT-CT imaging. Subsequently, a treatment dose of  $^{166}\text{Ho}$ -microspheres was injected and imaged with SPECT-CT. Lung shunting was calculated on  $^{99m}\text{Tc}$ -MAA scintigraphy. Mean lung doses were calculated on quantitative SPECT images for all three procedures and also on scintigraphy for  $^{99m}\text{Tc}$ -MAA. The activity in the lungs was converted into absorbed dose (Gy) corresponding to the net injected treatment dose. The pre-treatment estimations were compared to the lung dose after actual treatment, as measured with post-treatment SPECT.

#### RESULTS

No signs of radiation pneumonitis were seen in any patient during three months follow up. The median lung shunt based on  $^{99m}\text{Tc}$ -MAA scintigraphy was 4.1% (range 2.2 – 11.3%). The median lung dose after  $^{166}\text{Ho}$ -radioembolization was 0.2 Gy (range 0 – 0.7 Gy), based on quantitative SPECT. This lung dose was significantly overestimated by  $^{99m}\text{Tc}$ -MAA scintigraphy (median difference (?) 5.1 Gy, range 1.4 – 17.1 Gy,  $p < 0.001$ ) and by  $^{99m}\text{Tc}$ -MAA SPECT (? 2.3 Gy, range 0.5 – 11.8 Gy,  $p < 0.001$ ). The estimations on SPECT images of the  $^{166}\text{Ho}$ -scout dose did not differ significantly from treatment (? 0.0 Gy, range -0.7 – 0.3 Gy,  $p = 0.542$ ).

#### CONCLUSION

$^{99m}\text{Tc}$ -MAA lung shunt calculations significantly overestimate the mean lung dose after radioembolization with  $^{166}\text{Ho}$  microspheres. In contrast, a scout dose of  $^{166}\text{Ho}$ -microspheres accurately predicts the mean lung dose after treatment.

#### CLINICAL RELEVANCE/APPLICATION

The mean absorbed dose to lung parenchyma of patients treated with  $^{166}\text{Ho}$  radioembolization is significantly overestimated by  $^{99m}\text{Tc}$ -MAA planar scintigraphy and SPECT-based lung dose calculations.

### VSIR61-05 • Y-90 Cxs

**Robert J Lewandowski** MD (Presenter) \*

#### LEARNING OBJECTIVES

View learning objectives under main course title.

### VSIR61-06 • Trans-arterial Radioembolization (TARE) of Intermediate-advances HCC: Does Portal Vein Thrombosis Affect Survival ?

**Francesco Fiore** MD (Presenter) ; **Francesco Somma** MD ; **Roberto D'Angelo** MD ; **Rosa Ambrosio** MD ; **Sergio Setola** ; **Francesco Izzo** MD

#### PURPOSE

Our purpose is to assess and compare the survival of patients with portal vein thrombosis (PVT) and patients without PVT after a TARE using Y-90 microspheres of unresectable HCC, not responsive to other loco-regional treatments.

#### METHOD AND MATERIALS

Between November 2005 and February 2013, 81 TARE were performed in 74 patients (43% male; 57% female; range of age 28-84years) with unresectable HCC (size of lesions 1.1 to 5.5cm) and bilirubine values up to 2.6 mg/dl, 21 with PVT. Every patient was studied with Multislice Computed Tomography (MSCT) scans and angiography while just 12 of them underwent the embolization of the Gastro-duodenal artery, using micro-coils. In these cases, a previous study was performed with the injection of TC-99MAA through a 3F microcatheter. Proton-Pump Inhibitors (PPI) were administered to prevent gastritis and ulcers.

#### RESULTS

The average dose administered was 1.7GBq. After the treatment, fever and abdominal pain were found in 29 and 19 patients, respectively. No other side-effect was observed. According to the mRECIST criteria at least a partial response was found in 70% of patient three months after the procedure and in 90.5% at nine months. The mean survival of patients with PVT was similar to those



without thrombosis. Moreover, a regression of PVT was registered in more than 50% of patients.

#### CONCLUSION

TARE using Y-90 microspheres showed to be a safe and effective technique even in patients with PVT. Among the loco-regional treatments of intermediate-advanced HCC, TARE is extremely useful in case of relapse after trans-arterial embolization (TAE) or chemoembolization (TACE) in improving the survival of these patients.

#### CLINICAL RELEVANCE/APPLICATION

Portal vein thrombosis does not affect survival of patients who undergo the Y-90 TARE of intermediate-advanced HCC not responsive to other loco-regional

### VSIR61-07 • Debate: HCC With Portal Vein Thrombosis

**Charles E Ray** MD, PhD (Presenter) \* ; **Robert J Lewandowski** MD (Presenter) \*

#### LEARNING OBJECTIVES

1) Discern the impact of transcatheter intra-arterial embolotherapy in patients with hepatocellular carcinoma and portal vein thrombosis. 2) Understand the microembolic effects of radioembolization, and the potential advantages of this treatment over other intra-arterial embolotherapies. 3) Become familiar with the current literature regarding radioembolization of patients with unresectable hepatocellular carcinoma with portal vein thrombosis.

### VSIR61-08 • Thermal Ablation Cxs

**Daniel B Brown** MD (Presenter) \*

#### LEARNING OBJECTIVES

1) Techniques to avoid complications with thermal ablation. 2) How to manage complications of thermal ablation.

#### ABSTRACT

Complications are unusual with thermal ablation but can be severe. This presentation is designed to avoid complications as well as identify untoward events early after therapy to optimize management.

### VSIR61-09 • Evaluation of Thrombotic Risk in Hepatic Vessels during Microwave Tumor Ablations: Does Size Really Matter?

**Jason Chiang** BS (Presenter) ; **Bridgett J Willey** \* ; **Alejandro Munoz Del Rio** PhD ; **Christopher L Brace** PhD \*

#### PURPOSE

Microwave tumor ablation is a powerful tool that can more effectively overcome the "heat-sink" effect of nearby vasculatures. Such power may also increase the risk of thrombosing larger vessels, which can have devastating consequences for a patient whose liver is already compromised. The goal of this study is to correlate the risk of vascular thrombosis with vessel size, blood velocity and proximity to heating zone during microwave ablations.

#### METHOD AND MATERIALS

Microwave antennas were placed in-vivo, 5-20 mm away from a portal vein, hepatic vein and hepatic artery in a porcine liver (n=6). Vessel sizes, flow velocities and distance from antenna were measured under Doppler and ultrasound imaging. Microwave ablations were then created at 100 W for 5 minutes. Post-ablation ultrasound was used to determine presence of thrombus in each vessel. Uni- and multivariable logistic regressions were fitted to model the relationship predictors to thrombotic events in each kind of vessel. Fitted models were compared to each other using the area under the receiver operator characteristic curves (AUC); 95% confidence intervals for AUC were also obtained.

#### RESULTS

Thrombus formation was detected in 53.3% of portal veins (8/15), 13.3% of hepatic veins (2/15) and 0.0% in hepatic arteries (0/15). The hepatic vein AUC of velocity, spacing and diameter were 0.885 [95% CI: 0.617-0.989], 0.923 [0.667-0.997] and 0.904 [0.641-0.994], respectively. Portal vein AUC of velocity, spacing and diameter were 0.509 [0.163-0.853], 0.643 [0.340-0.946] and 0.536 [0.168-0.814], respectively. Multivariate prediction models of both hepatic and portal veins did not show significant increase in AUC over their respective individual univariate models.

#### CONCLUSION

The risk of thrombosis decreased with increasing vessel velocity, size and spacing in hepatic veins. Portal veins thrombosed at a rate four times higher than hepatic veins, but our analysis was not able to discriminate which factors were most relevant. Further study is required to elucidate the physical and biochemical mechanisms behind this discrepancy in thrombotic rates.

#### CLINICAL RELEVANCE/APPLICATION

Portal veins have greater, but less predictable risk for thrombosis compared to hepatic veins in microwave tumor ablation procedures.

### VSIR61-10 • The Effect on Renal Function Following Image Guided Radiofrequency Ablation (RFA) of Renal Tumors

**Tze M Wah** MBChB, FRCR (Presenter) ; **Walter Gregory** PhD ; **Henry C Irving** MBBS ; **Jon Cartledge** MD ; **Adrian D Joyce** MD ; **Peter J Selby** MD, DSc

#### PURPOSE

To analyse changes in GFR in patients who had image-guided RFA of their renal tumors and to correlate the percentage GFR change (% GFR change) with tumor size, polar position, tumor treatment location, the total size of the tumor treated per ablation session, number of tumors treated, and solitary kidney status.

#### METHOD AND MATERIALS

From June 2004-2012, a total of 165 patients (109 men, 56 women; mean age 67.7 years) had image-guided RFA of 200 renal tumors with size ranging from 1-5.6cm (mean= 2.9cm). The position of the renal tumors was: upper (n=63), middle (n=86) and lower (n=51). The tumor location was: exophytic (n=43), mixed (n=100), parenchymal (n=41) and central (n=16). All patients had renal function measured immediately before and at 24 hours post-RFA. Multivariate logistic regression analysis was performed to determine any association between % GFR change with the tumor size, polar position (upper, middle and lower pole of the kidney), tumor treatment location (exophytic, mixed, parenchymal and central), the total size of the tumor treated per ablation session, number of tumors treated and solitary kidney status.

#### RESULTS

The mean GFR pre- and post-renal RFA were: 54.7 ml/min/1.73m<sup>2</sup> (+/- SD 18.2 ml/min/1.73m<sup>2</sup>) vs. 52.7 ml/min/1.73m<sup>2</sup> (+/- SD 18.5 ml/min/1.73m<sup>2</sup>). There is a significant difference between the pre- and post-RFA GFR measurements (p 25% decrease in GFR) whilst in the majority (98%) of the patients renal function was preserved. The mean % change of GFR pre- and post-RFA was - 3.1% (+/- SD 15.2%). However, using multivariate logistic regression analysis there is no association between the % of GFR change with tumor size, polar position, tumor treatment location, the total size of the tumor treated per ablation session, number of tumors treated and solitary kidney status.

#### CONCLUSION

Preservation of the renal function can be achieved following image-guided RFA of renal tumors and the percentage of GFR change was not influenced by tumor factors or solitary kidney status.

#### CLINICAL RELEVANCE/APPLICATION

Any change in renal function following image-guided renal RFA is not influenced by tumors factors (size, polar position, treatment location, number of tumors treated) or solitary kidney status.

### **VSIR61-11 • Combination Therapy Cxs**

**Thuong G Van Ha** MD (Presenter) \*

#### LEARNING OBJECTIVES

View learning objective under main course title.

#### ABSTRACT

Combination therapy utilizing both transarterial chemoembolization and thermal ablation will be discussed with an emphasis on complications. Different techniques of TACE will be shown, in combination with either radiofrequency ablation or microwave ablation. Management of complications will also be discussed.

### **VSIR61-12 • Debate: Interventional Oncology - A Distinct Specialty/Interventional Oncology - We Are Radiologists, Not Oncologists**

**Daniel B Brown** MD (Presenter) \* ; **Charles E Ray** MD, PhD (Presenter) \*

#### LEARNING OBJECTIVES

View learning objectives under main course title.

### **VSIR61-13 • Literature Review: The Most Important IO Papers from 2012-13**

**Charles E Ray** MD, PhD (Presenter) \*

#### LEARNING OBJECTIVES

View learning objectives under main course title.

### **VSIR61-14 • Panel Discussion: Unknown Case Presentation**

#### LEARNING OBJECTIVES

View learning objectives under main course title.

### **VSIR61-15 • Wrap Up and Discussion**

#### LEARNING OBJECTIVES

View learning objectives under main course title.

---

## **Musculoskeletal Radiology Series: Elbow, Hand and Wrist Imaging**

**Friday, 08:30 AM - 12:00 PM • N228**



[Back to Top](#)

**VSMK61 • AMA PRA Category 1 Credit™:3.25 • ARRT Category A+ Credit:3.5**

#### **Moderator**

**Bruce B Forster**, MD \*

#### **Moderator**

**Mark D Murphey**, MD

### **VSMK61-01 • Sports Related Injuries of the Elbow**

**Bruce B Forster** MD (Presenter) \*

#### LEARNING OBJECTIVES

1) Demonstrate an understanding of the technical and procedure-related considerations in MR imaging of the elbow. 2) Identify the normal anatomic structures and variants within the four compartments of the elbow. 3) Diagnose common sports injuries of the elbow, using this compartmental approach.

#### ABSTRACT

### **VSMK61-02 • Accuracy of 3 Tesla MR Arthrography versus Conventional 3 Tesla MR Imaging of the Elbow as Compared with Arthroscopy**

**Thomas H Magee** MD (Presenter)

#### PURPOSE

MR arthrography of the elbow has been found to be useful in the diagnosis of full versus partial thickness tears of the collateral ligaments. MR arthrography is also useful for characterization of chondral defects. We assess the accuracy of 3 Tesla MR arthrography of the elbow versus conventional 3 Tesla MR imaging of the elbow as compared with arthroscopy.

#### METHOD AND MATERIALS

43 consecutive conventional elbow MR and MR arthrography exams performed on the same patients who went on to arthroscopy were reviewed retrospectively by consensus reading of two musculoskeletal radiologists. Full or partial thickness tears of the collateral ligaments, full or partial thickness tears of the extensor and flexor tendons, chondral defects and loose bodies in the joint space were assessed.

#### RESULTS

In thirty one patients, the diagnoses made on MR and MR arthrogram exams were the same. In seven patients MR arthrogram exams demonstrated additional findings that were not clearly demonstrated on conventional MR exams. There were three full thickness extensor tendon tears, three radial collateral ligament tears and one ulnar collateral ligament tear seen on MR arthrography exam that were not well seen on conventional MR exam. In five patients MR arthrogram demonstrated ligaments and tendons to be intact that appeared torn on conventional MR exam. There were three ulnar collateral ligaments and two common flexor tendons demonstrated to be intact on MR arthrography exam that appeared torn on conventional MR exam. All MR arthrography findings were confirmed at arthroscopy.

#### CONCLUSION

MR arthrography of the elbow is more accurate than conventional MR imaging of the elbow at three tesla. In seven cases MR arthrography demonstrated tendons and ligaments to be torn that appeared intact on conventional MR exam. In five cases MR arthrography demonstrated intact tendons and ligaments that appeared torn on conventional MR exam. These five cases are most likely due to the tears healing with fibrous tissue allowing the tendon and ligament tissues to coapt.

CLINICAL RELEVANCE/APPLICATION  
MR arthrography is more accurate in detection of intact or torn tendons and ligaments than conventional MR imaging of the elbow at three tesla. This is useful in pre surgical planning.

### VSMK61-03 • Entrapment Neuropathies of the Upper Extremity

**Ali M Naraghi** (Presenter)

#### LEARNING OBJECTIVES

1) Identify the common sites of nerve entrapment in the upper extremity. 2) Describe the normal peripheral nerve anatomy and muscle innervation in the upper extremity with an emphasis on sites of compression. 3) Recognize the imaging features peripheral nerve entrapment in the upper extremity.

#### ABSTRACT

### VSMK61-04 • T2 Mapping of the Median Nerve in the Wrist Joints: Preliminary Study in Patients with Carpal Tunnel Syndrome and Healthy Volunteers

**Ji Eun Lee MD** (Presenter) ; **Jang Gyu Cha MD** ; **Jong Kyu Han MD, PhD** ; **Soo Bin Im** ; **Sung Byung Kim**

#### PURPOSE

To perform a prospective quantitative analysis of median nerve T2 values and cross-sectional area (CSA) in patients with carpal tunnel syndrome (CTS) and in asymptomatic volunteers.

#### METHOD AND MATERIALS

Twelve CTS patients with positive nerve conduction results and 12 healthy volunteers (controls) were enrolled and underwent axial T2 mapping of the wrist joints. Median nerve T2 values and CSAs at the distal radioulnar joint, pisiform, and hook of hamate levels were compared between the groups.

#### RESULTS

The T2 values at the proximal and distal carpal tunnel were higher in the CTS patients than in the controls ( $p < 0.05$ ). The T2 values at the distal radioulnar joint did not differ between the groups ( $p = 0.99$ ). The CSAs of the median nerve at all levels of the carpal tunnel were significantly larger in the CTS patients than in the controls ( $p < 0.05$ ).

#### CONCLUSION

It is feasible to use T2 mapping to measure an increase of the median nerve T2 value in CTS patients. Quantitative measurements of T2 values can complement measurements of the median nerve CSA in the evaluation of CTS.

#### CLINICAL RELEVANCE/APPLICATION

T2 mapping can be useful for measuring an increase in the median nerve T2 values. Quantitative measurements of T2 values can complement measurements of the median nerve CSA in the evaluation of CTS.

### VSMK61-05 • Comparison of Various 3D and 2D MR Imaging Sequences of the Wrist at 3 Tesla

**Christoph Rehnitz MD** (Presenter) ; **Bastian Klaan** ; **Falko Stillfried** ; **Erick Amarteifio MD** ; **Hans-Ulrich Kauczor MD \*** ; **Marc-Andre Weber MD \***

#### PURPOSE

To quantitatively and qualitatively compare both image quality and diagnostic performance of 2D and 3D sequences for dedicated wrist imaging.

#### METHOD AND MATERIALS

16 healthy volunteers (mean age, 26.4 years) and 18 patients (mean age, 36.2 years) with wrist pain were examined using an 8-channel wrist-coil at 3 Tesla MRI. The imaging protocol consisted of 2D-proton-density fat-saturated (PDFs), isotropic 3D MEDIC, 3D-TrueFISP and 3D-PDFs-SPACE sequences. Signal-to-noise-ratios (SNR) and contrast-to-noise-ratios (CNR) of cartilage/bone/muscle/fluid and mean overall SNR/CNR were calculated using region-of-interest analysis. Qualitative analysis included overall image quality (OIQ), visibility of important structures and degree of artifacts rated on a five-point scale (0-4). ANOVA and adjusted Wilcoxon-signed-rank tests were applied. The study was approved by the institutional review board and all patients gave informed consent prior to inclusion.

#### RESULTS

Mean overall SNR/CNR for 2dPDFs; 3D-PDFs-SPACE; 3D-TrueFISP; 3D-MEDIC was 96/73; 43/28; 61/53; 77/45. SNR and CNR were higher (p

#### CONCLUSION

Standard 2D-PDFs sequence provides high SNR/CNR, image quality and robustness when compared to 3D sequences. Isotropic 3D-TrueFISP (cartilage) and 3D-MEDIC (ligaments/TFCC) exhibit additional advantages, while 3D-PDFs-SPACE is currently not advantageous.

#### CLINICAL RELEVANCE/APPLICATION

When imaging the wrist at 3 Tesla, the sequence protocol should include 2D-PDFs. An additional 3D-TrueFISP sequence can be recommended for assessing cartilage and a 3D-MEDIC for ligaments and TFCC.

### VSMK61-06 • Magnetic Resonance Microscopy of the Triangular Fibrocartilage Complex at 11.7T

**Paul A DiCamillo MD, PhD** (Presenter) ; **Sheronda Statum** ; **Christine B Chung MD** ; **Graeme M Bydder MBChB \***

#### PURPOSE

Anatomic studies of the Triangular Fibrocartilage Complex (TFCC) have been performed on clinical systems at field strengths up to 7T. In our study, we assessed the use of an 11.7T small bore system with high performance gradients and micro-array coils for detailed imaging of the TFCC.

#### METHOD AND MATERIALS

Human wrist samples were collected per institutional policy, and imaged on an 11.7T Bruker BioSpec 117/16USR system (Bruker BioSpin, Billerica, MA) fitted with a 750 mT/m gradient system, using solenoidal and four element semi-circular array coils. Both gradient and spin echo sequences were used (FLASH: 90-120um<sup>2</sup> isotropic resolution, TE 6ms, TR 25ms, fat sat, NEX 9-25, 4-6 hour scans; Multislice Spin Echo: 80x80x400um resolution , TE 7-14ms, TR 5000ms, 2 echoes, fat sat, NEX 5-15, 4-6 hour scans).

#### RESULTS

Detailed visualization of the TFCC was achieved at a spatial resolution well over 10 times greater than previously reported. Instead of the low signal, low contrast appearance seen in the TFCC with clinical T2 weighted images, with our acquisitions parameters and high performance system, the TFCC tissues displayed relatively high signal. Fiber structure in the upper and lower laminae, magic angle effects, entheses and the lamella layer of the disc were observed.

#### CONCLUSION

Unprecedented spatial resolution and contrast were achieved, with clear demonstration of detail in structures not previously not well visualized or seen at all. These results are likely to help in the recognition of injury and disease of the TFCC as stronger field strength systems become clinically available.

#### CLINICAL RELEVANCE/APPLICATION

High resolution 11.7T MR images of the TFCC were generated. These results may indicate what will be achievable on higher field clinical systems.

### VSMK61-07 • Sports Related Injuries of the Wrist

**Catherine N Petchprapa MD** (Presenter)

#### LEARNING OBJECTIVES

1) Review multiple common injuries of the wrist, as demonstrated on multiple imaging modalities.

### VSMK61-08 • Common Tumors in the Hand and Wrist

**Mark D Murphey MD** (Presenter)

#### LEARNING OBJECTIVES

1) Identify common tumors that affect the hand/wrist including giant cell tumor of tendon sheath, ganglion, enchondroma and synovial sarcoma. 2) Recognize the imaging appearance and spectrum of these common tumors of the hand/wrist. 3) Understand the pathologic basis of the imaging appearances that may allow differentiation of these lesions.

### VSMK61-09 • 11.7T Magnetic Resonance Microscopy of the Pulleys and Plates of the Fingers and Thumb

**Paul A DiCamillo MD, PhD** (Presenter) ; **Sheronda Statum** ; **Christine B Chung MD** ; **Graeme M Bydder MBChB \***

#### PURPOSE

Excellent anatomical studies on clinical systems have been done to demonstrate the detail of the digital pulleys and plates at fields up to 7T. In our study, using an 11.7T system with high-performance gradients and micro-array coils, we attempted to visualize details of these structures which have previously been refractory to MR imaging.

#### METHOD AND MATERIALS

Human fingers and thumbs were collected per institutional policy, firmly immobilized, and placed into the bore of an 11.7T Bruker BioSpec 117/16USR system (Bruker BioSpin, Billerica, MA) fitted with a 750 mT/m gradient system. Ten fields of view (**finger**: proximal, middle, distal phalanx, PIP, DIP and MCP; **thumb**: proximal, distal phalanx, IP and MCP) were independently imaged with both gradient and spin echo sequences (FLASH: 90-120um<sup>3</sup> isotropic resolution, TE 6ms, TR 25ms, fat sat, NEX 9-25, 4-6 hour scans; Multislice Spin Echo: 35x35x250um to 60x60x500um resolution, TE 7-14ms, TR 5000ms, 2 echoes, fat sat, NEX 5-15, 4-6 hour scans).

#### RESULTS

Detailed visualization of fibers in tendons, ligaments, pulleys, plates, and entheses of the fingers and thumb was achieved. A series of structures that correlate with anatomic descriptions of entities which have not previously been captured in detail in imaging studies was visualized. A partial list includes the cruciate pulleys of the finger; finger pulleys A<sub>1</sub> and A<sub>5</sub>; thumb pulleys A<sub>1</sub>, A<sub>V</sub>, A<sub>2</sub>; the oblique thumb pulley; and the fibrous structure of the palmar plates.

#### CONCLUSION

Unprecedented spatial resolution and contrast was achieved, with well over 10 times greater spatial resolution than previously reported. This allowed clear demonstration of the fiber direction in structures, as well as production of the first MR images of structures such as the cruciate pulleys of the finger. A high performance MR system together with coil repositioning for each of the 10 target locations was instrumental in meeting our resolution and contrast goals. These results are likely to help in the recognition of injury and disease of the pulleys and plates as stronger field strengths become clinically available.

#### CLINICAL RELEVANCE/APPLICATION

High resolution 11.7T MR images of the pulleys and plates of the finger were generated. These may facilitate the interpretation of normal anatomy as higher field clinical systems become available.

### VSMK61-10 • MR Findings in Avulsion Injuries at the Extensor Carpi Radialis Brevis Insertion and the Os Styloideum: A Case Series of Lesions in Hockey Players and Other 'Stick Swinging' Athletes

**Pranshu Sharma MD** (Presenter) ; **Adam C Zoga MD** ; **William B Morrison MD \*** ; **Diane M Deely MD** ; **Randall W Culp MD**

#### PURPOSE

To detail initial and follow-up imaging findings in athletes with avulsion injuries at the insertion of the Extensor Carpi Radialis Brevis (ECRB) tendon, and its relation to the os styloideum and carpal boss, with operative and 'return-to-play' correlation.

#### METHOD AND MATERIALS

A database of wrist MR exams over 18 months was searched for athletes with avulsion injuries at the dorsal wrist in the region of the extensor carpi radialis brevis (ECRB) insertion. 6 subjects were identified and demographics, athletic activity, and trauma vs. overuse were documented. The initial MR was reviewed by two MSK radiologists in consensus and the presence of an os styloideum or carpal boss, any synchondrosis or synostosis between the os and the base of third metacarpal were recorded. Bone marrow edema and displaced or nondisplaced fractures as well as fracture extension proximal or distal were noted. The insertion site of the ECRB was observed as directly on the os, directly on the base of third metacarpal, or both. MR findings and surgical findings when applicable were reviewed with a single hand surgeon. Any follow-up imaging to monitor healing was reviewed, and the interval to 'return-to-play' was documented.

#### RESULTS

3 were pro hockey players with forceful extension injuries. 1 was a collegiate golfer and the other 2 sustained falls on flexed wrists. 6 of 6 had os styloidia with bone marrow edema at the os. The ECRB inserted on the metacarpal base in 2, on the os in 2, and on both in 2. 3/6 had displacement of the os with a fracture extending to the metacarpal base at initial MR. No high grade tendon tear was observed. 3 went to surgery for os resection and cast immobilization and 1 for screw/plate fixation of the fracture and the os. The fixation subject was monitored for healing with CT and was able to return to hockey in 4 weeks, while 2 hockey players post os resection missed the remainder of the season but returned the following Spring (9 and 11 weeks).

#### CONCLUSION

There is an anatomical and injury spectrum in athletes with avulsion lesions at the ECRB insertion. The ECRB can insert on the os styloideum, the base of the metacarpal, or both. These injuries can be encountered in athletic activities involving repetitive wrist extension against resistance while holding a stick, such as hockey and golf.

#### CLINICAL RELEVANCE/APPLICATION

Location of the insertion of the ECRB and any fusion of the os to the metacarpal base should be noted to optimize treatment.

### VSMK61-11 • Eponyms to Know in Hand and Wrist Imaging

**Wilfred C. G Peh MD** (Presenter)

#### LEARNING OBJECTIVES

1) Review the imaging appearance of a variety of hand and wrist injuries that are named after physicians.

### VSMK61-12 • Flexor Carpi Radialis Tendinopathy and its Association with Scapho-trapezio-trapezoid and First Carpometacarpal Osteoarthritis

**Waseem K Khan MD (Presenter) ; Andrew R Palisch MD ; Suzanne S Long MD ; Adam C Zoga MD ; William B Morrison MD \***

#### PURPOSE

We sought to establish a potential association between flexor carpi radialis (FCR) tendinosis and/or tears and osteoarthritis of either the scapho-trapezio-trapezoid (STT) or first carpometacarpal (CMC) joints, as identified by magnetic resonance imaging (MRI).

#### METHOD AND MATERIALS

A retrospective analysis was performed by searching a database from a single institution for MRI exams of the wrist performed over a 15 month period with reports including the term "flexor carpi radialis". Exams with reports describing the tendon as 'normal' were excluded. Two MSK radiologists evaluated images and confirmed the presence of FCR tendinosis and/or FCR tears. The STT and first CMC joints were then evaluated for evidence of osteoarthritis at MR including eburnation, subchondral cysts/marrow edema, osteophytes and joint space narrowing. FCR tendinosis/tears were then correlated with findings of STT and 1st CMC osteoarthritis.

#### RESULTS

There were 26 wrists with FCR tendinosis and/or tear. M/F= 10/16, with a mean age of 57.8 years (14 – 80 years). The majority (24/26, 92%) had either STT (20/26, 77%) and/or first CMC (21/26, 81%) osteoarthritis. The two patients with no appreciable STT or first CMC osteoarthritis demonstrated only mild FCR tendinosis at MRI. 14/26 (54%) subjects had either partial (11) or complete (3) FCR tendon tears. 12/14 patients (86%) had tears positioned adjacent to the STT joint, including all three complete tears. The other 2 patients (14%) had tears located adjacent to the first CMC joint. In all FCR tears, volar spurs were noted extending from the affected joint and appeared to impinge upon the FCR.

#### CONCLUSION

This retrospective series suggests that there may be an association between FCR tendinosis or tear and osteoarthritis at the scapho-trapezio-trapezoid and first carpal-metacarpal joints. Further, partial or complete FCR tendon tears appear to be more often positioned near an STT joint with osteoarthritis. Potential etiologies of this association include osseous productive changes at the STT and 1st CMC joints impinging the FCR during dynamic activities.

#### CLINICAL RELEVANCE/APPLICATION

FCR tendinosis and tearing should be suspected and observed at MR if there are findings of osteoarthritis at either the STT or first CMC joints associated with volar/radial sided pain.

### **VSMK61-13 • Arthritides-What's Hot in the Rheumatology Literature**

**Eric Y Chang MD (Presenter)**

#### LEARNING OBJECTIVES

1) Discuss the roles of the radiologist in diagnosis and management of arthropathies. 2) Identify the various categories of disease modifying therapies (DMOADs and DMARDs). 3) Describe the imaging findings of rheumatoid arthritis and spondyloarthritis based on current literature.

### **Vascular Imaging Series: MR Angiography-Principles and Technique Optimization**

**Friday, 08:30 AM - 12:00 PM • E352**

**MR IR VA**

[Back to Top](#)

**VSVA61 • AMA PRA Category 1 Credit™:3.25 • ARRT Category A+ Credit:4**

### **VSVA61-01 • Contrast-enhanced and Time-resolved MRA**

**Stefan G Ruehm MD (Presenter) \***

#### LEARNING OBJECTIVES

1) Understand the general principles of contrast-enhanced and time-resolved MR Angiography. 2) Be familiar with sample clinical applications for time-resolved MR Angiography in several vascular beds. 3) Be aware of the major caveats in contrast enhanced MR Angiography at 1.5T and 3.0T and how to avoid them.

### **VSVA61-02 • Whole Body Cardiovascular Magnetic Resonance Imaging in the Detection of Occult Disease in Diabetes Mellitus**

**Graeme Houston MD, FRCR \* ; Jonathan Weir-McCall MBCh, FRCR (Presenter) ; Suzanne L Duce PhD ; Shona Matthew BSc, PhD \* ; Stephen Gandy ; Helen Colhoun ; Deirdre Cassidy ; Gill Reekie ; Jil J Belch ; Patricia Martin**

#### PURPOSE

The IMI-SUMMIT MRI study assessed whole body cardiovascular MR (WBCVMR) to provide surrogate markers of macrovascular disease in patients with diabetes mellitus. WBCVMR combines whole body contrast enhanced magnetic resonance angiography (WBCE-MRA) and cardiac MR(CMR) in a single examination. We compared WBCVMR in type 2 diabetic and non-diabetic patients, with and without symptomatic cardiovascular disease(CVD).

#### METHOD AND MATERIALS

156 subjects were divided into 4 groups: diabetics with (group 1, n=31) or without (group 2, n=55) CVD, and non-diabetics with (group 3, n=28) or without (group 4, n=29) CVD. WBCVMR was performed on 3T MRI (Siemens Trio, Erlangen, DE). WBCE-MRA was performed from skull vertex to feet following intravenous gadoterate meglumine (Dotarem, Guerbet, FR). The subtracted data were divided into 31 anatomical arterial segments. Each segment was scored according to degree of luminal narrowing: 0=normal, 1=

#### RESULTS

143 datasets were included, of which 87(60%) were male (13 excluded due to incomplete scan/inadequate image quality),. The mean age was 63.9±8.1 years. Mean WBAS were 0.41+/-0.45 (group 1), 0.17+/-0.17 (group 2), 0.49+/-0.4 (group 3), and 0.15+/-0.18 (group 4). Mean LVM(g) were: 61.6 +/-9.7 (group 1), 55.6+/-10.5 (group 2), 60.4+/-10.6 (group 3), and 52.6+/-8.7 (group 4). WBAS correlated with LVM (r=0.41; p

#### CONCLUSION

WBCVMR offers a robust investigation for detecting and quantitating whole body atheroma burden. Extensive arterial disease and silent myocardial scarring can be visualised in asymptomatic diabetic patients.

#### CLINICAL RELEVANCE/APPLICATION

Type 2 diabetics have an elevated risk of cardiovascular events which can occur in apparently healthy patients. Screening with WBCVMR may identify those at increased risk of future events.

### **VSVA61-03 • Feasibility Study of MR-tricks Sequence in Evaluation of the Dorsalis Pedis Artery and the First Dorsal Metatarsal Artery**

**Bo Sun (Presenter) ; Yue Dong ; Dianxiu Ning ; Qingwei Song BS, BEng ; Meiyu Sun**

#### PURPOSE

To study the feasibility of MR angiography of the dorsalis pedis artery and the first dorsal metatarsal artery (FDMA) by three-dimensional time-resolved imaging of contrast kinetics (TRICKS) sequences.

#### METHOD AND MATERIALS

43 cases with suspected or known soft tissue diseases of the ankle and foot were examined retrospectively by conventional MR sequences and TRICKS sequence on GE signa 1.5T HD echospeed MRI . MIP reconstruction was done to evaluate the image quality of arterial branches on ADW4.4 workstation and the evaluated criteria was divided into 4 grades according to the visualization of dorsalis pedis artery( grade 1-2), FDMA and toe web network(grade3-4). FDMA was dissected and categorized according to its location(superficial, intramuscular, absent), diameter[large( > 1.5mm ) , medium( 1.0-1.5mm ) , and small( second toe =Dfirst toe),main trunk type(Dsecond toe>Dfirst toe),fine small branch(Dsecond toefirst toe)]

#### RESULTS

8 cases(18.6%,8/43)in grade 4, 22(51.16%,22/43)in grade 3,8(18.6%,8/43) in grade 2 and 5(11.62%,5/43) in grade 1. In the grade 1 group, the dorsalis pedis arteries of 2 cases were absent and images of the other 3 cases were not clear because of severe venous contamination.

The TRICKS images of 38 cases(arterial scales=2 point) showed location and diameter of FDMA ,and the TRICKS images of 30 cases(arterial scales=3 point) showed branching pattern at the toe web of FDMA:( 1)Location:superficial (8), intramuscular(22 cases), intramuscular (8 cases), absent(0 cases);(2)Diameter: large(2 cases) , medium(25 cases) , and small(11 cases);(3)Branching pattern at the toe web:ramifying type(11 cases),main trunk type(5 cases),fine small branch(14 cases).

#### CONCLUSION

MR angiography of the dorsalis pedis artery and FDMA was achievable with MR TRICKS sequences, and it was useful for clinical evaluation of FDMA.

#### CLINICAL RELEVANCE/APPLICATION

MR angiography of the dorsalis pedis artery and FDMA with MR TRICKS sequences is available in preoperative evaluation for rebuilding thumb and finger by dissociating toe transplant.

### **VSVA61-04 • Renal MRA at 7T: How Much Gadolinium Do We Need?**

**Lale Umutlu MD (Presenter) \* ; Karsten J Beiderwellen MD ; Michael Forsting MD ; Mark E Ladd PhD ; Oliver Kraff MSc ; Thomas C Lauenstein MD**

#### PURPOSE

Renal impairment displays a relative contraindication to the application of Gadolinium- based contrast-agents. Hence, contrast dose reduction has become an important issue in the clinical setting. The aim of this trial was to determine whether contrast agent (CA) dose reduction to one-half and one-quarter of the standardized dosage allows for preserved image quality of renal MR angiography at 7T.

#### METHOD AND MATERIALS

12 healthy subjects underwent renal MR angiographic examinations on a 7T MR system (Magnetom 7T), utilizing a custom-built 8-channel RF body coil. Dynamic 3D FLASH data sets were obtained pre contrast and in arterial phase after the application of contrast agent. Examinations were performed at three different time points for injection of three dosages of CA (Gadobutrol, Bayer Healthcare): (1) 0.1 mmol/kg body weight (BW), (2) 0.05 mmol/kg BW and (3) 0.025 mmol/kg BW. Contrast ratios (CR) were measured pre and post contrast in the aorta and both renal arteries in correlation to adjacent psoas major muscle. Qualitative analysis with regard to delineation of the pre-contrast and post-contrast renal arterial vasculature was performed by two radiologists using a five-point-scale (5=excellent to 1= non diagnostic).

#### RESULTS

Non-enhanced T1w MRI provided an inherently high signal intensity of vasculature, yielding a good overall pre-contrast arterial delineation (mean 3.65). The application of contrast agent showed improved vessel delineation in subjective ratings of qualitative analysis for all three dosages, yielding comparable results with only minor improvement associated to increased dosage (mean aorta: 0.025Gd 4.4; mean0.05Gd 4.6; mean0.1Gd mean 4.80). Accordingly, quantitative analysis of contrast ratios showed minor increase of mean values with increasing Gadolinium dosage (mean right renal artery: 0.025Gd 0.36; mean0.05Gd 0.38; mean0.1Gd mean 0.42).

#### CONCLUSION

Our results demonstrate the successful facilitation of a significant dose reduction to one-quarter of the standardized dosage, while maintaining high image quality.

#### CLINICAL RELEVANCE/APPLICATION

The facilitation of a significant dose reduction to one-quarter while maintaining high image quality, may be of high diagnostic value for MRA examinations in patients with renal impairment.

### **VSVA61-05 • MR Contrast Agents for Vascular Imaging**

**Tim Leiner MD, PhD (Presenter) \***

#### LEARNING OBJECTIVES

1) To understand the different classes of contrast agents available for vascular imaging as well as their strengths and weaknesses. 2) To understand both acute and delayed safety concerns associated with administration of MR contrast agents for vascular imaging. 3) To understand proper contrast agent dosing for vascular MR imaging. 4) To understand basic principles underlying successful contrast injection.

#### ABSTRACT

### **VSVA61-06 • Gadofosveset-enhanced MR Venography of the Lower Extremities for Evaluation of Venous Reflux Disease: Feasibility and Comparison of Perforator Vein Imaging with Duplex Ultrasound**

**Andrew R Lewis MD (Presenter) ; Daniele Marin MD ; Holly L Nichols BS ; Daniel Geersen ; Cynthia K Shortell MD ; Charles Y Kim MD \***

#### PURPOSE

Duplex ultrasound (U/S) is the gold standard for imaging of venous reflux disease. CT and direct MR venography (MRV) have shown promising results, but are limited in the degree and extent of superficial vein opacification. Gadofosveset, a blood-pool agent, is uniquely well suited for venous imaging. The purpose of this study is to assess the feasibility of MRV of the deep and superficial venous system and to determine its accuracy in detection of perforator veins.

#### METHOD AND MATERIALS

Retrospective review of our imaging database from 9/2010 – 9/2012 yielded 58 patients (40 females, mean age 54) who underwent MRV of the abdomen, pelvis, and lower extremities as well as dedicated U/S evaluation of venous reflux disease of one or both legs. Axial MRV images were acquired during the equilibrium phase, approximately 5 minutes after IV gadofosveset injection. The lower extremity deep, superficial, and perforator veins were divided into 11 segments for evaluation. Two radiologists independently rated the visualization score of each venous segment on a scale of 1-4 with 4 being highest. Signal and contrast-to-noise ratios were calculated for the venous segments. The detection of enlarged perforator veins was assessed and compared to sonography.

#### RESULTS

Analysis was performed on 80 legs that underwent both MRV and U/S. The mean visualization scores for all analyzed venous segments were excellent (3.8-3.9 on a scale of 1-4). The SNR/CNR values were 280/165 for the femoral vein, 230/144 for the above-knee GSV, 394/237 for the below-knee GSV, 303/177 for the small saphenous vein, and 385/240 for superficial varices. 100% of pathologic perforator veins identified on dedicated U/S were detected on MRV. Additional occult enlarged perforator veins were identified on MRV

measuring up to 6mm in diameter.

#### CONCLUSION

MRV with gadofosveset allowed excellent visualization of varices, superficial, and perforator veins of the legs with a high SNR and CNR that was not previously possible with other contrast agents. The exceptional sensitivity for detection of perforator veins may enable improved treatment of venous reflux disease. Additional studies are warranted to correlate MRV findings with disease characterization and treatment outcomes.

#### CLINICAL RELEVANCE/APPLICATION

The excellent imaging quality of the entire venous system of the lower extremities with gadofosveset-enhanced MR venography may enable a new system for evaluation of venous reflux disease.

### **VSPA61-07 • MRA at 3T in Peripheral Arterial Occlusive Disease: Comparison of Gadoterate Meglumine - to Gadobutrol-MRA Using DSA as a Standard of Reference: A Randomized European Multicenter Trial**

**Christian Loewe MD (Presenter) \*** ; **Javier Arnaiz Garcia MD** ; **Denis Krause MD** ; **Luis Marti-Bonmati MD, PhD** ; **Manuela Aschauer MD** ; **Armando Tartaro MD** ; **Massimo Lombardi MD \*** ; **Marta Burrel MD, PhD** ; **Reynald Izzillo** ; **Michael M Lell MD \***

#### PURPOSE

To assess the diagnostic value of two contrast agents in CE-MRA at 3T in peripheral arterial occlusive disease (PAOD).

#### METHOD AND MATERIALS

189 patients were included in this double-blind trial. Patients randomly underwent peripheral CE-MRA with 0.1mmol/kg of either gadoterate meglumine (Dotarem®) or gadobutrol (Gadavist®). The primary endpoint was degree of agreement to DSA in stenosis detection and grading of both CE-MRA examinations. A non-inferiority analysis was performed based on two independent centralized readings. Secondary endpoints were specificity, sensitivity, positive/negative predictive values, diagnostic confidence, stenosis length, vessel diameter, signal-to-noise ratio and contrast-to-noise ratio. Safety and treatment recommendation were also recorded.

#### RESULTS

The non-inferiority was demonstrated for the primary endpoint. The sensitivity in the detection of significant stenosis for Reader 1 was 69.9% in gadoterate meglumine group compared to 71.0% in gadobutrol group ( $p=0.72$ ), whereas the specificities were 85.0% and 85.2% ( $p=0.84$ ), respectively. For Reader 2, sensitivities were 61.5% and 62.0% ( $p=0.77$ ) and specificities were 91.4% and 91.2% ( $p=0.51$ ). No difference in SNR and CNR was found between both groups ( $p = 0.72$  and  $p=0.73$ ), respectively as well as regarding the other secondary endpoints. There were no serious adverse events.

#### CONCLUSION

Contrast media with higher T1 relaxivity have been proposed to be advantageous as far as efficacy is concerned. However, the present study demonstrated the feasibility of PAOD evaluation at 3T and the lack of superiority of gadobutrol over gadoterate meglumine in terms of diagnostic accuracy despite the different Gd-concentrations and T1 relaxivities exhibited by the two contrast agents.

#### CLINICAL RELEVANCE/APPLICATION

Our study has demonstrated that there is no significant difference in terms of diagnostic accuracy when comparing Gd-DOTA-enhanced MRA and gadobutrol-enhanced MRA in an equimolar manner..

### **VSPA61-08 • Non-contrast MRA: TOF and SSFP Based Techniques**

**James C Carr MD (Presenter) \***

#### LEARNING OBJECTIVES

1) Understand the technical issues underlying non contrast MRA based on TOF and SSFP. 2) Become familiar indications and guidelines for using non contrast MRA. 3) Illustrate applicability of non contrast MRA in a variety of relevant clinical scenarios.

### **VSPA61-09 • Comparison of Non-contrast Enhanced SSFP MRA with Gadolinium Enhanced MRA in the Evaluation of the Post-operative Ascending Aorta**

**Emily Pang MD (Presenter)** ; **Gregory P King MD** ; **Simin Jeddiyan MD** ; **Anna E Zavodni MD, MPH**

#### PURPOSE

The objective of this study was to evaluate the comparability of non-contrast SSFP and gadolinium enhanced MRA sequences in the quantitative and qualitative assessment of the post-operative ascending aorta.

#### METHOD AND MATERIALS

After obtaining Research Ethics Board approval, we conducted a single center retrospective review of the 59 consecutive patients sent for MRI follow-up post ascending aortic replacement surgery between 2007 and 2012. Our analysis included 51 patients (mean age 67 +/- 3 years) with both non-contrast SSFP and gadolinium enhanced MRA sequences (8 patients were excluded due to not having one or both sequences performed). The images were independently evaluated by two cardiovascular fellowship trained radiologists with at least 2 years of experience, who measured the diameter of the thoracic aorta at several points including the root, ascending aorta, arch and descending aorta, as well as assessed for qualitative abnormalities. The datasets were compared using paired T-test, Bland-Altman, and kappa coefficient analysis (statistical significance was determined using a Bonferroni correction for multiple comparisons). Intra and inter-observer variability was also determined.

#### RESULTS

There was no statistically significant difference in measurements between non-contrast SSFP and gadolinium sequences, with the exception of the aortic annulus in patients who did not have valve replacement ( $p < 0.001$ ). We postulate that this finding was because the 3D gadolinium sequences allowed for measurements of the normally ovoid annulus in more than one dimension. Kappa analysis also demonstrated good agreement with regards to the quantitative observations. Inter and intra-observer variability was excellent (ICC >0.8).

#### CONCLUSION

Our results suggest that using an unenhanced SSFP MRA sequence is comparable to gadolinium enhanced MRA in the quantitative and qualitative evaluation of the post-operative ascending aorta. Adequate and accurate information is obtained from the non-contrast SSFP sequence such that intravenous gadolinium may be rendered unnecessary for surgical follow-up imaging, reducing the risk and inconvenience to the patient, as well as health care costs.

#### CLINICAL RELEVANCE/APPLICATION

Using unenhanced SSFP MRA may be sufficient in the post-operative MR imaging follow up of ascending aorta replacements, omitting the risks and costs associated with IV gadolinium administration.

### **VSPA61-10 • Performance of Non-enhanced ECG-gated Quiescent-interval Single Shot MRA (QISS-MRA) at 3 Tesla. A Comparison with Contrast-enhanced MRA and DSA**

**Jan Hansmann MD (Presenter)** ; **John N Morelli MD** ; **Henrik J Michaely MD \*** ; **Thomas Riestler MD** ; **Johannes Budjan MD** ; **Stefan O Schoenberg MD, PhD \*** ; **Ulrike I Attenberger MD \***

#### PURPOSE

To evaluate the diagnostic accuracy of a non-enhanced ECG-gated quiescent-interval single shot MR-Angiography (QISS-MRA) at 3T with

contrast-enhanced MRA (CE-MRA) and digital subtraction angiography (DSA) serving as the standard of reference.

#### METHOD AND MATERIALS

16 consecutive patients (9 male, 7 female, mean age 70±12 years) with peripheral arterial disease stages II-IV underwent a combined peripheral MRA protocol consisting of a large field-of-view QISS-MRA (acquisition time 18 min), continuous-table-movement MRA (acquisition time 62 sec), and an additional time-resolved MRA (acquisition time 96 sec) of the calves. DSA correlation was available in 8 patients. Image quality and degree of stenosis was assessed. Sensitivity and specificity of QISS-MRA was evaluated with CE-MRA and DSA serving as the standards of reference by two readers.

#### RESULTS

328 total segments were assessed. Overall sensitivity and specificity were, respectively, 81.1% and 83.5% for QISS-MRA vs CE-MRA. Relative to DSA, sensitivity for QISS-MRA was high (100% versus 91.2% for CE-MRA) in the evaluated segments; however, specificity was substantially less than that of CE-MRA (76.5% vs 94.6%, p). There was no significant difference in image quality between QISS-MRA and CE-MRA at the calf station (p=0.17). For the vasculature of the pelvis and thigh QISS-MRA was rated significantly lower compared to CE-MRA (p). Interreader agreement was very good for both QISS-MRA and CE-MRA (kappa=0.83 and 0.96 respectively).

#### CONCLUSION

Overall image quality and specificity of QISS-MRA at 3T are diminished relative to CE-MRA, potentially due to long acquisition times. However, when image quality is adequate, the high sensitivity of QISS-MRA may render it useful as a screening examination in patients with contraindications to gadolinium chelate administration.

#### CLINICAL RELEVANCE/APPLICATION

Due to its high sensitivity at 3 Tesla, QISS might serve as screening tool to rule out significant stenoses in patients with impaired renal function.

### **VSVA61-11 • Performance of Unenhanced MRA Using Spatial Labeling with Multiple Inversion Pulses Sequence to Depict Transplant Renal Vascular Anatomy and Complications**

**Hao Tang** (Presenter) ; **Daoyu Hu** MD, PhD ; **Zi Wang**

#### PURPOSE

To prospectively evaluate the performance of a new unenhanced magnetic resonance angiography (Unenhanced MRA) sequence, spatial labeling with multiple inversion pulses (SLEEK), to depict transplant renal vascular anatomy and complications in comparison to color doppler ultrasonography (CDUS) , digital subtraction angiography (DSA) and intraoperative findings.

#### METHOD AND MATERIALS

75 patients with renal transplant were examined with Unenhanced MRA using SLEEK and CDUS. DSA was performed in 14 patients. Surgery was performed for 7 patients. The ability to present transplant renal vascular anatomy and complications with SLEEK were evaluated by two experienced radiologists, and to correlate the results with CDUS, DSA and intraoperative findings.

#### RESULTS

#### CONCLUSION

Unenhanced MRA using SLEEK is a reliable diagnostic method for depicting transplant renal vascular anatomy and complications. It is relatively inexpensive and is not associated with renal complications. It can be as a good choice for screening renal vascular anatomy and complications, especially in patients with renal insufficiency.

#### CLINICAL RELEVANCE/APPLICATION

Unenhanced MRA using SLEEK is a reliable diagnostic method for depicting transplant renal vascular anatomy and complications, especially in patients with renal insufficiency.

### **VSVA61-12 • Hemodynamic Outcome Following Aortic Root Replacement with or without Hemiarch Replacement Assessed by 4D Flow MRI**

**Edouard Semaan** (Presenter) ; **Michael Markl** PhD ; **Chris Malaisrie** \* ; **Alex Barker** ; **Bradley D Allen** MD ; **Zoran Stankovic** MD ; **Patrick McCarthy** ; **James C Carr** MD \* ; **Jeremy D Collins** MD \*

#### PURPOSE

To evaluate aortic hemodynamics using 4D flow MRI following aortic root replacement (AR) or aortic root and hemiarch replacement (AR+HA), comparing to patients following non-mechanical aortic valve replacement (AVR) alone.

#### METHOD AND MATERIALS

IRB approval was obtained. 31 patients were recruited following open AVR (group 1: AR, n=16, 51±13 yrs; group 2: AR+HA, n=4, 60±10 yrs; group 3: AVR alone, n=11, 69±11 yrs). Aortic blood flow was measured using ECG and respiration synchronized 4D flow MRI (3-directional venc = 150cm/s, 2.0-2.8mm<sup>3</sup>, temp res 40-44msec) at 1.5 or 3T (Aera, Avanto, or Skyra, Siemens, Erlangen, GE) post-contrast administration. Data analysis included 3D blood flow visualization (EnSight, CEI, USA) based on time-resolved 3D pathlines and systolic 3D streamlines. Helical flow was assessed in the Ascending aorta (AAo), arch, and descending aorta on a 3-point Likert scale (360°). 3D pathlines qualitatively identified the existence of flow jets and the quadrant of flow impingement in the proximal, mid, and distal AAo. Flow uniformity was analyzed by quadrant dichotomizing systolic peak velocities at 1m/s. Peak systolic velocities and acceleration were quantified in 9 planes distributed throughout the thoracic aorta. Groups were compared using the student's t-test.

#### RESULTS

4D flow MRI revealed similar helical flow across groups (p>0.05). 72 % (8 of 11) of patients in group 3 demonstrated outflow jets impinging on the right anterior proximal aortic wall. Jet flow was seen in 52% (10 of 20) of patients in groups 1 and 2 and was preferentially directed towards the anterior wall. Flow profiles were asymmetric in 62%, 100%, and 72% of groups 1-3, respectively. There were significant differences between groups 1 and 2 compared to group 3 for peak acceleration and significant differences between groups 1 and 3 for peak velocities (p)

#### CONCLUSION

4D flow MRI characterized flow in AVR patients. Our preliminary findings demonstrate elevated peak systolic velocities and acceleration in patients with aortic grafts compared to patients with AVR alone. Follow-up studies are warranted to investigate the influence of these findings on ventricular loading and patient outcome.

#### CLINICAL RELEVANCE/APPLICATION

4D flow MRI demonstrates increased aortic peak velocities and acceleration status-post aortic replacement with graft material, suggesting increased ventricular loading with altered aortic compliance.

### **VSVA61-13 • 3D Cine PC VIPR as a Sensitive Indicator of Post-prandial Hyperemia with an Added Value of Avoiding Vortex and Helical Flow Portions**

**Masataka Sugiyama** (Presenter) ; **Yasuo Takehara** MD ; **Kevin M Johnson** \* ; **Oliver Wieben** PhD ; **Tetsuya Wakayama** PhD \* ; **Hiroyuki Kabasawa** ; **Shuhei Yamashita** MD ; **Harumi Sakahara** MD ; **Atsushi Nozaki** ; **Naoki Oishi**

#### PURPOSE

3D cine PC with vastly undersampled isotropic projection steady-state free precession imaging (VIPR) is a recently developed MR method that can cover full spatial and temporal data of the blood flow velocity. The purpose of our study is two folds i.e., 1) to test if 3D PC VIPR can be used for dietary stress test in detecting the post-prandial hyperemia of the SMA, and 2) to assess the flow patterns within SMA with streamline analysis for finding out the optimum plane to measure correct blood flow.



#### METHOD AND MATERIALS

All studies were conducted on a 3.0T MR imager with phased array coil. Five healthy volunteers (23 to 53 y.o.) were enrolled. Under 8 hr fasting, 2D cine PC and 3D cine PC VIPR were repeated before and after the intake of 400 Kcal supplementary diet. The measuring planes for the 2D cine PC were placed at the proximal portion, mid curved portion and the distal straight portion of the main trunk of SMA. With 3D cine PC VIPR, retrospective measurements at the corresponding planes were performed and the values were compared.

#### RESULTS

#### CONCLUSION

Newly developed 3D cine PC VIPR can be used for dietary stressed SMA flow measurement with an added value of delineating the vortex and helical flow portions in the SMA where the measurement should be avoided.

#### CLINICAL RELEVANCE/APPLICATION

3D cine PC VIPR is feasible as a dietary stress test for non-obstructive mesenteric ischemia by detecting the post-prandial hyperemia. The beauty of the method is retrospective flow analysis.

### **VSVA61-14 • Non-contrast MRA: Phase-contrast MRA**

**Scott B Reeder** MD, PhD (Presenter)

#### LEARNING OBJECTIVES

1) Understand the underlying principles of phase velocity MRA. 2) Be familiar with the currently available methods for phase velocity MRA. 3) Be familiar with important applications and examples of phase velocity MRA. 4) Understand current limitations and pitfalls associated with phase velocity MRA.

### **National Library of Medicine PubMed: Find Articles You Need: Searching PubMed/MEDLINE Efficiently**

**Friday, 10:30 AM - 12:00 PM • S401AB**



[Back to Top](#)

**ICIW61 • AMA PRA Category 1 Credit™:1.5 • ARRT Category A+ Credit:1.5**

**Holly A Burt**

**Chezire Aclimandos**

**Annabelle Nunez**, MA

**Wendy Wu**, MS

#### LEARNING OBJECTIVES

1) Understand how PubMed constructs a query and how to develop and refine effective search strategies in radiology. 2) Use PubMed tools including Clinical Queries, Related Articles, Single Citation Matcher and Loansome Doc. 3) Build focused searches using the Medical Subject Headings (MeSH) vocabulary for radiology and limit searches to radiology-oriented journals. 4) Understand how to save and download citations.

#### ABSTRACT

This hands-on workshop covers key searching techniques, changes to PubMed, and how to develop effective search strategies for PubMed and MEDLINE. Topics covered include: why keywords don't always give the results you expect, how to limit to specific journals, quick searches to find evidence-based citations, how to access full-text articles, and downloading citations to reference manager programs. The National Library of Medicine (NLM) provides free web access to nearly 24 million citations for biomedical and clinical medical articles through PubMed (available online at PubMed.gov). MEDLINE is a subset of PubMed which includes links to sites providing full text articles and to other related databases and resources.

### **Breast Imaging (Issues in Screening)**

**Friday, 10:30 AM - 12:00 PM • E450B**



[Back to Top](#)

**SST01 • AMA PRA Category 1 Credit™:1.5 • ARRT Category A+ Credit:1.5**

**Moderator**

**Susan G Roth**, MD

**Moderator**

**Sarah M Friedewald**, MD \*

### **SST01-01 • Mammography Outcomes by Screening Interval: Does Biennial Screening Affect Prognosis?**

**Laura Billadello** MD (Presenter) ; **Riti Mahadevia** ; **Paula M Grabler** MD ; **Ellen B Mendelson** MD \* ; **Lilian Wang** MD

#### PURPOSE

In 2009, the U.S. Preventative Services Task Force announced the recommendation for biennial screening mammography for women aged 50-74 years, despite evidence of mortality reduction with annual screening mammography beginning at age 40, as supported by the American College of Radiology (ACR), Society of Breast Imaging (SBI), and American Cancer Society (ACS). The purpose of this study is to use secondary endpoints of tumor size and lymph node positivity to compare the efficacy of screening mammography performed at various time intervals.

#### METHOD AND MATERIALS

Under IRB approval, a retrospective review of all screen-detected breast cancers between 2007-2010 was performed. Patients were divided into groups 1-3 based on time interval between screening mammograms, defined as 3 years. The three groups were controlled in terms of age, breast density, high risk status, and family history of breast cancer. Audit data as outlined by ACR BI-RADS, including % stage 0 or 1 cancers, % minimal cancer, and % positive axillary lymph nodes, were compared for the three groups. The size of invasive cancers was also compared.

#### RESULTS

There were 419 screen-detected cancers during the study period. 34 patients were excluded due to unknown screening interval or lack of surgical pathology and 24 patients were excluded for cancer detection on baseline mammography. To adjust for differences in age between groups, patients >75 years were excluded. This resulted in 332 patients, 207 in group 1, 73 in group 2, and 52 in group 3. There was no significant difference in age, breast density, high risk status, family history, or index histology between groups. The % stage 0 or 1 cancer and % minimal cancer did not differ between the groups (p=0.057 and p = 0.498, respectively). The size of invasive cancers was also not statistically different between the three groups (ANOVA, p=0.165). However, lymph node positivity was lowest in group 1, which was a statistically significant difference (8.7% vs. 20.5% and 15.4%, p = 0.002).

#### CONCLUSION

Screening mammography performed at an interval

#### CLINICAL RELEVANCE/APPLICATION

Screening mammography performed at an interval less than that recommended by the USPSTF significantly reduces the rate of lymph

node positivity, thereby improving patient prognosis.

### **SST01-02 • Incidental Breast Lesions: Factors Associated with Increased Risk of Malignancy and Lack of Follow-up**

**Eniola T Obadina MD (Presenter) ; Roberta M Strigel MD,MS ; Richard J Bruce MD \* ; Alejandro Munoz Del Rio PhD ; Frederick Kelcz MD, PhD**

#### **PURPOSE**

To evaluate the rate of malignancy of incidental breast lesions (IBLs) detected on non-breast imaging examinations, factors associated with malignancy, and compliance with recommended follow-up.

#### **METHOD AND MATERIALS**

Following IRB approval, a retrospective review of the electronic medical record using keyword search was performed to identify all patients (pts) without a known history of breast cancer who had an IBL detected on a non-breast imaging examination from 9/2008 to 8/2012. Outcomes were determined by follow-up with dedicated breast imaging and results of biopsy, if performed. Imaging modality of detection, IBL size, pt age and location at the time of the exam, follow-up and final outcome were recorded. Rates of imaging follow-up and malignancy were calculated. Kruskal-Wallis and Fisher's exact tests were used to identify factors associated with malignancy and compliance with follow-up.

#### **RESULTS**

293 pts were identified and ranged in age from 14 to 100 years (mean 59.6 years). 36/293 (12%) of pts were in the Emergency Department (ED) at the time of their non-breast imaging exam, 49/293 (17%) were inpatients, and 208/293 (71%) were outpatients. IBLs ranged in size from 0.4 to 7.2 cm (mean 1.53 cm). 242 pts had IBLs detected on CT (83%), compared to 25 pts with MRI-detected IBLs (8.5%) and 25 pts with PET-detected IBLs (8.5%). One pt had an IBL detected on a myocardial perfusion stress test. 121/293 (41%) pts underwent follow-up with dedicated breast imaging. There was a significantly increased rate of noncompliance with follow-up in ED pts (30/36; 83%), compared to 32/49 (65%) inpatients and 110/208 (53%) outpatients (p

#### **CONCLUSION**

Incidental breast lesions ultimately diagnosed as breast cancers are not rare (21%) and were most likely to represent malignancy if discovered on PET imaging. IBLs discovered as part of an ED visit were the most likely not to undergo follow-up.

#### **CLINICAL RELEVANCE/APPLICATION**

Incidental breast lesions identified on non-breast imaging exams represent malignancy in up to 21% of cases, emphasizing the need for dedicated breast imaging follow-up of these incidental findings.

### **SST01-03 • Surveillance of Women with Personal History of Breast Carcinoma Using MRI**

**Haiquan Liu (Presenter) ; Yanqing Hua MD ; Huadong Miao ; Weijun Peng MD**

#### **PURPOSE**

To determine the capability of MRI in detecting the second breast carcinoma among women with a personal history of breast carcinoma.

#### **METHOD AND MATERIALS**

This retrospective review of breast MRI examinations performed from 2007 to 2011 yielding 798 women who had a personal breast history. Of the 798 patients, 445 had adequate follow up data and 348 had MRI, mammography and ultrasound within 6 months intervals. The sensitivity, specificity of MRI in detecting the second breast carcinoma was calculated. The recall rate and PPV of MRI was also calculated.

#### **RESULTS**

Of the 798 patients, 49 second breast carcinoma was found and the incidence of the second breast carcinoma was 6.1%. Forty-five breast carcinomas were detected by MRI. The sensitivity and specificity of MRI in detecting the second breast carcinoma was 91.8% and 92.2%, respectively. The recall rate of MRI was 9.5% and PPV was 59.2%. The sensitivity of MRI, mammography and ultrasound in detecting the second breast carcinoma was 90.3%, 48.4% and 77.4%, respectively. The specificity was 95.3%, 93.4% and 95.9%, respectively.

#### **CONCLUSION**

We found that breast MRI surveillance of women with a personal history of breast cancer was clinically valuable in finding malignancies with a reasonable recall rate and PPV.

#### **CLINICAL RELEVANCE/APPLICATION**

For woman with history of breast carcinoma, breast MRI examination is valuable, especially when a patient has equivocal Clinical and Imaging Findings.

### **SST01-04 • Sensitivity, Specificity and Recall Rates for An Abridged Breast MRI Protocol in a Pure High-risk Screening Population**

**Laura Heacock MS, MD (Presenter) ; Amy N Melsaether MD ; Kristine M Pysarenko MD ; Samantha L Heller MD, PhD ; Ana P Klautau Leite MD ; Linda Moy MD**

#### **PURPOSE**

To evaluate the sensitivity, specificity and recall rates for an abridged MRI protocol.

#### **METHOD AND MATERIALS**

A retrospective review of 128 asymptomatic women with 195 findings who had a screening MRI was performed by 2 readers. Each reader was trained with 100 cases with a known cancer in an abridged protocol. Initially they evaluated the precontrast T1, first post-contrast T1 and first subtraction T1 post-contrast images blinded to the history and prior films. Then they assessed the images given the above information and once more with the addition of the pre-contrast T2 images. The scan time for the 3 T1-sequences was 4 mins; the scan time for the T2-sequence was 4 mins. The time to interpret the study and the confidence score was assessed for each study. Comparison was made to the original diagnostic interpretation.

#### **RESULTS**

Of 128 women, 22 (17.2%) BRCA carriers, 1 (0.8%) chest radiation, 73 (57%) family history, 20 (15.6%) personal history of breast cancer, 12 (9.4%) had atypia. Mean age was 48 years, range 25-82 years. Mean lesion size was 1.2cm (range 0.3 – 8cm). Of the 128 exams, 20 (15.6%) were originally assessed as BIRADS 1, 62 (48.4%) as BIRADS 2, 24 (18.8%) as BIRADS 3, 22 (17.2%) as BIRADS 4. Using the abridged protocol, 26 (20.3%) exams were assessed as BIRADS 0, 25 (19.5%) as BIRADS 1, 19 (14.8%) as BIRADS 2, 28 (21.9%) as BIRADS 3, 30 (23.4%) as BIRADS 4. Sensitivity was 100%; 3 cancers (2 DCIS and one invasive cancer) were identified by the readers. However, the specificity was 58% and an additional 31 findings were identified by the readers. Mean time for interpretation for readers was 50 secs (range 0.33 – 4.5 minutes). Both readers showed a significant increase in confidence (p

#### **CONCLUSION**

An abridged breast MRI in a pure screening population had a high sensitivity but low specificity and high recall rates. The addition of T2 images and prior films helped decrease the recall rate.

#### **CLINICAL RELEVANCE/APPLICATION**

In an abridged screening breast MRI exam, the number of sequences necessary to decrease the false-positive findings needs to be further evaluated.

### **SST01-05 • Screening Breast MRI in Patients Previously Treated for Breast Cancer: Diagnostic Yield for Cancer and False Positive Interpretation Rate**

**Catherine S Giess MD (Presenter) ; Patricia S Poole MD ; Sona A Chikarmane MD ; Dorothy A Sippo MD ; Robyn L Birdwell MD**

#### PURPOSE

To determine the cancer detection rate and rate of false positive interpretation of screening breast MRI in women previously treated for cancer

#### METHOD AND MATERIALS

IRB approved, retrospective review of the breast MRI database from 2009-2011 identified 3297 contrast enhanced screening exams, 1498 (45.4%) in women previously treated for breast cancer. MRI reports were reviewed to determine MRI findings, BIRADS assessments and patient demographics. The longitudinal medical record was reviewed to determine outcomes of short interval surveillance, biopsy results and cancers detected. False positive studies were considered BIRADS 3 assessments with no evidence of cancer on follow up or BIRADS 4/5 assessments benign on biopsy.

#### RESULTS

Patient age ranged from 26-88, mean 54 years. 10.1% (152/1498) exams were performed in known genetic mutation carriers. 11.2% (168/1498) screening exams were assessed as abnormal, including 79/1498 (5.3%) BIRADS 3 and 89/1498 (5.9%) BIRADS 4/5. Follow up data on BIRADS 3 exams included 40 (50.6%) without malignancy by imaging and/or clinical follow up  $\geq$  24 months, 27 (34.2%) with  $<$  24 months stability, and 12 (15.2%) upgraded to BIRADS 4/5, with 5 (41.7%) cancers. Cancer rate for BIRADS 3 lesions was 6.3%; 3 of 5 upgraded cancers occurred in mutation carriers. Biopsy results for BIRADS 4/5 exams were available in 81 lesions, with 22 (27.2%) cancers. Overall, 27 (1.8%) of 1498 screening MR exams had malignancy diagnosed during the study period. Average time interval from original cancer diagnosis was 7.8 years (range 1-23 years). 24/27 cancers had negative mammograms within 6 months prior to new cancer diagnosis. 7/27 (22%) of cancers were diagnosed in mutation carriers; an additional 8/27 (29.6%) were diagnosed in women with a positive family history.

#### CONCLUSION

Screening breast MRI in women previously treated for breast cancer detected cancer in 1.8% examinations, with a minority of exams requiring short term surveillance or biopsy, and positive predictive value of 27.2% for biopsies recommended. Nearly half of screen detected cancers in this population occurred in women without a genetic mutation or a positive family history of breast cancer.

#### CLINICAL RELEVANCE/APPLICATION

Screening breast MRI in women previously treated for cancer detects mammographically occult cancers, with acceptable positive predictive values and low false positive interpretation rates.

### **SST01-06 • Breast MRI Screening in Women Who had Undergone Breast Conserving Therapy for Cancers**

**Hye Mi Gweon MD (Presenter) ; Nariya Cho MD ; Ann Yi MD ; Woo Kyung Moon**

#### PURPOSE

The American Cancer Society reports insufficient evidence to recommend for or against MRI in surveillance of asymptomatic women with a personal history of breast cancer. The purpose of this study, therefore, was to retrospectively investigate the outcomes of the first round of MRI screening in women who had undergone breast conserving therapy for breast cancers.

#### METHOD AND MATERIALS

Between January 2008 and March 2012, 808 women who had undergone breast conserving therapy for breast cancers and subsequent screening breast MRI were identified. All women had an annual screening mammography prior to beginning MRI screening and all the results were negative. Women without at least 12-month follow-up data (n=102) and had metastatic disease (n=2) were excluded. A total of 704 women (median age 48, range 20-72 years) (initial stage 0: 27.3%, stage I: 37.2%, stage II: 30.3%, stage III: 5.3%) with 1069 screening breast MR examinations (one round: 389, two rounds: 265, three rounds: 50) formed our study group. The reference standard was based on biopsy and/or 12-month follow-up. The cancer detection rate, sensitivity, specificity, and positive predictive value (PPV) based on biopsy performed at the first round screen were analyzed. Median follow-up duration was 18.5 months (range, 12-53 months).

#### RESULTS

Of the 704 women, cancer was detected at MRI in 10 women (1.4%) at a median interval of 33 months (range, 14-56 months) between surgery and detection. The ten cancers included 7 (70%) invasive cancers and 3 (30%) DCIS and were found in 6 (60%) ipsilateral and 4 (40%) contralateral breasts and were 100% node negative among those staged. The median histologic size of the invasive cancers was 0.8cm (range, 0.4-1.4cm). Two (0.3%) interval cancers were found 6 months later by mammography and ultrasound, respectively. The sensitivity, specificity, and PPV of MRI were 83.3 % (10 of 12), 98.0% (678 of 692), and 41.7% (10 of 24).

#### CONCLUSION

A single MRI screening in women who had undergone breast conserving therapy for cancers detected 14 mammographically occult, node-negative breast cancers per 1000 women.

#### CLINICAL RELEVANCE/APPLICATION

Previous history of breast cancer therapy is a reasonable indication for breast MRI screening.

### **SST01-07 • Foci Detected on Screening MRI: Can They Be Safely Followed or Is Biopsy Required?**

**Dipti Gupta MD ; Raman Verma MD ; Morgan R Goldberg MD (Presenter) ; Erin I Neuschler MD ; Angelique C Floerke MD ; Riti Mahadevia ; Ellen B Mendelson MD \***

#### PURPOSE

While breast MRI has been established as the most sensitive tool for detecting breast malignancy, the increasing number of studies performed has led to an increasing number of MRI-guided biopsies. Previous studies demonstrate a highly variable positive predictive value of biopsied foci, ranging from 3% to 28%. This study attempts to evaluate the malignancy rate of suspicious foci identified on screening MRI and to determine if short-term follow-up can be safely performed in lieu of biopsy.

#### METHOD AND MATERIALS

In this IRB approved, HIPAA compliant retrospective study, 188 MRI-guided core biopsies of foci performed between January 2006 and March 2013 were retrieved from the report search system and reviewed. Suspicious foci identified during screening of the contralateral breast on MRI performed for extent of disease as well as suspicious foci on high-risk screening MRI were included. A focus was considered suspicious if it showed washout or plateau delayed phase kinetics, was the only enhancing focus in that breast or was more prominent than the background parenchymal enhancement. Foci biopsied in the breast ipsilateral to a known malignancy were excluded.

#### RESULTS

117/188 foci biopsied were in the ipsilateral breast as the known malignancy on MRI performed for extent of disease and were excluded. A total of 71/188 eligible patients were identified, which included 43 suspicious foci in the contralateral breast on MRI performed for extent of disease and 28 foci on high-risk screening MRI. 4/71 (5.6%) suspicious foci were positive for malignancy while 20/71 (28%) were high-risk lesions. Among suspicious foci on high-risk screening MRI, 3/28 (11%) were malignant and 5/28 (17%) had a high-risk pathology. 1/43 (2.2%) foci were malignant in the contralateral breast on extent of disease studies and 15/43 (35%) were high-risk lesions. The malignant and high-risk lesions are more likely to have type 2 and 3 kinetics (p=0.004) compared to benign foci.

#### CONCLUSION

The malignancy rate of foci is low in the contralateral breast on MRI performed for extent of disease. Given this, it may be reasonable to

follow foci in the contralateral breast, instead of recommending biopsy.

#### CLINICAL RELEVANCE/APPLICATION

As the rate of malignancy for a focus in the contralateral breast on extent of disease MRI is 2.2%, short interval follow up instead of biopsy may be reasonable.

### **SST01-08 • Impact of the Transition from Screen-film to Digital Screening Mammography on Interval Cancer Characteristics and Treatment-A Population based Study from the Netherlands**

**Joost Nederend MD (Presenter) ; Lucien Duijm MD, PhD ; Marieke W Louwman ; Frits H Jansen MD ; Adri C Voogd**

#### PURPOSE

In most breast screening programs screen-film mammography (SFM) has been replaced by full-field digital mammography (FFDM). We compared interval cancer characteristics at SFM and FFDM screening mammography.

#### METHOD AND MATERIALS

We included all 297 screen detected and 104 interval cancers in 60,770 SFM examinations and 427 screen detected and 124 interval cancers in 63,182 FFDM examinations, in women screened in the period 2008-2010. Breast imaging reports, biopsy results and surgical reports of all cancers were collected. Two radiologists reviewed prior and diagnostic mammograms of all interval cancers. They determined breast density, described mammographic abnormalities and classified interval cancers as missed, showing a minimal sign abnormality or occult.

#### RESULTS

The referral rate and cancer detection rate at SFM were 1.5% and 4.9‰ respectively, compared to 3.0% (p

#### CONCLUSION

FFDM resulted in a significantly higher cancer detection rate, but sensitivity was similar for SFM and FFDM. Interval cancers are more likely to be occult at prior FFDM than at prior SFM screening mammography, whereas their tumor characteristics and type of surgical treatment are comparable.

#### CLINICAL RELEVANCE/APPLICATION

Data on the impact of this transition on mammographic characteristics and tumor characteristics of interval breast cancer detected cancers are very limited.

### **SST01-09 • Breast Imaging Utilization Trends in the Medicare Population from 2005 to 2011**

**Richard E Sharpe MD, MBA (Presenter) ; David C Levin MD \* ; Vijay M Rao MD ; Laurence Parker PhD**

#### PURPOSE

This study aims to describe the utilization trends in screening mammography, diagnostic mammography, breast US and breast MR in the Medicare population from 2005 to 2011.

#### METHOD AND MATERIALS

The Medicare Part B Physician/Supplier Procedure Summary Master Files from 2005 through 2011 were used to determine the annual utilization rate of screening mammography, diagnostic mammography, breast ultrasound, and breast MR. Procedure volume counts were determined by tabulating global and professional component claims. Utilization rates per 1,000 women beneficiaries were calculated by dividing volume counts by the number of Medicare women beneficiaries for each year. Utilization rate and compound annual growth rate (CAGR) trends were evaluated.

#### RESULTS

For the 2005-2009 period, screening mammography utilization increased from 312 per 1,000 women in 2005 to 323 in 2009 (CAGR from 2005-2009=+0.9%); it then decreased to 311 in 2011 (CAGR for 2009-2011: -1.9%). Diagnostic mammography utilization decreased from 96 in 2005 to 92 in 2009 (CAGR=-1.3%); it further decreased to 86 in 2011 (CAGR: -3.4%). Breast MR utilization rate increased from 1.4 in 2005 to 3.9 in 2009 (CAGR=+28.4%); it then decreased to 3.6 in 2011 (CAGR=-3.7%). Breast US utilization increased from 37 in 2005 to 43 in 2009 (CAGR=+4.3%); it then increased to 45 in 2011 (CAGR=+1.7%).

#### CONCLUSION

For all breast examinations, the rate of change from 2005 to 2009 compared to 2009 to 2011 in all cases decreased, either going from a positive growth to a less positive rate, a positive to a negative rate, or from a negative to a more negative growth rate. Decreases in screening mammography, diagnostic mammography and breast MR utilization in recent years may be in part attributable to changes in the USPSTF recommendations. Continued increases in breast US utilization, albeit at a slower rate after 2009, may be secondary to whole breast US techniques and interest in US evaluation of women with mammographically dense breasts.

#### CLINICAL RELEVANCE/APPLICATION

In recent years, there has been negative growth in the utilization of all breast imaging examinations.

---

## **Cardiac (Coronary CT/MR V)**

**Friday, 10:30 AM - 12:00 PM • S502AB**

---



[Back to Top](#)

**SST02 • AMA PRA Category 1 Credit™:1.5 • ARRT Category A+ Credit:1.5**

**Moderator**

**Karin E Dill , MD**

**Moderator**

**Robert R Edelman , MD \***

### **SST02-01 • Comparison of Image Quality for Coronary CT Angiography Using Adaptive Iterative Dose Reduction 3D versus Filtered Back Projection**

**David Tso MD (Presenter) ; Andrew Van Der Westhuizen MD ; Patrick McLaughlin FFRCSI ; Darra T Murphy FFRCSI ; John R Mayo MD \* ; Savvas Nicolaou MD**

#### PURPOSE

The purpose of this study was to compare image quality of a Cardiac CT angiography (CCTA) utilizing Adaptive Iterative Dose Reduction 3D (AIDR 3D), an iterative reconstruction technology on a Toshiba CT scanner, and compare it with standard filtered back projections (FBP).

#### METHOD AND MATERIALS

59 consecutive patients were scanned with the Toshiba Aquilion ONE 320-slice MDCT scanner using a low-dose CCTA protocol. Two datasets for each patient were generated, one with iterative reconstruction (AIDR 3D) applied to the original dataset, and the other was unaltered as a FBP dataset. The two datasets were compared with respects to signal and noise measures of cardiac vascular structures. Qualitative image quality of the cardiac structures and coronary segments were assessed using a 4-point scale (3-clear, 2-minor motion, 1-significant motion, 0-non-diagnostic).

## RESULTS

The mean effective radiation dose for the CCTA was 1.97 mSv. When comparing FBP vs. AIDR 3D, there was higher signal in the FBP dataset vs. AIDR 3D in the aorta and coronary arteries (677.33 HU vs. 657.33 HU); p

## CONCLUSION

AIDR 3D improves qualitative visualization of cardiac anatomy in CCTA through iterative reconstruction in both raw and image data space. This enables CCTA scans to be performed at reduced radiation exposure to patients while producing images that are of diagnostic quality.

## CLINICAL RELEVANCE/APPLICATION

AIDR 3D improves qualitative visualization of cardiac anatomy in CCTA through iterative reconstruction process which can allow scans to be performed at much lower radiation doses.

### **SST02-02 • High-pitch Coronary CT Angiography in Dual-source CT during Free Breathing vs. Breath Holding**

**Bernhard Bischoff MD (Presenter) ; Felix G Meinel MD ; Maximilian F Reiser MD ; Hans-Christoph R Becker MD**

#### PURPOSE

Usually, coronary CT angiography (CCTA) is performed during breath hold to reduce motion artifacts caused by respiration. However, some patients are not able to follow the breathing command sufficiently due to deafness, hearing impairment, agitation or pulmonary diseases. The aim of this study was to evaluate the potential of high-pitch CCTA in free breathing patients when compared to breath holding patients.

#### METHOD AND MATERIALS

In this study we evaluated 40 patients with a heart rate of 60 bpm or below referred for CCTA for ruling out coronary artery disease who were examined on a 2nd generation dual-source CT system. The first consecutive 20 patients were examined using a prospectively ECG-triggered high-pitch scan protocol during breath holding in inspiration (scan delay 8 seconds, 70 ml contrast agent at 6 ml/s) while the second group of 20 consecutive patients was examined during free breathing (scan delay 4 seconds, 45 ml contrast agent at 6 ml/s). Heart rate prior to and during image acquisition was monitored. Image quality of each coronary artery segment according to the AHA 15-segment model was rated by two experienced readers who were blinded to the patients breathing status using a 4-point grading scale (1: non diagnostic - 4: excellent).

#### RESULTS

Patient and scan characteristics did not differ significantly between both study groups. Mean heart rate during image acquisition was 52 ±5 bpm in both groups. There was no significant difference in mean image quality, slightly favoring image acquisition during breath holding (see figure). Due to a smaller amount of injected contrast medium signal intensity was little but not significantly lower in free breathing patients (435 ±123 HU vs. 473 ±117 HU; p=0.648). Mean effective radiation dose was 0.92 ±0.42 mSv in breath holding patients and 0.94 ±0.41 mSv in free breathing patients (p=0.741).

#### CONCLUSION

In patients with a low heart rate who are not able to hold their breath adequately during CCTA images might also be acquired during free breathing without substantial loss of image quality when using a high pitch scan mode in 2nd generation dual-source CT. Furthermore, free breathing CCTA may allow to reduce the amount of injected contrast medium due to a shorter scan delay.

#### CLINICAL RELEVANCE/APPLICATION

High-pitch CCTA may be performed during free breathing without substantial loss of image quality.

### **SST02-03 • The Effect of Iterative Reconstruction on Quantitative CT Analysis of Coronary Plaque Composition**

**Richard A Takx MD (Presenter) ; Martin J Willeminck MD ; Ricardo P Budde MD, PhD ; Arnold Schilham PhD ; Pim A De Jong MD, PhD ; Tim Leiner MD, PhD \***

#### PURPOSE

To compare CT assessment of coronary plaque volume and composition using three levels of iterative reconstruction (IR) and filtered back projection (FBP) as the reference reconstruction.

#### METHOD AND MATERIALS

#### RESULTS

#### CONCLUSION

Application of IR to CCTA exams significantly improves objective image quality, and does not alter quantitative analysis of coronary plaque volume, composition and luminal area.

#### CLINICAL RELEVANCE/APPLICATION

Iterative reconstruction has the potential to reduce radiation exposure without affecting analysis of coronary plaque composition.

### **SST02-04 • Interobserver Variability of Coronary Atherosclerotic Plaque Characteristics Using a Semiautomatic Plaque Analysis Software**

**Azien Laqmani (Presenter) ; Thorsten Klink MD ; Marcus Quitzke ; Gerhard B Adam MD ; Gunnar K Lund MD**

#### PURPOSE

To evaluate the interobserver variability (IOV) of a dedicated semiautomatic plaque analysis software for the characterization of coronary atherosclerotic plaques.

#### METHOD AND MATERIALS

#### RESULTS

#### CONCLUSION

The dedicated semiautomatic plaque analysis software allows for a reproducible characterization of coronary atherosclerotic plaques. However, the IOV significantly deteriorates when the observers adjust the plaque segmentation based on individual experience.

#### CLINICAL RELEVANCE/APPLICATION

A standardized concept is essential for coronary plaque analysis in order to maintain reproducible plaque dimensions.

### **SST02-05 • Image Quality and Radiation Dose of Coronary Computed Tomography Angiography with Automatic Tube Potential Selection Technique**

**Ying Wang MD (Presenter) ; Huishu Yuan MD**

#### PURPOSE

To investigate the image quality and the radiation dose of automatic tube potential selection technique (ATPS) in dual-source computed tomography (DSCT) coronary computed tomography angiography (CCTA).

#### METHOD AND MATERIALS

325 patients (153 men and 172 women) consecutively enrolled in CCTA were randomly assigned into group A (n = 172) and group B (n = 153). The group A used ATPS (Care kV), and group B used conventional tube current modulation at 120 kV. All patients were scanned

with prospective ECG-triggered high-pitch helical mode or sequential mode according to the heart rate. The mean image quality score, attenuation, image noise, signal-to-noise ratio (SNR), contrast-to-noise ratio (CNR), volume CT dose index (CTDI<sub>vol</sub>), and effective dose (ED) were compared between the two groups with the 2-tailed Student *t* test or Mann-Whitney *U* test., A *P*-value < 0.05 was considered statistically significant. The interobserver variability of image quality scoring was determined by *Kappa* statistics.

#### RESULTS

The mean image quality score was not significantly different between group A and B (3.86 ± 0.23 vs. 3.85 ± 0.20, *P*>0.05). Imaging noise was significantly higher in group A than group B (25.6 ± 7.6 vs. 15.8 ± 4.0 HU, *PPP*<sub>vol</sub> and ED were both significantly lower in group A than group B (CTDI<sub>vol</sub>: 5.82 ± 6.85 vs. 10.32 ± 10.05 mGy; ED: 1.25 ± 1.24 vs. 2.19 ± 1.77 mSv, *PK*<sub>appa</sub>=0.59).

#### CONCLUSION

The use of ATPS for CCTA significantly reduced radiation dose while maintaining image quality.

#### CLINICAL RELEVANCE/APPLICATION

Automatic tube potential selection technique can maintain diagnostic image quality of coronary CTA as well as reduce radiation dose.

### **SST02-06 • Multi-detector Computed Tomography Angiography (MDCTA) in Asymptomatic Adults with Low and Intermediate Coronary Artery Disease Risk: Atherosclerotic Plaques Features**

**Radwa A Noureldin MD, MSc (Presenter) ; Riham H El Khouli MD, PhD ; Roderic I Pettigrew MD, PhD ; Ahmed M Gharib MBChB**

#### PURPOSE

MDCTA has a developing role in evaluating coronary artery disease (CAD) & ruling out significant stenosis non-invasively, yet it is not recommended for cardiovascular risk assessment in asymptomatic adult regardless of their risk score. We conducted this prospective study to evaluate the value of MDCTA examination in asymptomatic patients with low & intermediate risk for CAD.

#### METHOD AND MATERIALS

For our IRB approved study, we scanned 129 consecutive asymptomatic adults scanned with at least 64 detectors MDCTA scanner. Coronary arteries were categorized according to AHA 17-segment model. Number, size, quality of plaques & the degree of stenosis in each segment were assessed. Cardiac risk factors were evaluated & correlated to coronary arteries findings. Logistic regression & ROC curve analysis were performed.

#### RESULTS

Of 119 asymptomatic adults, 113 were included in the study (58 were females & 55 males), with mean age of 55±11. 73% (82/113) have low risk, 19.5% (22/113) intermediate risk, & only 5% (6/113) had high risk for CAD according to Framingham risk score (FrSc). Only 10 (8.8%) asymptomatic adults had completely normal CT scan with no plaques, all with low risk by FrSc. In 91.2% of cases, there were plaques with variable extent and in 22% of cases plaques caused moderate to severe stenosis. The best model to predict the total number of plaques in asymptomatic adults combined the age, gender, HbA1c level, C-reactive protein (CRP) level, calcium score (CaSc), & Framingham score (FrSc). For predicting the total number of large plaques, combining age, gender, & CaSc was the best model resulting in an AUC of 0.9. For predicting the total number of non-calcified plaques, combining the Tri-glyceride & CRP levels was the best model resulting in an AUC of 0.65. For the number plaques causing moderate to severe stenosis, combining age, gender, HbA1c, FrSc, & CaSc was the best model resulting in an AUC of 0.92.

#### CONCLUSION

MDCTA is useful in identifying coronary plaques in asymptomatic subjects with low or intermediate 10 years risk for CAD. We identified risk factors combined together enables the prediction of the risk of atherosclerosis in this specific population with good accuracy.

#### CLINICAL RELEVANCE/APPLICATION

MDCTA facilitated identification of multiple risk factors when combined that can predict the presence of coronary plaques in a group of asymptomatic adults with low & intermediate risk for CAD.

### **SST02-07 • Reduction of the Total Injection Volume of Contrast Material at Half Flow Rate in the First Four Seconds for 320-detector Row CT Coronary Angiography**

**Zhao-Hui Xian (Presenter) ; Xiang-Ran Cai ; Wen-Cai Yang ; Xu-Kai Mo ; Xiao-Bai Wang**

#### PURPOSE

To investigate the feasibility of half flow rate in the first 4 seconds to reduce the total injection volume of contrast material (CM) for 320-detector row computed tomography coronary angiography (CTCA).

#### METHOD AND MATERIALS

Ninety patients who underwent 320-detector row CTCA with heart rate =70 bpm and body weight =80 kg were recruited consecutively. They were randomly divided into two groups with a fixed injection of CM duration of 10 seconds: receiving 0.8 mL/kg body weight at a single flow rate (group 1; n=45), or receiving half flow rate in the first 4 seconds to reduce the total injection volume of CM by 20% (group 2; n=45). The concentration of CM was 350 mg of iodine per milliliter. All patients then received 30 ml of saline chaser with the same flow rate as the administration of CM. The groups were compared with respect to the attenuation values of the pulmonary trunk (PT), ascending aorta (AA), proximal and middle segments (vessel diameters >2.0 mm) of three coronary arteries and coronary sinus (CS).

#### RESULTS

The mean attenuation values of the PT and AA decreased slightly from group 1 to group 2, but did not achieve statistically significant differences (*p*>0.05). Also, there were no significant differences between the mean attenuation values at the proximal and middle segments of the right coronary artery, left anterior descending artery and left circumflex artery (*p*>0.05). However, the mean attenuation value in the CS for group 1 was higher than that for group 2 (*p*<0.05).

#### CONCLUSION

It was feasible to achieve sufficient and reliable evaluation of the coronary arteries in 320-detector row CTCA using half flow rate in the first 4 seconds, which could reduce the injection volume of CM by 20% compared to the single flow rate for 10 seconds.

#### CLINICAL RELEVANCE/APPLICATION

Variable flow rate of CM injection protocol contributes to achieving sufficient and credible evaluation of the coronary arteries, while reducing possible confounding of the coronary vein.

### **SST02-08 • Expanding the Role of 256-row Multidetector CT Coronary Angiography with Prospective ECG-gating and Iterative Reconstruction Algorithm in the Assessment of Coronary Artery Bypass: Evaluation of Dose Reduction and Image Quality**

**Davide Fior MD (Presenter) ; Davide Ippolito MD ; Pietro A Bonaffini MD ; Cammillo R Talei Franzesi ; Orazio Minutolo MD ; Sandro Sironi MD**

#### PURPOSE

To evaluate the diagnostic performance of high speed 256-row computed tomography coronary angiography (CTCA) in the follow-up of patients with coronary artery bypass grafting (CABG), using low-kV CT angiography protocol combined with prospective ecg-gating technique and iterative reconstruction algorithm (iDose4) compared with standard retrospective protocol.

#### METHOD AND MATERIALS

Thirty-seven non obese patients with known advanced coronary disease treated with artery bypass grafting were prospectively enrolled in our study. All the patients underwent 256MDCT (Brilliance iCT, Philips) CTCA using low-dose protocol (100kV; automated tube current

modulation; rotation time: 0,375s) combined with prospective ECG-triggering acquisition protocol and 4th generation iterative reconstruction technique (Idose4; Philips,Best,Netherlands), and all the length of the bypass graft was included in the evaluation. A total of 21 similar patients were enrolled in the control group and evaluated with a standard retrospective ECG-gated CTCA (120kV; 350mAs). Dose-length product (DLP) was directly provided by the scanners. On both CT scans regions of interest (ROIs) were placed in coronary arteries, in order to calculate standard deviation (SD) of pixel values and intravessel density (HU). Diagnostic quality was also evaluated using a 4-point scale (4 excellent, 3 good, 2 acceptable, 1 low).

#### RESULTS

Two radiologists performed a "double blind" reading of the exams (all considered diagnostic) and maximum intensity projection, curved planar reformatted images and volume rendering reconstructions were generated in both groups. Despite the statistically significant reduction of radiation dose (51% lower in the study group with a P-value Qualitative analysis did not reveal any significant difference in diagnostic quality of the two groups.

#### CONCLUSION

The development of high-speed multidetector CT scans combined with modern iterative reconstruction allows the use of low dose prospective CTCA protocols also in patients with CABG, maintaining high diagnostic performance despite the significant reduction in radiation dose.

#### CLINICAL RELEVANCE/APPLICATION

High speed CT scans combined with Idose4 allow an accurate evaluation of CABG with prospective ECG-gating protocols in a single breath-hold, obtaining a significant reduction in radiation dose.

### SST02-09 • Resident Interpretation of On-Call "Triple-Rule-Out" CT Studies in Patients with Acute Chest Pain

**Kevin G Garrett MD (Presenter) ; Justin R Silverman ; Aleksander Krazinski ; Lucas L Geyer MD \* ; Carlo Nicola De Cecco MD ; U. Joseph Schoepf MD \* ; Gary F Headden ; Philip Costello MD ; Felix G Meinel MD ; Pal Suranyi MD, PhD ; James G Ravenel MD**

#### PURPOSE

To evaluate the agreement between preliminary Radiology resident and final subspecialty attending interpretation of on-call, emergency "Triple-Rule-Out" (TRO) CT studies in patients with acute chest pain.

#### METHOD AND MATERIALS

Our department uses "peerVue" to track agreement between preliminary trainee and final subspecialty attending interpretation of on-call emergent imaging studies. This system enables grading preliminary resident reports as "Concur", "Minor Discrepancy" (not affecting patient management), and "Major Discrepancy" (affecting patient management). During a 24 month sampling period from April 2011 through March of 2013, 617 TRO studies were performed in an on-call setting, were initially evaluated by the on-call upper level resident and had "peerVue" data available. "peerVue" TRO grades were analyzed and compared with resident performance on 609 emergent non ECG-synchronized routine chest CT cases from the same period. In cases of flagged discrepancies, patient records were reviewed to determine eventual patient management and outcome.

#### RESULTS

There was agreement ("Concur") between preliminary Radiology resident and final subspecialty attending interpretation in 88.5% (n=546) of TRO cases. 10.4% (n=64) were graded as "Minor Discrepancy" and 1.1% (n=7) as "Major Discrepancy", with possible significance for patient management. In the interpretation of non ECG-synchronized routine chest CT cases (89.8% [n=547] "Concur"-rate), there were significantly (p

#### CONCLUSION

On-call resident interpretation of TRO CT studies in patients with acute chest pain is congruent with final subspecialty attending interpretation in the overwhelming majority of cases. Discrepancies are rare and did not affect patient management or outcome in our cohort. Resident performance in this domain is similar to performance in the interpretation of emergent non ECG-synchronized routine chest CT.

#### CLINICAL RELEVANCE/APPLICATION

With appropriate training, on-call resident interpretation of ECG-synchronized TRO CT studies is safe and trainee performance does not differ from more traditional interpretative tasks.

### Cardiac (Anatomy and Function II)

Friday, 10:30 AM - 12:00 PM • S504AB



[Back to Top](#)

**SST03 • AMA PRA Category 1 Credit™:1.5 • ARRT Category A+ Credit:1.5**

#### Moderator

**James C Carr , MD \***

#### Moderator

**Jeremy D Collins , MD \***

### SST03-01 • Should All Patients Undergoing Pulmonary Vein Isolation Have a Trans-esophageal Echocardiogram to Rule out Thrombus in the Left Atrial Appendage?

**Saurabh Jha MD (Presenter) ; Sahar J Farahani MBBS**

#### PURPOSE

Patients with atrial fibrillation (AF) undergoing pulmonary vein isolation (PVI) for catheter-guided ablation nearly always have a pre-procedural cardiac CT for 3 D guidance. These patients are at increased risk for thrombus in the left atrial appendage (LAAT), which results in cancellation of the procedure. This is a cost analysis to determine the optimal method of excluding LAAT, with the assumption that for patient convenience imaging is performed on the same day as the PVI.

#### METHOD AND MATERIALS

A simple diagnostic model was constructed on Tree Age Pro (2012). Patients with AF undergoing PVI were assumed to require pre-procedural cardiac CT. Two diagnostic strategies were explored for the detection of LAAT. The first was intracardiac US for LAAT flagged on cardiac CT. The second was TEE for all patients. Both TEE and intracardiac US were assumed to be perfect tests. If the patient had a positive TEE or a positive intracardiac US for LAAT the procedure would be abandoned. The outcomes included costs from a payer's perspective, number of cases of missed LAAT and number of procedures cancelled. The data were abstracted from published meta-analysis and varied with sensitivity analysis. Medicare fee for schedule was used for the costs of procedures.

#### RESULTS

Assuming a prevalence of LAAT in AF of 9 % and sensitivity and specificity of cardiac CT of 96 % and 92 %, the selective intracardiac US strategy was cheaper (\$417.93) than the strategy of TEE for all patients (\$503.20). In a cohort of 10, 000 patients with AF requiring PVI there would be 36 missed cases of LAAT using the cheaper strategy. The incremental cost incurred in detecting an additional case of LAAT was \$23, 686. If efficiency is desired such that patients must have imaging on the same day as the procedure then in a cohort of 10,000 patients there will be 864 cancellations with the cheaper strategy and 900 cancellations with the more expensive strategy.

#### CONCLUSION

In patients with AF undergoing PVI and same day imaging the strategy of selective intracardiac US on patients with cardiac CT provides for LAAT costs \$85.27 less than subjecting all patients to TEE; at the expense of missed LAAT such that the incremental cost of picking up an additional patient with LAAT is \$23, 686.

#### CLINICAL RELEVANCE/APPLICATION

LAAT has a high prevalence in patients with AF and this affects the management of the condition.

### SST03-02 • The Myocardial Cut-off Sign: A Finding of Left Ventricular Pseudoaneurysm

**Clinton E Jokerst MD (Presenter) ; Travis S Henry MD \* ; Constantine A Raptis MD ; Cylen Javidan-Nejad MD ; Fernando R Gutierrez MD ; Pamela K Woodard MD \***

#### PURPOSE

The purpose of this study is to describe/define the 'myocardial cut-off' sign and compare its sensitivity and specificity to other imaging findings which help distinguish left ventricular pseudo-aneurysms (LV PSA) from left ventricular true aneurysms (LV aneurysm).

#### METHOD AND MATERIALS

Retrospective chart review of patients who had undergone left ventricular repair at our institution was performed. Patients who had pre-operative cardiac imaging with either CT or MRI were identified and divided into 2 groups, those with surgically or pathologically proven LV aneurysms (n=15) and those with surgically or pathologically proven LV PSAs (n=15). The thickness of the sac wall was measured at the aneurysm neck and 1 and 2 cm distal to the neck. A decrease of 50% or more between the neck measurement and sac wall measurement was called a positive myocardial cut-off sign; a decrease of less than 50% was called negative. These measurements were made during diastole (when applicable) on images oriented in a plane perpendicular to the axis of the aneurysm/PSA in an effort to quantify how quickly the wall of the sac tapered. 2 measurements were obtained for each patient, one on either side of the neck. In addition, other imaging findings associated with LV aneurysms and PSAs were evaluated. Some of these included location, presence of pericardial enhancement, presence of thrombus, ratio of neck diameter to maximum sac diameter, and ratio of neck diameter to maximum sac depth. Sensitivities and specificities for these signs and findings were calculated.

#### RESULTS

The sensitivity and specificity of the myocardial cut-off sign measured 1 cm from the sac neck was 90% and 96.4% respectively. Apical location was 66.6% sensitive and 80% specific for LV aneurysms. Pericardial enhancement was 77.8% sensitive and 88.9% specific for LV PSAs. Thrombus was 93.3% sensitive and 73.3% specific for LV PSAs. The mean ratio of neck diameter to maximum sac diameter and to maximum sac depth was 1:1.1 and 1:0.7 for LV aneurysms; 1:2.3 and 1:1.9 for LV PSAs.

#### CONCLUSION

The myocardial cut-off sign is a sensitive and specific sign of LV PSA when measured at 1 cm from the sac neck. \* more in-depth statistical evaluation will occur prior to presentation!

#### CLINICAL RELEVANCE/APPLICATION

The myocardial cut-off sign is sensitive and specific for LV PSA. This is an important diagnosis to make as LV PSA is a surgical emergency and can be difficult to distinguish from LV aneurysm.

### SST03-03 • Systematic Comparison of CT Scan and Retrograde Venography for Depicting the Cardiac Venous System Prior to Cardiac Resynchronisation Therapy

**Marie-Michele Theriault MD (Presenter) ; Maria De La Paz Ricapito MD ; Felix paredes MD ; Patricia Diez Martinez MD ; Paul Farand ; Gerald Gahide MD, PhD**

#### PURPOSE

To assess the value of cardiac CT in comparison to retrograde venography for depicting the presence of a cardiac vein suitable to implant a left ventricular lead for Cardiac Resynchronization Therapy.

#### METHOD AND MATERIALS

Cardiac CT was performed in 41 consecutive patients (75.6% men) prior to Cardiac Resynchronisation Therapy procedure. Cardiac veins were systematically described by two readers (Inferior Interventricular Vein, Posterior Vein(s), Lateral Vein(s)) and compared to retrograde venography findings. The coronary sinus diameters, atrium area and distance between coronary sinus ostium and right atrium lateral wall were measured.

#### RESULTS

An inferior interventricular vein was demonstrated in all patients (41) on CT scan and in 41.5% patients (17) on venography. A posterior vein was demonstrated in 73.2% (n=30) of patients on CT scan and in 61% (n=25) on venography. A lateral vein was observed in 56.1% (n=23) on CT scan and in 51.2% (n=21) on venography. In comparison to venography, CT scan sensitivity for detecting cardiac veins was 100%. CT scan demonstrated significantly more veins than retrograde venography (p2 (IQR: 17.5 – 26.9 cm<sup>2</sup>). There was a good inter-observer agreement for the measures of coronary sinus ostium antero-posterior diameters (r: 0.83 ; p

#### CONCLUSION

Cardiac CT is an efficient tool for non-invasively depicting cardiac venous system tributaries suitable for Cardiac Resynchronisation Therapy. Its sensitivity for depicting those veins is significantly higher than retrograde venography.

#### CLINICAL RELEVANCE/APPLICATION

Cardiac CT could non-invasively help choosing patients with suitable veins for Cardiac Resynchronisation Therapy.

### SST03-04 • Comparison of Rapid Left Atrial Volume Determination: Gated Multidetector CT vs. Transthoracic Echo

**Daniel A Moses MBBS, FRANZCR (Presenter) ; Minh Truong MBBS, FRANZCR ; Liza Thomas MBBS, PhD ; Suzanne Eshoo MBBS, PhD**

#### PURPOSE

As CCTA become more ubiquitous, rapid LA volume estimation is desirable. We compared multidetector CT rapid volume estimation with transthoracic echo measurements.

#### METHOD AND MATERIALS

Retrospective study examining 51 patients undergoing retrospectively gated CCTA evaluation. Gated MDCT and TTE assessments were performed within 48 hours when there was no change in the patients clinical status. The CT images were reconstructed to reflect standard views from the TTE. The following measurements were obtained from the CT images (radiologists) and TTE (cardiologists), both at left ventricular end-systole and end-diastole.

1. Parasternal long axis view (PLAX): AP LA diameter.
2. AP-4 chamber view: maximum LA length and width, maximum and minimum left atrial area.

Measurements were compared using Pearson's correlation and Bland-Altman analysis.

Left atrial volume was calculated by the area-length and prolate ellipse methods (and indexed to BSA).

#### RESULTS

Comparison measurements were as follows: PLAX: TTE 3.7 ± 0.51 cm; MDCT 3.94 ± 0.56 cm 4-CH max length: TTE 5.22 ± 0.59 cm; MDCT 5.38 ± 0.54 cm 4-CH area-length: TTE 55.43 ± 19.12 cm<sup>3</sup>; MDCT 76.823 ± 27.2 cm<sup>3</sup> 4-CH min area: TTE 11.33 ± 3.65 cm<sup>2</sup>; MDCT 17.04 ± 3.87 cm<sup>2</sup> 4-CH max area: TTE 18.27 ± 3.81 cm<sup>2</sup>; MDCT 21.85 ± 4.46 cm<sup>2</sup> Prolate ellipse volume: TTE 41.12 ± 12.79 cm<sup>3</sup>; MDCT 52.52 ± 17.37 cm<sup>3</sup> When adjusted for surface area: 4-CH area-length: TTE 29 ± 10 mL/m<sup>2</sup>; MDCT 40 ± 14 mL/cm<sup>2</sup> Prolate ellipse volume: TTE 21 ± 6 mL/m<sup>2</sup>; MDCT 27 ± 9 mL/cm<sup>2</sup> There was modest correlation between measurements on MDCT and TTE: PLAX r = 0.57; max area r = 0.54; area length r=0.55; prolate ellipse r = 0.53. TTE measurements were systematically less than CT for all



methods. Bland-Altman plots demonstrate there was less agreement on larger LA sizes.

#### CONCLUSION

The systematically lower volume estimates by TTE likely relate to the reduced image spatial resolution and foreshortening on TTE when compared to gated MDCT. Anatomical landmarks (including the precise location of the LA wall and mitral valve) are much more easily appreciated on MDCT. Also the ability to manipulated the data set and achieve the desired imaging view is easier on MDCT.

#### CLINICAL RELEVANCE/APPLICATION

TTE is the most common modality for estimate of LA volume. Knowing how these relate to similar estimations of LA size on gated MDCT scan is important clinical information.

### **SST03-05 • Presence of Myocardial Fibrosis in Right Ventricle Detected on ECG Gated 320 Slice CT Might Be a Predictor of a Short Term Poor Prognosis in Subjects with Pulmonary Hypertension**

**Koya Ozawa MD (Presenter) ; Nobusada Funabashi MD, PhD ; Akihisa Kataoka MD ; Noriyuki Yanagawa MD ; Nobuhiro Tanabe ; Koichiro Tatsumi ; Yoshio Kobayashi**

#### PURPOSE

To evaluate significance of presence of myocardial fibrosis (MF), as represented by abnormal late enhancement on CT, in right ventricle (RV) in subjects with pulmonary hypertension (PH), we undertook ECG gated enhanced 320 slice CT.

#### METHOD AND MATERIALS

A total of 56 PH subjects confirmed on right heart catheterization (RHC) (15 males, mean age  $57 \pm 15$  years, 33 chronic thromboembolic PH (CTEPH), 21 pulmonary arterial hypertension (PAH), and 2 others) underwent ECG gated 320 slice CT (Aquilion one, Toshiba Medical) to evaluate pulmonary artery, RHC and transthoracic echocardiogram (TTE) within 3 months without any clinical incident. Prospective ECG gating was added and if there was abnormal enhancement in RV myocardium, we regarded this as MF. Subjects were followed for a median of 17 months.

#### RESULTS

Adverse events (AE) occurred in 11 subjects (5 males, mean age  $60 \pm 10$  years); cardiac death (3), heart failure (6), cerebral hemorrhage (2). MF in RV was detected in 16 subjects (5 males, mean age  $56 \pm 2$  years, 9 CTEPH, 6 PAH and 1 other). Comparing subjects with and without MF, only cardiac output (l/min) calculated on TTE was significantly lower in subject with than without MF ( $P < 0.05$ ). However, there were no significant differences between groups in other factors, especially hemodynamic state parameters, on CT, TTE and RHC. Significant differences between subjects with and without MF were seen at each time point when whole follow up period was compared by further Kaplan Meier analysis and log rank test ( $P = 0.031$ ).

#### CONCLUSION

Presence of MF in RV detected on ECG gated 320 slice CT may have a short term poor prognosis in PH subjects, even though there were no significant differences in hemodynamic state parameters acquired from CT, TTE and RHC (except cardiac output) on TTE between subjects with and without MF. In contrast to hemodynamic state parameters, which tend to change, presence of MF in RV is a permanent morphological parameter which may be useful for accurately predicting prognosis of PH subjects.

#### CLINICAL RELEVANCE/APPLICATION

Presence of MF in RV detected on ECG gated 320 slice CT may be useful for accurately predicting prognosis of PH subjects.

### **SST03-06 • Volumetric and Flow Measurements in Patients with Repaired Tetralogy of Fallot: Comparison of Transverse versus Short-axis Cine-MRI and Echocardiography**

**Juliane Schelhorn MD (Presenter) ; Ulrich Neudorf ; Kai Nassenstein ; Thomas W Schlosser MD**

#### PURPOSE

Patients with corrected tetralogy of Fallot (TOF) are prone to develop dilatation and dysfunction of the right ventricle resulting in long-term complications. For right ventricular (RV) volumetry MRI is the gold standard but it remains controversial whether axial or short-axis (SA) planes should be used for RV analysis. The aim of this study was to compare both algorithms for the assessment of RV function. Additionally we compared volumetric and flow data in MRI and echocardiography (Echo).

#### METHOD AND MATERIALS

31 MRI studies of 27 patients with TOF were retrospectively studied. End-systolic volume (ESV), end-diastolic volume (EDV), stroke volume (SV) and ejection fraction (EF) of the left and right ventricle and left myocardial mass were measured in axial and SA planes. Furthermore the inner diastolic right ventricular diameter (R VIDdiast) in Echo and pulmonary valve peak velocity (PVPV) were acquired in MRI and Echo.

#### RESULTS

Good correlation between axial and SA orientation was found for left ventricular ESV, EDV, myocardial mass and SV and for right ventricular ESV, EDV and SV in MRI ( $p=0.001$ ). For right ventricular volumetry no systematic difference between both stack orientations was found. R VIDdiast in Echo and right EDV in SA and in axial orientation in MRI correlated well ( $p=0.001$ ). Good correlation was found between PVPV in MRI and Echo ( $p=0.001$ ).

#### CONCLUSION

For right ventricular volumetry in MRI axial and SA slices provide comparable results with no systematic error. Due to its good correlation with right EDV in MRI the R VIDdiast in Echo can be recommended as practicable follow-up tool in clinical routine.

#### CLINICAL RELEVANCE/APPLICATION

We wanted to evaluate whether axial or short-axis planes for right ventricular volumetry in MRI in patients with corrected tetralogy of Fallot are more appropriate.

### **SST03-07 • Fusion of Body Surface Mapping and Imaging for the Assessment of Cardiac Arrhythmias**

**Hubert Cochet MD (Presenter) ; Frederic Sacher ; Meleze Hocini ; Bruno Quesson ; Pierre Jais ; Michel Montaudon MD ; Michel Haissaguerre ; Francois H Laurent MD**

#### PURPOSE

Non-invasive imaging with cardiac MDCT and delayed-enhanced (DE) MRI gives access to cardiac anatomy and myocardial substrate. Body surface mapping (BSM) enables a non-invasive assessment of cardiac activation. We evaluated the feasibility of BSM/imaging fusion for the assessment of cardiac arrhythmias.

#### METHOD AND MATERIALS

24 patients referred for electrophysiological procedure in the context of ventricular tachycardia (VT, N=10), Wolf-Parkinson-White syndrome (WPW, N=2), atrial fibrillation (AF, N=10) and scar-related ventricular fibrillation (VF, N=2) were studied. All patients underwent BSM and non-invasive imaging with MDCT (N=9) and/or DEMRI (N=18). When both MDCT and DEMRI had been performed, datasets were fused using landmark registration. BSM was performed using a 252-electrode vest enabling the computation of epicardial electrograms from body surface potentials. The epicardial geometry on which electrical activation was calculated from BSM acquisition was then registered to the geometry segmented from imaging, using an iterative coupled points algorithm. The output was a 3-dimensional cardiac model integrating cardiac anatomy (cardiac chambers, epicardium, coronary vessels, phrenic nerve), myocardial substrate (fibrosis from DEMRI, myocardial hypodensity or wall thinning from MDCT), and epicardial activation from BSM.

#### RESULTS

Acquisition, segmentation, and registration was feasible in all patients. In patients referred for VT, this enabled a non-invasive assessment of the earliest epicardial exit of the VT circuit, and its location with respect to myocardial substrate, coronary vessels, or phrenic nerve. In WPW patients, this helped understanding accessory pathways of unusual location, or resistant to prior ablation. In AF and VF patients this enabled a non-invasive analysis of rotor trajectories with respect to myocardial substrate. In 14 patients (10 VT, 1 WPW, 3 AF), 3-dimensional models were successfully integrated in navigation systems and used to guide mapping/ablation.

#### CONCLUSION

By combining information on anatomy, substrate and electrical activation, BSM and imaging fusion enables a comprehensive non-invasive assessment of cardiac electrical disorders. This might have applications for diagnosis, prognosis, or ablation targeting.

#### CLINICAL RELEVANCE/APPLICATION

Body surface mapping can be fused with other non-invasive cardiac imaging modalities to provide a comprehensive assessment of cardiac arrhythmias.

### SST03-08 • Biventricular Myocardial Strain Analysis in Patients with Arrhythmogenic Right Ventricular Cardiomyopathy (ARVC) Using Cardiac Magnetic Resonance Feature Tracking

**Philipp Heermann** (Presenter) ; **Dennis Hedderich** MD ; **Walter L Heindel** MD ; **Matthias Paul** MD ; **David C Maintz** MD ; **Alexander C Bunck**

#### PURPOSE

Fibrofatty degeneration of myocardium in ARVC causes detectable wall motion abnormalities. The aim of this study was to examine whether cardiac magnetic resonance (CMR) based strain analysis using feature tracking (FT) can serve as an observer-independent and quantifiable measure to confirm global and regional ventricular dysfunction in ARVC patients and support the detection of early forms of ARVC.

#### METHOD AND MATERIALS

We enrolled 20 patients diagnosed with ARVC, 30 with borderline-ARVC and 22 subjects with a positive family history but no signs of a manifest ARVC. 10 healthy volunteers (HV) served as controls. 15 ARVC patients received genotyping for placophilin-2 mutation (PKP-2), of which 8 were found to be positive. Cine MR datasets of all subjects were assessed for myocardial strain using FT (TomTec Diogenes Software). Global and segmental strain in radial, circumferential and longitudinal mode were assessed.

#### RESULTS

#### CONCLUSION

CMR based strain analysis using FT is an objective and useful measure for quantification of wall motion abnormalities in ARVC. It allows differentiation between manifest or borderline-ARVC and HV, even if ejection fraction is still normal.

#### CLINICAL RELEVANCE/APPLICATION

Importance of quantitative parameters in ARVC diagnosis is underlined by the modification of the Task Force Criteria 2010 and CMR-based strain promises to be a powerful measure to objectify diagnosis.

### SST03-09 • Morphological and Functional Evaluation of Right Ventricle on ECG-Gated 320 Slice CT Can Predict a Short Term Poor Prognosis in Subjects with Pulmonary Hypertension

**Koya Ozawa** MD (Presenter) ; **Nobusada Funabashi** MD, PhD ; **Akihisa Kataoka** MD ; **Noriyuki Yanagawa** MD ; **Nobuhiro Tanabe** ; **Koichiro Tatsumi** ; **Yoshio Kobayashi**

#### PURPOSE

To evaluate the morphological and functional parameters of right ventricle (RV) in subjects with pulmonary hypertension (PH) by electrocardiogram (ECG)-gated enhanced 320 slice computed tomography (CT).

#### METHOD AND MATERIALS

56 PH subjects (15 males, mean age  $57 \pm 15$  years, 33 chronic thromboembolic PH, 21 pulmonary arterial (PA) hypertension and 2 others) underwent retrospective ECG-gated 320 slice CT (Aquilion one, Toshiba Medical). To obtain not only images of the whole heart including RV and coronary arteries, but also images of the PA, all CT scans were obtained using a double volume conventional scan with retrospective ECG-gating with a 0.5 mm slice thickness with a downward direction. Tube voltage was set at 120 kV and tube current was set at 580 mA with tube current dose modulation. We injected 60 ml of contrast material (350 mgI/ml) at 3.5 ml/s, followed by injection of a saline-to-contrast material mixture (40 ml contrast material at 2.0 ml/s and 30 ml saline at 1.5 ml/s), followed by injection of 20 ml pure saline at 1.5 ml/s. CT images were reconstructed every 5% from 0-95% of ECG R-to-R interval and 4 dimensional (4D) images were obtained. Subjects were followed for a median of 17 months.

#### RESULTS

Adverse events (AE) occurred in 11 subjects (5 males, mean age  $60 \pm 10$  years); Cardiac death (3), heart failure (6), cerebral hemorrhage (2). Receiver operating characteristic (ROC) curves of RV end-diastolic volume (RVEDV) and end-systolic volume (RVESV) on CT showed area under curve (AUC) of 0.646 and 0.590, respectively, and best cutoff points of 125.2 mm<sup>3</sup> (sensitivity 72.7%, specificity 60%) and 113.5 mm<sup>3</sup> (sensitivity 54.5%, specificity 80%), respectively, to distinguish subjects with and without AEs. By Kaplan Meier analysis, there was significant differences in incidence of AEs between = and < 113.5 mm<sup>3</sup> of RVESV on CT (P=0.032). In a similar analysis, there was not significant differences in incidence of AEs between = and < 125.2 mm<sup>3</sup> of RVEDV on CT (P = 0.051).

#### CONCLUSION

Quantitative and qualitative morphological and functional evaluation of RV on 4D images of ECG gated 320 slice CT showing RVESV can predict short term poor prognosis in PH subjects.

#### CLINICAL RELEVANCE/APPLICATION

Presence of RVESV dilation on ECG-gated 320 slice CT should be considered for poor prognosis in PH subjects.

## Chest (Airways, Emphysema)

Friday, 10:30 AM - 12:00 PM • E451B

[CT](#) [CH](#)

[Back to Top](#)

SST04 • AMA PRA Category 1 Credit™:1.5 • ARRT Category A+ Credit:1.5

#### Moderator

**Yoshiharu Ohno**, MD, PhD \*

#### Moderator

**Katherine R Birchard**, MD

### SST04-01 • Assessment of Pathologic Air Trapping Using Density Mappings of Inspiration and Expiration Datasets in Multidetector Row CT: Comparison to Threshold-based Methods in Expiration and the Expiratory to Inspiratory Ratio of Mean Lung Density

**Olga Solyanik** MD (Presenter) ; **Sabine Dettmer** ; **Till Kaireit** ; **Tim Alten** ; **Frank K Wacker** MD \* ; **Hoehn-Oh Shin** MD

#### PURPOSE

To determine whether density mappings (DM) of HU values seen on inspiration and expiration computed tomography (CT) are more precise for the detection and quantification of pathologic air trapping (AT) than the threshold-based method (Exp) and the expiratory to inspiratory ratio of mean lung density (E/I-ratio MLD) in lung transplant patients.

#### METHOD AND MATERIALS

152 lung and heart-lung transplant recipients underwent paired inspiratory and expiratory CT examinations 6 months after transplantation and pulmonary function tests (PFTs) within six hours following the CT scans. The assessment of AT was performed using a threshold-based method on expiration with systematic variation of the HU range (-1000 HU to -750 HU), E/I-ratio MLD, and DM of HU values on inspiration and expiration. For Exp and DM, the ratio of the detected air trapping area (ATA) and the segmented total lung volume (TLV) seen on CT were compared to the ratio of the residual volume (RV) and the total lung capacity (TLC) on pulmonary function tests. RV/TLC beyond the 95th percentile of predicted was considered as pathologic. Detection of pAT was performed using Spearman rank correlation, receiver operating characteristic (ROC) analysis and the area under the ROC curve (AUC).

#### RESULTS

DM correlated significantly better with RV/TLC than other CT measures (DM:  $r=0.658$ ;  $p$

#### CONCLUSION

DM showed the highest correlation with RV/TLC in comparison to E/I-ratio MLD and Exp -820 to -950 HU and might to be the most suitable technique for detection of pathologic air trapping in patients after lung transplantation.

#### CLINICAL RELEVANCE/APPLICATION

Density mappings might be used as an imaging biomarker for the detection and quantification of pathologic air trapping.

### **SST04-02 • Dynamic Oxygen-enhanced MRI: Capability for Pulmonary Functional Loss Assessment and Clinical Stage Classification in Asthmatics as Compared with Quantitative Thin-section CT**

**Yoshiharu Ohno MD, PhD (Presenter) \* ; Shinichiro Seki ; Mizuho Nishio MD \* ; Hisanobu Koyama MD ; Maho Tsubakimoto MD ; Takeshi Yoshikawa MD \* ; Sumiaki Matsumoto MD, PhD \* ; Makoto Obara \* ; Marc Van Cauteren PhD \* ; Nobukazu Aoyama RT ; Akiko Kusaka RT ; Kazuro Sugimura MD, PhD \***

#### PURPOSE

To prospectively and directly compare the capability of dynamic oxygen-enhanced MR imaging (O<sub>2</sub>-enhanced MRI) and quantitative CT for pulmonary functional loss assessment and clinical stage classification in asthmatics.

#### METHOD AND MATERIALS

Thirty consecutive asthmatics (17 men and 13 women; age rang 27-78 years) underwent dynamic O<sub>2</sub>-enhanced MRI, thin-section MDCT and pulmonary function test (FEV<sub>1</sub>% and FEV<sub>1</sub>/FVC%). All asthmatics were classified into three stages ('Mild [n=12]', 'Moderate [n=12]' and 'Severe [n=6]') according to the Global Initiative for Asthma guideline. All dynamic O<sub>2</sub>-enhanced MRI were obtained by using respiratory-triggered inversion-recovery 2D HASTE sequence. From signal intensity-time course curves, relative enhancement ratio and wash-in time maps in each subject were generated by pixel by pixel analyses. Then, ROIs were placed over the lung, and averaged to determine mean relative enhancement ratio (MRER) and mean wash-in time (MWIT) in each subject. On quantitative CT in each subject, ratios between wall area and total area of bronchus in right apical and anterior basal bronchi was averaged as WA%, and mean lung density (MLD) of the entire lung was also measured. To compare the capability of dynamic O<sub>2</sub>-enhanced MRI and quantitative CT for pulmonary functional loss assessment, MRER, MWIT, MLD and WA% were correlated with FEV<sub>1</sub>% and FEV<sub>1</sub>/FVC%. To determine the capability of two modalities for clinical stage classification, MRER, MWIT, MLD and WA% were statistically compared among three clinical stages by means of Fischer's PLSD test.

#### RESULTS

FEV<sub>1</sub>/FVC% had significant and moderate correlations with MRER ( $r=0.50$ ,  $p=0.005$ ), MWIT ( $r=0.65$ ,  $p=0.005$ ) also had significant and moderate correlations with MRER ( $r=0.60$ ,  $p=0.0005$ ), MWIT ( $r=0.68$ ,  $p$

#### CONCLUSION

Dynamic oxygen-enhanced MR imaging has better capability for pulmonary functional loss assessment and clinical stage classification in asthmatics than quantitative CT.

#### CLINICAL RELEVANCE/APPLICATION

Dynamic oxygen-enhanced MR imaging has better capability for pulmonary functional loss assessment and clinical stage classification in asthmatics than quantitative CT.

### **SST04-03 • Relationship between Current Smoking, Visual CT Findings, and Emphysema Index in Cigarette Smokers**

**Sungshiick Jou (Presenter) ; Kunihiro Yagihashi MD ; Jordan Zach ; David A Lynch MBChB \***

#### PURPOSE

Quantitative CT (QCT) measures of emphysema are significantly lower in current smokers than in those that quit, even after adjustment for severity of COPD. The purpose of this study is to evaluate whether visual CT findings could account for the current smoker effect.

#### METHOD AND MATERIALS

500 current and former smokers were evaluated (50% current smokers, 53% male, 80% non-Hispanic white, mean age 62.8 ± SD 8.6). The cohort included 100 smoking controls, and 100 subjects within each of the GOLD stages 1-4. Subjects underwent high resolution volumetric CT at full inspiration. Following automated lung segmentation, extent of emphysema was defined as % voxels with attenuation values < -950 Hounsfield Units (HU) on inspiratory CT (%LAA-950HU). Each CT scan was visually scored by two radiologists for presence and extent of emphysema, ground glass opacity (GGO), centrilobular nodularity (CN), and airway wall thickening (AWT) within each lobe. Univariate analyses tested the relationship of smoking status to visual CT findings. To test whether the effect of smoking status can be attributed to visual findings, a multivariate model for %LAA-950HU was constructed containing previously described confounders in addition to the visual components associated with smoking status.

#### RESULTS

Current smokers displayed 23% less visual emphysema, 19% more AWT, and 188% more CN than former smokers (all  $p$

#### CONCLUSION

Current smokers have less emphysema, more airway wall thickening and centrilobular nodularity than former smokers. QCT emphysema index is reduced in current smokers, even after adjustment for physiologic severity and visual findings.

#### CLINICAL RELEVANCE/APPLICATION

The decreased emphysema index found in current cigarette smokers is not fully explained by visual findings such as ground glass abnormality, centrilobular nodularity and airway wall thickening.

### **SST04-04 • Relationships between QCT Airway Measures and Outcomes of Exacerbations**

**Alexander McKenzie BS (Presenter) ; David A Lynch MBChB \* ; John D Newell MD \* ; Douglas Stinson ; Joyce D Schroeder MD \* ; Douglas C Everett PhD ; Stephen Humphries ; Jordan Zach ; Meilan K Han \* ; Carla G Wilson ; Eric A Hoffman PhD \***

#### PURPOSE

Volumetric CT with quantitative analysis yields numerous measures of airway lumen and airway wall. The purpose of this study was to determine which airway measures are best associated with exacerbation frequency.

#### METHOD AND MATERIALS

8043 inspiratory CT scans from the COPDGene study were examined. Airway measures included inner diameter, inner area, outer area and airway wall thickness, in upper and lower lobes (segmental in all cases, subsegmental and sub-subsegmental in 330 cases). Ratios of upper and lower lobe airway parameters (e.g. RB1/RB10, LB1A/LB10A) were examined. Exacerbation outcome was defined as either one severe exacerbation requiring hospitalization, or more than one mild or moderate exacerbation. Univariate logistic regression was used to determine odds associated with exacerbation. Multivariate logistic regression included age, smoking history and status, % emphysema and FEV<sub>1</sub> percent predicted.

## RESULTS

On univariate analysis, measures of inner bronchial diameter and inner luminal area were consistently associated with significantly increased risk of exacerbation (odds ratios 1.05 to 3.15). Odds ratios increased as airway generation increased from the segmental to the subsegmental but remained consistent between the subsegmental and the sub-subsegmental. Multivariate regression decreased the odds ratios, but odds were consistently higher at higher generation airways (subsegmental, sub-subsegmental). Inner diameter of segmental airways in the upper lobes proved to be the most consistently high predictor of exacerbation (LB1 OR = 1.48, RB1 OR = 1.35). Exacerbations were better predicted when inner diameter measures were taken at the sub and sub-subsegmental level. Additionally, the inner diameter ratio of upper to lower lobe airways was strong predictors of exacerbation at the subsegmental level (LB1A/LB10A OR = 2.08, RB1A/RB10A OR = 2.86).

## CONCLUSION

Quantitative airway measures can all be used to predict exacerbation, and odds increase in more distal airways. Upper to lower lobe ratio of airway inner diameter is a strong predictor of exacerbation at the subsegmental level.

## CLINICAL RELEVANCE/APPLICATION

Quantitative evaluation of airway wall thickness may permit risk stratification and prophylaxis for COPD exacerbation, an important cause of morbidity and mortality in COPD.

### SST04-05 • Is Bronchial Imaging Affected by Temporal Resolution? Comparative Evaluation at 140 and 75 ms in 90 Patients

**Nunzia Tacelli MD (Presenter) ; Antoine Hutt MD ; Teresa Santangelo ; Colm F Murphy MD ; Martine J Remy-Jardin MD, PhD \* ; Jacques Remy MD \***

## PURPOSE

To evaluate the influence of temporal resolution (TR) on cardiac motion artifacts at the level of bronchial walls.

## METHOD AND MATERIALS

90 consecutive respiratory patients (mean age: 50.2 yr, mean heart rate: 81.2 bpm) underwent a noncontrast chest CT examination on a second-generation 128-slice dual-source CT system (Somatom Definition Flash, Siemens Healthcare, Forchheim, Germany). The examinations were obtained with dual-source, single-energy using the following parameters: collimation: 32x2x0.6 mm; rotation time: 0.28 s; weight-adapted selection of the kilovoltage (100 kVp -120 kVp); reference tube current-time product: 64 ref mAs; 4D dose modulation and a pitch of 2.0. Two series of images were systematically reconstructed using data from both tubes on a prototype workstation with a TR of 75 ms (i.e., optimized TR) (Group 1) and 140 ms (i.e., standard TR) (Group 2). Using a 4-point scale, two radiologists independently analyzed the presence and severity of cardiogenic artifacts at the level of 8 target bronchi, i.e., right (R) and left (L) B1, B5, B7 and B10 (total number of bronchi examined: n= 720).

## RESULTS

Cardiogenic artifacts were significantly less frequent and less severe in Group 1 than in Group 2 (p

## CONCLUSION

At 75 ms, most of bronchi can be depicted without cardiogenic artifacts.

## CLINICAL RELEVANCE/APPLICATION

Quantitative estimation of bronchial morphometry should integrate the influence of cardiac motion artifacts, themselves dependent on the temporal resolution of data acquisitions.

### SST04-06 • Comparison of CT Findings between Th2 Asthma and Non-Th2 Asthma: Can CT Findings Characterize Molecular Mechanism Based Phenotypes in Severe Asthma

**Kwang Nam Jin MD (Presenter) ; Chang Hyun Lee MD, PhD ; Hye-Ryun Kang ; Sujeong Kim ; Sang Min Lee MD ; Young Eun Bahn MD ; Kyunghye Lee MD ; Hyun-Ju Lee MD, PhD ; Jin Mo Goo MD, PhD \***

## PURPOSE

Recent studies suggest that asthma can be divided into at least 2 distinct phenotypes defined by degree of T helper type 2 (Th2) cell inflammation. The purpose of this study was to compare the CT findings between Th2 (eosinophilic) and non-Th2 (non-eosinophilic) driven asthma.

## METHOD AND MATERIALS

We enrolled 29 patients who have severe asthma with molecular based identification of the phenotype and underwent chest CT. Th2 type asthma was diagnosed in 21 patients and non-Th2 in 8. Two radiologists blinded to clinical information performed visual analysis in consensus for the extent and severity of bronchial wall thickening (BT), mucus plugging (MP), and the extent of bronchiectasis (BE). The extent of BT, MP, and BE was assessed as the number of involved lobes (range, 0-5) and the severity of BT and MP was evaluated as 4-point scores (range, 0-3). Quantitative analysis was available for the low lung attenuation with threshold -950 HU (LAA-950HU), LAA-856HU, and bronchial wall (thickness, inner luminal diameter, and wall area %; RB1, LB1+2, RB10, LB10) in 16 CT scans (13 Th2 vs 3 non-Th2).

## RESULTS

In the qualitative analysis, Th2 type showed more extensive BT (Th2, 3.1 ± 2.2 vs Non-Th2, 1.1 ± 1.4, p = 0.02) and MP (Th2, 1.9 ± 1.8 vs Non-Th2, 0.5 ± 0.8, p = 0.03). BE was equally observed in both types (Th2, 1.4 ± 1.9 vs Non-Th2, 0.4 ± 0.7, p = 0.19). Severity of BT and MP between Th2 and Non-Th2 types was not significantly different (Th2, 1.3 ± 1.0 vs Non-Th2, 0.6 ± 0.7, p = 0.15; Th2, 0.8 ± 0.8 vs Non-Th2, 0.5 ± 0.8, p = 0.67) but Th2 type was given slightly higher mean severity scores. LAA-950HU was not significantly different between Th2 and Non-Th2 types (Th2, 9.9 ± 14.5 vs Non-Th2, 9.1 ± 9.1, p = 0.46), however, LAA-856HU was significantly higher in Th2 type (Th2, 43.6 ± 40.0 vs Non-Th2, 37.8 ± 20.3, p = 0.002). Quantitative analysis of the segmental bronchial wall (RB1, LB1+2, RB10, LB10) showed no significant difference in the BT, inner luminal diameter and wall area % between Th2 and Non-Th2 (p < 0.05).

## CONCLUSION

In severe asthmatics, Th2 associated asthma showed more extensive bronchial wall thickening, mucus plugging, and air-trapping than non-Th2 asthma.

## CLINICAL RELEVANCE/APPLICATION

The radiologic findings on CT in severe asthma differentiating between Th2 vs Non-Th2 types may enhance characterization of phenotypes and personalized and phenotype-specific therapies for asthma.

### SST04-07 • 3D Lung Motion and Destruction Assessments from Inspiratory and Expiratory Thin-section MDCT: Utility for Pulmonary Functional Loss and Clinical Stage Evaluation in Smokers

**Hisanobu Koyama MD (Presenter) ; Yoshiharu Ohno MD, PhD \* ; Yasuko Fujisawa MS \* ; Shinichiro Seki ; Mizuho Nishio MD \* ; Takeshi Yoshikawa MD \* ; Sumiaki Matsumoto MD, PhD \* ; Naoki Sugihara MENG \* ; Hitoshi Yamagata PhD \* ; Kazuro Sugimura MD, PhD \***

#### PURPOSE

To evaluate the utility of three-dimensional (3D) lung motion and destruction assessments from inspiratory and expiratory CT for pulmonary functional loss and clinical stage evaluation in smokers.

#### METHOD AND MATERIALS

Forty-four consecutive smokers (36 men and 8 women, mean age 76.6 years) underwent inspiratory and expiratory thin-section MDCTs and pulmonary function test. According to the GOLD guideline, all smokers were divided into four clinical stages as follows: 'without COPD (n=6)', 'mild COPD (n=5)', 'moderate COPD (n=22)', and 'very and very severe COPD (n=11)'. 3D motion vector map was generated from inspiratory and expiratory CT in each smoker. Then, regional motion magnitudes were measured at the following three axes: horizontal, X-axis; ventrocaudal, Y-axis; and craniocaudal, Z-axis. Then, all mean magnitudes within the entire lung ( $MML_x$ ,  $MML_y$  and  $MML_z$ ) were normalized by lung volume from expiratory CT. Moreover, CT-based functional lung volume (FLV) on inspiratory CT was also assessed from total and low attenuation lung volumes in each subject. To evaluate the capability for pulmonary function loss assessment, all indexes were correlated with  $FEV_1\%$  and  $\%DL_{CO}/V_A$ . Then, principal component analysis (PCA) was performed for discriminating clinical stages by means of all indexes.

#### RESULTS

$FEV_1\%$  had significant correlation with  $MML_y$  ( $r=0.67$ ,  $pZ$  ( $r=0.38$ ,  $pCO/V_A$  had significant correlation with  $MML_z$  ( $r=0.40$ ,  $p0.89$ ): the first component called 'maintained structure and diaphragm motion' determined by FLV and  $MML_z$ , the second component called 'asynchronous chest wall motion' determined from  $MML_x$  and  $MML_y$  and the third component called 'synchronous chest wall motion' determined from  $MML_x$  and  $MML_y$ .

#### CONCLUSION

3D lung motion as well as destruction assessments is considered as a useful indicator for pulmonary functional loss and clinical stage evaluation in smokers.

#### CLINICAL RELEVANCE/APPLICATION

3D lung motion as well as destruction assessments from inspiratory and expiratory CT data is considered as a useful indicator for pulmonary functional loss and clinical stage evaluation in smokers.

### **SST04-08 • Radiation-induced Lung Injury (RILI) after Stereotactic Body Radiation Therapy (SBRT) in Patients with Emphysema: A Quantitative Analysis of CT Changes**

**Abraham Knoll MD (Presenter) ; Mary M Salvatore MD ; Miriam Knoll MD ; Ren-Dih Sheu PhD ; Sarah L Kerns PhD, MPH ; Yeh-Chi Lo PhD ; Kenneth E Rosenzweig MD \***

#### PURPOSE

While lung Stereotactic Body Radiation Therapy (SBRT) is the standard of care for medically inoperable patients with early stage lung cancer, there is often concern regarding the development of radiation induced lung injury (RILI) in patients with COPD due to their compromised lung volumes. We compared the volume of RILI on CT exams in patients with and without radiographic evidence of emphysema.

#### METHOD AND MATERIALS

A review of patients treated with lung SBRT in our department was performed and pre-treatment CT was reviewed by a Diagnostic Radiologist for evidence of emphysema. Patients were scored by number of pulmonary lobes with emphysema and severity of emphysema in each lobe (mild, moderate or severe). Each patient's baseline smoking history was recorded. The RILI was contoured by a Diagnostic Radiologist and Radiation Oncologist and total volume of observed fibrosis was recorded.

#### RESULTS

37 lung lesions were treated in 15 patients with emphysema and 17 patients without. A total of 37 FU-CT's were reviewed. At a median of 6 months after treatment (range 3 to 7 months), the mean volume of fibrosis in patients with and without emphysema was  $35.4 \text{ mm}^3$  and  $99.2 \text{ mm}^3$ , respectively. The presence and severity of emphysema was significantly inversely proportional to the total RILI ( $p=0.024$  and  $p=0.003$ , respectively). Age was not significantly associated with RILI ( $p=0.441$ ). The number of total lung lobes with emphysema was not significantly associated with RILI ( $p=0.276$ ). Smoking status was also not significantly correlated with RILI, although only 3 patients were never-smokers.

#### CONCLUSION

Patients with radiographic evidence of emphysema who are treated with lung SBRT have significantly decreased RILI on post-treatment FU-CT, as compared patients without emphysema. Within the subset of patients with emphysema, those with increased severity had significant decreases in RILI.

#### CLINICAL RELEVANCE/APPLICATION

Patients with COPD who are treated with SBRT for lung cancer have overall less RILI compared to those who do not have emphysema.

### **SST04-09 • Association Study between Quantitative Measurement of Diaphragm Using Volumetric CT and Pulmonary Function Tests in Patients with COPD**

**Sang Min Lee MD (Presenter) ; Yongjun Chang ; Jangpyo Bae MS ; Namkug Kim PhD ; Joon Beom Seo MD, PhD ; Sang Young Oh MD**

#### PURPOSE

To evaluate the relationship between quantitative morphological parameters of the diaphragm with three-dimensional reconstruction using CT and pulmonary function tests in patients with COPD.

#### METHOD AND MATERIALS

Non-contrast, inspiration volumetric CT of thirty patients (M:F=28:2; mean age, 62.2 years) with COPD (n; mild = 3, moderate = 15, severe = 7 and very severe = 5) were included. Pulmonary function tests (PFT) were performed in all patients within 1 week of CT imaging. Using in-house software, upper margin of diaphragm were segmented automatically. Based on initial diaphragm segmentation, quadratic 3D surface fitting was used to measure morphological parameters of the diaphragm including the diaphragm lengths on x, y, z axes (XDL, YDL, ZDL), quadratic fitting diaphragm lengths on z axis (FZDL), height from apex and base plane (H), shape index at apex (SIA), average curvature (C), curvature on apex (CA) and surface area (SA). In addition, the correlation between morphological parameters of diaphragm, emphysema index (EI) and PFT were assessed with Pearson correlation test.

#### RESULTS

Measured morphological parameters of diaphragm, EI and PFT were as follows:  $XDL=129.80\pm 11.66\text{mm}$ ,  $YDL=163.19\pm 13.45\text{mm}$ ,  $ZDL=71.27\pm 17.52\text{mm}$ ,  $FZDL=61.59\pm 16.98\text{mm}$ ,  $H=28.08\pm 56.58\text{mm}$ ,  $SIA=0.849\pm 0.052$ ,  $C=0.0081\pm 0.0017$ ,  $CA=0.0095\pm 0.0025$ ,  $SA=34381\pm 6680\text{mm}^2$ ,  $EI=22.1\pm 11.68$ ,  $Dico=15.78\pm 5.41$ ,  $FEV_1=55.9\pm 20.88$  and  $FEV_1/FVC = 47.68\pm 16.2$ . Measured ZDL, SIA, C, CA, and SA were negatively correlated with EI ( $r = -.421, -.382, -.384, -.411, -.415$ , respectively). And, XDL, ZDL, FZDL, SIA, C, CA, and SA were positively correlated with DLCO ( $r = .489, .540, .531, .496, .415, .469, .637$ , respectively) and CA was positively correlated with  $FEV_1/FVC$  ( $r = .402$ ).

#### CONCLUSION

The several quantitative morphological parameters of diaphragm decrease in relation to the progression of emphysema and decrease of PFT in COPD.

#### CLINICAL RELEVANCE/APPLICATION

Detailed analysis of morphological diaphragm changes is possible using volumetric CT and dedicated software. It may be helpful in the understanding of diaphragm changes in COPD.



SST05 • AMA PRA Category 1 Credit™:1.5 • ARRT Category A+ Credit:1.5

Moderator

Doug R Kitchin, MD

Moderator

Peter S Liu, MD

Moderator

Vincent M Mellnick, MD

**SST05-01 • CT Findings of Bowel Ischemia in Closed-loop Small Bowel Obstruction****Kazuaki Nakashima** (Presenter); **Hideki Ishimaru** MD; **Toshifumi Fujimoto**; **Takashi Mizowaki**; **Yohjiro Matsuoka** MD; **Masataka Uetani** MD; **Seigo Kimura**; **Sachie Yotsumoto**; **Kazunori Mitarai**; **Kei Kitamura**

## PURPOSE

Closed-loop small bowel obstruction (CL-SBO) is associated with a high risk for vascular impairment and considered as a surgical emergency, however, when the bowel is viable, preservation of the bowel is feasible. The aim of this study was to characterize contrast-enhanced CT (CECT) findings predicting bowel necrosis and ischemia in CL-SBO.

## METHOD AND MATERIALS

Thirty five patients with CL-SBO confirmed by laparotomy (n = 34) or multiplanar reconstruction of thin slice CT images (n = 1) were included. On the basis of the surgical findings, these patients were classified into three groups: necrosis group, (n = 16) and ischemia without necrosis (ischemia group; n = 11), and no ischemia (n = 8). One patient recovered only with conservative management was also included in no ischemia group. Two blinded radiologists retrospectively reviewed CECT including multiplanar reconstruction images, and evaluated 12 CT findings previously reported to be associated with bowel ischemia: (1) wall thickening, (2) target sign, (3) high attenuation of the wall at precontrast CT, (4) wall enhancement, (5) mesenteric edema, (6) whirl sign, (7) enhancement of mesenteric artery and (8) vein, (9) engorgement of the mesenteric veins, (10) small bowel feces, (11) ascites, and (12) intraperitoneal air. Sensitivity and specificity of each findings were compared among the three groups, and logistic regression analysis was performed.

## RESULTS

Intraperitoneal air, high attenuation of the wall, reduced enhancement of mesenteric arteries and small bowel feces sign showed high specificities of 100%, 100%, 89% and 89%, however low sensitivity of 25%, 31%, 44%, 31%, respectively, to predict bowel necrosis in CL-SBO. On multivariate logistic regression analysis, reduced wall enhancement, reduced enhancement of mesenteric veins and lack of the engorgement of the mesenteric veins were significant for predicting bowel necrosis or ischemia (p

## CONCLUSION

Reduced enhancement of wall and mesenteric vessels were reliable findings to detect ischemia. On the contrary, engorgement of the mesenteric veins was predictor of viable bowel.

## CLINICAL RELEVANCE/APPLICATION

Evaluation of engorgement of mesenteric vein and enhancement of wall and mesenteric vessels would help us to predict bowel ischemia or necrosis in the closed-loop small bowel obstruction.

**SST05-02 • Dual Energy CT Improves Visibility of Early Small Bowel Ischemia Compared to Conventional CT in a Swine Model****Theodora A Potretzke** MD (Presenter); **Christopher L Brace** PhD\*; **Meghan G Lubner** MD; **Lisa A Sampson**\*; **Bridgett J Willey**\*; **Fred T Lee** MD\*

## PURPOSE

To compare dual-energy CT (DECT) to conventional CT for the detection of early bowel ischemia in a swine model.

## METHOD AND MATERIALS

Ischemic bowel segments (n=7) were created in swine (n=4) by surgically occluding distal mesenteric vasculature. Ischemia was confirmed grossly and with Doppler ultrasound. DECT and conventional CT were performed in arterial, portal venous, and delayed phases on a single-source fast-switching dual-energy CT scanner. ROIs of bowel wall attenuation were used to compare contrast-to-noise ratios (CNR) between ischemic and perfused segments on iodine material density and monospectral images at 51keV, 65keV (approximates 80kVp), and 80keV (approximates 120kVp). ANOVA and post-hoc t-tests compared pixel intensities and CNR among segments and imaging groups.

## RESULTS

Ischemic bowel exhibited significantly lower attenuation than perfused segments on DECT-iodine material density and 51keV images (P

## CONCLUSION

DECT significantly improves the visibility of early bowel ischemia compared to conventional CT images. DECT may offer earlier and more confident diagnosis of bowel ischemia especially in the absence of late secondary signs. It may increase the sensitivity and specificity of CT for bowel ischemia.

## CLINICAL RELEVANCE/APPLICATION

Mortality from bowel ischemia is high and increases with delay in diagnosis. Dual-energy CT increases the conspicuity of differential enhancement and may allow earlier diagnosis of bowel ischemia.

**SST05-03 • Small Bowel Transplantation: MDCT Features of Wall Thickening with Pathologic Correlation****Michael Bazylewicz** MD (Presenter); **Christine Chan**; **Sandra J Allison** MD; **Angela D Levy** MD

## PURPOSE

To determine if MDCT features of bowel wall thickening allows differentiation between normal bowel, ischemic bowel, rejection, post transplant lymphoproliferative disease (PTLD), and infection in patients with small bowel transplants.

## METHOD AND MATERIALS

CT scans (n=57) from isolated and multivisceral small bowel transplant patients (ages 1-62, mean 26) were retrospectively reviewed with consensus reading by two radiologists blinded to pathology results. Patients had endoscopic biopsy within 3 days of CT scanning. Small bowel was assessed for wall thickening, attenuation and enhancement pattern, feces sign, pneumatosis, dilatation, mesenteric edema and adenopathy, ascites, anasarca, vascular patency, and whether the scan was done with oral or IV contrast. Demographic data obtained: age, gender, race, and transplant type. Kappa power analysis determined a goal of 20 patients per group would show at least a 60% correlation exists between groups. For the continuous variable, the differences in the averages were tested and the non-parametric Kruskal Wallis test was used since normality assumptions were not satisfied. Chi-square and Fisher's exact tests were used to investigate the differences for categorical variables. A p-value of

## RESULTS

No statistical differences in age (0.69 pediatric, 0.2 adult), race (0.6), or transplant type (0.56). Significant difference between the

normal and ischemia subgroup was observed in gender (0.04). No difference was observed in wall thickening (0.29), attenuation (0.66), bowel enhancement pattern (0.66), feces sign (0.1), pneumatosis (0.67), dilatation (0.11), mesenteric edema (0.8), mesenteric adenopathy (0.5), anasarca (0.89), vascular patency (0.5), those with oral contrast enhanced scans (0.23), or those with IV contrast enhanced scans (0.59). A general difference between the 5 categories was noted in the category of ascites (0.03), however specific analysis of normal vs. the four abnormal subgroups demonstrated no significant difference (ischemia 0.28, rejection 0.052, infection 0.55, PTLD 0.39).

#### CONCLUSION

There is no correlation between small bowel wall thickening in patients with small bowel transplant and the common complications including ischemia, rejection, PTLD, and infection.

#### CLINICAL RELEVANCE/APPLICATION

Small bowel wall thickening on MDCT in small bowel transplants is likely non-contributory in determining an underlying pathologic condition.

### **SST05-04 • Cine MR Enterography Grading of Small Bowel Peristalsis: Evaluation of the Antiperistaltic Effectiveness of Sublingual Hyoscyamine Sulfate**

**Peter M Ghobrial MD ; Flavius F Guglielmo MD (Presenter) ; Donald G Mitchell MD \* ; Ilana Neuberger MD ; Laurence Parker PhD ; Christopher G Roth MD \* ; Sandeep P Deshmukh MD ; Patrick L O'Kane MD \* ; Allison Borowski MD**

#### PURPOSE

To use a cine MR enterography (cine-MRE) pulse sequence to assess the effectiveness of a sublingual (SL) antiperistaltic agent, hyoscyamine sulfate.

#### METHOD AND MATERIALS

IRB approval was granted with an exemption for informed consent in this HIPAA compliant retrospective single-institution study. Of the 288 MR enterography exams performed between October 1, 2007 and January 15, 2011, 92 using SL hyoscyamine sulfate for antiperistalsis were included for review, each with cine MRE pre and post medication. These 184 cine MRE sequences were randomized, blinded for treatment, and independently reviewed by five attending abdominal radiologists, who rated the degree of bowel motility of each cine MRE sequence on a five point scale. Pre- and post-medication mean peristalsis ratings, standard deviation, mean difference, and treatment effect sizes were calculated. A repeated measures analysis of variance (ANOVA) test was performed, using a significance threshold of  $p=0.05$ .

#### RESULTS

Mean peristalsis ratings ranged from 2.63 to 3.34 before, to 2.36 to 3.03 after medication administration. The mean differences ranged from 0.22 to 0.46, which are treatment effect sizes of 0.10 to 0.18. The decrease in peristalsis observed by the five reviewing radiologists after SL hyoscyamine sulfate administration was significant ( $df 1/182$ ,  $f=7.35$ ,  $p$

#### CONCLUSION

While cine MRE sequences show decreased bowel peristalsis after use of SL hyoscyamine sulfate, the small size of the observed treatment effect is likely insufficient to justify its use for MR enterography.

#### CLINICAL RELEVANCE/APPLICATION

While it is possible to detect and quantify decreased bowel peristalsis caused by a sublingual anti-spasmodic agent during cine MRE, the decrease is likely too small to be of clinical significance.

### **SST05-05 • Ischemic Colitis: Is There a Relationship between the CT Findings, the Different Etiologies and the Timing of the Disease? A Clinical Study**

**Francesca Iacobellis MD (Presenter) ; Daniela Berritto MD ; Maria Paola Belfiore ; Giuliano Gagliardi ; Mariano Scaglione MD ; Maria A Mazzei MD ; Roberto Grassi MD**

#### PURPOSE

To define the CT findings of ischemic colitis (IC), according to the different etiologies and timing of the disease.

#### METHOD AND MATERIALS

A computerized search of all medical records was used to retrospectively identify 130 patients who were admitted with the suspected diagnosis of IC over a five-year period. From these, 52 patients with IC proven by endoscopy with biopsies or surgical pathology were considered for the enrollment in the present study. Among 52 patients, 32 subjects (17 men and 15 women; median age 74, range 51-94 years) that underwent at least one CT examination, constituted the object of the analysis. Their medical history and CT examinations were retrospectively reviewed

#### RESULTS

Among the 32 CT examinations performed in the acute phase in 62.5% no defects or occlusion of the superior mesenteric artery (SMA) or inferior mesenteric artery (IMA) was found whereas in 37.5% IMA occlusion was detected. In acute phase in 100% of patients the presence of pericolic fluid was found, undergoing progressive resorption from acute to sub-acute phase if an effective reperfusion occurred; the bowel wall thickening was observed in 28.1% patients in acute phase and in 86.4% patients evaluated in sub acute phase. The unthickened colonic wall was found in all conditions where ischemia is not followed by effective reperfusion, 71.9% of cases, and it was never found in chronic phase, when the colon appears irregularly thickened.

#### CONCLUSION

The results of this study showed that particular attention should be paid in the diagnosis of non-occlusive mesenteric ischemia (NOMI) before reperfusion representing the more difficult form of IC to detect at imaging, diagnostic difficulties may also be encountered in sub acute forms where the colon wall thickening could be misdiagnosed as normal wall with collapsed lumen, and in chronic forms where the irregular thickening of large bowel could be misdiagnosed if the patient's clinical history is unknown. CT has a crucial role, it allows to define the morpho-functional alterations associated with the IC distinguishing among acute, sub acute and chronic phases and allows to estimate the timing of the ischemic damage.

#### CLINICAL RELEVANCE/APPLICATION

The definition of the CT findings of ischemic colitis in relationship with the etiology and the timing of the disease has a crucial role to ensure a correct diagnosis and an appropriate treatment.

### **SST05-06 • Double Contrast-enhanced Ultrasonography Diagnosis of Rectal Lesions with Pathologic Correlation**

**Man Lu PhD (Presenter) ; Zhiqing Cai ; Jun Song ; Bin Song MD**

#### PURPOSE

Recently, transabdominal ultrasonography with a gastrointestinal contrast agent has been used widely in China to detect digestive disorders. Double Contrast Enhanced Ultrasonography (DCUS) combines both a gastrointestinal luminal contrast agent with an intravenous contrast agent for imaging of lesions. The purposes of this pilot study were to assess the value of DCUS in the preoperative diagnosis of rectal lesions.

#### METHOD AND MATERIALS

#### RESULTS

Of the 227 patients examined, there were 232 rectal lesions ( 72 rectal adenocarcinomas, 45 adenomas and 15 inflammatory mass). The study using DCUS showed unique vascular patterns in different rectal lesions. Rectal adenocarcinoma revealed earlier AT and TP

compared with normal rectal tissue ( $p < 0.05$ ), earlier AT and higher PI with adenoma, earlier TP and lower PI with inflammatory mass. Rectal adenoma had lower PI compared with normal rectal tissue ( $p < 0.01$ ). Rectal inflammatory mass had higher PI and earlier AT compared with normal rectal tissue.

Conclusions: DCUS is a valuable technique for differential diagnosis of benign and malignant rectal lesions in patients with pathology diagnosis. The parameters of the enhancement curves reflect the different perfusion status of the rectal lesions.

#### CONCLUSION

DCUS is a valuable technique for differential diagnosis of benign and malignant rectal lesions in patients with pathology diagnosis. The parameters of the enhancement curves reflect the different perfusion status of the rectal lesions.

#### CLINICAL RELEVANCE/APPLICATION

DCUS is a valuable technique for differential diagnosis of benign and malignant rectal lesions in patients with pathology diagnosis

### **SST05-07 • Neurogenic Bowel Dysfunction in Spinal Cord Injury Patients - Diagnostic Using Functional MRI. A Feasibility Study**

**Celine D Alt MD (Presenter) ; Cornelia Putz ; Cornelia Hensel ; Bjoern Wagner ; Norbert Wagner ; Hans-Juergen Gerner ; Hans-Ulrich Kauczor MD \* ; Lars Grenacher MD**

#### PURPOSE

Neurogenic bowel dysfunction represents a common clinical problem in spinal cord medicine, which severely affects the quality of life following spinal cord injury (SCI). The aim of this study was to evaluate functional MRI as a diagnostic tool to visualize neurogenic bowel dysfunction in SCI patients.

#### METHOD AND MATERIALS

In this prospective study, 20 Th1-10 SCI patients (AIS A) given written informed consent and the study proposal was approved by the local ethics committee. Examination was performed at a 3T scanner in lateral position with angled legs. The rectum was filled with ultrasonic gel. The protocol included T2w truFISP sequences in three planes at rest and in sagittal plane during defecation (30 measurements) and T2w turbo spin echo images in sagittal and axial plane. Evaluation included the hiatal width (H-line), the M-line, the anorectal angle (ARA) and the anorectal junction (ARJ). The rectal filling volume and the maximum rectum diameter were noted, until defecation procedure started.

#### RESULTS

#### CONCLUSION

MR-Defecography is feasible in SCI patients and may help to differentiate between different types of neurogenic bowel dysfunction.

#### CLINICAL RELEVANCE/APPLICATION

Dynamic MRI may serve as a diagnostic tool to guide therapeutic decision making in SCI patients suffering from neurogenic bowel dysfunction.

### **SST05-08 • MR Imaging of Perianal Fistulas: Value of Using a Balloon Rectal Double Channel Catheter**

**Shuohui Yang MD (Presenter) ; Fang Lu MD ; Songhua Zhan MD ; Wenli Tan MD ; Qiong Zhu MD**

#### PURPOSE

To investigate the value of using balloon rectal double channel catheter (BRDCC) for the diagnosis of perianal fistula patients in conventional MRI studies.

#### METHOD AND MATERIALS

18 perianal fistula patients with BRDCC and 18 patients without BRDCC underwent MR scans with a body coil. The number of fistulas, the internal openings, extensions and abscesses were counted. All MR findings were utilized to evaluate for the classification of the fistulas and compared with the surgery results.

#### RESULTS

#### CONCLUSION

By using BRDCC, conventional MRI can provide more information of the fistulas and their routes.

#### CLINICAL RELEVANCE/APPLICATION

Providing evidences of internal openings, extensions and abscesses of the anal fistula diagnosis and directing the operation of anal fistula

### **SST05-09 • Rectal MRI of Fistula-in-ano: Diagnostic Values of Diffusion-weighted Imaging (DWI)**

**Minho Park MD (Presenter) ; Sung Kyoung Moon ; Seong Jin Park MD, PhD ; Joo Won Lim ; Dong Ho Lee MD ; Young Tae Ko MD, PhD**

#### PURPOSE

To investigate the diagnostic performance of DWI in fistula-in-ano.

#### METHOD AND MATERIALS

This study included 46 patients who underwent rectal MRI to evaluate fistula-in-ano from March 2011 to March 2012. A history of Crohn's disease (CD) and fistulectomy were reviewed. Two radiologists retrospectively reviewed rectal MRI with consensus three times at 2-week intervals. The first review assessed the presence of perianal lesions, fistula type, and lesion conspicuity with T2WI. The second review assessed fistula conspicuity with CE-FS-T1WI and T2WI. The third assessed fistula conspicuity with DWI with a b-value of 1000 and T2WI. Lesion conspicuity was scored from 1 to 4 as follows: 1, unclear fistula tract; 2, visible fistula tract with unclear margin; 3, distinct fistula tract with partial obscuration; and 4, distinct fistula without obscuration. The lesion conspicuity was compared between CE-FS-T1WI and DWI using the Wilcoxon rank-sum test. Lesion conspicuity according to the clinical history was assessed using the Mann-Whitney U-test.

#### RESULTS

Of the 46 patients, 39 had perianal lesions in rectal MRI: 30 patients with CD and 9 without. Nine patients (23.1%) had fistulectomy histories. There were 14 complex fistulas (35.90%), 12 intersphincteric fistulas (30.76%), 5 trans-sphincteric fistulas (12.82%), 4 perianal abscesses (10.26%), and 4 anal fissures (10.26%). The mean lesion conspicuity score of T2WI, CE-FS-T1WI, and DWI with a b-value of 1000 was  $3.11 \pm 0.689$ ,  $3.29 \pm 0.732$ , and  $3.55 \pm 0.724$ , respectively. There was no significant difference between CE-FS-T1WI and DWI ( $p=0.096$ ). Lesion conspicuity was significantly better with DWI than T2WI ( $p=0.010$ ). With DWI, lesion conspicuity was significantly better in the patients with CD than those without CD ( $p=0.004$ ).

#### CONCLUSION

The lesion conspicuity of DWI with a b-value of 1000 was similar to that of CE-FS-T1WI, and significantly better in the patients with CD.

#### CLINICAL RELEVANCE/APPLICATION

DWI with a high b-value could help to inform clinicians about fistula shape and type.



**SST06 • AMA PRA Category 1 Credit™:1.5 • ARRT Category A+ Credit:1.5****Moderator****Michael S Gee**, MD, PhD**Moderator****Aliya Qayyum**, MBBS \***SST06-01 • Image Quality on Liver CT Based on Sinogram Affirmed Iterative Reconstruction Algorithm****Boris Schulz MD (Presenter)**; **Boris Bodelle MD**; **Petra Siebenhandl**; **Martin Beeres MD**; **Firas Al-Butmeh**; **Claudia Frellesen**; **Thomas J Vogl MD, PhD****PURPOSE**

To evaluate efficiency of sinogram affirmed iterative reconstruction technique, regarding noise and image quality on contrast enhanced computed tomography (CT) of the liver.

**METHOD AND MATERIALS**

CT examinations were performed upon 32 patients (128 slice CT, 120kV, 180mAs, activated tube current modulation, 0.6mm collimation). Each examination was reconstructed at standard filtered back projection (FBP) and 5 different SAFIRE strengths in 5mm images in transversal direction with soft tissue kernel. Image noise was defined as standard deviation (SD) of Hounsfield units (HU) in air, and signal to noise ratio (SNR) of the liver was defined as mean liver HU per liver SD. Subjective image quality was evaluated by three raters using a 5-point scale (1=non-diagnostic image quality, 5=excellent image quality).

**RESULTS**

Average image noise was 6.2HU (FBP), vs. 5.7HU (SAFIRE 1), vs. 5.0 (SAFIRE 2) 4.4HU (SAFIRE 3), 3.8HU (SAFIRE 4), 3.1HU (SAFIRE 5). SNR of the liver consecutively increased when using the iterative reconstruction algorithms from 8.4 (FBP) to 9.3 (SAFIRE 1) to 10.4 (SAFIRE 2) to 12.2 (SAFIRE 3) to 15.1 (SAFIRE 4) to 17.5 (SAFIRE 5). The differences in image noise and SNR of each SAFIRE-strength to FBP was statistically significant (p

**CONCLUSION**

Sinogram affirmed based iterative reconstruction technique significantly reduces image noise and increases SNR for examinations of the liver. However subjective image quality decreases with strong iterative strengths.

**CLINICAL RELEVANCE/APPLICATION**

Since subjective image quality decreased slightly with iterative reconstructive techniques, mild iterations are recommended to enhance image quality on liver CT.

**SST06-02 • The Clinical Utility of Diffusion-weighted-Imaging of the Abdomen with Ultra-high B-values****Melissa Ong MD (Presenter)**; **Johannes Budjan MD**; **Stefan Haneder MD**; **Stefan O Schoenberg MD, PhD \***; **Ulrike I Attenberger MD \***; **Henrik J Michaely MD \*****PURPOSE**

To evaluate the clinical utility of diffusion-weighted-imaging (DWI) of the abdomen with ultra-high b-values.

**METHOD AND MATERIALS**In this retrospective IRB approved study 46 consecutive patients (30 women, 16 men, mean age 54±17.5) who underwent abdominal MR-exams including a DWI-EPI sequence with b-values of 50, 800 and 2000 s/mm<sup>2</sup> on a 3T MRI-system (Siemens Skyra) were included. Overall image quality with regard to detection of pathology and degree of artifacts as well as lesion conspicuity in the b800 and b2000 images were compared by two board-certified radiologists (1: preferring b2000; 2: preferring b800; 0: no difference). Quantitative analysis included determination of signal-to-noise ratio of sample tissues including the kidneys and the ventral and dorsal subcutaneous fat.**RESULTS**

Reader 1 preferred the b2000 image in 30 (67%) patients, reader 2 in 32 (71%) patients. The b800 image was preferred in only 2 (4%) patients by both readers. Interobserver agreement was k=.706 for overall image quality. Lesion conspicuity was rated better in the b2000 images in 31 (69%) patients and the b800 images in 1 (2%) patient by reader 1, in 27 (60%) and 2 patients (4%) by reader 2. Measure of agreement was k=.494 for lesion conspicuity. There were no differences observed regarding artifacts. The signal-to-noise ratio measured 37.47 (±14.96) vs. 15.74 (±4.07) and 41.46 (±16.21) vs. 16.90 (±5.52) in the b800 and b2000-images for the left and right kidney, 9.22 (±3.18) vs. 12.05 (±3.75) and 9.80 (±2.52) vs. 12.14 (±2.93) for the ventral and dorsal fat, respectively.

**CONCLUSION**DWI imaging of the abdomen with ultra-high b-values of 2000 s/mm<sup>2</sup> is feasible for lesion detection with good to acceptable image quality.**CLINICAL RELEVANCE/APPLICATION**

Ultra-high b-values should be used in a clinical routine as a feasible tool for lesion detection.

**SST06-03 • Multiphasic Contrast Enhanced Free Breathing 3D Imaging and Liver Perfusion Mapping Using Through-time 3D Spiral GRAPPA Acceleration****Yong Chen**; **Gregory R Lee**; **Katherine Wright**; **Mark A Griswold PhD \***; **Nicole Seiberlich PhD \***; **Vikas Gulani MD, PhD (Presenter) \*****PURPOSE**

The goal of this work is to demonstrate high spatiotemporal resolution quantitative DCE liver MRI using a 3D stack-of-spirals acquisition, through-time non-Cartesian GRAPPA reconstruction, non-rigid body motion correction, and application of a dual-input single compartment model for quantitative perfusion mapping.

**METHOD AND MATERIALS**

MRI experiments were performed on a Siemens 3T Skyra scanner with normal volunteers (N = 4), and 0.1 mmol/kg Gadobenate (Multihance, Bracco, NJ) was given. T1-weighted 3D volumes were acquired using a stack-of-spirals gradient echo sequence. 120 volumes were acquired with a temporal resolution of 1.6~1.9 seconds, while the subjects were breathing freely. To accelerate the acquisition, data were undersampled in-plane with a reduction factor of 6, and reconstructed using through-time non-Cartesian GRAPPA. The reconstructed volumes were registered using FMRIB's Non-linear Image Registration Tool (FNIRT). A dual-input single-compartment model was established to retrieve liver perfusion parameters from DCE-MRI data.

**RESULTS**Images with high spatial resolution of 1.9x1.9x3 mm<sup>3</sup> are obtained with whole liver coverage. With the high imaging speed of less than 2 sec/volume, a free-breathing scan is achieved, and subtle dynamic changes in contrast enhancement are captured. The free-breathing 3D images were registered with almost no residual motion in liver tissue. Quantitative whole liver 3D perfusion maps were obtained and the perfusion parameters are all in good agreement with published literature from CT and MR.**CONCLUSION**

In this study, a high spatiotemporal resolution 3D liver imaging technique was developed using a stack-of-spirals acquisition and

through non-Cardesian GRAPPA acceleration. This technique allows fast imaging of the whole liver during free breathing and accurate quantification of liver perfusion.

#### CLINICAL RELEVANCE/APPLICATION

Free-breathing abdominal scans with through-time spiral GRAPPA can provide diagnostic images from patients with difficulty breath-holding and additional quantitative information of liver perfusion.

### **SST06-04 • 4D Flow MRI with k-t GRAPPA in the Quantitative Assessment of PV Hemodynamics in Patients with Advanced Liver Cirrhosis: Initial Results and Comparison to Age-matched Controls**

**Zoran Stankovic MD (Presenter) ; Edouard Semaan ; Michael Markl PhD ; Marie Wasielewski ; Maria Carr ; Robert J Lewandowski MD \* ; Riad Salem MD, MBA \* ; James C Carr MD \* ; Jeremy D Collins MD \***

#### PURPOSE

To qualitatively and quantitatively evaluate blood flow hemodynamics in the portal venous (PV) system of patients with advanced liver cirrhosis compared to age-matched controls at non-contrast 4D flow MRI with contrast-enhanced 4D flow MRI as the standard of reference.

#### METHOD AND MATERIALS

In an ongoing study, time-resolved 4D flow MRI was applied at 3T ( $v_{enc}=50\text{cm/sec}$ , spatial resolution= $2.1\times 2.5\times 3.0\text{mm}^3$ ) with and without a blood pool contrast agent in 20 datasets representing 5 patients with advanced liver cirrhosis (age= $55\pm 6$ years) compared to 5 healthy age-matched controls (age= $53\pm 9$ years). k-t GRAPPA was used with an acceleration factor  $R=5$  to reduce scan time. 3D PV flow visualization based on 3D streamlines and time-resolved particle traces. Flow quantification was performed in the PV system with retrospective extraction of time-resolved peak velocities and net flow over the cardiac cycle. Bland Altman (BA) analyses compared the datasets before and after contrast application (mean bias $\pm 2$ SD).

#### RESULTS

Qualitative image analysis was successfully performed in the PV system with clear resolution of all branches except the superior mesenteric vein in one patient. Quantitative analyses demonstrated similar results before and after contrast for peak velocities (BA: $0.012\pm 0.029$ ), while net flow values demonstrated a -7% bias for the non-contrast analysis (BA: $-0.141\pm 0.412$ ). Comparing patients with liver cirrhosis and age-matched controls significant differences for peak velocities were seen only in the intrahepatic portal vein before and in the right intrahepatic portal vein branch after contrast application (p

#### CONCLUSION

4D flow MRI enabled quantitation of comprehensive 3D flow characteristics in the portal venous system in patients with liver cirrhosis and visualized abnormal blood flow hemodynamics. Non-contrast 4D flow MRI analyses demonstrated similar peak velocity assessment compared to a contrast-enhanced acquisition, although net flow was underestimated by 7%; field inhomogeneities may have accounted for the bias in net flow.

#### CLINICAL RELEVANCE/APPLICATION

4D flow MRI may improve quantification of altered liver blood flow hemodynamics in patients with advanced liver cirrhosis enabling quantitative analysis without Gadolinium based contrast media.

### **SST06-05 • Quantification of Hepatic Blood Flow, ADC and Stiffness in Fasting and Post-prandial Conditions: Prospective Study at 3T**

**Guido H Jajamovich PhD (Presenter) ; Hadrien Dyvorne PhD ; Ersin Bayram PhD \* ; Claudia Donnerhack ; Richard L Ehman MD \* ; Bachir Taouli MD \***

#### PURPOSE

Techniques such as MR Elastography (MRE), phase contrast (PC) and diffusion-weighted imaging (DWI) have potential for non-invasive detection of liver fibrosis, cirrhosis and portal hypertension. Since portal flow and liver stiffness (LS) may be altered by food intake, changes in LS, portal vein (PV) flow, PV velocity and liver ADC might be observed and may lead to decreased reproducibility. This prospective study quantifies reproducibility (in fasting conditions) and post-prandial changes in PV flow/velocity, LS, and liver ADC at 3T.

#### METHOD AND MATERIALS

11 healthy volunteers and 7 patients with HCV cirrhosis were enrolled in this prospective IRB approved study. All subjects underwent 3T MRI (MR750, GE Healthcare), including 2D PC (pulse triggered,  $V_{ENC}=50\text{ cm/s}$ , slice perpendicular to portal vein), axial SS EPI DWI (free breathing, 16 b-values from 0 to  $800\text{ mm}^2/\text{s}$ ) and MRE (4 slices through the liver). All subjects were initially scanned twice after 6 hours of fasting to assess reproducibility of each technique, and then scanned again 20 minutes after a 700 Kcal liquid meal. To quantify PV flow and velocity, a ROI was drawn in the PV on PC images. Mean LS and liver ADC were obtained by placing a ROI in the right hepatic lobe on LS maps and diffusion images. The coefficients of variation (CV) were computed for the two scans in fasting state. Wilcoxon paired tests and Mann-Whitney U tests were performed to assess differences in these metrics before and after caloric intake (average from the 2 fasting scans was used for comparison) and differences between patients and volunteers, respectively.

#### RESULTS

PV flow, PV velocity, liver ADC and LS showed good to excellent reproducibility in fasting state, with CVs ranging from 3.6%-11.8%. PV flow, PV velocity and LS were all significantly higher in postprandial state (p

#### CONCLUSION

These results indicate that caloric intake is a factor to consider in interpreting PC-based PV flow/velocity and MRE-based hepatic stiffness measurements. LS can be used to separate cirrhotic patients from healthy volunteers.

#### CLINICAL RELEVANCE/APPLICATION

Liver blood flow and metabolism (portal venous flow/velocity and liver stiffness) are altered significantly in the postprandial state, showing the importance of undergoing MRI in a controlled state.

### **SST06-06 • Start of Hepatocyte Uptake in Gadoxetate Disodium (Gd-EOB-DTPA) Enhanced MRI in Normal Liver Parenchyma**

**Hanke Schalkx MD (Presenter) ; Marijn Van Stralen PhD ; Kenneth Coenegrachts MD ; M.A.A.J. van den Bosch ; Wouter B Veldhuis MD, PhD ; Maarten S Van Leeuwen MD, PhD**

#### PURPOSE

To evaluate the enhancement pattern of normal liver parenchyma in contrast-enhanced (CE) magnetic resonance imaging (MRI) using gadoxetate disodium, with special emphasis on the start of the hepatocyte uptake.

#### METHOD AND MATERIALS

23 patients without chronic liver disease underwent CE-MRI with gadoxetate disodium (Gd-EOB-DTPA, Primovist or Eovist, Bayer, Netherlands) on a 1.5T MRI system (Philips, Best, The Netherlands) using a 4D-THRIVE key-hole protocol [1] resulting in a total of 17 3D-acquisitions up to 20 minutes. After contrast administration of  $0.25\text{ mmol/kg}$  gadoxetate disodium at  $1\text{ ml/s}$  the first dynamic scan ( $t=0$ ) was triggered on left ventricle filling. Signal intensity of liver parenchyma was measured on all scans, averaged over 3 regions-of-interest. Parenchymal enhancement was calculated as the relative signal intensity (SI) increase with respect to pre-contrast parenchymal intensity.

#### RESULTS

The initial, portal phase induced, parenchyma peak with a relative SI of 0.53 (SD=0.18) occurred at mean  $37.6\text{ s} \pm \text{SD } 14.3\text{ s}$ . After the initial peak, 12/21 patients (57%) showed gradual increase in enhancement until 20 min. In 2/21 patients (2%) enhancement remained within  $-/+ 5\%$  of the initial peak intensity. After the initial peak, 7/21 Patients (33%) demonstrated a decrease in SI of minimal 10% before parenchymal intensity gradually increased up to 20 min. The decrease in enhancement occurred at  $68.9\text{ s} \pm 7.8\text{ s}$  and max 76 sec.

## CONCLUSION

After the initial, dynamic phase induced, parenchyma peak, three different enhancement patterns were observed. Increase in parenchymal enhancement due to gadoxetate disodium uptake started at mean 37.6 sec, and no later than 76 sec. [1] Beck, G.M., et al., J Magn Reson Imaging, 2008. 27(6): p. 1461-7.

## CLINICAL RELEVANCE/APPLICATION

In CE-MRI after gadoxetate disodium, hepatocyte uptake already influences parenchymal enhancement in the early dynamic phases, potentially influencing lesion detection and characterization.

### **SST06-07 • Gadobenate Dimeglumine Enhanced Liver MRI: Quantitative Analysis of Hepatobiliary Phase According to Incremental Flip Angle**

**Eunjung Lee** (Presenter) ; **Dae Jung Kim** MD

#### PURPOSE

To evaluate effects on hepatobiliary phase with using gadobenate dimeglumine (BOPTA) enhanced 3D T1-weighted (T1) gradient echo sequence (GRE) magnetic resonance imaging (MRI) during increasing the flip angle.

#### METHOD AND MATERIALS

A total of 43 patients, who had a BOPTA enhanced MR exam for evaluation of focal lesion in the liver, were enrolled during three months. Hepatobiliary phase fat suppressed 3D T1 GRE sequences with 10°, 20°, 30° flip angles (FAs) were obtained at 90 min. Signal intensity (SI) of the liver in precontrast phase and hepatobiliary phase with each FAs was measured using region-of-interest (ROI), as large as possible, 2 times measurement at each hemiliver. Noise estimates were derived by recording three times the standard deviation of the noise measured anterior to the liver, outside of the body. SI of each hepatic lesions (long axis = 10 mm) in hepatobiliary phase with each FAs was also measured using ROI, as large as possible. The relative enhancement (RE) of liver parenchyma at hepatobiliary phase with each FAs was calculated, as following:  $RE = (SI\text{-post} - SI\text{-pre})/SI\text{-pre}$ . The signal to noise ratio (SNR) of liver parenchyma at hepatobiliary phase with each FAs was calculated, as following:  $SNR = SI\text{-liver} / SI\text{-noise}$ . The lesion-to-liver contrast to noise ratio (CNR) at hepatobiliary phase with each FAs was calculated, as following:  $CNR = (SI\text{-lesion} - SI\text{-liver}) / SI\text{-noise}$ . Analysis of variance with the Sheffe method was used to evaluate statistical significance of the differences in RE, SNR and CNR values, according to the each FAs.

#### RESULTS

The RE values of hepatic parenchyma was significantly different in each FAs (10°, RE=0.73; 20°, RE=0.65; 30°, RE=0.52; p=0.002). The SNR of hepatic parenchyma values was not significantly different in each FAs (10°, SNR=26.3; 20°, SNR=25; 30°, SNR=23.3; p=0.093). Twenty five patients out of all patients had 41 lesions, which were consisted with 5 benign lesions and 36 malignant lesions. The CNR of lesions was not significantly different in each FAs (10°, CNR=-5.9; 20°, CNR=-7.9; 30°, CNR=-8.1; p=0.223).

#### CONCLUSION

Increasing the FA on hepatobiliary phase of BOPTA enhanced MRI affects only relative hepatic parenchyma enhancement.

#### CLINICAL RELEVANCE/APPLICATION

Hepatobiliary phase with high degree of flip angle on BOPTA enhanced MRI decreased only hepatic parenchyma enhancement and didn't affect contrast noise ratio of the lesion.

### **SST06-08 • Respiratory Motion Artifact Affecting Arterial-phase Imaging-Comparison of Gadoxetate Disodium and Gadobenate Dimeglumine and Exam Recovery Using Multi-arterial Phase Acquisitions**

**Jason A Pietryga** MD (Presenter) ; **Lauren M Burke** MD ; **Tracy A Jaffe** MD ; **Mustafa R Bashir** MD \*

#### PURPOSE

To compare the rates of moderate/severe respiratory motion artifact on arterial-phase magnetic resonance imaging (MRI) when using gadoxetate disodium versus gadobenate dimeglumine intravenous contrast, and to assess if obtaining multiple arterial phases salvages some studies with motion.

#### METHOD AND MATERIALS

This is an IRB-approved HIPAA-compliant study. A retrospective search identified consecutive outpatients who had undergone contrast-enhanced MR imaging of the abdomen using either gadoxetate disodium or gadobenate dimeglumine over a period of three months using identical imaging protocols. Three board-certified radiologists (blinded to the contrast agent used) independently reviewed the following T1-weighted series for motion artifact: precontrast, three rapid arterial phases obtained in a single breath hold, portal venous phase, and late dynamic phase. Series were scored for severity of respiratory motion on a scale of 1(none) to 5 (nondiagnostic), and timing of each arterial phase was assessed. Motion scores were compared between exams obtained with the two contrast agents for: number of exams with new (not present on precontrast phase) moderate (motion =3) or severe (=4) motion on at least one arterial phase, and exams where at least one well-timed late arterial phase had less than severe (

#### RESULTS

275 qualifying examinations were identified (166-gadoxetate/109-gadobenate). Exams performed with gadoxetate had higher rates of new moderate (42.8% vs. 16.8%, p

#### CONCLUSION

Transient moderate and severe motion artifact in the hepatic arterial phase occurs at a higher rate with gadoxetate disodium than with gadobenate dimeglumine. A multi-arterial phase acquisition scheme can recover a proportion of those examinations partially affected by arterial phase motion.

#### CLINICAL RELEVANCE/APPLICATION

Increased rates of significant motion artifact are seen when imaging the liver in the arterial phase with gadoexetate contrast vs. dimeglumine. Multi-arterial phase acquisition may salvage some exams.

### **SST06-09 • Liver MRI with Gadofosveset Trisodium**

**Laurent Milot** MD, MSc (Presenter) ; **Shoichet Martin** MD ; **Helen Cheung** MD ; **Caitlin T McGregor** MD ; **Megan Snoyer** ; **Masoom A Haider** MD \* ; **Liang Zeng** ; **Chirag Patel** MBBS, MRCP ; **George Tomlinson** ; **Calvin Law** MD, FRCPC

#### PURPOSE

To illustrate the benefits and limitations of liver imaging performed with an intravascular blood pool agent Gadofosvest Trisodium (Gadfos) compared with an extracellular Gadolinium (EcGd) agent Gadobutrol.

#### METHOD AND MATERIALS

#### RESULTS

#### CONCLUSION

Enhancement pattern of background vessels/liver parenchyma and benign lesions is similar for both agents but Ablavar does not accumulate in metastatic lesions over time, a key differentiating feature. Pitfall may exist in some cases of NET.

#### CLINICAL RELEVANCE/APPLICATION

Liver imaging with Ablavar may help in the characterization of small equivocal liver lesions, especially in the context of patients with known adenocarcinoma.

**SST07 • AMA PRA Category 1 Credit™:1.5 • ARRT Category A+ Credit:1.5****Moderator**  
**Raj M Paspulati**, MD  
**Moderator**  
**Julia R Fielding**, MD**SST07-01 • A New Look at the Female Pelvis: Ultra-high-Field (7T) MR Imaging****Lale Umutlu** MD (Presenter)\*; **Oliver Kraff** MSc; **Sonja Kinner** MD; **Anja Fischer** MD; **Stefan Maderwald** PhD, MSc; **Michael Forsting** MD; **Mark E Ladd** PhD; **Thomas C Lauenstein** MD**PURPOSE**

MR imaging of the female pelvis has been established in clinical diagnostics for the assessment of possible uterine or ovarian pathologies. The increase of the magnetic field strength to 3 Tesla pelvis MRI has been proven beneficial with regards to improvement of the spatial resolution. Hence, with the successful introduction of 7 T MRI to in-vivo research body imaging, the aim of this study was to investigate the feasibility and diagnostic potential of 7 T contrast-enhanced MR imaging of the female pelvis.

**METHOD AND MATERIALS**

14 healthy female volunteers were examined on a 7T whole-body MR system (Magnetom 7T, Siemens Healthcare) utilizing a custom-built 8-channel transmit/receive radiofrequency body coil suitable for RF-shimming. The examination protocol included: 1) T1w fs 2D FLASH 2) T1w fs 3D FLASH 3) T2w TSE. For dynamic imaging, Gadobutrol was injected intravenously and 4 repetitive T1w 3D FLASH sequences were obtained. For visual qualitative image analysis of T1w imaging two readers assessed the delineation of (1) pelvic anatomy, (2) of vasculature, (3) tissue contrast and (4) overall image quality was assessed using a five-point scale (5= excellent vessel delineation to 1= non-diagnostic). For T2w MRI, the zonal anatomy of the uterus and the conspicuity of the ovaries were evaluated. Additionally, image impairment due to artifacts was assessed.

**RESULTS**

For the T1w sequences, 2D FLASH imaging was rated with higher scores for all assessed structures than 3D FLASH MRI, with highest scores for overall image quality (meancontrast-enhanced2D FLASH 4.80) and tissue contrast (meancontrast-enhanced2D FLASH 4.90). T2w TSE imaging yielded a moderate to high delineation of the zonal anatomy of the uterus with mean scores ranging from 3.60 for endometrium to 4.75for myometrium. Overall image impairment due to artifacts was rated strongest for T2w MRI (2.90) and least for 2D FLASH MRI (mean 4.05).

**CONCLUSION**

This pilot study of dedicated 7 Tesla MRI of the female pelvis demonstrates the feasibility and potential of in vivo ultra-high-field pelvic imaging, providing good overall image quality and transitioning the associated higher SNR into high spatiotemporal resolution imaging.

**CLINICAL RELEVANCE/APPLICATION**

The high-quality delineation of anatomical details and non-enhanced vasculature may lead to a more accurate diagnosis of pelvic parenchymatous and vasculature disease using 7T MRI.

**SST07-02 • Spectrum of Pelvic Venous Congestion in Pudendal Neuralgia in Female Patients****Olga M Kalinkin** MD (Presenter); **Rohit Khanna** MD; **Diana Atashroo** MD; **Andrea Chen** MD; **Michael Hibner** MD, PhD**PURPOSE**

Pudendal neuralgia is a painful condition with poorly understood etiology. Dilated vessels accompanying the pudendal nerve in anatomically narrowed spaces may cause extrinsic mass effect on the nerve. We are evaluating the presence of pelvic venous congestion in the patients with pudendal neuralgia.

**METHOD AND MATERIALS**

A retrospective analysis of the dedicated contrast enhanced pelvic MRI examination performed for 146 female patients with pudendal neuralgia clinically assessed by pelvic surgeons specialized in treatment of pudendal neuralgia. Diameter and localization of dilated venous vessels along the course of pudendal nerve in the interligamentous space, Alcock's canal, at the inferior rectal branch, perineal branch, dorsal clitoral branch, caliber of vessels of the parauterine or paravaginal (in case of hysterectomy) venous plexus were assessed. Correlation of type of pelvic venous congestion with clinical symptom laterality was performed.

**RESULTS**

Among 146 female patients, 81 patients (55%), aged from 26 to 79 years, were found to have dilated venous pelvic vessels. Supralelevator pelvic venous congestion is identified as dilatation of parauterine or paravaginal venous plexus without or with focally dilated vessels along the course of pudendal nerve in 34 and 28 patients respectively. Infralevator pelvic venous congestion as isolated dilated vessels in Alcock's canal or interligamentous space and focally dilated small branches of pudendal nerves was seen in 13 patients and 6 patients respectively. 57 patients (90%) with supralelevator pelvic venous congestion have bilateral site of pain or bilaterality of physical exam findings. In 7 from 19 patients the presence of isolated dilated veins along the pudendal nerve in Alcock's canal or interligamentous space (infralevator unilateral pelvic congestion) are not associated with laterality of pain or symptoms.

**CONCLUSION**

Spectrum of pelvic venous congestion in the female patients with pudendal neuralgia is ranging from diffuse supralelevator parauterine (paravaginal) venous plexus dilatation to isolated infralevator focal venous dilatation of pudendal veins in Alcock's canal or interligamentous spaces or small venous varices along the branches of pudendal veins.

**CLINICAL RELEVANCE/APPLICATION**

Differentiation of supralelevator versus infralevator pelvic venous congestion may guide the pelvic surgeon to select an appropriate treatment with gonadal vein ligation versus focal venosclerotherapy.

**SST07-03 • Urinary Bladder Neck Dysfunction in Male Patients: Evaluation with MRI and with Voiding MR-Cystourethrography****Marco Di Girolamo** MD (Presenter); **Alberto Trucchi**; **Ines Casazza**; **Matteo Cappucci** MD; **Andrea Tubaro**; **Vincenzo David** MD**PURPOSE**

To evaluate with MRI male patients with urinary bladder neck dysfunction, studying the anatomical aspect of bladder neck and performing voiding MR-cystourethrography.

**METHOD AND MATERIALS**

We have evaluated with MRI 21 male patients with urinary bladder neck dysfunction diagnosed with pressure-flow study. All the patients had undergone US in the month proceeding MRI and patients with BPH were excluded. The MR examinations were performed with an 1.5 Tesla superconductive magnet with the patient placed in supine position and using a phased-array body coil. The patients had urine-filled bladders and sagittal and oblique coronal TSE T2-weighted scans were performed (TR:6250ms; TE:90ms;sl.thick.:3mm; acq.time:3'38"). The oblique coronal scans were parallel to the plane of the bladder neck. 15 patients underwent also voiding MR-cystourethrography

performed with T1-weighted spoiled 3D gradient-echo acquisitions on sagittal plane performed (TR:12ms; TE:2,7ms; flip-angle:40°; sl.thickness: 2mm; acq.time:12s) after the filling of bladder lumen with contrast-material-enhanced urine obtained by the i.v administration 20 mg of furosemide followed by the i.v. administration of ¾ of the normal dose of a paramagnetic contrast agent (Magnevist, Bayer Pharma, Germany).

#### RESULTS

The entire MR examination lasted no longer than 10 minutes for each patient. We detected 18 patients with abnormality of smooth muscular structures of the bladder neck and 3 patients with bladder neck cyst. MRI allowed a perfect evaluation of the different smooth detrusor muscles of the bladder neck. In patients with the typical urinary bladder neck dysfunction, we detected the hypertrophy of posterior smooth muscular structures of bladder neck and the kyphosis of prostatic urethra. Only 6 patients were able to perform voiding MR-cystourethrography that showed the characteristic radiological features.

#### CONCLUSION

MRI with voiding MR-cystourethrography could be performed in male patients with bladder outlet obstruction in order to visualize the anatomical aspect of the bladder neck. These anatomical information are useful to determine the causes of voiding obstruction, to diagnose urinary bladder dysfunction and to establish the best therapeutic approach.

#### CLINICAL RELEVANCE/APPLICATION

MRI with voiding MR-cystourethrography could be performed to diagnose urinary bladder neck dysfunction and can substitute conventional retrograde and voiding cystourethrography

### **SST07-04 • The Value of Dynamic Magnetic Resonance Imaging in Interdisciplinary Treatment of Pelvic Floor Dysfunction**

**Ulrike I Attenberger** MD (Presenter) \* ; **John N Morelli** MD ; **Alexander Herold** ; **Peter Kienle** MD, PhD ; **Werner Kleine** ; **Axel Hacker** ; **Christopher Baumann** ; **Julia Heinzlbecker** ; **Stefan O Schoenberg** MD, PhD \* ; **Henrik J Michaely** MD \*

#### PURPOSE

To determine the value of dynamic pelvic floor MRI relative to standard clinical examinations in treatment decisions made by an interdisciplinary team of specialists in a center for pelvic floor dysfunction

#### METHOD AND MATERIALS

60 women were included in this IRB approved retrospective analysis. All patients were referred for dynamic pelvic floor MRI by an interdisciplinary team of specialists of a pelvic floor center. All patients were clinically examined by an urologist, gynecologist, a proctological and colorectal surgeon. The specialists assessed individually and in consensus, whether (1) MRI provides important additional information not evident by physical examination and in consensus whether (2) MRI influenced the treatment strategy and/or (3) changed management or the surgical procedure.

#### RESULTS

MRI was rated essential in the treatment decisions of 22/50 cases, leading to a treatment change in 13 cases. In 12 cases, an enterocele was diagnosed by MRI but was not detected on physical exam. In 4 cases an enterocele and in 2 cases a rectocele were suspected clinically but not confirmed by MRI. In 4 cases, MRI proved critical in assessment of rectocele size. Vaginal intussusception detected on MRI was likewise missed by gynecologic exam in 1 case.

#### CONCLUSION

MRI allows diagnosis of clinically occult enteroceles, by comprehensively evaluating the interaction between the pelvic floor and viscera. In nearly half of cases, MRI changed management or the surgical approach relative to the clinical evaluation of an interdisciplinary team. Thus, dynamic pelvic floor MRI represents an essential component of the evaluation for pelvic floor disorders.

#### CLINICAL RELEVANCE/APPLICATION

In an interdisciplinary center for pelvic floor disorders dynamic pelvic floor MRI leads to a significant change in clinical management

### **SST07-05 • Cervical Evaluation by Virtual Hysterosalpingography before Embryo Transfer**

**Javier Vallejos** MD (Presenter) ; **Patricia M Carrascosa** MD \* ; **Carlos Capunay** MD ; **Ana Carla L Vasconcelos** MD ; **Mariano Baronio** ; **Jorge M Carrascosa** MD

#### PURPOSE

To compare cervical catheter test and virtual hysterosalpingography (VHSG) in the evaluation of cervix before embryo transfer.

#### METHOD AND MATERIALS

We evaluated 100 patients with history of infertility. The day of examination, a gynaecologist performed a cervical test with a Wallace catheter. Then, patients underwent VHSG performed with a 256-slice CT scanner. CT images were evaluated by a radiologist, and the cervical patency, utero-cervical angle and the presence of cervical pathology were determined.

#### RESULTS

There was a good correlation ( $r=0,92$ ) in cervical patency evaluation between both methods. Unsuccessful cervical catheter test was observed in 35% of patients. In these patients, Virtual HSG detected polyps, adhesions and sinuous cervical canal, while cervix was normal in 23 patients, but the utero-cervical angle was  $< 90^\circ$ .

#### CONCLUSION

Virtual HSG findings correlate with cervical catheter test in the evaluation of cervical patency. Moreover virtual HSG provides anatomic information useful to identify the probable cause of failure of embryo transfers and prevent them.

#### CLINICAL RELEVANCE/APPLICATION

Virtual HSG allows a complete description of the cervical canal, providing important prognostic information to the gynecologist prior to the completion of embryo transfer.

### **SST07-06 • Value of Contrast Enhanced Sonography in Acute Pelvic Pain in Women and Children: Initial Experience**

**Sandrine Chapuy** (Presenter) ; **Philippe Manzoni** MD ; **Adrian I Kastler** MD, MSc ; **Sebastien L Aubry** MD, PhD ; **Bruno A Kastler** MD, PhD

#### PURPOSE

To study the feasibility and value of contrast enhanced ultrasound (ECUS) in acute pelvic pain in women and children.

#### METHOD AND MATERIALS

Seventeen adnexal torsion were included in this retrospective study (16 patients from 21 days to 58 years, including 3 pregnant women) after local ethics committee approval between 2008 and 2012. ECUS imaging findings were compared to regular non enhanced US and to either pathological findings in case of surgery and to follow up imaging in the remaining cases.

#### RESULTS

Thirteen adnexal torsion were confirmed, 9 of which occurred on a pathological ovary. ECUS sensitivity and positive predictive value were 84.6%. We report two cases of false negative and two cases of false positive. Ovary Vascularization assessment was possible in all 13 cases as opposed to 30.8% in Doppler mode, showing hypovascularization of ovary in ECUS in 58.8% against 15.4% in Doppler mode. In the three cases of ECUS performed pregnant women, imaging findings showed no transplacental passage. No adverse events were noted in all cases.

#### CONCLUSION

Our study showed that ECUS allowed accurate diagnosis of adnexal torsion in 84.6% of cases. ECUS is a feasible, safe and useful tool in the assessment of acute pelvic pain in women and children.

#### CLINICAL RELEVANCE/APPLICATION

Contrast enhanced US is a useful tool in the early diagnosis of adnexal and provides crucial information on ovary perfusion which may help conservative surgical management

### SST07-07 • Comparison of the Pelvic Floor before Pregnancy and 6 Weeks after Delivery: An MRI Study

**W. Thomas Gregory MD ; Terri E Reichner MD ; Amanda Holland BS ; Amy S Thurmond MD (Presenter) \***

#### PURPOSE

Pelvic organ prolapse is linked to parity, and for millennia has resulted in stress urinary incontinence and other symptoms which affect large numbers of women and limit their ability to work and socialize. We used MRI to evaluate changes in the pelvic floor before and after a first pregnancy. We compared these changes between those undergoing cesarean delivery and those having a vaginal delivery.

#### METHOD AND MATERIALS

This is a subgroup from an ongoing prospective cohort study of nulliparous women planning pregnancy. Participants have a standardized evaluation before pregnancy (Visit 1), 6 weeks after delivery (Visit 2), and then 6 months after delivery (Visit 3). At all three visits the participant has an interview with questionnaire, clinical pelvic exam, transperineal and endoanal 3D ultrasound, electromyography (EMG) of the pelvic floor and anal sphincter muscles, and pelvic MRI using a 3 Tesla magnet. This report focuses on MRI findings of the women who have completed Visits 1 and 2.

#### RESULTS

In 42 women, there was no significant change in bony measurements before and after pregnancy and delivery. There were however significant differences in the soft tissue measurements, including statistically significant inferior position of the bladder neck 6 weeks after delivery in all women, which was related to descent of the puborectalis muscle. This was more pronounced following vaginal delivery (31 women) compared to cesarean delivery (15 women). This was particularly evident during the dynamic maneuvers of kegel and valsalva. Interestingly, the pre-pregnancy values of bladder neck descent were larger in the women who ended up needing cesarean delivery.

#### CONCLUSION

Our data supports observations that after a first pregnancy women who had a vaginal delivery are 5 to 6 times more likely to have measurable pelvic prolapse than women who had cesarean delivery. Universal cesarean delivery to avoid future pelvic prolapse would not however be safe or cost effective. The comparison of pelvic structures in the same woman before and after delivery has not been done before, and may help us predict the women in whom the benefits of cesarean delivery for maintaining pelvic support, outweigh the risks.

#### CLINICAL RELEVANCE/APPLICATION

This is the first large study to image the pelvic floor anatomy in women before and after their first delivery of a child.

### SST07-08 • Endometriosis: Is there a Way to Differentiate between Silent Fibrotic Adhesions and DIE with MRI?

**Lucia Manganaro MD ; Valeria Vinci MD (Presenter) ; Silvia Bernardo MD ; Paolo Sollazzo ; Maria Eleonora Sergi MD ; Matteo Saldari ; Carlo Catalano MD**

#### PURPOSE

Feasibility of contrast enhanced (CE) MRI with rectal filling to differentiate between recto-sigmoid DIE and silent fibrotic adhesions, and to assess the severity of infiltration.

#### METHOD AND MATERIALS

From October 2011 and April 2013 We enrolled 18 women coming with either ultrasound or clinical suspect of posterior endometriosis. We performed a pelvic MRI examination on 1.5T system, with intravenous administration of gadobenate dimeglumine (Gd-BOPTA) and rectal filling with ultrasonographic gel. We evaluated the presence of recto-sigmoid involvements and its nature by taking in consideration the different CE behaviour. All patients underwent to laparoscopy within 1 month from MRI.

#### RESULTS

MRI diagnosed posterior cul-de-sac obliteration in 15/18 patients. 5/15 cases MRI reported fibrotic strand between uterus and rectum. In other 6/15 cases, MRI detected wide nodules (mean diameter 18mm) on the Rectal surface, involving at full depth the muscularis mucosa, these nodules were easily visible thanks to the difference of CE between the lesion and the normal enhancing surrounding muscularis mucosa. In all cases overlying mucosa was intact. In 4/15 cases MRI detected smaller implants on the rectal wall, (mean diameter 8 mm); 3/4 appeared to involve partially the rectal wall, thus were suggestive for DIE; on the contrary 1/3 showed to be clearly remarkable from rectal wall in CE phase, therefore we suggested to be a pseudo-nodular adhesion. MRI findings were compared to laparoscopy, which demonstrated that the small implants suggestive for pseudo-nodular adhesion was indeed a implants of DIE (False negative); 1 case of small implants reported as DIE on MRI revealed to be fibrotic adhesion (False positive). We achieved a 92% sensitivity and a 75% specificity.

#### CONCLUSION

This study shows that CE MRI and rectal filling are suitable for the diagnosis of recto-sigmoid endometriosis and mainly in differentiating between fibrotic adhesions and DIE. Moreover, CE MRI may allow to detect the severity of infiltration through rectal wall. All these information are important to guide the surgeon towards a resection or shaving of the nodules of DIE, or for the lysis of the adhesions.

#### CLINICAL RELEVANCE/APPLICATION

CE MRI associated to rectal filling proved to be suitable to differentiate between adhesions and DIE ; differentiate between these two type of manifestation is crucial for the surgical planning.

### SST07-09 • Diffusion Weighted Imaging in the Evaluation of Hormonal Cyclic Changes in Abdominal Wall Endometriomas

**Berhan Genc ; Mecit Kantarci (Presenter) ; Aynur Solak ; Neslin Sahin MD ; Mine Genc ; Hayri Ogul ; Oya Sivrikoz ; Berhan Pirmoglu MD**

#### PURPOSE

To investigate the utility of diffusion weighted (DW) Magnetic Resonance (MR) imaging in the diagnosis of abdominal wall endometrioma (AWE) and to compare ADC values of AWE with uterine endometrium, during different two phases of menstrual cycle.

#### METHOD AND MATERIALS

21 women with 25 AWE lesions, ages between 27 – 42 (mean: 32.8), with regular menstrual cycle were included in the study. The mean and standard deviation of the apparent diffusion coefficient (ADC) values of normal endometrium/AWE were calculated for menstrual and luteal phases. All examinations were performed with a 1.5 T magnet (b values: 50, 400 and 800 mm/s<sup>2</sup>). The results were analyzed by means Shapiro Wilk, Pearson correlation test, ANOVA test and Paired sample t-test per data.

#### RESULTS

The ADC values of the endometrium were different in the two phases of the menstrual cycle (menstrual phase: 0.924±0.256; luteal phase: 1.256±0.215) Similarly the ADC values of AWEs were different in these phases (menstrual phase: 0.924±0.171, luteal phase: 1.171±0.135). Both ADC measurements (AWE and uterine endometrium) were significantly lower in the menstrual phase than during the luteal phase and statistical significant difference was observed between menstrual and luteal phase (p < 0.05). There was no significant difference in ADC values between endometrial layer and AWE, in the same phase (p=0.216 for menstrual phase, p=0.104 for luteal phase, paired sample t-test).

## CONCLUSION

This study demonstrated that the DWI features of AWEs were significantly similar to the uterine endometrial tissue in all patients and they show similar cyclic changes on ADC measurements. These preliminary results suggest that ADC values of lesion close to the uterine endometrium may be used to differentiate AWE from the other pathologic conditions of abdominal wall.

## CLINICAL RELEVANCE/APPLICATION

DWI particularly ADC measurements together with uterine endometrial lining, provide useful information for diagnosis of AWE.

## Informatics (Segmentation, Measurement and CAD)

Friday, 10:30 AM - 12:00 PM • E353A

[Back to Top](#)



**SST08 • AMA PRA Category 1 Credit™:1.5 • ARRT Category A+ Credit:1.5**

### Moderator

**Ayis T Pyrros, MD \***

### Moderator

**Mohammed I Quraishi, MD**

## **SST08-01 • Bag-of-Words Representation of White Matter in Diffusion Tensor Imaging and Its Application to Diagnosis of Schizophrenia**

**Chi Wai Cheung** (Presenter) ; **Kin Yin Cheung** ; **Siu Ki Yu** PhD

### PURPOSE

Diagnosis of Schizophrenia can be performed in Diffusion Tensor Imaging (DTI) by detecting the abnormalities in white matter. In this study, we propose a bag-of-words representation of white matter in DTI, apply it to diagnose Schizophrenia, and compare it with the Parzen window model.

### METHOD AND MATERIALS

In a DTI scan, a diffusion tensor can be estimated for each voxel by a least-squares method. The affine-invariant scalar measures including Frobenius Norm (FN), Fractional Anisotropy (FA) and Mode (MD) describe the shape of the tensors. We define a word  $w$  as a triple of the quantized scalar measures of a voxel (i.e.  $w \rightarrow$ ). The vocabulary size is therefore  $|N(FN) \times N(FA) \times N(MA)|$ , where  $N()$  is the number of the bins of a measure. A DTI scan is represented as a set of words and it is called a bag-of-words representation. This representation captures the correlations between scalar measures of diffusion tensors. To diagnose Schizophrenia, feature vectors specifying the occurrences of the words of white matter are calculated and used to train a classification function using Support Vector Machines, which is then used to classify the DTI scans. The public MIDAS/NAMIC Brain Multimodality dataset which contains DTI scans of 10 Normal Controls and 10 Schizophrenic cases was used to compare the classification function with a Parzen window model based on a probabilistic representation. We performed stratified random sub-sampling validation. In each trial, 30% of total samples are randomly selected as the testing samples and the remaining samples are the training samples. We performed 1000 trials in total and the results presented below are averaged over all trials.

### RESULTS

For the Parzen window model, the sensitivity and specificity are 0.595 and 0.513 respectively. For the classification function based on our proposed presentation, the sensitivity and specificity are 0.717 and 0.59, giving 20.5% and 15% improvements respectively.

### CONCLUSION

The results show that the classification function based on the proposed representation outperforms the Parzen window model based on the probabilistic representation for diagnosis of Schizophrenia using DTI.

### CLINICAL RELEVANCE/APPLICATION

Bag-of-words Representation of White Matter in Diffusion Tensor Imaging gives high accuracy in diagnosis of Schizophrenia

## **SST08-02 • A Platform for the Comparison of Lung Nodule Segmentation Algorithms: Methods and Preliminary Results**

**Jayashree Kalpathy-Cramer** MS, PhD (Presenter) ; **Binsheng Zhao** DSc ; **Dmitry Goldgof** PhD ; **Yuhua Gu** ; **Xingwei Wang** ; **Sandy Napel** PhD \* ; **Robert J Gillies** PhD \* ; **Hao Yang** ; **Yongqiang Tan** PhD

### PURPOSE

Accurate and reproducible segmentation of lung nodules is an important step in the assessment of response to therapy in lung cancer patients. Four institutions, Massachusetts General Hospital (MGH), (Stanford University (SU), Moffitt Cancer Center (MCC), and Columbia University Medical Center (CUMC)), members of the NCI's Quantitative Imaging Network, sought to create and test a platform for comparing these algorithms on shared datasets.

### METHOD AND MATERIALS

The data set used for this evaluation consisted of 52 tumors in 41 CT volumes from 5 collections available in The Cancer Imaging Archive (including the RIDER, LIDC and FDA phantom collections, as well as two collections from SU and MCC). CUMC, MCC, and SU provided the outputs for 3 runs (each initialized with unique seeds) of their own segmentation algorithms (SU=region growing with gray-value statistics; CUMC= marker-controlled watershed and active contours; MCC= ensemble segmentation using region-growing algorithm and automatically selected multiple seed points). We used the TaCTICS platform, which allows participants to submit results in a variety of formats (e.g., png, DICOM-seg), to perform statistical analysis and visualization of results, including bias (phantom volume estimates) and repeatability. Dice coefficients ("overlap") and Hausdorff distances ("surface distance") were calculated for all pairs of segmentations for each nodule.

### RESULTS

Graphical display of all metrics allowed easy detection of outlying algorithms and challenging nodules. Average tumor volumes were between 33 and 56,641 ml. Dice coefficients for all pairwise comparisons varied from 0.54 to 0.97 (mean:0.85, s.d=0.17) with 1.0 being perfect. The intra-algorithm agreement was higher than the inter-algorithm agreement (average Dice: 0.95 vs 0.81), and was typically higher for larger volumes. Repeated measures ANOVA showed no statistically significant difference between algorithms in terms of repeatability.

### CONCLUSION

Our platform allows for easy comparison of evolving segmentation algorithms, is easily generalizable to a wide range of tumor types and imaging modalities, and could speed the development of robust algorithms.

### CLINICAL RELEVANCE/APPLICATION

This platform can facilitate advancement and evaluation of segmentation algorithms for lesions seen in medical image volumes, critical for precision diagnosis and assessment of treatment response.

## **SST08-03 • A Method for Segmenting Multi-focal Radiotracer Uptake in PET Images to Quantify Tuberculosis in Rabbits**

**Brent Foster** (Presenter) ; **Ulas Bagci** PhD, MSc ; **Ziyue Xu** PhD ; **Awais Mansoor** PhD ; **Bappaditya Dey** ; **Brian Luna** ; **William Bishai** ; **Sanjay K Jain** MD ; **Daniel J Mollura** MD

#### PURPOSE

To develop a novel segmentation method that can identify and quantify diffuse and multi-focal uptake regions using small animal model PET images that have a diagnosis of a pulmonary infection.

#### METHOD AND MATERIALS

Our segmentation approach is based on affinity propagation (AP) clustering and uses a novel distance metric and a probability density function that is estimated from a smoothed histogram. An overview of the proposed method is as follows: (i) the PET image histogram was estimated and smoothed by using a diffusion based kernel density estimation, (ii) a novel similarity function was constructed to determine how similar the histogram data points are to each other, based on two constraints: probability based and intensity based constraints, with the assumption that points that are more similar are more likely to belong to the same classification, and (iii) the AP clustering was applied to the similarities between the data points in order to find optimal thresholding levels that can separate the significant uptake regions into several tissue labels. Our proposed method was tested using an infectious disease small animal model that consisted of imaging ten rabbits at weeks 0,5,10,15,20,30, and 38 with FDG-PET—and all rabbits were infected with an aerosolized Mycobacterium Tuberculosis. Two experts segmented the images to define the ground truth for comparison.

#### RESULTS

The Dice Similarity Coefficient (DSC) and the sensitivity and specificity were calculated between the segmentation regions that were found by the proposed method and then compared to expert delineations. An average DSC of  $89.06 \pm 9.82\%$  with a sensitivity of  $97.87 \pm 7.09\%$  and a specificity of  $83.70 \pm 15.32\%$  were achieved. The Pearson correlation coefficient between the delineation performances of the two expert observers was  $R^2=0.85$  (p

#### CONCLUSION

Current PET segmentation techniques focus on focal uptake regions and are not well suited for multi-focal uptake regions, commonly found in infectious lung diseases. Our proposed segmentation method quantified the multi-focal uptake regions with high accuracy and within seconds—and it outperformed the state-of-the-art methods.

#### CLINICAL RELEVANCE/APPLICATION

This method can be used to segment diffuse and multi-focal FDG uptake normally seen in PET images from patients with infectious diseases like TB.

### **SST08-04 • Evaluation of a Novel Software for Fully Automated Detection of Osteoporosis in Abdominal MDCT Scans Performed for Other Clinical Indications, as an Aid to the Radiologist**

**Einat Blumfield MD (Presenter) \* ; Jay S Leb MD ; Anthony Blumfield MSc \***

#### CONCLUSION

The use of Radnostics software may increase early detection of OP in patients who have abdominal MDCT scans for other clinical indications.

#### Background

Osteoporosis (OP) is a common condition that increases the risk of fractures without significant trauma. Early detection and therapy may diminish fracture risk. While Screening with bone densitometry is considered the gold standard for diagnosing OP, the compliance for this test is low. OP may be detected in CT scans; however it is under-reported by radiologists. An automated method for detection of OP may improve the rate of early diagnosis. Novel software, for automated spine segmentation and OP detection was developed by Radnostics® (Scarsdale, NY). The software performs phantomless measurement of bone mineral density (BMD) in vertebral bodies and presents the radiologist with an image (figure) on PACS that includes average BMD and density values and a sagittal image of the spine. The process is fully automated and takes < 5 minutes per scan. The purpose of this study is to evaluate the efficacy of the software as an aid to the radiologist.

#### Evaluation

In this retrospective, IRB exempt study, 198 consecutive subjects (182F, 16M, age 34-89, mean-65.5+/-9 y) who had DXA and CT scans within a period of

#### Discussion

The use of the software resulted in a 275% increase in the rate of reporting osteopenia in abdominal CT scans with only 3 additional FP cases. The Radnostics software is efficient as an aid to the radiologist. It provides the radiologist with an image that contains data needed for evaluation of bone mineralization and does not require any manual intervention.

### **SST08-05 • Semi-automatic Quantitative Measurement of Breast Background Parenchymal Enhancement and Breast Cancer Risk**

**Ya Wang (Presenter) ; Malcolm Pike ; Valencia King MD ; Janice S Sung MD ; Elizabeth A Morris MD ; Eve Burstein ; Erin E Onstad ; Jonine L Bernstein ; Jennifer Brooks PhD ; Joseph O Deasy PhD**

#### PURPOSE

Breast fibroglandular tissue (FGT) amount, as measured by mammographic density or breast MRI, is an established breast cancer risk factor. Our recent study found that background parenchymal enhancement (BPE) on MRI of an unaffected breast is also strongly associated with breast cancer risk. To significantly reduce the intra- and inter-reader variability inherent in visual FGT and BPE classification, we developed a semi-automatic quantitative method and tested it on the MRIs in the aforementioned study.

#### METHOD AND MATERIALS

Contrast-enhanced breast MRI sequences were obtained for 39 breast cancer cases and 78 for control group. Our segmentation algorithm was applied to the central slice images, providing an automatic classification of voxels into FGT and non-FGT. An "enhancement image" within the breast area was obtained by subtracting the baseline from the post-injection image. We defined a subtraction voxel with a signal intensity of 10 or greater as positive and the percentage of positive subtraction voxels within the FGT area (BPE-W) was calculated. The set of BPE-W from all cases and controls was then divided into quartiles. The lowest two and highest two quartiles were combined and a conditional logistic regression for matched case-control groups, adjusted for menopausal status, was used to calculate the relative risk of being a case in the high (versus low) BPE group. These results were compared to those from Reader 1 in the original study, who had used BI-RADS conventions to classify BPE as minimal, mild, moderate, or marked.

#### RESULTS

Our method successfully analyzed 31 of the 39 cases with at least one matched control apiece. The relative risk (RR) of being a case using BPE-W was significant (p = 0.003) and was estimated at 5.6. The RR calculated using Reader 1's BI-RADS classifications for the same subset of cases and controls is 11.6 (p = 0.001).

#### CONCLUSION

The results from our semi-automatic quantitative method measuring BPE were similar to those obtained from visual classification of MRI's using the BI-RADS system. The large and significant RR was obtained using only the central slice from the breast MRI, and our method is likely to produce even more informative results when entire breast is analyzed.

#### CLINICAL RELEVANCE/APPLICATION

Our semi-automatic quantitative method supports earlier results suggesting BPE as a risk factor for breast cancer, and shows better reproducibility by reducing inter- and intra-reader variability.

### **SST08-06 • Bi-ventricular Volume Estimation for Cardiac Functional Assessment**

**Zhijie Wang (Presenter) ; Mohamed Ben Salah ; Ismail Ben Ayed \* ; Ali Islam MD ; Aashish Goela MD ; Shuo Li PhD \***

#### CONCLUSION



Developed a nearly real-time method to estimate the volumes of both RV and LV with minimum user input. The method was tested on short-axis MR images of 35 subjects and was demonstrated as a promising tool that enables semi-automated functional assessment for RV as well as LV simultaneously.

#### Background

Estimation of the two cardiac ventricles' volumes is of significant clinical importance for the purpose of cardiac functional assessment. Although very powerful semi-automated solutions have been employed for the left ventricle (LV), the estimation task is still performed manually or visually for the right ventricle (RV) in routine clinical use. We have developed a semi-automated method to efficiently estimate the volumes of RV as well as LV simultaneously with neither manual nor auto contouring.

#### Evaluation

Following IRB approval, 35 patients (22 men, 13 women, avg 52±17 yrs) underwent cardiac cine MR images using 1.5T GE scanner with FIESTA image sequence. A subject sequence consists of 20 frames of 3D images in short-axis view. For each subject, only two landmarks were placed at the attachment spots of the right ventricular wall to the left ventricular septal wall in the first frame on each slice. Then our method simultaneously estimated the volumes of both RV and LV, and computed their ejection fractions. The results on the 35 subjects were compared with gold standard created by a human expert manually contouring the biventricular endocardia.

#### Discussion

A comprehensive validation on 35 subjects demonstrates that the estimated volumes of RV and LV are highly correlated to gold standard with correlation coefficients 0.9470 and 0.9812. Furthermore, the coefficient of the correlation between the RV/LV ejection fraction and gold standard are also as high as 0.8635 (RV) and 0.9676 (LV). Overall, the performance is lower on RV than on LV, which is expected due to the complex motion and geometry of RV. The whole bi-ventricular volume estimation process takes on average 1.26 seconds per subject and can be further optimized.

### SST08-07 • Enhancement of CADx Accuracy by Using Multiple Slices from Various Views in 3D Liver Ultrasound

**Ye-Hoon Kim** (Presenter) ; **Moon Ho Park** ; **Junghoe Kim** ; **Baek Hwan Cho** ; **Yeong Kyeong Seong** PhD ; **Kyoung-Gu Woo** ; **Min Woo Lee**

#### CONCLUSION

3D US liver CADx using multiple slices in the vicinity of the lesion center and combination of their various views can enhance the diagnostic accuracy for liver cancer.

#### Background

The objective of this study is to enhance the performance of 3D US Computer-Aided Diagnosis (CADx) for liver cancer. The proposed 3D US liver CADx uses multiple slices and various views from 3D volume for diagnosis of benign and malignant tumors. Our CADx system segments the lesion and extracts the features and then classifies lesions as benign for cyst and hemangioma and as malignants for hepatocellular carcinoma.

#### Evaluation

2D (1024x768) and 3D (512x510x256) US images of liver lesions were acquired for this research from 44 patients (22 benign and 22 malignant cases) respectively by using 2D and 3D US probes from Feb. 2012 to Mar. 2013. The accuracy of our CADx was 1) 80.8% by only a 2D slice containing a lesion; 2) 81.9%, 78.8%, 74.4% by using a center slice of the lesion with three orthogonal views, respectively; 3) 81.8% by combining three orthogonal views of the lesion (total 3 slices); 4) 85.5%, 79.0%, 75.5% by using seven slices of the lesion for three orthogonal views, respectively; 5) 84.0% by combining seven slices of the lesion with their three orthogonal views (total 21 slices). The seven slices include a center slice which bisects a lesion and additional slices in the vicinity of the lesion center in 3D volume. 2D lesion contour for ground truth was obtained by a radiologist and 3D lesion volume was obtained semi-automatically. Majority voting was used to classify lesions from the multiple slices and views. The 10-fold cross-validation and averaged accuracy of 100 iterations were used for performance evaluation.

#### Discussion

The combination of three orthogonal views only at the center of the lesion was less effective to improve the 3D CADx accuracy. However because our 3D US liver CADx can use additional information of the 3D volume, the combination of multiple slices and their different views outperformed the case of combining multiple views only at the center of the lesion (p

### SST08-08 • SyN and ART: Quantitative Evaluation of Two Leading Open-source Image Registration Software Tools for Automatic Segmentation and Measurement of the Corpus Callosum on MR Images of Multiple Sclerosis Patients

**Paxton Smith** MEng (Presenter) ; **David K Li** MD \* ; **Anthony Trabousee** MD \* ; **Roger Tam** PhD

#### PURPOSE

The emergence of robust neuroimage analysis software enables automatic volumetry of brain structures commonly associated with neurodegenerative disease such as multiple sclerosis (MS). However, the application of such software is not standardized, and it is unclear how much variability can be expected from the choice of tools. In our study, we demonstrate the use of two open-source, state-of-the-art image registration tools, namely SyN (Symmetric Normalization) and ART (Automatic Registration Toolbox), in the automatic measurement of the corpus callosum area (CCA) in the mid-sagittal plane (MSP). Our goal was to find whether significant differences in volumetry exist between the tools when applied to our task, to the extent that tool selection could impact the outcome of clinical studies.

#### METHOD AND MATERIALS

We randomly selected 100 3-D, T1-weighted axially acquired MR images of patient brains from a recent MS clinical trial. Image format was 256 x 256 x 180 with 0.976 mm x 0.976 mm x 1 mm voxel size and the AC-PC line manually centered in the volume during acquisition. Extra-cranial regions were deleted from the images using BET, and the CC was manually segmented in the MSP using ITKSNAP to provide ground truth. Patient brains were affinely registered to the MNI152 reference using FLIRT followed by non-linear transformations with SyN v1.9 and ART v2.0. The JHU CC label for the MNI152 atlas was then propagated to patient space using the corresponding inverse transformations.

#### RESULTS

The overlap between the automatic and manual segmentations was measured with the Dice coefficient (SyN = 0.764, ART = 0.769). The Wilcoxon test (p = 0.475) showed no significant difference between SyN and ART. The correlation of CCAs between automatic and manual segmentations was measured with Spearman's rank coefficient (SyN  $\rho = 0.815$   $p = 9.41e10^{-24}$  vs. ART  $\rho = 0.507$   $p = 1.60e10^{-7}$ ), showing that the SyN and manual segmentations were more strongly correlated.

#### CONCLUSION

SyN and ART perform very similarly for common metrics in ours and past studies; however, there is sufficient difference in the volumetric correlation to ground truth that they cannot be considered equivalent.

#### CLINICAL RELEVANCE/APPLICATION

Leading image registration tools, SyN and ART, perform similarly for most common metrics, but to compare results between clinical studies, standardization of the image analysis pipeline is critical.

### SST08-09 • Fully Automated Segmentation of Multiple Organs in Contrast-enhanced Abdominal CT: Preliminary Study

**Jing Liu** (Presenter) ; **Qiang Li** PhD \*

#### PURPOSE

Organ delineation in CT is a key component to computer-aided detection, radiotherapy planning, and pre-surgical planning. We developed a generic algorithm for fast and robust segmentation of multiple abdominal organs from contrast-enhanced CT scans.

## METHOD AND MATERIALS

The fully automatic algorithm segments organs using a set of atlases, i.e., pre-learned abdominal organ shapes and inter-organ spatial relationship models. The algorithm consists of five major steps. First, a test image was filtered with an edge-preserving non-local-mean filter. Second, the centroid of an organ of interest (OOI) on the test image was identified by context-driven Generalized Hough Transform (cGHT) using organ atlases. Third, a probability map indicating the likelihood of being the OOI was assigned to image pixels according to the localized centroid and atlas of the OOI. Fourth, the initial organ segmentation was achieved by graph-cut method for maximizing the likelihood for the label assignment with a smoothness penalty. Finally, initial organ segmentation was refined by a fast adaptive erosion-dilation (AdaED) method. In this preliminary study, the algorithm was used for segmenting liver, spleen, left and right kidneys from 10 test CT scans. Livers, spleens and both kidneys on test images were manually segmented by two radiologists prior to the application of automatic algorithm and were used as reference standard. The segmentation algorithm was evaluated by Jaccard overlap scores between automatic segmentation and reference standard. The algorithm will be applied to the segmentation of more organs in more CT scans in the upcoming months.

## RESULTS

The cGHT correctly localized all organs of interest on 10 test images. The Jaccard scores for segmentation of liver, spleen, left and right kidneys were  $89.3 \pm 2.5\%$ ,  $86.6 \pm 5.0\%$ ,  $90.0 \pm 3.1\%$  and  $90.6 \pm 3.0\%$ , respectively.

## CONCLUSION

The use of cGHT, likelihood-based graph-cut and AdaED achieved, respectively, very efficient organ localization, initial segmentation and segmentation refinement in abdominal CT scans. The preliminary results showed that the automatic organ segmentation method is robust and accurate. We thank Drs. F. Li and C. Zhang for manual organ delineation.

## CLINICAL RELEVANCE/APPLICATION

An automated segmentation algorithm greatly improves efficiency/consistency for organ contouring, and facilitates computer-aided detection, radiotherapy and pre-surgical planning in clinical practice.

## Neuroradiology/Head and Neck (Advanced Head and Neck Imaging)

Friday, 10:30 AM - 12:00 PM • N226



[Back to Top](#)

**SST09** • AMA PRA Category 1 Credit™:1.5 • ARRT Category A+ Credit:1.5

### Moderator

**Suresh K Mukherji, MD**

### SST09-01 • Vascular Communications between Donor and Recipient Tissues One Year after Successful Full Face Transplantation

**Kanako K Kumamaru MD, PhD (Presenter)**; **Geoffroy C Sisk**; **Michael L Steigner MD \***; **Elizabeth George MBBS**; **Bohdan Pomahac MD**; **Frank J Rybicki MD, PhD \***; **Kurt Schultz RT \***; **Dimitris Mitsouras PhD**; **David S Enterline MD \***; **Ericka M Bueno PhD**

### PURPOSE

To noninvasively study vascular changes that have implications on graft survival and rejection, future surgical planning, and our understanding of the underlying biology changes after full face transplantation.

### METHOD AND MATERIALS

Three full face transplant patients (single anastomosis bilaterally of artery and vein) for whom clinical findings were previously reported (NEJM 2012; 366:715-22) were, for the first time, evaluated for vascular reorganization 1 year after successful transplantation using a previously described 320 x 0.5 mm detector row dynamic CT angiography protocol (AJNR 2012, Aug 9, PMID 22878008).

### RESULTS

Consistent, extensive vascular re-organization was observed among the recipients. Diverted external carotid artery (ECA) or facial artery angiosomes were found to be perfused from newly opened, elaborate collateral circulation. Using the metric of arterial blood flow (BF) at the temporal region expressed as the percentage of the BF at the internal carotid artery, allograft tissue was slightly less perfused when the facial artery was the only donor artery when compared to an ECA-ECA anastomosis ( $4.4 \pm 0.4\%$  vs  $5.7 \pm 0.7\%$ ). However, allograft BF was higher than the recipient normal neck soft tissue. Blood flow to the recipient's tongue was maintained, despite the fact that the recipient lingual arteries were not always preserved. On the side where the lingual artery was ligated, blood flow was redistributed from a contralateral artery. Venous drainage was adequate for all patients, including patients for whom the recipient internal jugular vein was anastomosed in end-to-end fashion on one side.

### CONCLUSION

Despite extensive surface contact between the donor and the recipient, disruption of recipient's blood supply depends on extensive collateralization rather than new vessel ingrowth from the donor tissues. These findings guide both surgical planning and the assessment of potential complications for larger scale face transplant studies.

### CLINICAL RELEVANCE/APPLICATION

A single anastomosis bilaterally of artery and vein is adequate for full face transplantation, evidenced by substantial arterial flow demonstrated on dynamic CT angiography.

### SST09-02 • Value of Dynamic Volume Imaging with 320-detector Row CT in the Pre-transplantation Evaluation of Head and Facial Skin Flap: Initial Experience

**Kaiyuan Xu (Presenter)**; **Xuelin Zhang**; **Xing Chen \***

### PURPOSE

To investigate the value of dynamic volume perfusion CT scanning in the pre-transplantation evaluation of blood supply of head and facial flaps with 320-Detector row computed tomography(CT).

### METHOD AND MATERIALS

Whole-head dynamic volume perfusion CT scan was performed in 576 patients with a 320-Detector row CT system. All the patients enrolled had normal internal carotid arteries but due to other reasons referred to CT perfusion examination. Volume perfusion data were generated and then analyzed with the body perfusion software. BF(Blood Flow) value of each separate skin flap within the scan region was measured. The numbers of flap arteries and veins that can be found in dynamic CTA images are summarized.

### RESULTS

We succeeded to measure BF value of each skin flaps in the head or face for all the patients. BF value of the forehead flap, the eyelid flap, the nasal dorsum flap, the buccal flap, the parietal flap, occipital flap, cervical flap was ( $127 \pm 7.7$ )ml/min, ( $268.0 \pm 31.1$ )ml/min, ( $229.0 \pm 50.9$ )ml/min, ( $67.8 \pm 9.5$ )ml/min, ( $140.3 \pm 5.5$ )ml/min, ( $163.8 \pm 15.5$ )ml/min, ( $123.5 \pm 12.5$ )ml/min, respectively. There are significant difference between the flaps in different region, among which BF value of the buccal flap was the lowest. Arteries and vein of flaps was observed through different phases. Display rate of arteries and vein that can be found on dynamic CTA image was 100% for all flaps.

### CONCLUSION

Whole-head dynamic volume CT perfusion using 320-detector row MDCT is able to offer effective reference for assessing blood supply and vessel anatomy of different skin flaps for the patient who is going to undergo skin flap autotransplantation. Fusion of perfusion map and CT anatomical images were helpful to the analysis and orientation of flaps.

#### CLINICAL RELEVANCE/APPLICATION

Whole-head perfusion can be used as a method of preoperative assessment of the skin flap perfusion and avoid operation complications effectively, which has the potential to improve diagnostic utility.

### **SST09-03 • MRI Displays Affection of the Deep Temporal Artery and the Temporal Muscle in Patients with Giant Cell Arteritis**

**Simon Veldhoen MD (Presenter) ; Thorsten Klink MD ; Julia Geiger MD ; Peter Vaith ; Cornelia Glaser ; Thomas Ness ; Dirk Duwendag ; Marcus Both MD ; Thorsten A Bley MD**

#### PURPOSE

Giant cell arteritis (GCA) is a vasculitis of large and medium-sized arteries. Dedicated MRI protocols have been developed to detect vasculitic changes of the superficial cranial arteries noninvasively. This study assesses the involvement of the deep temporal artery and the temporal muscle in MRI of patients with active GCA.

#### METHOD AND MATERIALS

99 patients who received MRI and subsequent temporal artery biopsy (TAB) were included. TAB was positive in 61 and negative in 38 patients. TAB negative patients served as reference group. Contrast enhanced T1-weighted spin-echo images were acquired utilizing 1.5T and 3T MRI scanners at three academic medical centres. Mural contrast enhancement and wall thickening of the deep temporal artery and contrast enhancement of the temporal muscle were defined as their inflammatory involvement and assessed by two radiologists with experience in vasculitis imaging. Correlation analyses between individual MRI results and jaw claudication were performed to test for a concordance of clinical symptoms and MRI findings.

#### RESULTS

Patients with active GCA showed inflammatory affection of the deep temporal artery in 34.4% (n=21) and 49.2% (n=30). Bilateral involvement was found in 80% (n=19) and 90.5% (n=24). Temporal muscle involvement was observed in 19.7% (n=12) and 21.3% (n=13), respectively, and occurred bilaterally in all cases. Relative risk for jaw claudication was increased to 2.1 [1.5; 3.1] for GCA patients. Its presence correlated with inflammatory MRI findings in the deep temporal artery (r=0.38; p=0.01) as well as in the temporal muscle (r=0.31; p=0.01).

#### CONCLUSION

MRI is able to assess vasculitic changes in the deep temporal artery and in the temporal muscle. Both structures were affected simultaneously in a remarkable number of GCA patients. A substantial correlation of clinical symptoms and MRI results was observed.

#### CLINICAL RELEVANCE/APPLICATION

MRI is able to display the involvement of the deep temporal artery and the temporal muscle in patients with active GCA.

### **SST09-04 • Evaluation of Head and Neck Arteriovenous Malformations with 4D Contrast-enhanced MR Angiography at 3T**

**Yasuhiko Iryo (Presenter) ; Toshinori Hirai MD ; Mika Kitajima MD ; Yoshinori Shigematsu ; Minako Azuma ; Yasuyuki Yamashita MD \***

#### PURPOSE

Four-dimensional contrast-enhanced MR angiography (4D CE-MRA) at 3T may replace digital subtraction angiography (DSA) for certain diagnostic purposes in patients with arteriovenous malformations (AVMs) in the head and neck region. The purpose of this study was to compare the agreement between DSA and 4D CE-MRA findings for the evaluation of head and neck AVMs.

#### METHOD AND MATERIALS

Six patients with facial AVMs (4 men, 2 women; aged 15 - 83 years, mean 39.2 years) underwent 4D CE-MRA at 3T and DSA. The AVMs were located tongue, lip, scalp, orbit, nose and cheek in one each. 4D CE-MRA combined randomly segmented central k-space ordering, keyhole imaging, sensitivity encoding, and half-Fourier imaging; it yielded total acceleration factor was 88. We obtained 30 dynamic scans every 1.9 sec at an acquired spatial resolution of 0.9×0.9×1.5 mm; the matrix was 256×256. Two independent observers reviewed 4D CE-MRA images with regard to the nidus size, main arterial feeders and venous drainage. The venous drainage was recorded as being extracranial, intracranial, or extra- and intracranial veins. Interobserver and intermodality agreement was assessed by  $\kappa$  statistics.

#### RESULTS

On 4D CE-MRA, the interobserver agreement was excellent for main arterial feeders ( $\kappa = 1.0$ ) and good for the nidus size and venous drainage ( $\kappa = 0.63$  and  $0.67$ , respectively). Intermodality agreement was excellent for main arterial feeders and venous drainage ( $\kappa = 0.92$  and  $1.0$ , respectively) and good for the nidus size ( $\kappa = 0.63$ ).

#### CONCLUSION

The agreement between 4D CE-MRA and DSA findings was good to excellent with respect to the nidus size, main arterial feeders and venous drainage in head and neck AVMs.

#### CLINICAL RELEVANCE/APPLICATION

4D CE-MRA is a reliable tool for assessing head and neck AVMs, although it is not able to replace DSA for the detailed evaluation.

### **SST09-05 • Visualization of the Intraparotid Facial Nerve with 3T MRI**

**Hiroyuki Fujii MD (Presenter) ; Akifumi Fujita MD ; Yukio Kimura MD ; Edward K Sung MD ; Osamu Sakai MD, PhD \* ; Hideharu Sugimoto MD**

#### PURPOSE

It is important to know the spatial relationship of the intraparotid facial nerve to a parotid tumor since the location of the tumor influences the duration and difficulty of the surgery. Recently, several study have proposed MRI techniques to visualize the intraparotid facial nerve by 3-dimensional reversed fast imaging with steady-state precession with diffusion weighted imaging (3D-PSIF-DWI) and three-dimensional double-echo steady-state with water excitation (3D-DESSWE). The purpose of this study is to evaluate the visualization of the intraparotid facial nerve with both sequences using 3T MRI, and compare the utility of this application in clinical practice.

#### METHOD AND MATERIALS

We evaluated 72 parotid glands of 36 consecutive patients during routine clinical MR examination. We performed both 3D-PSIF-DWI and 3D-DESSWE sequences using our 3T MR scanner (MAGNETOM Skyra, Siemens). Two observers initially assessed the images independently, but later resolved inconsistencies by collaborative review and consensus agreement. The certainty of identifying the intraparotid facial nerve was evaluated and divided into four categories; (1) Excellent: branch of the facial nerve identified; (2) Good: distal facial nerve trunk identified; (3) Fair: proximal facial nerve trunk identified; and (4) Poor: intraparotid facial nerve not identified.

#### RESULTS

Both 3D-PSIF-DWI and 3D-DESSWE were successfully obtained in all 36 patients (72 parotid glands). The intraparotid facial nerve was identified in 62 parotid glands (86.1%; Excellent:17, Good:25, Fair:20) with 3D-PSIF-DWI sequence and in 71 parotid glands (98.6%; Excellent:40, Good:15, Fair:16) with 3D-DESSWE sequence.

#### CONCLUSION

Using 3T MRI, both 3D-PSIF-DWI and 3D-DESSWE sequences can adequately demonstrate the course of the intraparotid facial nerve. 3D-DESSWE demonstrated better than 3D-PSIF-DWI in visualization intraparotid facial nerve.

#### CLINICAL RELEVANCE/APPLICATION

Knowledge about the course of the intraparotid facial nerve in relation to a parotid tumor is important for preoperative planning, and can optimize the surgical approach to prevent facial nerve damage.

### SST09-06 • High Resolution Diffusion-weighted MR Imaging in the Head and Neck: A New Approach

**Thorsten Klink MD** (Presenter) ; **Daniel Chong** ; **Dechen W Tshering-Vogel** ; **Nedelina Slavova** ; **Berthold Kiefer PhD \*** ; **Harriet C Thoeny MD**

#### PURPOSE

To evaluate whether diffusion-weighted MR images acquired with readout-segmented echo planar imaging (RESOLVE) are superior to single-shot echo planar imaging (ssEPI) in the head and neck region.

#### METHOD AND MATERIALS

After ethics committee approval and written informed consent, 10 volunteers were prospectively included in our MRI study of the head and neck region. The 3T MR study protocol included axial T2w-TSE, ssEPI, and RESOLVE acquisitions. Image analysis was performed by two independent observers. DWI was qualitatively evaluated by visual assessment using a 10-point score, and quantitatively by measuring SNR and ADC values of various predefined structures. Image distortion was assessed qualitatively and quantitatively by measuring the diameter of anatomical structures on RESOLVE and ssEPI images in comparison to T2w images. The RESOLVE sequence was additionally tested in four patients. Differences were considered statistically significant, when  $p=0.05$  applying the non-parametric Mann-Whitney-U test.

#### RESULTS

Quality of RESOLVE images was significantly higher in comparison to ssEPI (Quality scores, RESOLVE  $7.51 \pm 0.18$  and ssEPI  $4.50 \pm 0.32$ ;  $p < 0.05$ ).

DWI of the head and neck acquired with the RESOLVE sequence had superior image quality at comparable SNR and ADC levels in ten healthy volunteers, and were of diagnostic quality in four patients. Significant less image distortion is the key advantage of RESOLVE over ssEPI and may therefore improve image interpretation of DWI in this challenging region.

#### CLINICAL RELEVANCE/APPLICATION

RESOLVE produced superior image quality and less distortion; this new approach for DWI in the artifact- and distortion-susceptible head and neck region may improve image interpretation.

### SST09-07 • Objective Evaluation of Salivary Gland Function Using Diffusion-weighted MR Imaging: Follow-up of Radiation-induced Xerostomia

**Yun-Yan Zhang** (Presenter) ; **Dan Ou** ; **Yajia Gu MD** ; **Xia-Yun He** ; **Weijun Peng MD** ; **Jian Mao BA** ; **Lei Yue**

#### PURPOSE

To investigate the value of diffusion-weighted (DW)-MRI as a noninvasive tool to assess salivary gland function for follow-up of patients with radiation-induced xerostomia.

#### METHOD AND MATERIALS

A HIPAA-compliant waiver of authorization was granted by the institutional review board. Twenty-three consecutive patients with nasopharyngeal carcinoma were examined with a 3T unit pre-radiotherapy (RT), and 1 week and 1 year post-RT. Clinical xerostomia was also assessed according to the Radiation Therapy Oncology Group/European Organization for Research and Treatment of Cancer morbidity scoring system. A DWI sequence was performed once on the salivary glands at rest, then continually repeated on the parotid glands immediately after oral ascorbic acid stimulation over a mean period of 21minutes. Apparent diffusion coefficient (ADC) maps for salivary glands before and after stimulation were calculated. The maximum ADC of the parotid glands (pADCmax) and the time to pADCmax (pTmax) during stimulation were also obtained. Findings before and after RT were compared.

#### RESULTS

#### CONCLUSION

The ADC value is a sensitive indicator for salivary gland dysfunction, and it changes earlier than clinical xerostomia. DW-MRI is potentially useful for noninvasively evaluating the severity of radiation-induced xerostomia.

#### CLINICAL RELEVANCE/APPLICATION

DW-MRI could noninvasively evaluate the functional changes of salivary glands before and after RT and the ADC value may be a early prediction for the severity of radiation-induced xerostomia.

### SST09-08 • Evaluation of Enhanced Modernize Collaborative Management of Neck Lumps

**Kit H Chow MBBCh, FRCR** (Presenter) ; **Rathinavelu Balamurugan MBBS** ; **Unnikrishnan Anoop MBBS, FRCR** ; **Saravana Ammamuthu MBBS** ; **Jyothi Rao**

#### PURPOSE

Chesterfield Royal Hospital (CRH) implemented an enhanced modernized collaborative one-stop system in 2008, which included the use of specialist neck Ultrasound (US) and US-guided biopsy. We evaluated this innovative model of diagnostic management of neck lumps.

#### METHOD AND MATERIALS

1. Prospective Survey of Patient's Satisfaction (n=100) 2. Prospective 3 months study of impact of US and US guided biopsy on patients referred to CRH rapid access H&N lump clinic 3. Retrospective study of 60 patients with H&N Lymphoma in CRH presented over a 4 years period. This provides an evaluation of effectiveness of core biopsy provided by this radiology service.

#### RESULTS

#### CONCLUSION

The result shows this of model managing neck lumps is faster, cheaper, clinically less invasive and represents a successful formula for patients, radiologists, referring clinicians and commissioners of services.

#### CLINICAL RELEVANCE/APPLICATION

Radiologists should develop an ambition to work beyond their traditional boundary and use their skills to extend their role by running neck lump clinics, which, offer H&N US and US guided biopsy.

### SST09-09 • Preliminary Prospective Study on Contrast-enhanced Ultrasound (CEUS) in the Quantitative Assessment of Uveal Melanoma (UM) Response to Gamma Knife Radiosurgery (GKR): Do Changes in Tumor Vascularization Precede Diameter Reduction?

**Caterina Colantoni** (Presenter) ; **Massimo Venturini MD** ; **Giulio Modorati** ; **Maura Di Nicola** ; **Giulia Agostini** ; **Alessandro Del Maschio MD**

#### PURPOSE

Tumor thickness is worldwide accepted as the most useful parameter to evaluate UM response to GKR, which on average occurs at 12 months. According to the modified response evaluation criteria in solid tumors (mRECIST), in case of hypervascular lesions, changes in vascularization precede diameter reduction after treatment. Our aim was to prospectively analyze CEUS as a tool to quantitatively assess the response of UM to GKR, investigating if changes in quantitative parameters expressing tumor vascularization precede diameter

reduction.

#### METHOD AND MATERIALS

Our study had institutional review board approval, and written consent was obtained. From 2012 to 2013, 10 patients (mean age, 66 years) affected by UM were enrolled and submitted to a complete ophthalmological evaluation before and after GKR. US and CEUS (ATL-Philips, IU-22, 5-9 MHz linear probe; Sonovue, Bracco) were performed by the same experienced radiologist at baseline (b-GKR), 3 (3-GKR), and 6 (6-GKR) months after GKR. UM transverse diameter (TD), thickness (Th), and different quantitative parameters (area under the curve in the wash-in phase; wash-in perfusion index (WiPI); peak enhancement (PE); mean transit time; wash-in rate (WiR); rise time (RT); time to peak) were calculated by the same operator using a dedicated and off-line imaging software (Sonotumor, Bracco). Comparisons between each parameter were made using the Wilcoxon analysis.

#### RESULTS

At US the mean tumor diameters (TDxTh, mm) were: b-GKR=10.7x8.3, 3-GKR=8.8x7.4, 6-GKR=9.4x6.6, with statistical significance at 6 months (P=.031).

At CEUS the quantitative parameters were: PE (arbitrary units, a.u): b-GKR=2\*10<sup>7</sup>, 3-GKR=3\*10<sup>7</sup>, 6-GKR=8\*10<sup>5</sup> (P=.018); WiR: b-GKR=4\*10<sup>6</sup>, 3-GKR=5\*10<sup>6</sup>, 6-GKR=8\*10<sup>4</sup> (P=.028); WiPI (cm<sup>3</sup>/sec): b-GKR=6\*10<sup>7</sup>, 3-GKR=1\*10<sup>8</sup>, 6-GKR=2\*10<sup>6</sup> (P=.028). At 6-GKR tumor mean diameters decreased in 8/10 patients, while UM enhancement in 10/10.

#### CONCLUSION

CEUS is a feasible and reproducible method for the quantitative assessment of UM vascularization; it showed a reduction in UM enhancement at 6 months after GKR, earlier than tumor diameter changes, even though further studies with a larger population and a longer follow-up are needed.

#### CLINICAL RELEVANCE/APPLICATION

CEUS could be a useful additional tool to conventional US or the first choice technique to monitor UM response to GKR, in order to better predict the long-term survival of patients.

## Neuroradiology (Cerebral Ischemia, Hemorrhage and Vessel Wall Imaging)

Friday, 10:30 AM - 12:00 PM • N227



[Back to Top](#)

**SST10** • AMA PRA Category 1 Credit™:1.5 • ARRT Category A+ Credit:1.5

#### Moderator

**Ashok Srinivasan**, MD \*

#### Moderator

**Jalal B Andre**, MD

**SST10-01 • Does Transfer Status Affect Outcomes in Acute Ischemic Stroke Patients Treated Endovascularly?**

**Maryam Soltanolkotabi** MD (Presenter) ; **Farnoosh Feiz** MD ; **Ali Shaibani** MD ; **Michael C Hurley** MBBCh ; **Yvonne Curran** MD ; **Sameer A Ansari** MD, PhD

#### PURPOSE

To study the effect of transfer status on endovascularly treated AIS patients' outcomes.

#### METHOD AND MATERIALS

We retrospectively analyzed consecutive anterior circulation AIS patients that underwent IAT at 4 institutions from 2006-2011. We excluded patients selected using perfusion imaging. Patient demographics, medical risk factors, presentations, technical, and clinical (NIHSS and mRS scores) outcomes, complications, and mortality were studied. Symptom-onset, groin puncture, and end-of-procedure times were recorded. THRIVE scores were calculated. Successful recanalization was defined as TIC I=2b. Good functional outcome was defined as mRS 0-2 at 90 days. Patients were categorized into those who were transferred from outside institutions and those who presented directly to the CSCs.

#### RESULTS

116 patients were studied. 68 (58.6%) were transferred from outside institutions. Transfers and nontransfers were similar in THRIVE scores (p=0.300), median symptom-onset to groin puncture times (306 vs. 315 minutes; p=0.572), successful recanalization (p=0.574), and symptomatic ICH (13.2 vs. 10.4, p=0.776), but differed by age (59 vs. 69 years; p=0.002), prior stroke (3% vs. 22%, p=0.002), cardiac history (17.9 vs. 36.6%, p=0.040), baseline NIHSS (20 vs. 17, p=0.005), and location of occlusion (45.6% vs. 22.9% ICA, p=0.012). Transfer patients had significantly worse outcomes at 90 days (mRS 0-2: 16.2% vs. 60.4%, p In multivariate analysis, transfer status was an independent predictor of poor functional outcome (adj. OR 0.05, 0.011-0.222), adjusting for relevant covariates.

#### CONCLUSION

Transferred AIS patients have worse functional outcomes at 90 days than non-transfers, independent of baseline risk factors, stroke severity, time to IAT, and procedural success/complications. Further investigation should focus on residual factors that may contribute to our findings such as baseline/final infarct volumes, pre-morbid functional status, and post-stroke care.

#### CLINICAL RELEVANCE/APPLICATION

Access to intra-arterial therapy (IAT) for acute ischemic stroke (AIS) is limited to comprehensive stroke centers (CSCs) with timely access deemed critical for success. Inter-hospital transfers rep

**SST10-02 • Diffusion Tensor Imaging Study on Wallerian Degeneration of Pyramidal Tract after Pontine Infarction**

**Miao Zhang** (Presenter) ; **Jie Lu** MD ; **Dongdong Rong** ; **Zhilian Zhao** PhD ; **Yanxiang Cao** ; **Kuncheng Li** MD

#### PURPOSE

To investigate dynamic process in Wallerian degeneration (WD) of the pyramidal tract after pontine infarction using diffusion tensor imaging (DTI), as well as its relationship with clinical prognosis.

#### METHOD AND MATERIALS

Nineteen patients with pontine infarction underwent five DTI examinations during a period of 6 months (7, 14, 30, 90 and 180 days after onset). Clinical neurological assessments were performed. Nineteen healthy control subjects age-sex matched were recruited. The fractional anisotropy (FA) values were measured at medulla, cerebral peduncle, posterior limb of internal capsule and precentral gyrus cortex at five time points. The FA values in the infarcted sides were compared with the contralateral sides and control subjects, and their relationships with clinical scores were analyzed.

#### RESULTS

The FA values at the medulla, cerebral peduncle, posterior limb of internal capsule and precentral gyrus cortex ipsilateral to infarct significantly decreased progressively with time. This trend was the most significant during 7~14 days after stroke, then it became slow during 14~30 days and stable during 30~180 days after stroke. The relative FA (rFA) values at the medulla and above the pons

correlated positively with the Fugl-Meyer (FM) scores in 90 and 180 days. The rFA values above the pons correlated negatively with the modified Rankin scale (mRS) scores in 90 days.

#### CONCLUSION

DTI can detect secondary WD of pyramidal tract much earlier after pontine infarction. The decreased FA value of pyramidal tract in early stage may predict motor outcome.

#### CLINICAL RELEVANCE/APPLICATION

It is suggested that the progressive anterograde and retrograde degeneration in the pyramidal tract following a pontine infarct may slow down the process of neurological recovery.

### **SST10-03 • Functional MRI (fMRI) in Patients with Spastic Hemiplegia after Stroke, Treated with Botulinum Toxin: The Role of 'Motor Imagery' in the Demonstration of Central Effects and Brain Plasticity**

**Alessandro Stecco MD (Presenter) ; Roberta Matheoud ; Stefano Carda ; Marco Perchinunno ; Emanuele Malatesta ; Alessandro Carriero MD ; Carlo Cisari**

#### PURPOSE

Botulinum toxin is considered a first-line treatment of focal spasticity in post-stroke patients. The aim of our study is to describe the central nervous system effects of botulinum toxin by a fMRI analysis, assuming that in case of absence of influence, the brain fMRI pattern should not be modified after therapy.

#### METHOD AND MATERIALS

We enrolled 17 patients (10 healthy volunteers as a control group and 7 patients with ischemic stroke with hemiplegia spastic upper limb). All patients underwent three fMRI with execution of a motor imagery task (finger tapping), one before starting treatment with botulinum toxin (T0), one after 4 weeks (T1) and the last after 8 weeks (T2), the task was repeated twice every same session. Between T0, T1 and T2 was not carried out any physical therapy, but only passive muscle stretching.

#### RESULTS

The analysis on the healthy volunteer sample confirmed that the motor imagery paradigm showed efficacy and reliability in activating the motor cortex.

The group analysis on the patients sample showed activation but with a progressive focalization of cerebral activations, in particular a progressive reduction of the supplementary motor area (SMA and Brodmann 6 areas).

#### CONCLUSION

First of all our data confirmed the efficacy of "motor imagery" fMRI paradigms as a "window" to study the brain after stroke and its motor recovery.

We demonstrated a kind of modification induced on the brain cortical reorganization after stroke, by mean of a peripheral therapy as botulinum toxin injection.

#### CLINICAL RELEVANCE/APPLICATION

These data, with the pattern of progressive reduction and delimitation of cortical activations during therapy, are in line with the "small world network" theory of cortical reorganization after stroke

### **SST10-04 • Dual-energy CT (DECT) and Non-enhanced CT (NECT) in the Characterization of Intracerebral Hemorrhage (ICH) or Iodinated Contrast Material in CT Follow-up after Endovascular Treatment for Acute Ischemic Stroke**

**Federico X Zarco Contreras MD (Presenter) ; Antonio Lopez Rueda ; Camilo Pineda Ibarra MD ; Sebastian Capurro ; Miren L Olondo MD ; Sergio Amaro MD ; Luis San Roman MD ; Jordi Blasco MD \* ; Juan Miguel Macho ; Laura Oleaga**

#### PURPOSE

To assess the accuracy of DECT and NECT in the characterization of hyperattenuation areas on CT follow-up after endovascular treatment for acute ischemic stroke, in order to determine the start of early heparin treatment.

#### METHOD AND MATERIALS

A retrospective study in 35 patients with hyperattenuation areas on CT follow-up after endovascular treatment for acute ischemic stroke were reviewed. DECT was used for imaging at 80 and 140kV, and a three-material decomposition algorithm was used to obtain virtual unenhanced images and iodine overlay images. Source images (mixed 140/80 kV) were consider as NECT. Two neuroradiologists with over 10 years of experience were designated for double-blind readings. DECT and NECT were used in order to classify the findings into 6 categories: Contrast Extravasation (CE), Hemorrhagic Infarction (HI) types 1 and 2, Parenchymal Hemorrhage (PH) types 1 and 2, and Remote Hematoma (RH). CT/MRI Follow-up images were used as the standard of reference. According to our clinical management protocol, early heparin treatment is indicated to CE, H1 and H2. The six categories were dichotomized according to the indication of early heparin treatment: heparin treatment (CE, HI1 and HI2) and no heparin treatment (PH1, PH2 and RH). The sensitivity, specificity and accuracy of DECT and NECT in the prospective characterization of hyperattenuation areas were obtained. All analyses were performed with the use of SPSS software (ver. 20, SPSS Inc, Chicago, IL)

#### RESULTS

The sensitivity, specificity, and accuracy of NECT were 58% (7 of 12 areas), 100% (23 of 23 areas), and 85% (30 of 35 areas), respectively. According to the agreement, the kappa-weight index between readers was 0.53, and the kappa index in the dicotomization sample was 0.60.

The sensitivity, specificity, and accuracy of DECT were 83% (10 of 12 areas), 100% (23 of 23 areas), and 95% (33 of 35 areas), respectively. According to the agreement, the kappa-weight index between readers was 0.71, and the kappa index in the dicotomization sample was 0.85.

#### CONCLUSION

DECT is more accurate and more consistent than NECT in the characterization of hyperattenuation areas on CT follow-up after endovascular treatment for acute ischemic stroke.

#### CLINICAL RELEVANCE/APPLICATION

DECT is more accurate than NECT, achieving an excellent agreement, in the purpose of decide early heparin treatment after endovascular approach for acute ischemic stroke.

### **SST10-05 • Initial Findings of Blood-brain Barrier Permeability in Predicting Delayed Cerebral Infarction in Aneurysmal Subarachnoid Hemorrhage**

**Jana Ivanidze MD, PhD (Presenter) ; Kartik Kesavabhotla ; Sirish Kishore MD ; Ajay Gupta MD ; Pina C Sanelli MD**

#### PURPOSE

Aneurysmal subarachnoid hemorrhage (aSAH) patients are at increased risk of delayed cerebral ischemia (DCI) resulting in infarction. Since its pathophysiology is not well understood, early detection and treatment of DCI remains challenging. We hypothesize that blood brain barrier permeability (BBBP) increases prior to occurrence of infarction related to DCI. The purpose of this study is to assess whether alterations in BBBP, measured as permeability surface (PS) using CTP, precede development of infarction related to DCI in aSAH patients.

#### METHOD AND MATERIALS

This is a retrospective study of aSAH patients included in an IRB-approved clinical trial. Inclusion criteria are patients with CTP performed with extended scanning technique for analysis of PS. Exclusion criteria were patients who did not develop an infarction related to DCI,

based on follow-up CT. All CTP data were post-processed using CT perfusion 4D software (GE Healthcare) for generation of PS, CBF, CBV and MTT maps. Using the integrated registration tool, the NCCT with the infarction region was superimposed on the CTP maps for co-registration of the exact infarct location. As an internal control for each patient, a "mirror ROI" was placed in the contralateral non-infarcted region. Paired t-tests were performed for each CTP parameter.

#### RESULTS

A total of 13 patients were included in the statistical analysis with 13 infarction (delayed cerebral ischemia, DCI) regions. PS elevation was observed in all cases in ROI that represented subsequently developed DCI compared to the contralateral brain parenchyma without DCI (mean DCI 0.449; mean control 0.198;  $p = 0.0002$ ). By contrast, the conventional clinically used CTP parameters CBF, CBV and MTT did not show any significant difference to the contralateral ROI on pre-DCI CTP (CBF mean DCI 15.76; mean control 16.34;  $p = 0.9296$ ; CBV mean DCI 1.89; mean control 1.54;  $p = 0.0528$ ; MTT mean DCI 9.76; mean control 7.89;  $p = 0.0917$ ).

#### CONCLUSION

These preliminary data show that a relative increase in blood brain barrier permeability compared to the contralateral brain parenchyma appears to precede the development of delayed cerebral ischemia in patients with aneurysmal subarachnoid hemorrhage.

#### CLINICAL RELEVANCE/APPLICATION

Permeability changes prior to the development of irreversible cerebral infarction may lay the foundation for the development of new treatment strategies targeted towards stroke prevention.

### **SST10-06 • 3T High Resolution Vessel Wall Imaging in Acute Perforator Infarction within the Territory of Middle Cerebral Artery**

**Younghen Lee MD (Presenter) ; Doran Hong MD ; Hyung Suk Seo ; Bo-Kyung Je MD, PhD ; Sang-II Suh ; Jin Man Jung ; Do Young Kwon ; Moon Ho Park**

#### PURPOSE

Recently, 3T high-resolution vessel wall imaging (HRVW) has been introduced to compensate limitation of 3-dimensional time-of-flight magnetic resonance angiography (TOF MRA) which only shows the vascular lumen of intracranial artery diseases by demonstrating wall appearances. We aimed to evaluate the vessel wall characteristics of the ipsilateral middle cerebral arteries (MCA) in acute striatocapsular infarction presumed to be perforator occlusion using HRVW in addition to TOF MRA.

#### METHOD AND MATERIALS

Forty-seven consecutive patients (M:F=31:16, mean age=59.6±12.9 years) with acute striatocapsular infarctions presumed by perforator occlusion, displayed on the DWI, were retrospectively enrolled. According to the lesion diameter, we classified them either 1) perforator arterial infarction (PAI)50%,n=7). Additionally stroke risk factors including atherosclerosis and cardioembolic indicators were assessed.

#### RESULTS

Of the included 47 patients with acute PAI within MCA territory, 25 showed wall enhancement, 10 showed wall thickening, and 9 showed eccentric narrowing. HRVW demonstrated additional vessel wall abnormalities in eighteen (45.0%) from 40 patients classified as normal M1 on TOF MRA, moreover, 12 (41.4%) from twenty-nine patients with PAI< 2cm whose ipsilateral MCA was normal on TOF-MRA.

Abnormal vessel wall findings to suggest intracranial atherosclerosis were more commonly depicted by HRVW than TOF MRA in patients (p < 0.05).

#### CONCLUSION

Based on our preliminary results, HRVW imaging could provide more additional findings to suggest relationship of intracranial

atherosclerosis in acute PAI

#### CLINICAL RELEVANCE/APPLICATION

HRVW imaging could provide more additional findings beyond the scope of TOF-MRA

### **SST10-07 • Temporal Patterns of Intracranial Vessel Wall Imaging Using High Resolution MRI: A Follow-Up Study**

**Emmanuel C Obusez MD (Presenter) ; Ferdinand K Hui MD \* ; Rula Haggi-Ali ; Stephen E Jones MD, PhD**

#### PURPOSE

High-Resolution Magnetic Resonance Imaging (HRMRI) is an emerging tool for evaluating intracranial artery disease. Vessel wall characteristics of intracranial vasculopathy have been described on HRMRI. We investigated HRMRI arterial wall characteristics of non-atherosclerotic intracranial diseases to determine wall pattern changes over a follow up period.

#### METHOD AND MATERIALS

We retrospectively reviewed high resolution 3-tesla MRI vessel wall studies performed on 29 patients with confirmed diagnosis of large to medium cerebral vessel disease over a follow up period. The high resolution vessel wall imaging protocol included black-blood contrast-enhanced T1-weighted sequence with fat suppression and time-of-flight (TOF) MRA of the circle of Willis. Clinical and demographic data and vessel wall characteristics including enhancement, wall thickening, and lumen narrowing were collected.

#### RESULTS

Clinical and radiographic diagnosis included CNS vasculitis (13), RCVS (13), moyamoya (2), intracranial dissection (1). In the CNS vasculitis group, 9 showed smooth, concentric wall enhancement and thickening, 3 with smooth, eccentric wall enhancement and thickening, and 1 without wall enhancement and thickening. Six of 13 had follow-up imaging, 4 showed stable smooth, concentric enhancement and thickening consistent with initial imaging findings and 2 with resolution of initial imaging findings. For RCVS, 10 showed diffuse, uniform wall thickening without and with mild enhancement. Nine of 10 had follow-up imaging, 8 with complete resolution of initial findings. For moyamoya, 2 of 2 patients at initial and follow-up imaging showed severe, irregular, vessel narrowing and occlusion without wall thickening, while 1 of 2 showed patchy wall enhancement. Intracranial dissection showed irregular, eccentric enhancement and wall thickening with a dual lumen separated by an enhancing intimal flap and attenuation of initial findings at follow-up imaging.

#### CONCLUSION

Post-gadolinium high-resolution 3-tesla MRI appears to be a feasible tool in differentiating vessel wall patterns of intracranial arteriopathy over a follow up period.

#### CLINICAL RELEVANCE/APPLICATION

Study of the evolution of HRMRI wall patterns may improve radiographic diagnoses and may serve as a surveillance modality to identify changes in wall morphology with intracranial disease progression.

### **SST10-08 • Wall Enhancement of the Cerebral Arteries after Gadolinium Injection: Evaluation by MRI Using MSDE-3D-TSE Sequence**

**Morio Nagahata MD (Presenter) ; Makoto Obara \* ; Yasuko Minagawa ; Seina Sato ; Satoko Nagahata MD ; Rei Kondo MD, PhD ; Shinjiro Saito MD, PhD ; Takamasa Kayama MD, PhD**

#### PURPOSE

Motion sensitized driven equilibrium (MSDE) method can reduce the intraluminal blood signal, even in the post-contrast MR imaging. In this paper, we investigate the wall enhancement of cerebral arteries after injection of gadolinium using MSDE-3D-TSE sequence.

#### METHOD AND MATERIALS

A retrospective review was undertaken of consecutive 231 Gd-enhanced brain MR examinations with additional post-contrast MSDE-3D-TSE scan from May 2011 to March 2013. MSDE-3D-TSE sequence was performed in three directions (axial, coronal, and sagittal) with a high resolution protocol consisting of T1w 3D-TSE sequence, TR/TE 425/12.8, 50 sections, 0.72x0.95x0.70mm voxel size, and a 384x342-imaging matrix on a 3T Achieva scanner (Philips). Among the 231 brain examinations, we evaluated the wall enhancement of each main arterial segment such as ICA (C1), M1, vertebral artery (VA), and basilar artery (BA) on MSDE-3D-TSE

images. All images were analyzed by experienced neuroradiologist and neurosurgeons in consensus and classified as strong wall enhancement (equal to choroid plexus), faint enhancement (increased wall signal than pre-contrast scan), and no enhancement. In this study, we excluded the abnormal arterial segments such as occlusion, existing stenosis, fusiform dilatation, and dissection. Objective vessels of almost-normal morphology, which we could evaluate on post-contrast MSDE images, were 341 ICAs, 310 M1s, 78 VAs, and 122 BAs.

#### RESULTS

Strong wall enhancement, equally to choroid plexus, was observed in 0.88% of ICAs, 3.2% of M1s, 23.1% of VAs, and 0.82% of BAs. Faint enhancement was observed in 5.6% of ICAs, 1.3% of M1s, 30.8% of VAs, and 3.3% of BAs. Strongly enhancing M1 wall was observed only at the affected side of distal cortical embolism or perforating arterial infarcts in our series. Wall enhancement of VA was, however, observed frequently without symptoms suggesting vascular pathology.

#### CONCLUSION

We could evaluate the enhancement of cerebral arterial wall using MSDE-3D-TSE sequence. In MCA, strong enhancement may mean some pathological change. In VA, strong enhancement does not always mean the vascular pathology, although it is often observed.

#### CLINICAL RELEVANCE/APPLICATION

Wall enhancement of normal cerebral arteries revealed by post-contrast MSDE-3D-TSE sequence should be an important data for evaluating the pathological wall enhancement by post-contrast MRI in future.

### SST10-09 • Effect of Insurance Status on Imaging Utilization for Acute Ischemic Stroke

**Waleed Brinjikji** (Presenter) ; **Abdulrahman M El-Sayed** DPhil ; **Jennifer S McDonald** PhD \* ; **Alejandro A Rabinstein** MD ; **Harry J Cloft** MD, PhD \*

#### PURPOSE

Previous studies have demonstrated that socioeconomic disparities exist in imaging utilization for both acute and chronic disease. We studied a large nationwide database to determine if insurance-based disparities exist in the utilization of imaging for acute ischemic stroke.

#### METHOD AND MATERIALS

Inpatients with a primary diagnosis of acute ischemic stroke from 11/2005 through 12/2011 were identified from the Perspective database. Patients were stratified into four groups according to insurance status: 1) uninsured, 2) Medicaid, 3) Medicare and 4) private insurance. Utilization rates of head CT, CT perfusion, head MRI, non-invasive head angiography (including head CTA and head MRA), non-invasive neck angiography (including neck CTA and neck MRA), carotid ultrasound, and echocardiography were compared using a chi-squared test. A multivariable logistic regression model adjusting for potential confounding variables was fit to determine the association between insurance status and imaging.

#### RESULTS

A total of 210212 patients were included in this study. 10396 patients (5.0%) were uninsured, 14243 patients (6.8%) had Medicaid, 153209 patients (72.9%) had Medicare and 32364 patients (15.4%) had private insurance. Utilization rate of MRA/CTA head was 55.9% for private insurance patients compared to 36.1% for Medicare patients (P

#### CONCLUSION

Significant disparities exist in the utilization of neuroimaging for acute ischemic stroke based on patient insurance status. More research is needed to address these disparities.

#### CLINICAL RELEVANCE/APPLICATION

Significant insurance-based disparities exist in the utilization of advanced imaging for acute ischemic stroke. Further studies are needed to better understand and address these disparities.

## Neuroradiology (Quantitative Neuroimaging)

Friday, 10:30 AM - 12:00 PM • N230

[MR](#) [BQ](#) [NR](#)

[Back to Top](#)

**SST11 • AMA PRA Category 1 Credit™:1.5 • ARRT Category A+ Credit:1.5**

**Moderator**

**Pratik Mukherjee**, MD, PhD \*

**Moderator**

**Haris I Sair**, MD

### SST11-01 • Geometrical Assessment of the Membranous Semicircular Canals: Using Three-dimensional Reconstructed High Resolution Magnetic Resonance Imaging of the Inner Ear

**Ahmed F Emam** MBCh (Presenter) ; **Nagy N Naguib** MSc ; **Nour-Eldin A Nour-Eldin** MD, MSc ; **Mohammed A Alsubhi** BMBS ; **Thomas J Vogl** MD, PhD

#### PURPOSE

To estimate the angles between and to assess the length of the Superior (S), Posterior (P), Lateral (L), Crus commune (CC) semicircular canals (SCC) of the Inner Ear using three dimensional (3D) reconstruction of the high resolution MR-Imaging sequences

#### METHOD AND MATERIALS

The retrospective study was performed on 2100 SCC's (in 350 patients with a mean age of 48.5 year). Measurements were performed using 3D reconstruction of a high resolution MR-Imaging ISO-Space sequence with 0.6 mm slice thickness. 3D reconstructions were performed using Advantage Workstation for diagnostic imaging. The assessment was manually performed for each side in all patients. For each side the angles between the superior and posterior SCC (X), between the Superior and lateral SCC (Y) and between the Posterior and lateral SCC (Z) were measured. In addition, the individual length of each SCC and the CC was performed. The mean, standard deviation (SD) and range of each measurement were calculated.

#### RESULTS

Of the 2100 angles measured 37 were not visualized due to unclear appearance of the SCC in the region of the angle. In addition the length of 163 SCCs was not assessed due to fragmentation or unclear visualization. The angles between the left SCCs showed a mean value of X: 108.31° (SD:10.15, Range:77°-145°), Y: 72.11° (SD:12.28, Range:41°-116°) and Z: 84.85° (SD:12.45, Range:48°-123°). The angles between the right SCCs showed a mean of X: 110.34° (SD:10.26, Range:80°-150°), Y: 71.13° (SD:13.15, Range:42°-113°), and Z: 85.33° (SD:13.07, Range:48°-138°).

The mean Length of the Superior, Posterior, Lateral, Crus commune SCC of the left Inner Ear was S: 19.66mm (SD:1.64, Range:14-25mm), P: 21.54mm (SD:1.99, Range:7.3-27mm), L: 13.31mm (SD:1.48, Range:8-18mm) CC: 3.78mm (SD:0.44, Range:3-5mm). The mean Lengths on the right side were S: 19.47mm (SD:1.67, Range:15-26mm), P: 22.30mm (SD:2.06, Range:16-29mm), L: 13.39mm (SD:1.46, Range:7-18mm), CC: 3.78mm (SD:0.44, Range:2.7-5mm).

#### CONCLUSION

This descriptive study showed that angles between the Semicircular canal planes have a wide range of degrees..



#### CLINICAL RELEVANCE/APPLICATION

Contrary to previous reports in the literature (that the angle between the SCCs is around 90°) the current study results shows a wide range of variations between the angles.

### SST11-02 • Clinical Evaluation of Synthetic Brain MRI at 3.0 Tesla

**Michael Nelles** MD (Presenter) ; **Juergen Gieseke** DSc ; **Dariusch R Hadizadeh Kharrazi** MD ; **Horst Urbach** MD ; **Hans H Schild** MD

#### PURPOSE

Prospective intra-individual comparison of synthetic quantitative versus regular MR imaging (MRI) of the brain at 3.0T.

#### METHOD AND MATERIALS

A 3.0T MR system (Achieva 3.0T TX, Philips Healthcare, The Netherlands) and a stand-alone postprocessing software (SyntheticMR, Sweden) were used to create T1, T2 and FLAIR contrast-weighted synthetic MR images of the brain. The quantitative mapping was based on the QRAPMASTER method ("Quantification of Relaxation Times and Proton Density by Multiecho acquisition of a saturation-recovery using Turbo Spin-Echo Readout"), using a multislice, multiecho, and multidelay acquisition with a scan time of 4:50 minutes. 25 consecutive patients underwent MRI of the brain including synthetic quantitative and regular T1, T2 and FLAIR sequences. Contrast ratios (CRs) were calculated between gray matter (GM) and white matter (WM) for synthetic and regular sequences. Diagnostic quality of synthetic MR examinations was scored as follows: Score of 4, excellent (sharp depiction of the GM/WM junction and subcortical GM without interfering artifacts). Score of 3, adequate for diagnosis (minor artifacts or noise present not interfering with image interpretation). Score of 2, questionable for diagnosis (impaired by artifacts, noise and / or changes in contrast). Score of 1, non-diagnostic.

#### RESULTS

#### CONCLUSION

Synthetic quantitative MRI is capable of generating accurate conventional contrast images within a clinically acceptable time. The diagnostic image quality is readily comparable to that of regular MRI sequences in the majority of cases.

#### CLINICAL RELEVANCE/APPLICATION

Synthetic MRI holds the promise of replacing the acquisition of different regular MR series in selected patients, suitable for disease monitoring in e.g. MS or glioma patients.

### SST11-03 • Multivariate Longitudinal Shape Statistics of Brain Lateral Ventricles during the First Eighteen Months of Human Life

**Lucile Bompard** (Presenter) ; **Shun Xu** ; **Martin Styner** ; **Wei Gao** ; **Valerie L Jewells** DO ; **Beatriz Paniagua** ; **Weili Lin** PhD

#### PURPOSE

The human brain undergoes dramatic structural changes in the first few years of life. Of particular interest are the lateral ventricles (LVs) of the brain because of their association with many psychiatric and developmental disorders. The primary aim of this research is to discern the temporo-spatial growth characteristics of the LVs to develop a normative data-base.

#### METHOD AND MATERIALS

24 healthy subjects were imaged using a 3T MR scanner as frequently as 3 months from 2 weeks of age to 12 months of age, and again at 18 months. A minimum of 4 scans was performed per subject. T2- weighted images were employed to segment the LVs, resulting in 127 left and 119 right LVs. Due to significant variation, the tail of the ventricular horn was manually removed. Subsequently, a densely sampled surface representation was computed for each LV using spherical harmonics based point distribution models, allowing group analysis of the spatiotemporal growth of the LVs during the first 18 months of life. Volumetric measures, cross-sectional areas, and growth rates were calculated.

#### RESULTS

Volumetric measurements reveal a continuous growth of the LVs in the first 12 months, followed by 11±27% reduction from 12 to 18 months. In addition, the left LV is consistently larger (10±23% at 2wks and 9±20% at 18month) than that of the right LV. By grossly separating the LVs into the anterior and posterior horns and the mid-body, additional insights are revealed. Measurements of regional cross-sectional areas of LVs, the mid-body mainly elongates and the horns thicken with time. Specifically, the ventricle horns exhibit the fastest growth rates between 0 – 3 months, followed by a progressively reduced growth rate between 3 – 12 months. In addition, the posterior horn consistently outgrows the anterior horn. In contrast, the temporal changes of thickness of the mid-body are mainly from dorsal to ventral, with the fastest growth rate between 0 – 3 months.

#### CONCLUSION

The LV growth exhibits both temporal and regional specific patterns during the first 18 months of life. Our results offer new insights into the unique growth patterns of human ventricle.

#### CLINICAL RELEVANCE/APPLICATION

This detailed normative spatiotemporal growth characteristics of LVs during the first 18 months of life provide important references for the delineation of early abnormal LV growth.

### SST11-04 • Whole Brain Volumetric and Morphometric Analysis of Patients with Maple Syrup Urine Disease

**Emilie R Muelly** PhD (Presenter) ; **Don Bigler** ; **Gregory J Moore** MD, PhD ; **Kevin Strauss** ; **D. Holmes Morton** ; **Julie A Mack** MD

#### PURPOSE

Maple syrup urine disease (MSUD) is an inherited metabolic disorder that impairs branched chain amino acid metabolism. Rapid elevations of circulating branched chain amino- and ketoacids cause life-threatening encephalopathy. Despite dietary treatment, achievement of metabolic control varies and patients remain at risk for acute decompensation. Liver transplantation has been shown to eliminate metabolic volatility. Reversible decreases in N-acetylaspartate (NAA) have been demonstrating using magnetic resonance spectroscopy during both acute and chronic states of disease. These findings may reflect structural or functional differences. Volumetric analysis may add value to interpretation of neurochemical findings.

#### METHOD AND MATERIALS

Quantitative proton magnetic spectra were obtained for 37 patients (26 on dietary therapy, 11 status-post liver transplantation) and 26 sibling controls using a Siemens Magnetom Trio 3 Tesla scanner. Whole brain and segmented volume calculations of the images were made using SPM5 in Matlab. Brain morphometry dimensional measurements were measured using Osirix. A three-way ANCOVA (accounting for age as a cofactor) with Tukey post-hoc testing were used to identify group differences.

#### RESULTS

Total brain parenchyma as a percentage of total brain volume was greater in patients on dietary therapy compared to controls (p = 0.02). Gray and white matter percentages of total brain volume individually did not differ between groups. Total whole brain volume and morphometry did not differ between groups.

#### CONCLUSION

Our results support the hypothesis that low NAA levels in MSUD patients reflect impaired neuronal energy production rather than neuronal loss. However, our methods prevent us from detecting decreases in neuronal density that do not change tissue size and also do not specifically evaluate brain regions in which low NAA levels were detected. Furthermore, increased total brain parenchyma may reflect subtle chronic edema. Further study, such as analysis of T2\* and regional morphometric data, is needed to explore these possibilities.

#### CLINICAL RELEVANCE/APPLICATION

Patients with maple syrup urine disease have increased total brain parenchymal volume.

### SST11-05 • DTI Correlates of Cognition in Conventional MRI Normal Appearing Brain in Patients with Vitamin B12 Deficiency

**Rakesh K Gupta** MD, MBBS (Presenter) ; **Pradeep K Gupta** MSc ; **Ravindra K Garg** MD, MBBS ; **Bhaswati Roy** ; **Abhinav Yadav** BS ; **Yogita Rai** PhD ; **Ram K Rathore** DSc ; **Chandra M Pandey** PhD ; **Ponnada A Narayana** PhD

#### PURPOSE

Deficiency of vitamin B12 may result in neuronal degeneration and brain damage which influences the cognition. We hypothesized that patients with clinical symptoms of subacute combined degeneration (SACD) and biochemical evidence of Vitamin B12 deficiency should have a cognition decline and microstructural brain changes on advanced MRI even when conventional MRI appears normal.

#### METHOD AND MATERIALS

Patients with SACD of the cord were recruited for the study. Patients underwent nerve conduction velocity and biochemical analysis for serum Vitamin B12, and homocystine. Hematology including the type of anemia was also performed. All patients with Vitamin B12 deficiency and clinical features of SACD were subjected to the complete imaging cervical spine and brain imaging. Patients with normal brain MRI with or without imaging changes in the cervical spine were included for cognition tests. Based on these criteria, 51 patients and 46 age and sex matched controls were enrolled in this study. 3D-T1 weighted and DTI was performed in all these subjects. FSL based VBM and TBSS analysis were performed for volumetric and white matter fiber tracts changes quantification.

#### RESULTS

No significant changes in grey and white matter volumes were observed in patient compared to control using VBM. Significant reduction of FA and increase in MD and RD values were observed in various brain regions in patients compared to controls. Most of the Neuropsychological score were significantly altered in patients compared to controls and few of these showed significant correlation with FA and RD in some of the brain regions.

#### CONCLUSION

Decrease in FA and increase in MD and RD results of WM microstructure suggests its alteration probably due to demyelination of the fibers secondary to Vitamin B12 deficiency. These patients, though present clinically with SACD, have generalized involvement of the white matter of the CNS and have associated decline in cognition. Correlation of some of the NPT scores with region specific white matter changes confirms that the abnormalities in NPT relate to the changes in the white matter microstructures.

#### CLINICAL RELEVANCE/APPLICATION

Vitamin B12 deficiency has generalized effect on the CNS white matter even when it manifests as SACD as evidenced by cognition and brain microstructural alteration.

### SST11-06 • Reliability of 3D Pseudo-continuous Arterial Spin-labeling MR Imaging for Measuring Visual Cortex Perfusion on Two 3T Scanners

**Diandian Huang** (Presenter) ; **Xin Lou** MD, PhD ; **Lin Ma** MD ; **Bing Wu** ; **Kai-Ning Shi**

#### PURPOSE

The visual cortex cerebral blood flow (CBF) values are closely associated with visual perception. Perfusion MRI can be used to identify patients with ischemic changes of visual cortex who may benefit from reperfusion therapies. The risk of nephrogenic systemic fibrosis, however, limits the use of contrast agents. Our objective was to evaluate the reliability and reproducibility of three dimensional arterial spin labeling (3D pCASL), an alternative noninvasive perfusion technique, to detect CBF of visual cortex *in vivo*.

#### METHOD AND MATERIALS

Twelve healthy subjects were scanned three times on two 3.0T MR scanners with 3D pCASL technique. The 1st test and 3rd test were done on scanner-1, while the 2nd test was on scanner-2. Intervals between tests were among 10-15 days. The 3D pCASL data with two post labeling delay time (PLD) of 1.5 and 2.5 seconds was acquired during every scanning. Volumetric T1-weighted images were also acquired for image registration. The CBF values of visual cortex (included brodmann 17, brodmann 18, brodmann 19) were extracted for comparison. The intra- and inter-scanner reliability and reproducibility were evaluated with the intraclass correlation coefficient (ICC) and Bland-Altman plot.

#### RESULTS

The relative CBF values of visual cortex were 16-84 ml/min/100g (PLD=1.5s) and 27-75 ml/min/100g (PLD=2.5s). Compared with 1st test and 2nd test, the ICC was 0.685 at PLD=1.5s and 0.754 at PLD=2.5s. Compared with 2nd test and 3rd test, the ICC was 0.719 at PLD=1.5s and 0.903 at PLD=2.5s. Compared with 1st test and 3rd test, the ICC was 0.821 at PLD=1.5s and 0.831 at PLD=2.5s. Higher reliability (ICC=0.829) for PLD 2.5s compared to PLD 1.5s (ICC=0.743) were demonstrated in inter-scanners. At intra- and inter-scanner, the Bland-Altman showed the reproducibility at PLD=2.5s is better than that at PLD=1.5s.

#### CONCLUSION

Although inter-scanner reliability is slightly lower than intra-scanner, there is a very high similarity of the outcomes at different time from two scanners. The 3D pCASL technique is available for measuring the CBF at visual cortex with high reliability and reproducibility. It should be used for MR research on blood flow of visual cortex at multiple centers.

#### CLINICAL RELEVANCE/APPLICATION

The 3D pCASL can measure CBF values of visual cortex with high reliability and reproducibility and offers a noninvasive way to access the etiology and diagnosis of posterior visual pathway disease.

### SST11-07 • Adaptation and Slow Recovery of Metabolic Activity in Human Visual Cortex Coupled with a Modest Change in Cerebral Blood Flow

**Farshad Moradi** MD (Presenter) ; **Richard B Buxton** PhD

#### PURPOSE

We recently demonstrated sub-additive flow and metabolic response non-linearity in human visual cortex consistent with adaptation. A disproportionately larger adaptation of metabolic response compared to blood flow was observed. These results indicate an aspect of metabolic activity corresponding to neural adaptation (or fatigue) that has a different neurovascular coupling from stimulus driven activation. We examine if the adaptable aspect of metabolic activity is coupled with high flow and whether or not it recovers during inter-stimulus intervals.

#### METHOD AND MATERIALS

Six observers participated in the experiment. CBF and BOLD responses to continuous (46 s) and intermittent (7.6 s on and off x 3) peripheral gratings were measured using a dual gradient-echo optimized multipulse pseudo-continuous arterial spin labeling sequence. A 2x2 design (continuous vs. intermittent, two contrast levels) was used. The difference between initial and final 18 s of activity during each epoch (?CBF vs. ?BOLD) were determined. ?CMRO2 was estimated using a modified calibrated BOLD method.

#### RESULTS

If the adaptable aspect of metabolic activity is coupled with high flow then the neurovascular-coupling ratio is expected to increase over time with prolonged stimulation in the continuous condition. If the adaptable aspect of metabolic activity recovers during interstimulus intervals then the neurovascular-coupling ratio should remain the same over time in the intermittent condition. A positive change in neurovascular coupling would result a ?BOLD that is disproportionately greater than ?CBF. Contrary to both predictions, ?BOLD was negative compared to ?CBF in all conditions, indicating a significantly lower neurovascular coupling ratio at the end of each epoch

compared to the beginning.

#### CONCLUSION

The adaptable aspect of metabolic activity is coupled with a lower flow modulation compared to the input-driven modulation and does not recover during short inter-stimulus intervals. Our findings are consistent with the hypothesis that cerebral blood flow in human visual cortex is driven by both metabolic activity and visual input via independent mechanisms.

#### CLINICAL RELEVANCE/APPLICATION

Numerous pathologic conditions affect the regulation of cerebral blood flow. Our results provide insight into physiological modulations of neurovascular coupling and role of adaptation nonlinearity.

### SST11-08 • Evaluation of WBAA with Registration-based Cube Propagation for Brain Atrophy Quantification

**Martin Lillholm** MSc, PhD (Presenter) \* ; **Akshay Pai** ; **Lauge Sorensen** ; **Mads Nielsen** PhD \* ; **Jon Sparring** \* ; **Sune Darkner** ; **Erik B Dam** PhD \*

#### PURPOSE

Atrophy for the whole brain and sub-structures is becoming common as study outcome in clinical trials assessing the efficacy of potential treatments of diseases involving dementia. In this study, we evaluated the sensitivity to change related to progression of Alzheimer's disease of a novel software framework, WBAA.

#### METHOD AND MATERIALS

The recently defined Alzheimer's disease neuroimaging initiative (ADNI) standardized collection ('ADNI1:Annual 2 Yr 1.5T' at [adni.loni.ucla.edu](http://adni.loni.ucla.edu)) with 504 subjects (169 normals, 234 mild cognitively impaired, and 101 alzheimer) including baseline and 12-month 1.5T T1 magnetic resonance imaging (MRI) scans was used. The MRIs were processed using longitudinal FreeSurfer and the whole brain atrophy application (WBAA 1.0 by Biomediq) that performs non-rigid registration followed by atrophy estimation quantification using cube propagation (CP). The WBAA was also evaluated with CP replaced by the common Jacobian integration (JI) method. Sensitivity to change was evaluated by atrophy differences between healthy and Alzheimer subjects quantified using Cohen's D and required study sample sizes.

#### RESULTS

As example, quantifications of the hippocampus atrophies estimated using WBAA were -1.3% and -0.6% for the Alzheimer and healthy subjects whereas the ventricle estimates were +9.3% and +4.1%, respectively. Corresponding Cohen's D for WBAA on these two regions were 1.1 and 1.0. For whole-brain, hippocampus, ventricles, and medial temporal lobe, the WBAA Cohen's D were 0.7, 1.1, 1.0, and 1.3. The corresponding sample sizes were 173, 124, 113, and 87. For WBAA with JI, Cohen's D were 0.5, 1.1, 1.0 and 1.2; with sample sizes 230, 139, 112, and 101. For longitudinal FreeSurfer, Cohen's D were 0.7, 1.0, 1.0, and 1.3; with sample sizes 183, 152, 118, and 102.

#### CONCLUSION

The WBAA using CP for brain atrophy quantification provided sensitivity equal or superior to leading, competing methods. Specifically, the WBAA sample sizes were generally lower.

#### CLINICAL RELEVANCE/APPLICATION

Unlike longitudinal FreeSurfer, WBAA allows quantification of final atrophy estimates directly after each visit. Adding the matching/improved sensitivity, WBAA seems appropriate for clinical trials.

### SST11-09 • Tumor Cellularity and the Extravascular-Extracellular Space: Using Quantitative Imaging to Evaluate Correlation Between ADC and DCE MRI in Human Gliomas, Meningiomas and Cerebral Lymphomas

**Hannu T Huhdanpaa** MD (Presenter) ; **Darryl Hwang** PhD ; **Naira Muradyan** PhD \* ; **Steven Cen** PhD ; **Michael Booker** ; **Alexander Lerner** MD ; **Deborah Commins** ; **Anandh G Rajamohan** MD ; **Paul E Kim** MD ; **Orest B Boyko** MD, PhD \* ; **John L Go** MD ; **Eu-Meng Law** MBBS \* ; **Mark S Shiroishi** MD

#### PURPOSE

The apparent diffusion coefficient (ADC) determined from diffusion tensor (DTI) MR imaging can give an impression of the extravascular-extracellular space (EES) and has been shown to be inversely correlated with tumor cell density. Parametric maps such as the EES fraction ( $v_e$ ) derived from dynamic contrast enhanced (DCE) MRI also characterize EES. The purpose of this study was to determine if there is a correlation between ADC and DCE metrics such as  $v_e$ , blood-brain barrier transfer constant ( $K_{trans}$ ),  $K_{ep}$  ( $K_{trans}/v_e$ ), and fractional plasma volume ( $v_p$ ) for gliomas, cerebral lymphomas and meningiomas. Figure 1 demonstrates ADC and  $v_e$  parametric maps for a glioma.

#### METHOD AND MATERIALS

18 gliomas (grade I-IV), 2 lymphomas and 5 meningiomas were retrospectively evaluated. DTI and DCE images were acquired during the same MRI exam. DCE-MRI images were postprocessed in CADvue. Metrics extracted from DCE MRI were:  $v_e$ ,  $v_p$ ,  $K_{trans}$ , and  $K_{ep}$ . ADC maps were generated by the MR scanner. DCE and ADC images were co-registered and 3-dimensional regions of interest were drawn on parametric maps. Voxel-wise correlation between ADC and DCE parameters were examined using scatter plots and tested by random effects model. Mean and median values were extracted using Spearman correlation.

#### RESULTS

Overall, mean ADC correlated negatively with mean  $v_e$  ( $r = -0.48$ ,  $p = 0.03$ ) as well as with median  $v_e$  ( $r = -0.52$ ,  $p = 0.01$ ). The result of voxel level analysis using random effects model did not show significant correlation between ADC and  $v_e$  ( $r = 0.09$ ,  $p = 0.09$ ). No statistically significant correlation was observed between ADC and the other parameters,  $v_p$ ,  $K_{trans}$ , and  $K_{ep}$ .

#### CONCLUSION

Our results showed a negative correlation between ADC and both mean as well as median  $v_e$ , and no significant correlation between ADC and the other DCE parameters. This is in agreement with a prior study performed in breast cancer, while another study in breast cancer as well as one in glioblastoma found no correlation. These results likely reflect limitations in our understanding of these metrics though limitations in imaging technique may be confounders.

#### CLINICAL RELEVANCE/APPLICATION

Determination of the relationship between ADC and DCE MRI metrics such as extravascular-extracellular volume fraction ( $v_e$ ) may provide new imaging biomarkers of brain tumor cellularity

### ISP: Nuclear Medicine (Cardiovascular Imaging)

Friday, 10:30 AM - 12:00 PM • S505AB



[Back to Top](#)

SST12 • AMA PRA Category 1 Credit™:1.5 • ARRT Category A+ Credit:1.5

Moderator

Akash Sharma, MD

Moderator

Pamela K Woodard, MD \*

SST12-01 • Nuclear Medicine Keynote Speaker: New Horizons in Cardiovascular Imaging with PET/MRI

### SST12-03 • FDG-PET/CT: Do Contrast Enhanced CT for Attenuation Correction and Ultra-HD-PET Influence the SUV-values in Large Vessel Walls?

Ingo Janssen (Presenter) ; Inga Buchmann ; Florian M Vogt MD

#### PURPOSE

To optimize large-vessel-imaging in FDG-PET/CT we evaluated, if contrast enhanced CT (ceCT) for attenuation correction (AC) in FDG-PET-CT and ultraHD-(high-definition-PET+ time of flight) (uHD) compared with iterative reconstruction (IR) may lead to differences in large-vessel-SUV.

#### METHOD AND MATERIALS

50 patients (pat), who underwent FDG-PET/CT in malignant-disease-staging, were included in this retrospective study. All pat were unsuspecting for large-vessel-vasculitis. 25 pat underwent FDG-PET-CT with ceCT for AC (group A; 100 ml Xenetix® 300 i.v, delay 50 sec) and 25 pat FDG-PET-CT with non-contrast (nc) CT for AC (group B).  $242 \pm 15$  MBq FDG were applied i.v. PET-CT-scans with acquisition of uHD and IR data started  $82 \pm 19$  min p.i. (Biograph mCT, Siemens). SUVmax-values in identical localizations in the wall of ascending aorta, aortic arch and descending aorta were evaluated by VOI-analysis in all patients. Further a SUVmax/mediastinal-bloodpool (MB)-ratio and SUVmax/liver-bloodpool(LB)-ratio were calculated. MB was determined by drawing a VOI directly inside of the ascending aorta, LB by drawing a VOI in visually physiological liver-tissue. Mean SUVmax, mean MB-ratio and mean LB-ratio of both groups were compared in uHD and IR. Significance level was defined as  $p = 0.05$ .

#### RESULTS

Mean SUVmax-values in group A were significantly higher than in group B (uHD: p

#### CONCLUSION

CeCT for AC in FDG-PET/CT shows significant higher SUVmax-values in aortic wall and uHD demonstrates significant higher aortic-wall to background-contrasts. These results may significant influence the interpretation of large-vessel-vasculitis imaging in FDG-PET/CT.

#### CLINICAL RELEVANCE/APPLICATION

Further studies have to be performed, to evaluate the influence of ceCT for AC and uHD-PET on vasculitis-imaging in FDG-PET/CT.

### SST12-04 • 11C-Choline PET/CT Evaluation of Atherosclerotic Disease

Ann Packard MD (Presenter) ; Geoffrey B Johnson MD, PhD ; Christopher H Hunt MD ; Mark A Nathan MD ; Patrick J Peller MD \*

#### PURPOSE

Choline is known to be a prominent constituent of atherosclerotic plaque. This study measures the 11C-Choline accumulation in the abdominal aorta compared to vessel wall calcification and conventional risk factors of atherosclerotic disease.

#### METHOD AND MATERIALS

The 11C-choline PET/CT database was searched retrospectively from 1999-2012 for patients with data related to atherosclerotic risk factors, including medications, laboratory data, and medical history with an accrual target of 100 patients. PET/CT scans were evaluated blinded to clinical information by a Nuclear Medicine physician with 25 years of PET/CT experience, for radiotracer activity and calcium quantification. The aorta was analyzed from the renal arteries to the bifurcation. Max SUV was obtained from an ROI placed around the aorta on axial imaging at the level of peak activity. Max SUV ratios of aorta to blood pool were calculated. Clinical atherosclerotic risk factors were correlated to 11C-choline max SUV/BP ratio. Basic statistical analysis included Students-T test and ANOVA.

#### RESULTS

All 11C-Choline PET/CTs were performed for prostate cancer recurrence. Of a cohort of 900 11C-choline PET/CTs, 104 patients with adequate clinical data were targeted, and of these, 94 had complete imaging, and had a mean age of 69.6 (SD 8.33 yrs, range 45-86) at the time of scan; 50 had prior or active smoking history, 38 were on statin therapy for hyperlipidemia, and 14 had prior cardiovascular events including MI or stroke. Patients with a prior cardiovascular event had a higher max SUV ratio ( $2.99 \pm 0.599$ , p

#### CONCLUSION

Patients with prior cardiovascular events and those on statin therapy had higher choline uptake within the abdominal aorta. No relationship was found between choline and calcium, or a difference in calcium score between groups stratified for cardiovascular risks.

#### CLINICAL RELEVANCE/APPLICATION

11C-Choline PET/CT may be useful in evaluating and identifying active atherosclerotic vascular disease in patients receiving PET/CTs for other reasons.

### SST12-05 • Quantification of Myocardial Blood Flow and Coronary Flow Reserve with an Innovative Tc-99m Sestamibi Dynamic SPECT/CT Method: Validation with Coronary Angiography in a Pilot Study

Chung-Chieh Huang (Presenter) ; Fu-Chung Chen ; Po-Nien Hou ; Guang-Uei Hung ; Ran Klein \* ; Robert Dekemp PhD \* ; Wan-Chen Chen ; Bailing Hsu

#### PURPOSE

Myocardial blood flow (MBF)/coronary flow reserve (CFR) quantification with positron emission tomography has demonstrated the incremental value in diagnosis and risk stratification of coronary artery disease (CAD) over perfusion alone images, but its widespread utilization is limited in areas without appropriate flow tracers. This study investigates the diagnostic value of a dynamic SPECT/CT (dSPECT) method as a potential utility for flow quantification.

#### METHOD AND MATERIALS

Fifteen patients who underwent clinically indicated dipyridamole-stress/rest Tc99m-sestamibi myocardial perfusion SPECT were enrolled to evaluate both perfusion and dSPECT MBF/CFR. Coronary angiography for all patients confirmed 9 CAD with  $\geq 50\%$  stenosis (5 one-vessel, 1 two-v, 3 three-v). In addition, 5 low-likelihood (LL) patients with normal perfusion were included to obtain the range of LL MBF/CFR. dSPECT images were quantitatively reconstructed and analyzed for MBF/CFR with 1-tissue/2-kinetic compartmental flow model, tracer extraction correction and rest heart rate/pressure product correction using FlowQuant program. Traditional perfusion images were interpreted visually with a 17-segment model to create summed stress scores (SSS). Receiver-operating characteristic (ROC) analysis was used to evaluate the diagnostic performance of stress MBF (SMBF), CFR and SSS in detecting CAD.

#### RESULTS

Global SMBF and CFR of CAD group ( $1.31 \pm 1.03$  ml/min/g and  $1.61 \pm 0.94$ ) were significantly lower than those of non-CAD ( $2.42 \pm 0.51$  ml/min/g,  $p=0.016$  and  $3.06 \pm 0.66$ ,  $p=0.0038$ ) and LL groups ( $2.81 \pm 0.38$  ml/min/g,  $p=0.0023$  and  $2.78 \pm 0.67$ ,  $p=0.02$ ). No significant difference was noted between non-CAD and LL groups for global SMBF and CRF ( $p=0.18$  and  $0.51$ ). For vessel-based CAD (prevalence: 16 of 45 vessels, 36%) detection, area under the ROC curve (AUC) for territorial SSS ( $0.548 \pm 0.091$ ) was significantly smaller than that of SMBF ( $0.812 \pm 0.063$ ,  $p=0.009$ ) or CFR ( $0.815 \pm 0.063$ ,  $p=0.011$ ).

#### CONCLUSION

Our preliminary results suggest that dSPECT is a simple and effective method for the quantitation of MBF and CFR that can enhance the accuracy for CAD diagnosis without adding extra radiation burden to patients.

#### CLINICAL RELEVANCE/APPLICATION

Traditional MPI likely underestimate the extent and severity of perfusion abnormality in multi-vessel CAD, dSPECT MBF/CFR quantitation is clinically feasible and can enhance the diagnostic performance

## **SST12-06 • A Comparative Analysis of Myocardial Perfusion on Gated SPECT vs Coronary Atherosclerosis and Coronary Calcium Score on 64-slice CT**

**Parul Mohan** MBBS, MD (Presenter) ; **Harsh Mahajan** MD, MBBS ; **Upendra Kaul** MBBS, MD

### **PURPOSE**

Currently both gated SPECT and multislice CT are available for functional imaging i.e. assessing the haemodynamic consequences of CAD and anatomical imaging i.e. visualizing the coronary artery tree respectively. The aim of the current study was to compare the results of 64-slice CT and gated SPECT on a regional basis (per vessel distribution territory) in patients with known or suspected CAD.

### **METHOD AND MATERIALS**

One hundred and fifty patients underwent both gated SPECT for myocardial perfusion imaging and 64-slice CT for coronary calcium scoring and coronary angiography. The coronary calcium score was determined for each coronary artery. Coronary arteries on multislice CT angiography were classified as having no CAD, insignificant stenosis (0% luminal narrowing). Gated SPECT findings were classified as normal or abnormal (reversible or fixed defects) and were allocated to the territory of one of the various coronary arteries.

### **RESULTS**

In coronary arteries with a calcium score of 10 or less, the corresponding myocardial perfusion was normal in 94 %. In coronary arteries with extensive calcifications (score > 400), the percentage of vascular territories with normal myocardial perfusion was lower, 52%. Similarly, in most of the normal coronary arteries on 64-slice CT angiography, the corresponding myocardial perfusion was normal on SPECT in >94%. In contrast, the percentage of normal SPECT findings was significantly lower in coronary arteries with obstructive lesions

### **CONCLUSION**

Although a relationship exists between the severity of CAD on multislice CT and myocardial perfusion abnormalities on SPECT, analysis on a regional basis showed only moderate agreement between observed atherosclerosis and abnormal perfusion. Accordingly, 64-slice CT and gated SPECT provide complementary rather than competitive information, and further studies should address how these two modalities can be integrated to optimize patient management.

### **CLINICAL RELEVANCE/APPLICATION**

The comprehension of the data derived by the use of coronary angiography and cardiac radionuclide imaging is of paramount importance

## **SST12-07 • Inter-platform Reproducibility for Quantitative Assessment of Arterial [18F] Fluorodesoxyglucose (FDG) Uptake in Large Peripheral Vessels: A PET/CT Study**

**Birgit Langhans** (Presenter) ; **Axel Rominger** ; **Markus Hacker** ; **Peter Bartenstein** ; **Maximilian F Reiser** MD ; **Tobias Saam** MD \*

### **PURPOSE**

FDG-PET/CT is able to quantify arterial wall inflammation and is increasingly used in clinical trials to assess effects of new anti-atherosclerotic therapies. The objective of this study was to analyse inter-platform reproducibility of FDG uptake.

### **METHOD AND MATERIALS**

20 cancer patients were examined by whole-body FDG-PET/CT on two different platforms (platform 1: GE Discovery 690; platform 2: Siemens Biograph 64) with a median time between the first and second scan of 3.6 [2.8, 5.0] months. The maximum standardized uptake value (SUV<sub>max</sub>), the mean venous blood-pool (SUV<sub>bp</sub>) and the target-to-background ratio (TBR=SUV<sub>max</sub>/SUV<sub>bp</sub>) were determined in the aortic arch, ascending, descending, and abdominal aorta and both iliac and carotid arteries.

### **RESULTS**

Mean SUV<sub>max</sub>, averaged across all arterial territories were significantly higher on platform 1 compared to platform 2, with a mean difference of 0.25±0.31 (SUV<sub>max</sub>1: 2.86 vs. SUV<sub>max</sub>2: 2.61; p=0.002). However, mean TBR values did not differ significantly between the platforms (TBR1 2.25 vs. TBR2 2.10; p=0.2). When the vascular territories were assessed separately, SUV<sub>max</sub> was significantly higher on platform 1 in the aortic arch, ascending, descending and abdominal aorta. No significant differences in SUV values were found in iliac and carotid arteries. TBR values for the different vascular territories did not differ significantly, except for the aortic arch.

### **CONCLUSION**

SUV<sub>max</sub> measurements differ significantly across different platforms, but not the TBR values. For serial assessment of vessel wall inflammation we therefore recommend to use the identical platform or alternatively to use TBR measurements instead of SUV measurements.

### **CLINICAL RELEVANCE/APPLICATION**

Hybrid imaging by PET/CT is a promising technology for the localization of vulnerable plaques based on the uptake of various molecular imaging agents indicative of inflammatory processes.

## **SST12-08 • Optimizing 18F-FDG-PET Imaging of Vessel Wall Inflammation - The Impact of 18F-FDG Circulation Time, Dose, Uptake Parameters, and Fasting Blood Glucose Levels**

**Jan Bucerius** (Presenter) ; **Venkatesh Mani** PhD ; **Colin Moncrieff** ; **Josef Machac** MD \* ; **Valentin Fuster** MD ; **Michael E Farkouh** ; **Ahmed Tawakol** MD \* ; **James Rudd** MD, PhD ; **Zahi A Fayad** PhD \*

### **PURPOSE**

<sup>18</sup>F-fluorodeoxyglucose (FDG) positron emission tomography (PET) is increasingly used for imaging of vessel wall inflammation. However, limited data is available regarding the impact of methodological variables, i. e. patient's pre-scan fasting glucose, the FDG circulation time, the injected FDG dose, and of different FDG uptake parameters, in vascular FDG-PET imaging.

### **METHOD AND MATERIALS**

195 patients underwent vascular FDG-PET/CT of the aorta and the carotids. Arterial standard uptake values (mean SUV<sub>max</sub>) as well as target-to-background-ratios (mean TBR<sub>max</sub>) and the FDG blood pool activity in the superior vein cava (SVC) and the jugular veins (JV) were quantified. Vascular FDG uptake classified according to tertiles of patient's pre-scan fasting glucose levels, the FDG circulation time, and the injected FDG dose was compared using ANOVA. Multivariate regression analyses were performed to identify the potential impact of all variables described on the arterial and blood pool FDG uptake.

### **RESULTS**

Tertile analyses revealed FDG circulation times of about 2.5 h and pre-scan glucose levels of less than 7.0 mmol/l showing favorable relations between the arterial and blood pool FDG uptake. FDG circulation times showed negative associations with the aortic mean SUV<sub>max</sub> values as well as SVC- and JV FDG blood pool activity but a positive correlation with the aortic- and carotid mean TBR<sub>max</sub> values. Pre-scan glucose was negatively associated with aortic- and carotid mean TBR<sub>max</sub> and carotid mean SUV<sub>max</sub> values, but correlated positively with the SVC blood pool uptake. Injected FDG dose failed to show any significant association with the vascular FDG uptake.

### **CONCLUSION**

FDG circulation times and pre-scan blood glucose levels significantly impact FDG uptake within the aortic and carotid wall and may bias the results of image interpretation in patients undergoing vascular FDG-PET/CT. FDG dose injected was less critical. Therefore, circulation times of about 2.5 h and pre-scan glucose levels less than 7.0 mmol/l should be preferred in this setting.

### **CLINICAL RELEVANCE/APPLICATION**

Standardization of vascular FDG-PET/CT imaging methodology and protocols to non-invasively assess vascular inflammation.

## **SST12-09 • FDG PET CT To Evaluate Response of Cardiac And Extracardiac Sarcoidosis to Immunosuppressive Therapy**

**PURPOSE**

To evaluate the response to immunosuppressive therapy in patients with active cardiac and extra cardiac Sarcoidosis on serial FDG PET CT scans. To assess differences in response of cardiac and extra cardiac disease to immunosuppressive therapy.

**METHOD AND MATERIALS**

Retrospective evaluation of eighteen patients with biopsy proven Sarcoidosis who underwent serial FDG PET scans (twenty nine data sets) to assess disease activity in response to therapy. The interval between serial scans ranged between three and twelve months. Patients received immunosuppressive therapy including prednisone, methotrexate or both. The response of cardiac disease was categorized as progressive if there was increase in inflammation or scar, stable if no change was noted and response if decrease in disease activity was noted. The extracardiac disease was graded as response, resolution, stable and progressive disease.

**RESULTS**

The extracardiac disease showed resolution or partial response in 11 patients, progression in 3 patients, stable disease in 2 patients and negative scan in 2 patients. Cardiac disease showed response in 7 patients, progression in 5 patients and stable disease in 6 patients. In 7 patients extracardiac disease showed treatment response or resolution, whereas cardiac disease progressed or remained stable. In 3 patients who had progression of extracardiac disease, cardiac disease also progressed or remained stable. In all patients response to therapy of both cardiac and extracardiac disease correlated well with a self-perceived response to therapy.

**CONCLUSION**

Serial FDGPET CT scans are a good objective indicator of response to therapy and correlate well with clinical well-being in patients who respond to therapy. Cardiac disease is more resistant to treatment compared to extracardiac disease.

**CLINICAL RELEVANCE/APPLICATION**

Response to therapy is a very important guiding factor in optimizing dosage of toxic immunosuppressive agents in patients with Sarcoidosis and FDG PET CT is probably the most reliable tool available.

---

**Pediatrics (Interventional)**

**Friday, 10:30 AM - 12:00 PM • N229**



[Back to Top](#)

**SST13 • AMA PRA Category 1 Credit™:1.5 • ARRT Category A+ Credit:1.5**

**Moderator**

**Anne Marie Cahill** , MBCh

**Moderator**

**Kamlesh U Kukreja** , MD \*

**SST13-01 • Long-term Outcome of Percutaneous Interventions of Hepatic Venous Outflow Obstruction after Pediatric Living Donor Liver Transplantation**

**Minoru Yabuta** MD (Presenter) ; **Toshiya Shibata** MD ; **Ken Shinozuka** ; **Toyomichi Shibata** MD ; **Hiroyoshi Isoda** MD ; **Kaori Togashi** MD, PhD \*

**PURPOSE**

To evaluate retrospectively the long-term outcome of percutaneous interventions of hepatic venous outflow obstruction (HVOO) after pediatric living donor liver transplantation (LDLT).

**METHOD AND MATERIALS**

Between October 1997 and December 2012, 48 patients (24 male, 24 female; median age, 6 years) who had undergone LDLT were confirmed to have HVOO at percutaneous hepatic venography and manometry, and underwent percutaneous interventions, including balloon angioplasty with / without stent placement. Technical success, patency rates, stent placement and major complications were evaluated.

**RESULTS**

Technical success was achieved in 92 of 93 sessions (99.0%). During follow-up periods ranged from one to 182 months (median, 51.5 months), 28 patients were treated with a single session of balloon angioplasty and 20 who developed recurrent stenosis were treated with repeated balloon angioplasty or stent placement. The rate of primary, primary assisted, and secondary patency at 1-, 3-, 5-, 10-years after the initial balloon angioplasty were 0.64, 0.57, 0.57 and 0.52 respectively, 0.98, 0.95, 0.95 and 0.95 respectively, and 1.0, 1.0, 1.0 and 1.0 respectively. A major complication was seen in a session of a patient, where a stent was migrated to the right atrium.

**CONCLUSION**

Balloon angioplasty with / without stent placement was an effective treatment for HVOO after LDLT.

**CLINICAL RELEVANCE/APPLICATION**

Percutaneous interventions such as balloon dilation and stent placement were effective in patients with HVOO after LDLT.

**SST13-02 • The Influence of Liver and Spleen Volume Changes after Percutaneous Transhepatic Angioplasty for Portal Venous Stenosis in Pediatric Living-donor Liver Transplant Recipients**

**Manabu Nakata** MD (Presenter) ; **Waka Nakata** MD ; **Hideharu Sugimoto** MD

**PURPOSE**

To quantify the changes in liver and spleen volumes after percutaneous transhepatic angioplasty (PTA) for portal venous stenosis (PVS) occurring in patients after pediatric living-donor liver transplantation.

**METHOD AND MATERIALS**

Twenty consecutive patients (8 males, 12 females; mean age 4.8 years) who underwent PTA for PVS from August 2005 to September 2011 after pediatric liver transplantation were included. Liver and spleen volumes (LV, SV) were quantified using computed tomography (CT) before PTA, 3 months, 12 months, 24 months, and 36 months after PTA. Spleen volume-to-standard spleen volume ratio (SV/SSV) and LV/SV were calculated at each time point. Statistical analyses of comparison between pre- and postoperative data were performed. The correlation of LV and SV at each time point was analyzed.

**RESULTS**

LV significantly increased by an average of 28% within 6 months after PTA and remained increased significantly through 36 months. SV/SSV significantly decreased an average of 24% within 6 months and remained decreased significantly through 36 months, although SV had no significant difference between pre- and post-operative data. LV/SV significantly increased by an average of 36% within 6 months after PTA, and thereafter had no significant differences. SV at each follow-up time point significantly negatively correlated with LV.

**CONCLUSION**

Improvement of splenomegaly and liver enlargement occur and continue during 36 months after PTA, with negative correlations between

liver and spleen volumes. These data indicate that liver and spleen volumes are influenced by portal venous flow and recovery of these volumes may take at least 36 months.

#### CLINICAL RELEVANCE/APPLICATION

Splenomegaly is improved within 6 months after PTA, although the decrease in spleen volume may continue at least 36 months. This information may be utilized for application and evaluation of PTA.

### **SST13-03 • Non-invasive Measures that Guide Indication, Pathology and Outcome of Percutaneous Biliary Intervention in Paediatric Transplantation**

**Anushka Lijutikov** MBBS, FRCR (Presenter) ; **Navaratne Subhachandra** MBBS, FRCR ; **Pauline A Kane** MBBS, FRCR ; **John B Karani** MBBS, FRCR ; **Maria E Sellars** MD, FRCR ; **Anil Dhawan** MD, FRCPC ; **Nigel Heaton**

#### PURPOSE

Biliary complications adversely impact on graft survival following transplantation in paediatric recipients. Interventions are technically challenging and carry risk in infants and children; therefore, selection is critical. The purpose of this study was to evaluate the diagnostic utility of non-invasive parameters which singularly, or in combination, guide the need for intervention.

#### METHOD AND MATERIALS

Reference to pre-procedural non-invasive imaging and graft function from the transplant database between 2008 -2012 formed the study cohort. This retrospective study reviewed these parameters in predicting findings, pathology and outcome of intervention.

#### RESULTS

There were 49 interventions in 40 recipients (ages 4 months-16 years, M:F 21:19) transplanted between 1997-2012. (Total transplant cohort 582). Indications included EHBA, PFIC, ALF. Operative technique was left lateral segment (37) including live related (22) and whole grafts (3). Key findings were non-cholestatic enzyme rise (34), increasing duct calibre on ultrasound (34), MRCP diagnosis of anastomotic strictures (27) and cholangiopathy (7). Diagnostic PTC was successful in all with findings of anastomotic strictures (24), cholangiopathy (7), bile leaks (4). Balloon dilatation of strictures was successful in 20. External biliary drains were placed in 4. The positive predictive values (PPV) in diagnosing anastomotic stricture and cholangiopathy are non-cholestatic enzyme rise 70.3% and 34.6%, USS duct calibre 63% and 30%, MRCP 78% and 43 %. The combined tests PPVs are 85% and 55.5%.

#### CONCLUSION

The combination of non-invasive measures of graft assessment allows most appropriate selection for biliary intervention in paediatric liver transplant recipients but MRCP is the best single predictor of biliary complications

#### CLINICAL RELEVANCE/APPLICATION

Biliary complications adversely affect graft survival in paediatric recipients. Interventions are technically challenging and carry risk hence selection of the correct patient is crucial

### **SST13-04 • Pediatric Soft Tissue Tumors: Deterministic Factors for Safety and Accuracy of Diagnostic Yield in Image-guided Percutaneous Core-needle Biopsies**

**Michael R Acord** MD (Presenter) ; **Raja Shaikh** MD ; **Gulraiz A Chaudry** MBChB

#### PURPOSE

To assess lesion-related and technical factors that affect diagnostic yield and safety in image-guided percutaneous core-needle biopsies (PCNB) of soft tissue tumors in children.

#### METHOD AND MATERIALS

Institutional review board approval was obtained for a retrospective study of 150 PCNB performed at our institution from January 2003 to January 2013. Medical records and radiologic data were evaluated on all PCNB performed on soft tissue lesions, excluding vascular malformations. Technical details of the procedure, demographic characteristics of the patients, and radiologic features of the lesions such as the location, size, imaging nature and enhancement were recorded. Procedure-related complications and repeat PCNB or other testing due to poor or non-diagnostic yields were noted. Associations between the radiologic characteristics of the lesion, technical factors and diagnostic yield were evaluated using bivariate and multivariate logistic regression.

#### RESULTS

Mean patient age was 11.4 ± 7.1 years. Ultrasound guidance was used in 80% of cases. General anesthesia was the most common form of sedation (86% of cases). Mean number of core biopsies was 6.4 ± 3.2 per case. The overall diagnostic yield was 80%. On bivariate analysis, procedures taking less number of cores (OR 0.75 95% CI 0.57 to 0.99, p=0.04) and involving benign lesions (OR 0.14 94% CI 0.03 to 0.69, p=0.02) were associated with non-diagnostic biopsies. Using a lower gauge needle showed a trend toward improving diagnostic success (OR 1.87 95% CI 0.93 to 3.71, p=0.08). On multivariate analysis, the only factor that predicted low diagnostic yield was whether the lesion was benign (OR 0.14 95% CI 0.02 to 1.00, p=0.05).

#### CONCLUSION

Image guided PCNB is a safe and accurate method for the diagnosis of pediatric soft tissue tumors. Particular attention should be paid toward lesions that appear benign on pre-procedure imaging in order to improve diagnostic yield.

#### CLINICAL RELEVANCE/APPLICATION

Percutaneous core needle biopsy of soft tissue tumors is a minimally invasive technique compared to open biopsy and has a low complication rate providing an early diagnosis.

### **SST13-05 • Pilot Study Evaluating Parenchymal Perfusion and Renal Blood Flow Using Color-coded Imaging in Pediatric Renal Artery Angioplasty**

**Tiffany Hwang** (Presenter) \* ; **Erin Girard** PhD \* ; **Anne Marie Cahill** MBChB

#### PURPOSE

*syngo* iFlow is a color-coded imaging adjunct used to interpret digital subtraction angiography (DSA). This study investigates the ability of *syngo* iFlow to evaluate changes in flow and parenchymal perfusion in patients undergoing angioplasty for renal artery stenosis (RAS).

#### METHOD AND MATERIALS

20 children underwent 30 percutaneous angioplasty procedures for RAS. For each stenotic artery that underwent angioplasty, pre- and post-stenotic regions of interest (ROI) were chosen. The difference in time to peak (dTTP) maximum contrast opacification values (given by iFlow) between these 2 ROIs represented flow rate across the stenosis. ROIs were drawn in the relevant parenchymal pole (upper, middle, and/or lower) to assess perfusion. 44 poles from the 20 patients were assessed for time to peak (TTP) opacification values. Only 35 of these poles had sufficient data to compute inflow rate, measured by the slope of the linear regression of contrast opacification vs time, representing contrast values between 15-75% of maximum opacity.

#### RESULTS

iFlow measured significantly improved flow across stenosis following angioplasty as indicated by dTTP (p=0.0001). dTTP decreased in 23/30 cases, of which 12 demonstrated dTTP=0 seconds post-angioplasty, possibly due to complete flow restoration. No change in dTTP was demonstrated in 5/30 cases. dTTP increased in 2/30 cases, correlating with mural dissection and intraluminal thrombus. iFlow measured significantly improved perfusion following angioplasty as indicated by TTP (p=.0008). TTP decreased in 31/44 poles, indicating an improvement in flow. No change in TTP was seen in 6/44 poles. An increase in TTP was demonstrated in 7/44 poles, 3 of which correlated with dissection and thrombus. Using inflow slope as a second measure, iFlow demonstrated improved perfusion in 20/35 poles, but this was not significant (p>0.05).

## CONCLUSION

This pilot study demonstrates the ability of iFlow to quantitatively and significantly assess differences in parenchymal perfusion and flow rates across stenotic vessels following angioplasty procedures. Thus, iFlow in general may provide the physician with more objective evidence of improved vascular flow and perfusion in other vascular interventions.

## CLINICAL RELEVANCE/APPLICATION

The ability of iFlow to quantify vascular parameters can provide the physician with objective measurements of altered vascular flow during angioplasty procedures and can guide the interventional plan.

### **SST13-06 • Implementation of a Fluoroscopy Competency Check-off for Radiology Trainees: Impact on Reducing Radiation Dose in the Pediatric Population**

**Sweta Shah** (Presenter) ; **Stephane Desouches** DO ; **Lisa H Lowe** MD ; **Brenton D Reading** MD

## PURPOSE

The purpose of this study is to determine the impact of implementing a fluoroscopy competency check-off aimed at decreasing radiation dose in three common pediatric fluoroscopic studies.

## METHOD AND MATERIALS

A fluoroscopy competency check-off form was developed for PGY 2-6 radiology trainees performing pediatric procedures. Techniques used to limit radiation exposure for three common pediatric radiologic studies were discussed. Additionally, a pediatric radiologist supervised and assessed each trainees' competency and technical skill prior to independent performance of the three procedures. Radiation dose and exposure time were recorded for 171 oropharyngeal motility (OPM), 176 voiding cystourethrogram (VCUG), and 171 upper GI (UGI) exams in 24 trainees for the six months preceding implementation of the competency check-off and in 114 OPM, 145 VCUG, and 132 UGI exams in 23 trainees for the six months after implementation. A paired t-test was then used to compare the mean radiation dose for each procedure in the two groups.

## RESULTS

A statistically significant reduction in radiation dose was found for OPM and VCUG exams after competency implementation. The mean radiation dose of the OPM exam decreased from 7.75 to 5.33 mGy pre- and post- competency implementation respectively, with a total reduction of 31% ( $P = 0.023$ ). The mean radiation dose of the VCUG exam decreased from 3.90 to 2.59 mGy pre- and post- competency implementation respectively, with a total reduction of 33% ( $P = 0.033$ ). No statistically significant reduction was seen for the UGI exam.

## CONCLUSION

Implementation of a fluoroscopy competency check-off for radiology trainees reduced radiation dose in pediatric patients undergoing both OPM and VCUG studies.

## CLINICAL RELEVANCE/APPLICATION

This study demonstrates that exposing trainees to a competency check-off can help decrease the radiation dose, thereby reducing the risk of excess radiation exposure in the pediatric population.

### **SST13-07 • A System for Real-time Mapping of Pediatric Skin Dose during Fluoroscopic Cardiac Procedures**

**Daniel Bednarek** PhD (Presenter) \* ; **Vijay Rana** \* ; **Stephen Rudin** PhD \*

## PURPOSE

To provide the clinician with a real-time visual graphic display showing the distribution of skin-dose for pediatric patients undergoing fluoroscopic cardiac interventional procedures.

## METHOD AND MATERIALS

We have developed a software system to track skin dose during fluoroscopic interventional procedures and to provide a graphic representation of the cumulative dose distribution in real time. Originally the program and graphics were developed and verified for adult patients. To use the system with pediatric patients, an open-source software application was used to create a series of 3D patient graphic models with varying heights ranging from 60 to 128 cm and with three weight ranges for each height. The model most closely matching the patient is selected at the beginning of the procedure and the skin dose is calculated at each point on the graphic within the x-ray beam for each exposure pulse and the cumulative distribution is displayed in a color-coded mapping. To verify that the correct dose is calculated, measurements were made with a 6 cc ionization chamber placed on the surface of a pediatric phantom (Kyoto Kagaku PBU-70, 105 cm height, 20 kg weight) at various locations on the torso; exposures were made for a range of projections with the heart at C-arm gantry iso-center and chamber readings were compared with those of the tracking system. Similar measurements were made with a water-filled phantom of similar dimensions.

## RESULTS

Using a matching patient graphic, the ratio of dose tracking system reading to ionization chamber reading had an average value of 1.08 +/- 0.04 for fluoroscopy and 0.99 +/- 0.05 for DA mode with the pediatric phantom, while the values agreed with the chamber within 2% for the water phantom over a range of cardiac RAO/LAO and CRA/CAU projections.

## CONCLUSION

With the newly developed patient graphic models, accurate tracking of skin dose is possible in real-time during pediatric fluoroscopic interventional procedures, enabling the clinician to reposition the C-arm to avoid exceeding the threshold for deterministic skin effects.

## CLINICAL RELEVANCE/APPLICATION

The system developed facilitates the management of risk for deterministic skin effects for pediatric patients during interventional fluoroscopic procedures.

### **SST13-08 • MRI of Vascular Anomalies: Value of Diffusion Imaging**

**Sebastien Benali** MD (Presenter) ; **Josee Dubois** MD ; **Francoise F Rypens** MD ; **Chantale Lapierre** MD ; **Gilles P Soulez** MD \*

## PURPOSE

MRI diffusion-weighted imaging (DWI) is a new method to evaluate the diffusion of intra and extracellular water. The goal of this study is to characterize diffusion imaging parameters in vascular anomalies (VA) and compare them to malignant soft tissue tumors.

## METHOD AND MATERIALS

## RESULTS

The mean ADC values at b=1000-500 were estimated at 3.05±0.08, 3.37±0.24 and 3.01±0.09 respectively for VM, LM and hemangiomas and at 2.96±0.08 for soft tissue tumors. At b=1000-500, ADC values were significantly higher for LM as compared to VM ( $p=0.01$ ) and hemangiomas ( $p=0.03$ ). However, no significant difference could be demonstrated between VM, hemangiomas and soft tissue tumors. At b=1000, ADC values were estimated at 3.82±0.14, 4.23±0.18 and 3.74±0.15 respectively for VM, LM and hemangiomas and at 3.46±0.11 for soft tissue tumors. The latter displayed significantly lower ADC values than VM and LM ( $p=0.0001$ ) and hemangiomas ( $p=0.02$ ). No significant correlation between contrast enhancement and ADC values was observed ( $r=-0.056$ ).

## CONCLUSION

All VA presented high ADC values. At b=1000-500, LM displayed significantly higher values as compared to VM and hemangiomas. At b=1000, malignant soft tissue tumors showed significantly lower ADC values than VM, LM and hemangiomas. DWI could be a useful tool to characterize VA and discriminate them from malignant lesions.



#### CLINICAL RELEVANCE/APPLICATION

Diffusion imaging can characterize and differentiate vascular anomalies from soft tissue malignant tumors. Soft tissue malignant tumors display higher ADC coefficient than brain and organ tumors.

### SST13-09 • Novel Use of MRI/X-ray Overlay for Interventional Radiology Sclerotherapy Procedures in the Pediatric Population

**Tiffany Hwang** (Presenter) \* ; **Erin Girard** PhD \* ; **Anne Marie Cahill** MBBCh

#### PURPOSE

Fluoroscopic imaging is used for navigation during lesion-targeting interventional radiology procedures, such as sclerotherapy for vascular malformations, as it provides real-time information. However, fluoroscopy provides only a 2D image of 3D anatomy and does not visualize the lesion. On the other hand, magnetic resonance imaging (MRI) provides quality soft tissue contrast for lesion visualization. *syngo* 3D/3D fusion and *iPilot* dynamic software programs (Siemens Healthcare AG, Forchheim, Germany) allow 3D MR images to be overlaid on real-time fluoroscopy images, enhancing lesion visualization during interventional procedures. This study describes our experience using this software to target lesions and compares procedure and fluoroscopy times between software assisted and unassisted cases.

#### METHOD AND MATERIALS

20 children, mean age 11.5 years, underwent sclerotherapy procedures with MRI/x-ray image overlay assistance for vascular malformations. Their average procedure and fluoroscopy times were compared to those of 100 software-unassisted sclerotherapy procedures using a 2-tailed t-test (p

#### RESULTS

Both average procedure and fluoroscopic times of software-assisted cases (47.11; 4.97 min) were higher than those of unassisted cases (42.54; 4.72 min), but not to a statistically significant degree (p=0.37; 0.84). The physician reported that MRI overlay increased therapeutic confidence in 17/20 cases and determined the interventional plan in 10/20 cases. Of these 10 cases, changes made included adding a clarifying ultrasound (1), not performing a post-procedural DynaCT (2), determining post-procedural extubation (3), or a combination of these changes (3). The 3/20 cases that did not confer useful knowledge occurred with diffuse vascular malformations, where MR overlay was suboptimal due to unclear lesion boundaries.

#### CONCLUSION

In this study we showed that MRI/x-ray overlay during sclerotherapy can confer additional information to improve treatment confidence and guide the interventional plan while not significantly increasing procedure or fluoroscopy time.

#### CLINICAL RELEVANCE/APPLICATION

MRI/x-ray overlay during sclerotherapy procedures may improve clinical care by providing physicians with additional information on the distribution of sclerotherapy agent, with respect to a prior MRI.

### Physics (CT-Dose Optimization)

Friday, 10:30 AM - 12:00 PM • S403B

QA PH CT

[Back to Top](#)

SST14 • AMA PRA Category 1 Credit™:1.5 • ARRT Category A+ Credit:1.5

#### Moderator

**Cynthia H McCollough**, PhD \*

#### Moderator

**Robert G Gould**, DSc

### SST14-01 • ACRIN PA 4006: Effect of Device Technical Factors on Patient Dose in a Prospective Digital Breast Tomosynthesis Screening Trial

**Mathew Thomas** BS (Presenter) ; **Yohei Matsutani** ; **Emily F Conant** MD \* ; **Andrew D Maidment** PhD \*

#### PURPOSE

To characterize the effect of kVp, mAs, and filter-anode combinations on mean glandular dose (MGD) in digital mammography (DM) and digital breast tomosynthesis (DBT).

#### METHOD AND MATERIALS

A prospective multi-site trial was conducted to compare the recall rates of DM and DBT. The DBT image set consisted of 2D and 3D images obtained at approximately a 15% reduced dose effected by using a phototimer setting of "-1"; the DM images were acquired without modification of dose. All image data were stored in a centralized DICOM server and the image metadata were automatically extracted from the DICOM headers. These data included breast laterality, image orientation, kilovoltage (kV), exposure (mAs), target and filter materials, entrance surface dose and mean glandular dose (MGD). Regression analysis was performed to ascertain the influence of the various acquisition parameters on MGD.

#### RESULTS

The 2D component of the combined-DM/DBT acquisition was on average 18.5% less than (p

#### CONCLUSION

For both DM and DMT, the key determining factor of MGD is mAs. The kVp of DM and 2D DBT images is significantly lower than the kVp of 3D DBT images for breast thicknesses in the range of 70-100mm due to filter change in DM.

#### CLINICAL RELEVANCE/APPLICATION

This paper characterizes the key technical parameters that determine the cumulative dose exposure for patients during digital breast tomosynthesis screening.

### SST14-02 • Assessment of Patient Dose from CT Localizer Radiographs

**Natalia Saltybaeva** (Presenter) ; **Bernhard Schmidt** PhD \* ; **Daniel Kolditz** PhD \* ; **Willi A Kalender** PhD \*

#### PURPOSE

CT localizer radiographs (LR), also known e.g. as topogram or scout view, in the past were not perceived as contributing significantly to the effective dose of a CT examination. In modern low-dose CT, however, this contribution has to be taken into account. The purpose of our study was to assess typical LR dose values based on simulations and measurements.

#### METHOD AND MATERIALS

Four anthropomorphic phantoms representing 2 adults (male and female, Rando-Alderson Research Laboratories, New York, USA) and 2 children (5 and 1 y.o., CIRS, Norfolk, VA, USA), equipped with 30-60 TLD chips, underwent LR scans (SOMATOM Definition Flash, Siemens AG, Forchheim, Germany). Three different body regions (head, thorax, and abdomen-pelvis) and three positions of the X-ray tube (AP, PA and lateral) were considered. We simulated 3D dose distribution for each setup using a validated Monte Carlo tool (ImpactMC, CT Imaging GmbH, Erlangen, Germany) and compared simulated and measured dose values point by point. Organ and effective doses for the different LRs were calculated and compared to typical dose values in CT examinations.

#### RESULTS

The differences between measured and simulated dose values for all projections (AP, PA and lateral) were below 15% on average. Organ doses varied significantly depending on the tube position; the largest differences were observed for breast dose in female chest LR (AP: 2.4 mSv vs. PA: 0.5 mSv). Overall effective dose values per LR ranged from 0.04 mSv for adult head to 0.7 mSv for 1 y.o. child abdomen. This adds from 5% to 42% to effective dose of typical low-dose CT exams.

#### CONCLUSION

MC simulations provide accurate estimates of LR dose distributions. Localizer radiographs may contribute substantially to organ and effective dose of the total CT examination. Organ doses from LRs can be significantly reduced by choosing the appropriate projection angle.

#### CLINICAL RELEVANCE/APPLICATION

Dose from localizer radiographs should be taken into account. LR parameter optimizations should be performed in order to decrease total dose of CT examinations.

### **SST14-03 • CT Radiation Dose Optimization of Coronary Calcium Scanning: Comparing Different Image Reconstruction Methods at 100kVp and 120kVp**

**Joerg Blobel** PhD (Presenter) \* ; **Jurgen Mews** \* ; **Joanne Schuijf** \* ; **Willem Overlaet** \*

#### PURPOSE

The effects of tube voltage reduction and different reconstruction methods on coronary calcium scoring remain largely unknown. We performed a quantitative phantom study to determine the lowest applicable volume CTDI thresholds ( $CTDI_{vol}$ ) at 100kVp versus 120kVp while controlling Agatston and volume score accuracy.

#### METHOD AND MATERIALS

ECG-gated volume scans of an anthropomorphic thoracic phantom with calcium calibration inserts, containing 200, 400 and 800mg HA/cm<sup>3</sup> calcium mass spheres of 1, 3 and 5mm diameter (QRM GmbH, Germany), were performed on 320-row CT (Aquilion ONE, Toshiba Medical Systems, Japan). Using 100kVp and 120kVp with 10-580mA variations in 32 steps, each acquisition was reconstructed with Filtered Back-Projection (FBP), Quantum Denoising Software (QDS) and Adaptive Iterative Dose Reduction (AIDR 3D). To determine the minimum  $CTDI_{vol}$  thresholds for the six groups a statistical 2S-outlier test (WinStat 2007.1 software) was performed on the semi-automatically detected Agatston and volume scores. The Kruskal-Wallis-Test was used to evaluate statistical differences between the three reconstructions and both kVp scan series.

#### RESULTS

At equal kVp settings, there were no significant differences in average scores between the three reconstruction methods ( $p > 0.21$ ). The use of 100kVp, as compared to 120kVp, resulted in a 3% lower Agatston score average (672 vs. 694,  $p3$ , pvol thresholds were reduced from 5.98mGy to 2.37mGy (120kVp, QDS), 1.86mGy (120kVp, AIDR 3D), 4.13mGy (100kVp, FBP), 1.94mGy (100kVp, QDS) and 1.12mGy (100kVp, AIDR 3D) (Fig.). The averages of 10 repeated scans at low dose level (1.12 mGy, AIDR3D, 100kVp) showed no significant difference with the reference group (12 dose steps, FBP, 120kVp) for both Agatston ( $p=1.00$ ) and volume ( $p=0.75$ ) score.

#### CONCLUSION

Mean dose reductions of 37% using 100kVp instead of 120kVp and 71% using the novel iterative reconstruction AIDR 3D instead of FBP can be achieved for coronary calcium scanning. Combining 100kVp with AIDR 3D resulted in an 81% lower  $CTDI_{vol}$  threshold compared to a standard scan protocol (120kVp, FBP).

#### CLINICAL RELEVANCE/APPLICATION

Considerable radiation dose reduction can be achieved for coronary calcium scanning using AIDR 3D at 100kVp. Low dose coronary calcium scanning is possible with good accuracy and reproducibility.

### **SST14-04 • Synthetic Cone-beam CT for Determining Patient- and Task-specific Minimum-dose Techniques in Repeat Scans**

**Adam S Wang** PhD (Presenter) \* ; **Joseph W Stayman** PhD \* ; **Yoshito Otake** \* ; **Jeffrey H Siewerdsen** PhD \*

#### PURPOSE

To evaluate a newly developed method (Synthetic Cone-Beam CT) for accurately determining the impact of lower-dose techniques in C-arm CBCT, allowing identification of minimum-dose protocols suitable to a given imaging task in scenarios that require repeat scans.

#### METHOD AND MATERIALS

An initial CBCT acquired at nominal scan protocol at the beginning of a procedure provides a patient-specific basis for synthetic CBCT. To accurately simulate lower-dose techniques, noise of the proper magnitude and correlation is added to the projections, accounting for object-dependent noise levels and correlations introduced by the detector. The resulting noisy projections are then reconstructed to yield synthetic CBCT images accurately portraying the image quality in lower-dose scans. Validation studies were conducted on a mobile C-arm using a 16 cm acrylic phantom to first assess the detector signal-variance relationship and correlations. Synthetic CBCT was then applied to a head phantom (100 kVp, 320 mAs initial scan), synthesizing projections across a range of lower-dose techniques (160, 80, 40, and 20 mAs). Real CBCT scans were also obtained at each technique for image quality comparison.

#### RESULTS

Comparison of synthetic and real CBCT images across the full range of techniques demonstrated accurate noise magnitude (within ~3%) and correlation (matching noise-power spectrum, NPS). Other image quality characteristics (e.g., spatial resolution, contrast, beam hardening, and scatter) remain intact and are realistically presented in synthetic CBCT. Generating synthetic CBCT for a broad range of protocols gives a useful method to select minimum-dose techniques that accounts for complex factors of imaging task, patient-specific anatomy, artifacts, and physician preference.

#### CONCLUSION

Synthetic CBCT accurately portrays the increased noise in lower-dose protocols while preserving other image quality characteristics, providing a method to define minimum-dose, task-specific protocols in repeat CBCT. Ongoing work includes translation to clinical studies and application to iterative reconstruction, where potential dose reduction is even greater and synthetic CBCT accurately portrays low-dose limits that are difficult to predict.

#### CLINICAL RELEVANCE/APPLICATION

Selection of minimum-dose, task-specific techniques for intraoperative C-arm cone-beam CT is enabled by synthesizing patient-specific images that accurately reflect image quality at lower dose.

### **SST14-05 • Preliminary Clinical Evaluation of an Online Intrascan Motion-correction Algorithm for Interventional C-arm Flat-detector CT**

**Julia Wicklein** \* ; **Oliver Beuing** \* ; **Martin Skalej** MD, PhD \* ; **Steffen Serowy** \* ; **Willi A Kalender** PhD \* ; **Yiannis Kyriakou** PhD (Presenter) \* ; **Holger Kunze** MS \*

#### PURPOSE

Intrascan Motion-artifact-correction in C-arm-based flat-detector CT (FD-CT) is an important issue in interventional imaging because of longer scan times as compared to Multi-Slice CT. Our aim was the development and evaluation of an online image-content-based motion-correction technique without using any kind of markers or external motion knowledge.

#### METHOD AND MATERIALS

The correction method is based on a gradient descent method, minimizing a gray-value entropy criterion optimizing the underlying acquisition trajectory parameters. It is formed as a multistep approach, including a global, local and projection wise optimization. We are

using a locally rigid variation of the systems trajectory parameters like detector- or source-translation or a detector rotation to compensate patient motion. The retrospective evaluation of 30 arbitrary (with weak and strong motion, without motion artifacts) patient head scans included 5s 3D angiography and 20s soft-tissue protocols. All scans were performed on an Artis Q System (Siemens AG). For each dataset three volumes were computed: 1) original reconstruction using the system's geometry calibration (OR), 2) motion corrected reconstruction without any system information (MCR) and 3) motion corrected reconstruction using the system's geometry calibration as initialization (MCR+). Two neuroradiology experts performed a visual evaluation according to a 5-point grading scale with respect to general image quality, motion-artifact-content and spatial resolution of the structures of interest, e.g. 3D vessels.

#### RESULTS

The average scores for OR, MCR and MCR+ were 2.75, 3.0 and 3.15, respectively. The combined compensation of unknown trajectories and unknown patient motion (MCR) can lead to comparable results to OR. Both experts confirmed a distinct reduction of artifacts by the motion correction algorithm (MCR+), e.g. blurring and streaks. Especially for 3D angiography even small distal vessels were depicted clearly. MCR+ application on soft-tissue protocols illustrated a constantly better delineation of bone and soft-tissue in the border zones.

#### CONCLUSION

Image-based motion correction is possible without a-priori knowledge of the motion pattern and can improve interventional FD-CT imaging.

#### CLINICAL RELEVANCE/APPLICATION

Using the proposed algorithm enables good image quality even for unsteady patients and can be helpful for longer FD-CT acquisitions in cases where anaesthesia is contraindicated.

### **SST14-06 • Supervised Conversion of Ultra-low-Dose to Higher-dose CT Images by Using Pixel-based Machine Learning: Phantom and Initial Patient Studies**

**Kenji Suzuki** PhD (Presenter) \* ; **Yipeng Liu** MS ; **Toru Higaki** PhD ; **Yoshinori Funama** PhD ; **Kazuo Awai** MD \*

#### PURPOSE

Reduction of radiation dose in CT is highly demanded. Our purpose was to develop a supervised pixel-based machine-learning technique for converting ultra-low-dose (ULD) CT to "virtual" higher-dose (HD) CT images with less noise or artifact.

#### METHOD AND MATERIALS

We developed a pixel-based machine-learning technique based on a massive-training artificial neural network (MTANN) filter that is trained with input ULDCT images and corresponding "teaching" HDCT images. Through training, the MTANN learns the relationship between the input and teaching images to convert ULDCT into HDCT images. Once trained, the MTANN no longer requires HDCT images; and it produces HDCT-like images from non-training ULDCT images. To train our MTANN filter and make a reference, we acquired 6 sets of CT scans of an anthropomorphic chest phantom (Kyoto Kagaku, Kyoto, Japan) with a tube voltage of 120kVp, tube currents of 10, 25, 50, 100, 150, and 300 mA, and a collimation of 5 mm. A 10 mA ULDCT image and the corresponding 300 mA HDCT image were used for training our MTANN filter. To evaluate the performance of our MTANN, we acquired ULDCT scans of 3 patients with a tube voltage of 120kVp and a tube current of 10 mA. The effective radiation dose of an ULDCT study was 0.1 mSv. We evaluated the image quality of CT images by using signal-to-noise ratio (SNR) in each image.

#### RESULTS

With our trained MTANN filter, noise and artifacts (e.g., streaks) in ULDCT images (0.1 mSv) were reduced substantially, while details of soft tissue such as pulmonary vessels and bones were maintained. The average SNR of 0.1 mSv ULDCT images for patients was improved from 2.3 ( $\pm$  1.8) to 13.0 ( $\pm$  2.5) dB (two-tailed t-test; P

#### CONCLUSION

With our supervised MTANN dose-reduction technique, the image quality of 0.1 mSv ULDCT was improved substantially to the quality comparable to 1.5 mSv HDCT; thus, radiation dose can potentially be reduced by 93%.

#### CLINICAL RELEVANCE/APPLICATION

Advantage of our technique over iterative reconstruction is substantial reduction of radiation dose in CT with a very short processing time, which would be beneficial to patients and radiologists.

### **SST14-07 • The Influence of kV and Patient Positioning on CT Image Quality and Dose: Why Low kV CT Scans Have a Higher Sensitivity to Patient Positioning**

**Timothy P Szczykutowicz** PhD (Presenter) \* ; **Frank N Ranallo** PhD ; **Kara Gill** MD ; **Myron A Pozniak** MD \*

#### PURPOSE

Higher levels of noise non-uniformity were noticed in our pediatric scans. Investigation into the problem led to the conclusion that due to the low kV used for pediatric scans, errors in patient positioning caused larger increases in noise non-uniformity for pediatric patients relative to similar adult protocols using higher kV settings. The purpose of this work is to explore the physical reason behind this effect and provide guidelines to avoid this problem in the clinic.

#### METHOD AND MATERIALS

Several clinical cases flagged by our pediatric radiologists were analyzed and motivated an anthropomorphic phantom study. A pediatric protocol was applied using 80 and 140 kV. The phantom was purposely mis-centered low by 0 and 6 cm. The noise uniformity was reported as the ratio of the standard deviation in uniform region located in the anterior and posterior regions of the phantom. In addition, a numerical simulation was performed in which a bowtie filter was forward projected using an 80 and 140 kV polychromatic spectra and the transmitted fluence examined. This numerical study was meant to provide insight onto why changing the kV can influence noise uniformity when a patient is mis-centered.

#### RESULTS

It was found that the noise non-uniformity of the 80 and 140 kV scans was 1.33 and 1.27 at 0 cm offset and 1.86 and 1.58 at 6 cm offset respectively. The numerical simulation showed the 140 kV spectra provided a 23% wider fluence profile than 80 kV when both spectra were normalized to have equal fluence through the center of the bowtie.

#### CONCLUSION

Novel to this study, it was shown that the degree of non-uniformity depends on kV and the physical reason for this effect was shown via phantom measurements and numerical simulation. This study identifies a new reason to stress the importance of patient positioning, especially for low kV exams (i.e. pediatrics).

#### CLINICAL RELEVANCE/APPLICATION

Low kV settings, commonly used in pediatric protocols, can increase the chance for an un-diagnosable scan due to the higher dependence of noise non-uniformity on patient mis-centering at lower kVs.

### **SST14-08 • Radiation Dose in Dual-energy Computed Tomography: Axial Dose Distributions in Specific Thoracic and Abdominal Regions**

**Kosuke Matsubara** PhD (Presenter) ; **Haruka Koshida** ; **Keita Sakuta** RT ; **Tadanori Takata** ; **Kichiro Koshida** PhD ; **Yukihiro Matsuura** RT ; **Toshifumi Gabata** MD

#### PURPOSE

Polyenergetic x-rays with low (100 or 80 kVp) and high tube voltage [140 kVp with or without a tin (Sn) filter] are used in dual-energy computed tomography (DECT). We aimed to evaluate the radiation doses administered during thoracic and abdominal DECT and compare them with those administered during single-energy CT (SECT) of the same regions.

#### METHOD AND MATERIALS

A 128-section dual-source CT device (SOMATOM Definition Flash; Siemens Healthcare, Erlangen, Germany), an anthropomorphic female phantom (RAN-110; Phantom Laboratory, Salem, NY, USA), and calibrated radiophotoluminescent glass dosimeters (RPLDs) (GD-302M; Chiyoda Technol, Tokyo, Japan) were used to acquire axial absorbed dose distributions in specific regions of the thorax and abdomen that were imaged using CT with one SE (120 kVp) and three DE (100 and Sn/140 kVp, 80 and Sn/140 kVp, and 140 and 80 kVp) modes. The energy modes were in accordance with the standard clinical protocols for thoracic and abdominal CT, and the tube current was adjusted so that the displayed volumetric CT dose indices (CTDIvol) were equivalent among the four energy modes. Axial absorbed dose distributions in the thoracic and abdominal regions were acquired by placing RPLDs within all holes of one thoracic or abdominal section and pasting them around the section.

#### RESULTS

The absorbed doses in the thoracic region were  $12.8 \pm 2.3$ ,  $12.5 \pm 2.2$ ,  $11.7 \pm 1.9$ , and  $12.2 \pm 1.6$  mGy ( $p < 0.01$ , Friedman's test) when the 120 kVp, 100 and Sn/140 kVp, 80 and Sn/140 kVp, and 140 and 80 kVp modes, respectively, were used. The corresponding values for the abdominal region were  $24.8 \pm 2.2$ ,  $24.3 \pm 2.0$ ,  $22.9 \pm 1.7$ , and  $23.3 \pm 1.6$  mGy ( $p < 0.01$ ), respectively. The doses absorbed at the surface and center of the abdomen were higher and lower, respectively, when the 140 and 80 kVp mode was used than when the other three modes were used for abdominal CT.

#### CONCLUSION

DECT can be performed with a radiation dose that is equivalent to or lower than that required during SECT when the displayed CTDIvol is equivalent. The additional Sn filter used in abdominal DECT can approximate the axial absorbed dose distribution of DECT to that of SECT.

#### CLINICAL RELEVANCE/APPLICATION

DECT has advantages over SECT. Evaluation of the radiation dose administered during DECT is necessary to determine its indications for application and the energy modes required.

### **SST14-09 • CT Image Quality Improvement and Dose Reduction Potential with Model-based Iterative Reconstruction Using Autopsy Imaging in the Abdomen: Evaluation of Image Noise and DOSE Estimation with Different Noise Index**

**Tomokatsu Tsukamoto** (Presenter) ; **Takashi Takahata** RT ; **Yue Dong** ; **Keisuke Nishihara** MD ; **Kazunari Mesaki** MD ; **Hiroki Mori** MD ; **Ye Ju** ; **Katsuhide Ito** MD

#### PURPOSE

To assess the dose reduction potential and image quality improvement with model-based iterative reconstruction algorithm (Vevo) using autopsy imaging by comparing image noise and DOSE (DLP mGy-cm) with the adaptive statistical iterative reconstruction (ASiR) and the filtered back projection (FBP) reconstructions.

#### METHOD AND MATERIALS

With institutional review board approval, 8 autopsy imaging (AI) underwent abdomen CT with different noise index (NI: 8.5, 10.5, 14.5, 20.5, 30.5) on Discovery CT750HD was included. In addition to the 3 sets of 0.625mm slice thickness CT images were reconstructed with FBP, 50% ASiR and Vevo. The image noise (SD) was measured with the same size of regions of interest at the same slice in 3 locations for liver and pelvis. The image noise reduction ratio was defined by SD (at NI30.5)/SD (at NI8.5). Using a 5-point score (1: poor; 3: diagnosis, 5 excellent), 3 radiologists independently and graded overall noise and delineation of the abdomen image.

#### RESULTS

For the Liver, the image noise reduction with Vevo compared with FBP and 50%ASiR for the NI: 8.5, 10.5, 14.5, 20.5, 30.5 and the average were (47.3%, 52.2%, 61.0%, 70.6%, 79.0% and  $62.0 \pm 13.0\%$ ) and (37.7%, 32.2%, 44.4%, 58.1%, 70.1% and  $48.5 \pm 15.5\%$ ), respectively; for Pelvis, (49.2%, 54.3%, 66.3%, 74.1%, 79.8% and  $64.7 \pm 12.9\%$ ) and (28.5%, 34.9%, 52.4%, 63.3%, 71.8% and  $50.2 \pm 18.4\%$ ), respectively. The reduction ratio (NI30.5/NI8.5) of image noise about (Liver and Pelvis) for the Vevo, 50%ASiR and FBP were (1.5 and 1.5), (3.2 and 3.9) and (3.9 and 3.9), respectively. All the differences were statistically significant between Vevo and FBP ( $p$  CONCLUSION

The model-based iterative reconstruction algorithm (Vevo) advanced reconstruction algorithms greatly reduced image noise to compare FBP and ASiR .

#### CLINICAL RELEVANCE/APPLICATION

Vevo reconstruction technique has the ability to reduce radiation dose through their improvement in image quality compared with the current algorithms such as FBP and ASiR.

## **Physics (Image-guided Radiation Therapy II)**

**Friday, 10:30 AM - 12:00 PM • S403A**

**PH** **RO** **CT**

[Back to Top](#)

**SST15 • AMA PRA Category 1 Credit™:1.5 • ARRT Category A+ Credit:1.5**

**Moderator**

**Peter Balter** , PhD \*

**Moderator**

**Lei Xing** , PhD \*

**SST15-01 • Artifact-resistant Motion Estimation for Motion-compensated CT**

**Marcus Brehm** ; **Thorsten Heuser** (Presenter) ; **Pascal Paysan** PhD \* ; **Markus Oelhafen** DPhil, DSc \* ; **Marc Kachelriess** PhD

#### PURPOSE

Image quality of respiratory-correlated 4D volumes from flat detector cone-beam CT scans (4D CBCT) is deteriorated by severe sparse projection artifacts. These artifacts complicate motion estimation and therefore motion compensation. The aim is to robustly estimate motion in presence of dominating image artifacts and to allow for a subsequent motion-compensated image reconstruction that guarantees full dose usage.

#### METHOD AND MATERIALS

To estimate respiratory motion in artifact-dominated images we developed a patient-specific artifact model: A 3D reconstruction of the 4D data is segmented into air, soft tissue, and bone by simple but robust hard thresholding (at -800 HU, +300 HU). The resulting three-valued image is forward projected and the thus-obtained rawdata undergo a 4D reconstruction (phase binning and independent reconstruction of each respiratory phase) yielding 4D CBCT images free of patient motion but full of sparse projection artifacts. The artifacts change from respiratory phase to respiratory phase. Deformable registration of those artifact volumes yields an approximation of the "motion" induced by the artifacts. This information is used to correct motion vector fields that were estimated on the conventional 4D CBCT volumes. The method is verified using simulated rawdata obtained by deforming a clinical patient dataset by realistic deformation fields, and by processing patient data acquired with the TrueBeam 4D CBCT system (Varian Medical Systems).

#### RESULTS

The motion-compensated reconstructions, from simulated and patient data, do not contain any streak artifacts, they are free from motion blurring, and their image noise is similar to the standard 3D reconstruction. The high temporal resolution is maintained. Pulmonary blood vessels that have been hidden by motion blurring or streak artifacts before now become clearly visible.

#### CONCLUSION

The proposed patient-specific artifact model allows for a robust registration between images that are severely degraded by artifacts. Combined with motion compensation one is able to remove streak and motion artifacts while maintaining a good spatial and good temporal resolution. Full dose usage is guaranteed because now all data contribute to each time frame.

#### CLINICAL RELEVANCE/APPLICATION

High quality 4D images are a prerequisite for precise adaptive radiation treatment.

### **SST15-02 • The Effect of CT Image Quality on Deformable Image Registration in Radiotherapy**

**Vern P Hart** PhD (Presenter) ; **Guang-Pei Chen** PhD ; **Allen Li** PhD

#### PURPOSE

Various CT modalities of different image quality are used to plan and guide radiation therapy (RT). This work is to assess the effect of CT image quality on deformable image registration (DIR) and its impact on auto-segmentation and dose accumulation in adaptive RT (ART).

#### METHOD AND MATERIALS

A variety of CT data sets with different soft-tissue contrasts were acquired for prostate cancer patients in different treatment fractions. Conventional diagnostic CT with standard protocols (SCT) and high soft-tissue contrast protocols (increased dose) (HCT), kilovoltage cone beam CT (CBCT), and megavoltage tomotherapy CT (MVCT) were registered using an in-house DIR tool based on the symmetric force Demons algorithm. Targets and critical organs were contoured on the SCTs and populated to other CT images with DIR. Of particular interest was the impact of soft-tissue contrast on intensity-based algorithms. DIR results were assessed with the Dice similarity coefficient (DSC) and were correlated with differences in image quality observed between CT image types.

#### RESULTS

Differences in soft-tissue contrast had a significant impact on DIR accuracy, as demonstrated in the registration of SCT-SCT, SCT-HCT, SCT-CBCT, and SCT-MVCT between different fractions. The inclusion of binary masking partly compensated for this effect and yielded excellent results. In the case of SCT-CBCT registration, binary masking provided DSC values exceeding 96, 97, and 98% for rectum, prostate, and bladder, respectively. Initial results have also shown that contour smoothing using morphological warping can improve accuracy in the absence of binary masks on daily images, which is of interest for ART.

#### CONCLUSION

Decreased soft-tissue image contrast generally leads to decreased DIR accuracy during ART. A number of techniques can be implemented to improve the accuracy of contouring and dose mapping. Binary masking provides excellent results and research is currently underway to increase the clinical robustness of this approach, such as auto-segmentation for mask generation and morphological smoothing of image contours. These approaches would allow ART based on commonly used CT modalities.

#### CLINICAL RELEVANCE/APPLICATION

DIR is essential in ART for accounting for interfraction variations and thereby improving RT delivery accuracy. As such, compensating for decreased CT quality in DIR is of great interest to ART.

### **SST15-03 • Deformable Registration Guided Correlation of Post-radiotherapy Recurrent Disease to Pre-radiotherapy PET Positive Volume in Patients with Head and Neck Cancer**

**Michalis Aristonhanous** (Presenter) ; **Abdallah S Mohamed** MD, MSc ; **Adam S Garden** MD ; **David I Rosenthal** \* ; **Clifton D Fuller** MD, PhD \*

#### PURPOSE

Investigate the predictive role of pre-radiotherapy (pre-RT) FDG-PET/CT scans for head and neck cancer local and/or regional recurrence (LRR).

#### METHOD AND MATERIALS

Thirty-five patients that developed LRR following radiotherapy (RT) for primary SCC of the head and neck between May 2003 and July 2010 were identified under an IRB approved protocol. Each patient had an FDG-PET/CT scan on average 2 months prior to RT. The PET-based gross tumor volume (GTV) was defined utilizing an automated segmentation algorithm developed in-house to obtain a pre-RT GTV-PET. The recurrent disease was identified and contoured on follow up post-radiotherapy (post-RT) CT imaging to obtain the GTV-REC. The post-RT CT scan was fused to the pre-RT PET/CT using an in-house developed deformable registration algorithm. The deformation map was applied to the contours to obtain GTV-REC\_def that was registered to the pre-RT PET/CT. A uniform 1cm margin was added to the GTVs to account for the various uncertainties in the segmentation and registration process. Several SUV statistics inside the recurrent and PET defined GTVs were obtained and analyzed, along with the overlap of the GTV-REC\_def with the GTV-PET.

#### RESULTS

Primary sites were oral cavity (8.6%), oropharynx (68.5%), and hypopharynx (22.9%). The mean (range) GTV-PET and GTV-REC\_def were 29.2ml (3.1-145.6ml) and 10.9ml (0.9-92.9ml) respectively with the Pearson correlation coefficient between the two volumes being 0.82. The SUV maximum in the GTV-PET and GTV-REC\_def+1cm was found to have no statistically significant difference. Finally, an overlap of 1 between GTV-REC\_def and GTV-PET+1cm indicating complete inclusion of the recurrence in the pre-RT defined GTV-PET was obtained for 68.6% of the cases, and increased to 82.9% for an overlap greater than 0.5.

#### CONCLUSION

The results suggest that the volume of the PET positive GTV on a pre-RT FDG-PET scan can be predictive of the size of disease in cases of recurrence. In addition, utilizing deformable registration to relate the recurrent GTV to the pre-RT SUVs on the FDG-PET scan confirmed that greater than 80% of recurrence occurs within or at the PET positive volume boundary.

#### CLINICAL RELEVANCE/APPLICATION

Predictions of post-radiotherapy recurrent disease patterns based on pre-radiotherapy PET characteristics can result in treatment plan strategy modifications that improve loco-regional control.

### **SST15-04 • Monte Carlo Based Estimation of Pediatric Dose from CBCT Imaging Head Protocols for Patient Positioning and Target Localization in Radiotherapy**

**Kyle McMillan** (Presenter) \* ; **Maria Zankl** PhD ; **Michael F McNitt-Gray** PhD \* ; **Dan Ruan** PhD \*

#### PURPOSE

The purpose of this investigation is to estimate the organ doses to a pediatric patient undergoing repeat CBCT imaging as part of an image-guided radiation therapy (IGRT) procedure.

#### METHOD AND MATERIALS

A Monte Carlo model was developed with application to kV-CBCT dose quantification on the Varian On-Board Imager platform. This model was validated against experimental measurements with an average agreement within 4%. Using this validated model, dose to a pediatric patient was simulated for the GSF "Child" model. This whole-body voxelized phantom was derived from CT imaging data of a 7-year-old female and contains 144 slices of 8 mm thickness with each slice consisting of a 256 x 256 matrix of 1.54 mm x 1.54 mm pixels. Simulations were performed using a standard-dose, low-dose and high-quality head CBCT protocol. For each protocol, the clinical default x-ray field size of 27.2 x 18.4 cm<sup>2</sup> at 100 cm source-to-surface distance was simulated. The reference center of the scan was set in the infratentorial region of the brain, and dose was tallied in all relevant organs near the collimated x-ray beam. Results for each simulated protocol were reported for both an individual scan as well as the accumulated dose expected from 30 repeated scans throughout the course of an IGRT treatment regimen consisting of 5 treatment fractions a week for 6 weeks.

## RESULTS

For a standard-dose protocol, dose per scan to the brain, skull, lens of the eye, head skin and cervical spine was 2.9, 10.6, 0.47, 3.3 and 14.9 mGy, respectively. These doses were decreased by a factor of 2 when the low-dose protocol was used and increased by a factor of 5 when the high-quality protocol was used. Accumulated dose as high as 2240 mGy was observed for the cervical spine when the high-quality protocol was used for all 30 repeated scans.

## CONCLUSION

Dose to bony structures such as the skull and cervical spine is significantly higher than dose to soft tissue. In pediatric patients whose bones are in a proliferative state, this CBCT imaging dose increases the risk of retardation of growth and induction of bone cancer. Therefore, it is important that the dose from CBCT imaging of pediatric patients be carefully considered and monitored.

## CLINICAL RELEVANCE/APPLICATION

Organ-specific dose quantification from this study provides distributional knowledge about CBCT imaging dose and facilitates designing protocols to reduce risk of late effects in pediatric patients.

### SST15-05 • 4D Cone Beam CT in Image Guided Radiation Therapy without Data Truncation Artifacts

**Kai Niu** MS (Presenter) ; **Ke Li** MS ; **Guang-Hong Chen** PhD \*

## PURPOSE

To evaluate the capability of solving the data truncation and detector shift problem common in clinical applications of 4D cone beam CT (CBCT) using an adapted Prior Image Constrained Compressed Sensing (PICCS) reconstruction method and to quantify the robustness of the adapted PICCS-4DCBCT algorithm under different data truncation conditions.

## METHOD AND MATERIALS

## RESULTS

For PICCS-4DCBCT, the rRMSEs are 0%, 4%, 6%, 7% for each case from no data truncation to most aggressive data truncation. In contrast, for TV-CS, the corresponding rRMSEs are 4%, 6%, 8%, 9%, and for FDK, the rRMSEs are 17%, 18%, 19% and 20%. The UQIs for PICCS-4DCBCT images are 1, 0.996, 0.991 and 0.986 (score=1 means perfect); for TVCS, the UQIs are 0.970, 0.957, 0.951 and 0.947, and for FDK images, the UQIs are 0.630, 0.630, 0.630 and 0.629.

## CONCLUSION

(1) PICCS-4DCBCT offers much better image quality and reconstruction accuracy compared with TV-CS and E-FDK at all data truncation levels. (2) No meaningful variations in performance were observed when the amount of truncation was changed.

## CLINICAL RELEVANCE/APPLICATION

PICCS-4DCBCT can be performed accurately and stably with almost arbitrary data truncation scanning conditions in 4DCBCT to guided radiation therapy for lung cancers.

### SST15-06 • Optimization of the Design of Portal Imaging Systems Incorporating Thick, Segmented Scintillating Detectors Employed for Megavoltage Cone-beam CT through a Novel Hybrid Modeling Technique

**Langechuan Liu** (Presenter) ; **Larry E Antonuk** PhD ; **Hao Jiang** ; **Youcef El-Mohri** PhD ; **Qihua Zhao** PhD

## PURPOSE

Active matrix flat-panel imagers (AMFPIs) incorporating thick, segmented scintillators have demonstrated order-of-magnitude improvements in DQE at radiotherapy energies compared to systems based on conventional phosphor screens. Such improved DQE values facilitate megavoltage cone-beam CT (MV CBCT) at clinically practical doses – providing distinct advantages over kV CBCT performed using additional on-board imaging equipment. However, the MV CBCT performance of such AMFPIs is highly dependent on the design parameters of the scintillators. In this presentation, a theoretical examination of imaging performance as a function of these parameters is reported.

## METHOD AND MATERIALS

The imaging performance of various scintillator designs was examined through a hybrid approach involving Monte Carlo simulation of radiation transport and determination of optical point spread functions. For each design, a full tomographic scan of a contrast phantom incorporating various soft-tissue inserts was simulated at a total dose of 3 cGy. This novel technique was validated through comparisons of theoretical predictions of contrast, noise and contrast-to-noise ratio (CNR) with measurement results obtained from a 1.13 cm thick, 1016  $\mu\text{m}$  pitch BGO prototype.

## RESULTS

Theoretical values for contrast, noise and CNR were found to be in close agreement with measurements for the BGO prototype, strongly supporting the validity of the modeling technique. For various other scintillator designs, results for CNR demonstrate improvement by a factor of  $\sim 2.2$  when the scintillator thickness is increased from 1.13 to 6 cm, and an improvement by a factor of  $\sim 2.6$  when the pitch is increased from 508 to 1016  $\mu\text{m}$ . Finally, optimization of design based on a trade-off between thickness and pitch, along with evaluation of the corresponding spatial resolution performance, is discussed.

## CONCLUSION

A new technique to model both radiation and optical effects was validated and employed to accurately evaluate the MV CBCT performance of MV-AMFPIs incorporating various segmented scintillator designs. It appears that significant improvement in the imaging performance of such AMFPIs can be achieved through optimization of scintillator design parameters.

## CLINICAL RELEVANCE/APPLICATION

Enhanced performance of MV-AMFPIs with segmented scintillators should greatly facilitate soft tissue visualization in external beam radiotherapy through MV CBCT imaging at clinically practical doses.

### SST15-07 • 2D kV Orthogonal Pair vs. 3D Cone Beam CT Localization for Breathhold Breast Radiation Therapy Treatment

**Michelle Howard** BS (Presenter) ; **Sean S Park** MD, PhD ; **Robert W Mutter** MD ; **Elizabeth S Yan** MD ; **Deanna H Pafundi** PhD ; **Debra Brinkmann** PhD

## PURPOSE

To assess the accuracy of breast and heart localization between 3D cone beam CT (3D-CBCT) registration to soft tissue and 2D kV orthogonal pair (2D-OP) registration to bony anatomy for assessment of matching criteria and imaging modality for accurate localization of breast and heart for left-sided breast patients treated with breath-hold (BH) technique. Previous research has shown a linear correlation between major coronary events and increased radiation dose to heart [1]. 1. Darby SC, et al. Risk of ischemic heart disease in women after radiotherapy for breast cancer. NEJM 2013; 368(11):987-98.

## METHOD AND MATERIALS

3D-CBCT and 2D-OP from 9 left-sided breast cancer patients treated with BH were retrospectively reviewed. Weekly 3D-CBCTs were acquired after manual 2D-OP registration to chest wall (anterioposterior) and sternum (lateral) was applied. 3D-CBCT images were then compared offline to planning CT with automatch applied to breast tissue, heart, or spine using translations only. The role of 2D vs 3D imaging for daily patient positioning was also evaluated.

## RESULTS

## CONCLUSION

Shift differences between 3D breast tissue automatic and 2D bony manual match were = 5mm in 7 patients and = 1cm in 4 patients. Accurate patient positioning is sensitive to the breast tissue placement and the degree of body roll which are difficult to ascertain with 2D imaging. 3D-CBCT registration allows for improved assessment and accurate localization of breast tissue, heart, and body roll. Further analysis will evaluate the dosimetric impact to heart based on localization to 2D-OP manual registration and 3D-CBCT automatch to breast, heart, and spine.

#### CLINICAL RELEVANCE/APPLICATION

This investigation will directly impact clinical practice decisions on which imaging modality and matching criteria are used daily to localize left-sided BH breast radiation therapy patients.

### SST15-08 • CT Number Changes Observed during Radiotherapy for Head and Neck Cancer

Ion Moraru (Presenter)

#### ABSTRACT

**Purpose/Objective(s):** Radiation induced anatomic changes, such as tumor regression, are common during the delivery of radiotherapy (RT) for head and neck cancer. In an effort to measure treatment response and identify indicators for adaptive RT, we investigate changes of CT number in target and organs at risk (OAR) from the CT data acquired during RT delivery and study correlations with anatomic variations.

**Materials/Methods:** Daily diagnostic-quality CT data acquired using an in-room CT (CT-on-Rails) for image-guided IMRT of 9 patients with stage III and IV squamous cell carcinoma of the oropharynx were analyzed. The patients were treated with 70 Gy in 35 fractions concurrently with chemotherapy. The gross tumor volume (GTV) and OARs were contoured on each daily CT set. All selected patients exhibited GTV reduction over the course of the treatment. We examined the distribution of CT numbers in Hounsfield units (HU) of various volumes of interest (VOI), including GTV and spinal cord, on daily CT sets. Statistical analysis of CT number distributions was performed for each patient for different fractions and trends were examined across the entire cohort. Various parameters including the mean, width, CT number of peak and asymmetry of each histogram were used to measure differences in the CT number distributions.

**Results:** Patient-specific changes in the CT number histograms as a function of fraction number for the GTV and spinal cord were observed. For the GTV, the mean CT number was observed to vary as much as +28% (+13 HU) and -27% (-12.5 HU) over 30 fractions, corresponding to +40% (+17.5 HU) and -38% (-18 HU) shifts in the CT number of the histogram peaks, respectively. These were associated with large differences in the histogram widths, namely 24% and 48%, and strong changes in symmetry, which may indicate that only part of the GTV experiences a shift CT numbers over the course of treatment for these patients. By contrast, a much more limited range of changes in the mean CT numbers was observed for the spinal cord, namely between +7.5% (+2.5 HU) and -11% (-4 HU), with less modifications in histogram width and symmetry. These maxima in the mean were not correlated with the data from those patients exhibiting the largest shifts in the GTV. This supports the idea that the observed differences in CT distributions of the GTV are largely radiation induced, as the spinal cord typical receives limited radiation dose.

**Conclusions:** Radiation induced non-negligible, patient-specific CT number changes were observed in volumes of interest during the delivery of RT for head and neck cancer. The pattern of variation is complex and no strong trend and/or correlation with tumor regression is identified for the small group of patients studied. More work is required to understand the mechanisms involved in these changes and how these will be used for adaptive RT to account for radiation response.

### SST15-09 • Offline CBCT Quantification of Translational and Rotational Displacements Using Automated Image Matching in Head and Neck Radiotherapy: A Feasibility Study

Jillian Hayes (Presenter) ; Maeve L McGarry BSc ; Gregory Perkins BSc ; Rabih W Hammoud MSc, BSc ; Saju Divakar ; Mohamed P Riyas MBBS, MD ; Noora Al Hammadi

#### Vascular/Interventional (MR Guidance/Topics of Interest)

Friday, 10:30 AM - 12:00 PM • E350



[Back to Top](#)

SST16 • AMA PRA Category 1 Credit™:1.5 • ARRT Category A+ Credit:1

#### Moderator

Dmitry J Rabkin, MD, PhD

#### Moderator

Elizabeth M Hecht, MD

### SST16-01 • Utilization of the iPad for Patient Education during Informed Consent in Interventional Radiology: A Randomized Controlled Trial

Sahil V Mehta MD (Presenter) ; Lauren E Ferrara MD ; Seth J Berkowitz ; William C Lo ; Salomao Faintuch MD \*

#### PURPOSE

To evaluate if interactive media presented on an iPad improves patient understanding and confidence during the informed consent process in interventional radiology.

#### METHOD AND MATERIALS

Patients were randomized into 4 groups. The control group (C) received an electronic consent form on the iPad. The second group was shown their radiology images (I) on an iPad. Dynamically displayed images were used to explain the patient's disease and planned intervention. The third group was shown interactive anatomic drawings (D) of their disease and planned intervention. The final group was shown a short video animation about the procedure to be performed (V). Patients completed a survey to rate their experience.

#### RESULTS

Fifty-six consecutive patients completed the study, 14 in each group. Procedures included venous access, nephrostomy, gastrostomy, fibroid and chemo embolization, tumor ablation, angiogram and biopsy. Use of the iPad was graded as significantly helpful to understand the reasoning for the procedure by 86% of patients in the imaging group (I), 79% in the drawing group (D) and 71% in the video group (V), compared to 43% of controls (p

#### CONCLUSION

Patients reacted positively to use of the iPad during informed consent, even when used as a simple replacement for a paper form. Nonetheless, clinical images and interactive drawings significantly improved patient understanding and confidence in the procedure to be performed. While videos were considered helpful, they were received less positively by patients, perhaps due to a reduction in interactivity with the provider. The iPad is a useful tool to help build a patient-physician relationship before an interventional procedure.

#### CLINICAL RELEVANCE/APPLICATION

The iPad can be very helpful during informed consent for interventional radiology procedures. It can significantly increase patient understanding, confidence and satisfaction.

### SST16-02 • Radiology Milestones: A Multiyear Study of Resident Experience with Radiologic Procedures at a Large Academic Medical Center

Adam B Prater MD (Presenter) ; Bradley S Rostad MD ; Emily Ebert BS ; Rachel Kearns BS ; Thomas W Loehfelm MD, PhD ; Brent Little MD ; Christopher P Ho MD ; Mark E Mullins MD, PhD

#### PURPOSE

The American College of Graduate Medical Education (ACGME) and the American Board of Radiology (ABR) initiated the Radiology Milestones Project in 2012 to create a framework for assessing the competency of radiology residents. An analysis of procedures performed by prior residents might help guide the assessment of procedural competency of current and future residents. Our study documented the most common types and numbers of procedures performed by radiology residents in a large academic center over a ten year period.

#### METHOD AND MATERIALS

Institutional review board approval was obtained. Resident procedure logs from graduating class years 2002 to 2012 were de-identified and organized into a secure electronic database. Summary statistics for each procedure type were calculated.

#### RESULTS

Resident procedure logs consisted of both paper and electronic forms, which varied in the number of resident participation and in the types and numbers of procedures documented. Over a ten year period, 110 residents recorded a total of 13,678 procedures consisting of 70 different procedure types. The most common recorded procedures were vascular catheter insertion, CT-Guided abdominal biopsies and drain placement, fluoroscopic Lumbar puncture, and ultrasound guided thoracentesis, paracentesis and thyroid biopsies. However, the numbers and types of procedures recorded for each resident varied considerably (mean  $124 \pm 75$ , max 331, min 15).

#### CONCLUSION

Although a wide variety of procedures are performed by residents during residency, resident procedural experience, as measured by procedure log data, varies significantly between residents even within the same program. This may be due to variability in resident procedure logging practices and procedures performed as data are manually entered by residents and are possibly underreported. Given the future directions suggested by the Radiology Milestones Project, our findings highlight the need for national guidelines regarding procedure requirements, and a more accurate method of acquiring radiology procedure data.

#### CLINICAL RELEVANCE/APPLICATION

The future of graduate medical education is geared towards data-driven metrics that can accurately depict resident progress and competence.

### **SST16-03 • Magnetically Assisted Remote Controlled Endovascular Catheter for Interventional MRI: In Vitro Navigation at 1.5T**

**Aaron D Losey** MS (Presenter); **Prasheel Lillaney**; **Alastair Martin** \*; **Daniel L Cooke** MD; **Mark W Wilson** MD; **Maythem Saeed** DVM, PhD; **Steven W Hetts** MD \*

#### PURPOSE

Using real-time MRI for interventional procedures affords a wealth of physiologic and structural information. The promise of endovascular MR guided procedures remains unrealized in part because of the lack of MR compatible catheters and guide wires. Innovative techniques for guiding a catheter in the magnetic field of the MR scanner have been proposed, but limited functionality has been described to date. This study evaluates navigation of a magnetically assisted remote controlled (MARC) catheter compared to guidance without magnetic assistance in vitro at 1.5T.

#### METHOD AND MATERIALS

#### RESULTS

#### CONCLUSION

We have developed and tested MARC catheters for endovascular navigation. At angles of 45 degrees or greater magnetic assistance was significantly faster than non-assisted guidance. The MARC catheter provides a novel opportunity to navigate effectively in interventional MRI environment. Preclinical in vivo studies are underway.

#### CLINICAL RELEVANCE/APPLICATION

Real-time MR guided catheter navigation with the MARC catheter could revolutionize minimally invasive procedures by advancing local treatment of stroke, cardiac arrhythmias and solid tumors.

### **SST16-04 • Non-enhanced T1-weighted Imaging of the Visceral Arteries at 7 Tesla**

**Anja Fischer** MD (Presenter); **Oliver Kraff** MSc; **Stefan Maderwald** PhD, MSc; **Karsten J Beiderwellen** MD; **Thomas C Lauenstein** MD; **Lale Umutlu** MD \*

#### PURPOSE

Aim of the study was to assess the feasibility of different non-contrast-enhanced T1-weighted (w) sequences for imaging of the visceral arteries of the upper abdomen at 7 Tesla.

#### METHOD AND MATERIALS

12 healthy volunteers were examined on a 7 T whole-body MR-system utilizing a custom-built 8-channel transmit/receive coil and radiofrequency shimming. The following non-enhanced sequences were acquired: (1) T1w 2D FLASH, (2) T1w 3D FLASH and (3) Time of flight (TOF)-MRA in transversal orientation. The following visceral arteries were evaluated (1) both common hepatic arteries, (2) coeliacal and splenic artery, (3) superior and (4) inferior mesenteric artery. For qualitative analysis, image quality and the presence of artifacts were assessed using a five-point scale (image quality: 5 = excellent vessel delineation to 1 = non-diagnostic; artifacts: 5 = no artifact to 1 = non-diagnostic). Contrast Ratios (CR = (Svessel-Sliver)/(Svessel+Sliver)) of the above named arteries in correlation to adjacent visceral tissue or psoas muscle were calculated for quantitative assessment. For statistical analysis, a Wilcoxon Rank Test was applied.

#### RESULTS

All three sequences provided a homogenous hyperintense delineation of the assessed visceral arteries. Qualitative image analysis showed a superiority of TOF MRA, providing best overall image quality (TOF 4.17, 2D FLASH 3.42, 3D FLASH 3.46) and highest mean values for image quality for all analyzed vessel segments. TOF MRA showed least impairment due to artifacts (overall artifacts TOF 4.08, 2D FLASH 3.50, 3D FLASH 3.46). Quantitative image analysis confirmed the superiority of the TOF sequence showing significant higher CR values for all visceral arteries due to an effective suppression of background signal (e.g. right hepatic artery TOF 4.25, 2D FLASH 3.54, 3D FLASH 3.33; p

#### CONCLUSION

Non-contrast-enhanced T1w imaging in general and, TOF MRA in particular, appear to be promising techniques for good quality assessment of visceral arteries without the need of contrast media at 7 Tesla.

#### CLINICAL RELEVANCE/APPLICATION

Non-enhanced MRA of visceral arteries at 7 T may bear the potential to be a good alternative to contrast-enhanced MRA, particularly for examination of patients with renal insufficiency.

### **SST16-05 • MR Lymphangiography in Clinical Diagnostics of Focal Lesions of the Lymphatic Vessel System in Peripheral Lymphedema**

**Frederik F Strobl** MD (Presenter); **Carolin Burgard**; **Mayo Weiss**; **Maximilian F Reiser** MD; **Mike Notohamiprodjo**

#### PURPOSE

Lymphoceles or focal dermal backflow form part of focal lesions of the peripheral lymphatic system. Focal dermal backflow is a frequent drainage pattern in the imaging of primary and secondary lymphedema and stands for a diffuse leakage of the tracer into subcutaneous tissue. In addition to lymphoscintigraphy, the magnetic resonance (MR) lymphangiography provides a valuable morphological and anatomical gain in information. Patients with this aforementioned disease pattern can benefit from this kind of information in pre- and



postsurgical diagnostic procedures. The purpose of this study was to compare findings of MR lymphangiography with those of lymphoscintigraphy in the assessment of focal lesions of the lymphatic vessel system in peripheral lymphedema.

#### METHOD AND MATERIALS

In this study, 44 consecutive patients with uni- or bilateral lymphedema and lymph vessel transplants of the lower extremities were included. MR lymphangiographies were performed with a 3.0-T fat-saturated three-dimensional gradient-echo MR after gadopentetate dimeglumine injection. Results of MR lymphangiography and lymphoscintigraphy were reviewed separately by a radiologist and a nuclear physician and concordance of the two techniques regarding existence, localization, distribution and confidence were examined.

#### RESULTS

With lymphoscintigraphy, which constituted the standard diagnostic procedure, focal lesions like lymphoceles or focal dermal backflow could be diagnosed in 23 patients. This result was confirmed by MR lymphangiography in 19 patients. Thus, there exists an excellent sensitivity of 83% and a specificity of 84% for MR lymphangiography. In addition, MR lymphangiography depicted auxiliary information about the anatomical constitution of lymph vessels or lymphoceles and showed a better differentiation between focal multiple or diffuse lesions.

#### CONCLUSION

Imaging findings of both techniques, the MR lymphangiography and the lymphoscintigraphy, showed an excellent correlation. Due to superior morphological and anatomical resolution, MR lymphangiography provides supplementary information for pre-surgical work-up in patients with focal lesions of the lymphatic vessel system in peripheral lymphedema.

#### CLINICAL RELEVANCE/APPLICATION

MR lymphangiography can provide 3D anatomical information without radiation exposure. Therefore it is a valuable alternative to lymphoscintigraphy in patients with peripheral lymphedema.

### **SST16-06 • Thermal versus Mechanical Disruption of Mice Melanoma due to MR Guided HIFU, a Feasibility Study**

**Martijn Hoogenboom** MSc (Presenter) ; **Martin J Van Amerongen** MSc ; **Iringo Kovacs** ; **Gosse Adema** ; **Arend Heerschap** PhD ; **Jurgen J Futterer** MD, PhD

#### PURPOSE

MR guided HIFU is an upcoming technique for non-invasive tumor treatment, however the differences in pathologic and immunologic effects by thermal or mechanical HIFU treatment is uncertain. The purpose of this feasibility study is to differentiate between mechanical and thermal HIFU ablation and to visualize the different pathologic and immunologic effects.

#### METHOD AND MATERIALS

Nine C57Bl/6n wild type mice were subcutaneously injected with B16F10 tumor cells at the right femur. After 9-10 days the tumor size was >8x8 mm. A 3MHz, 16 channel phased array HIFU system with an acoustic energy of 43-46W, was placed in a 7T animal MR scanner. An in-house made gelpad and degassed water was used for acoustic coupling.

The ablation process was visualized using MR guided thermometry (FLASH sequence, proton resonance frequency shift method: TR/TE=40/4ms, flip angle 25°, 5slices, 0.3mm inter-slice distance, voxel size 0.78x0.78x1.5mm<sup>3</sup>, 3.8s/dynamic, 0.5°C temperature accuracy).

Three different treatment strategies (3-6 spots) were applied in each tumor, 3 mice per strategy, respectively. First, continuous wave (CW) mode, 4 seconds ablation. Second, pulsed wave (PW) mode, 120shots of 20ms, pulse repetition frequency (PRF) of 4. Third, PW-mode, 500shots of 5ms, PRF 4. The mice are sacrificed 3 days after treatment, the tumor is removed for pathological evaluation, using HE-staining.

#### RESULTS

Temperatures of >35,

#### CONCLUSION

Thermal and mechanical HIFU treatment create different pathologic and immunologic responses, further research is necessary for quantification of these differences.

#### CLINICAL RELEVANCE/APPLICATION

Pathologic and immunologic effects due to HIFU are still uncertain, before testing on humans a mice set up is created for a good evaluation of these effects.

### **SST16-07 • MR-guided Focused Ultrasound Ablation of Pancreatic Cancer: A Totally Non-invasive Treatment for Pain Palliation and Tumor Control of Locally Advanced Lesions (Stage III)**

**Fulvio Zaccagna** MD (Presenter) ; **Alessandro Napoli** MD ; **Gaia Cartocci** ; **Gulia Brachetti** ; **Fabrizio Boni** ; **Vincenzo Noce** MD ; **Luca Bertaccini** ; **Maurizio Del Monte** ; **Carlo Catalano** MD

#### PURPOSE

To evaluate the feasibility of MR-guided focused ultrasound (MRgFUS) ablation for pain palliation and local tumor control in selected patients with unresectable primary pancreatic adenocarcinoma.

#### METHOD AND MATERIALS

6 patients with histologically proven unresectable pancreatic adenocarcinoma, who were clinically unable (n 4) or refused (n 2) to undergo chemo-radiation therapy, underwent MRgFUS treatment on a dedicated 3T unit featuring the ExAblate 2100 system (InSightec). All lesions were evaluated for device accessibility prior to treatment. MRgFUS procedures were performed in general anesthesia with constant breath control. Clinical assessment included evaluation of symptoms severity with visual analogue scale (VAS) before and after treatment. . After treatment all patients underwent CHT with the same chemotherapy scheme. Imaging follow-up, including both CT and MR examinations, was performed immediately after treatment and at 3 and 6 months in order to evaluate the effects of MRgFUS on the targeted tumor and the absence of procedure-related complications.

#### RESULTS

#### CONCLUSION

Our preliminary clinical experience suggests that MRgFUS is a feasible and repeatable ablative technique in selected patients with unresectable and device-accessible pancreatic adenocarcinoma.

#### CLINICAL RELEVANCE/APPLICATION

MRgFUS treatment for locally advanced pancreatic tumor is a safe procedure and could be repeated without increase of adverse event risk.

### **SST16-08 • The Synergy of High-intensity Focused Ultrasound and Low-dose Generic Chemotherapeutic Virtually Eliminates Multi-drug Resistant Solid Tumor Cells**

**Howard Q Vo** MD, MS (Presenter) ; **Yoo-Shin Kim** PhD ; **Brian E O'Neill** PhD

#### PURPOSE

Despite medical advances, multidrug-resistant (MDR) cancers continue to challenge the patients. Their clinical prognoses may further be complicated by the need for additional surgical procedures and/or radiotherapy. In this study, we seek to evaluate a new strategy in which the synergy of high-intensity focused ultrasound (HIFU) and a single low dose of a generic chemotherapeutic is utilized to attack MDR solid tumor cells.

#### METHOD AND MATERIALS

This strategy is partly an outgrowth of an in-house Phase 4 clinical trial in which MRI-guided HIFU was used to treat uterine fibroids. The clinical procedure was adapted for the 3-day *in vitro* study during which human uterine sarcoma cell line (MES-SA/Dx5 (ATCC® CRL1977™)), known for resistance to multiple drugs such as Doxorubicin (Dox), was paradoxically treated with Dox.

Day 1: Each data sample consisted of ~20K cells grown inside a well of 8-well glass slides (Lab-Tek). The well was then filled with McCoy's media and incubated at 36 °C for 4h. Afterward each well was sealed and secured onto a fixture before being submerged in a warm degassed water bath. The targets for HIFU therapy are the center points of the 4 quadrants of each well's base. The constant HIFU parameters for each well were acoustic pressure 7MPa, RF 1Hz, focal-zone depth and 30 sec/sonication/center point while duty cycle (DC) ranged 0-60% between the wells. 2h after HIFU treatment, the wells were unsealed and incubated overnight.

Day 2: Cell media for each well was replaced with fresh media containing [Dox] 0-1 ug/mL prior to repeating the HIFU procedure from 24h earlier.

Day 3: After 24h of exposure to Dox, cell survivability study was performed to determine the contributions of HIFU-mediated necrosis and Dox-mediated apoptosis.

#### RESULTS

Cell survivability decreased by increasing [Dox] or DC. In the Dox-only group (DC 0%), average survivability was 93% for [Dox] 0.5 ug/mL while in the HIFU-only group ([Dox] 0 ug/mL), average survivability was 42% for DC 50%. In contrast, there was virtually no survivability of sarcoma cells for [Dox] 0.5 ug/mL and DC = 50%.

#### CONCLUSION

The synergy of HIFU and low-dose Doxorubicin was successful in virtually eliminating MDR uterine sarcoma cells.

#### CLINICAL RELEVANCE/APPLICATION

A combination of HIFU and a low-dose generic chemotherapeutic may be a promising alternative to existing treatments (regular-dose multidrug regimen, surgery or radiotherapy) against some MDR cancers.

### **SST16-09 • Non-Vascular Interventional Procedures in an Urban General Hospital: Analysis of 2001-2010 with Comparison to the Previous Decade**

**Peter F Hahn MD, PhD (Presenter) \* ; Alexander R Guimaraes MD, PhD \* ; Ronald S Arellano MD ; Peter R Mueller MD \* ; Debra A Gervais MD \***

#### PURPOSE

Non-vascular image-guided procedures such as biopsy and fluid drainage are accepted medical care. Having previously reported an analysis of the 21324 cases in the 1991-2000 fiscal years, we undertook a comparative study of procedures performed by the same abdominal interventional group from October, 2000 through September, 2010.

#### METHOD AND MATERIALS

With IRB approval a 20-year quality assurance database verified against the radiology information system was queried for procedure location (eg. pleura, liver, bowel, abdomen) and type (eg. biopsy, catheter insertion, transient drainage), demographics and trends. New hospital numbers assigned each year served to normalize for overall hospital activity.

#### RESULTS

We performed 50195 IR procedures in 24309 distinct patients (M:F 12625:11684; average age 60), 940 procedures in under-20's and 571 in patients 90 or older. 15345, 4377 and 1754 patients had 1, 2 or 3 procedures; 470 had 10 or more. 27 supervising radiologists and 277 individuals participated as operators, double the previous decade. Biopsy (4.8% average yearly increase), abdominal drainage (7.3%), paracentesis (12.9%), tube manipulation (13.0%), suprapubic tube insertion (21.0%), and gastrostomy (44.6%) all increased strongly (p

#### CONCLUSION

Referrals for non-vascular IR procedures have doubled over two decades, outpacing growth in new hospital patients and requiring increased resource allocation.

#### CLINICAL RELEVANCE/APPLICATION

Since some specialized procedures like biliary and renal drainage have not increased proportionately, newly trained operators may have diminished experience with these more demanding cases.

### **Friday Imaging Symposium: MR Imaging of Common Musculoskeletal Injuries (An Interactive Session)**

**Friday, 12:30 PM - 03:00 PM • E350**



[Back to Top](#)

**SPMK61 • AMA PRA Category 1 Credit™:2.5 • ARRT Category A+ Credit:3**

#### **Moderator**

**Mark D Murphey, MD**

#### LEARNING OBJECTIVES

1) To recognize the common patterns of meniscal injuries on MR imaging and their clinical importance. 2) To identify the MR appearance of hip labral tears and patterns of femoroacetabular impingement syndrome (FAI). 3) To describe the common MR patterns and locations of rotator cuff tears and the importance of associated tendon retraction and muscle atrophy. 4) To recognize the patterns of injury and MR appearance associated with cruciate and collateral ligament injuries of the knee.

### **SPMK61A • MR of the Menisci**

**Mark D Murphey MD (Presenter)**

#### LEARNING OBJECTIVES

View learning objectives under main course title.

### **SPMK61B • MR of the Hip Labrum**

**Donna G Blankenbaker MD (Presenter)**

#### LEARNING OBJECTIVES

View learning objectives under main course title.

### **SPMK61C • MR of the Rotator Cuff**

**William B Morrison MD (Presenter) \***

#### LEARNING OBJECTIVES

View learning objectives under main course title.

## SPMK61D • MR of the Cruciate and Collateral Knee Ligaments

Mini N Pathria MD (Presenter)

### LEARNING OBJECTIVES

View learning objectives under main course title.

## Disclosure Index

### A

**Attenberger, U. I.** - Research Consultant, Bayer AG  
**Awai, K.** - Research Grant, Toshiba Medical Sysmtes Research Grant, Hitachi Medical Corporation Research Grant, Bayer AG Research Consultant, DAIICHI SANKYO Group Research Grant, Eizai Ltd

### B

**Balter, P.** - Research, Koninklijke Philips Electronics NV  
**Bashir, M. R.** - Research support, Bracco Group Research support, Siemens AG Consultant, Bayer AG Consultant, Siemens AG  
**Bayram, E.** - Employee, General Electric Company  
**Bednarek, D.** - Research Grant, Toshiba Corporation  
**Ben Ayed, I.** - Employee, General Electric Company  
**Beuing, O.** - Consultant, Siemens AG  
**Blasco, J.** - Speakers Bureau, Stryker Corporation  
**Blobel, J.** - Employee, Toshiba Corporation  
**Blumfield, A.** - Co-founder, Radnostics LLC  
**Blumfield, E.** - Co-founder and President, Radnostics LLC Spouse, Co-founder, Radnostics LLC Spouse, CEO, Radnostics LLC  
**Boonn, W. W.** - Founder, Montage Healthcare Solutions, Inc Shareholder, Montage Healthcare Solutions, Inc  
**Borm, P.** - Employee, Nano4Imaging GmbH  
**Boyko, O. B.** - Consultant, Bracco Group Consultant, Patient Comfort Systems, Inc  
**Brace, C. L.** - Shareholder, NeuWave Medical Inc Consultant, NeuWave Medical Inc  
**Brem, R. F.** - Board of Directors, iCAD, Inc Board of Directors, Dilon Technologies LLC Stock options, iCAD, Inc Stockholder, Dilon Technologies LLC Consultant, U-Systems, Inc Consultant, Dilon Technologies LLC Consultant, Dune Medical Devices Ltd  
**Brown, D. B.** - Consultant, Cook Group Incorporated Consultant, Biocompatibles International plc  
**Bruce, R. J.** - Officer, World IT Solutions, LLC  
**Brunken, R.** - Research Grant, Bracco Group Research Grant, Astellas Group  
**Bydder, G. M.** - Research Grant, General Electric Company

### C

**Carr, J. C.** - Speaker, Lantheus Medical Imaging, Inc  
**Carrascosa, P. M.** - Research Consultant, General Electric Company  
**Chen, G.** - Research funded, General Electric Company Research funded, Siemens AG Research funded, Varian Medical Systems, Inc Research funded, Hologic, Inc  
**Chen, X.** - Employee, Toshiba Corporation  
**Chung, J. H.** - Research Grant, Siemens AG  
**Cleveland, R. H.** - Research Consultant, Alexion Pharmaceuticals, Inc Editor, Springer Science+Business Media Deutschland GmbH  
**Cloft, H. J.** - Researcher, Johnson & Johnson  
**Collins, J. D.** - Consultant, C. R. Bard, Inc  
**Conant, E. F.** - Consultant, Hologic, Inc  
**Coursey, C. A.** - Research support, Becton, Dickinson and Company

### D

**Dam, E. B.** - Shareholder, Biomediq A/S Employee, Biomediq A/S  
**De Baere, T. J.** - Consultant, Terumo Corporation Speaker, Covidien AG Speaker, Terumo Corporation Speaker, General Electric Company Consultant, General Electric Company Consultant, Guerbet SA Speaker, Guerbet SA  
**Dekemp, R.** - Shareholder, FlowQuant Consultant, Jubilant Life Sciences Limited Shareholder, Jubilant Life Sciences Limited  
**DeStigter, K. K.** - Medical Advisory Board, Koninklijke Philips Electronics NV Consultant, Koninklijke Philips Electronics NV

### E

**Edelman, R. R.** - Research support, Siemens AG Royalties, Siemens AG  
**Ehman, R. L.** - CEO, Resoundant, Inc  
**Enterline, D. S.** - Consultant, Bracco Group Speakers Bureau, Bracco Group Consultant, General Electric Company Research support, Siemens AG Research support, Koninklijke Philips Electronics NV

### F

**Faintuch, S.** - Consultant, Boston Scientific Corporation  
**Farnsworth, C.** - CEO, HealthHelp Board of Directors, Vital Decisions LLC  
**Fayad, Z. A.** - Research Grant, Merck & Co, Inc Research Grant, Pfizer Inc Research Grant, F. Hoffmann-La Roche Ltd Research Grant, Takeda Pharmaceutical Company Limited Research Grant, DAIICHI SANKYO Group Research Grant, Siemens AG Research Grant, VIA Pharmaceuticals, Inc Research Grant, Guerbet SA Research Consultant, Merck & Co, Inc Research Consultant, VIA Pharmaceuticals, Inc Research Consultant, BG Medicine, Inc  
**Forster, B. B.** - Beneficial trust, Doyen Medical, Inc  
**Friedewald, S. M.** - Consultant, Hologic, Inc Scientific Advisory Board, Hologic, Inc  
**Fujisawa, Y.** - Employee, Toshiba Corporation  
**Fuller, C. D.** - Research Consultant, General Electric Company

### G

**Gervais, D. A.** - Research Grant, Covidien AG  
**Geyer, L. L.** - Speaker, General Electric Company  
**Gillies, R. J.** - Scientific Advisory Board, Intezyne, Inc  
**Girard, E.** - Employee, Siemens AG  
**Go, J.** - Research Grant, Guerbet SA Research Grant, Toshiba Corporation  
**Griswold, M. A.** - Research support, Siemens AG Royalties, Siemens AG Royalties, General Electric Company Royalties, Bruker Corporation Contract, Siemens AG  
**Guimaraes, A. R.** - Speakers Bureau, Siemens AG Expert Witness, Siemens AG  
**Guimaraes, M.** - Consultant, Cook Group Incorporated Consultant, Terumo Corporation Consultant, Bayer AG Consultant, Baylis Medical Patent holder, Cook Group Incorporated Research Grant, Terumo Corporation

**Gulani, V.** - Research support, Siemens AG  
**Gupta, R. T.** - Consultant, Bayer AG Speakers Bureau, Bayer AG

## H

**Haberland, U.** - Employee, Siemens Healthcare  
**Hahn, P. F.** - Stockholder, Abbott Laboratories Stockholder, Covidien AG Stockholder, CVS Caremark Corporation Stockholder, Kimberly-Clark Corporation Stockholder, Landauer, Inc  
**Haider, M. A.** - Consultant, Bayer AG  
**Hall, T. J.** - Equipment support, Siemens AG  
**Han, M. K.** - Advisory Board, Boehringer Ingelheim GmbH Advisory Board, Pfizer Inc Advisory Board, GlaxoSmithKline plc Advisory Board, F. Hoffmann-La Roche Ltd Advisory Board, Novartis AG Advisory Board, Forest Laboratories, Inc Speakers Bureau, Boehringer Ingelheim GmbH Speakers Bureau, Pfizer Inc Speakers Bureau, GlaxoSmithKline plc Speakers Bureau, F. Hoffmann-La Roche Ltd Speakers Bureau, Novartis AG Speakers Bureau, Forest Laboratories, Inc Consultant, Novartis AG Consultant, United Biosource Corporation Royalties, UpToDate, Inc  
**Henry, T. S.** - Travel support, Siemens AG Spouse, Employee, F. Hoffmann-La Roche Ltd  
**Hetts, S. W.** - Consultant, Silk Road Medical Inc Consultant, Medina Medical Inc Research Grant, Stryker Corporation Data Safety Monitoring Board, Stryker Corporation  
**Hoffman, E. A.** - Founder, VIDA Diagnostics, Inc Shareholder, VIDA Diagnostics, Inc  
**Houston, G.** - Director, Vascular Flow Technologies Ltd Shareholder, Vascular Flow Technologies Ltd Grant, Guerbet SA  
**Hudgins, P. A.** - Stockholder, Amirsys, Inc Consultant, Amirsys, Inc Author, Amirsys, Inc  
**Hughes, C.** - Employee, General Electric Company Consultant, General Electric Company Consultant, Hologic, Inc Consultant, Siemens AG Consultant, Toshiba Corporation  
**Hui, F. K.** - Speakers Bureau, Terumo Corporation Speakers Bureau, Penumbra, Inc Stockholder, Blockade Medical Inc  
**Hurwitz, L. M.** - Research Grant, Siemens AG Research Grant, General Electric Company  
**Hwang, T.** - Intern, Siemens AG

## J

**Jhaveri, K. S.** - Research Grant, Bayer AG  
**Johnson, K. M.** - Research support, General Electric Company

## K

**Kalender, W. A.** - Consultant, Siemens AG Consultant, Bayer AG Founder, CT Imaging GmbH Scientific Advisor, CT Imaging GmbH CEO, CT Imaging GmbH  
**Kanne, J. P.** - Research Consultant, PTC Therapeutics, Inc Research Consultant, Perceptive Informatics, Inc  
**Karczmar, G. S.** - Research Consultant, Perceptive Informatics, Inc Research Consultant, BioClinica, Inc  
**Kauczor, H.** - Research Grant, Boehringer Ingelheim GmbH Research Grant, Siemens AG Speakers Bureau, Boehringer Ingelheim GmbH Speakers Bureau, Bayer AG Speakers Bureau, Siemens AG  
**Khorasani, R.** - Stockholder, Medicalis Corp Royalties, Medicalis Corp Advisory Board, General Electric Company  
**Kiefer, B.** - Employee, Siemens AG  
**Kim, C. Y.** - Research Grant, Bayer Inc Research Grant, Lantheus Medical Imaging, Inc Consultant, Lantheus Medical Imaging, Inc  
**Kinahan, P. E.** - Research Grant, General Electric Company Co-founder, PET/X LLC  
**Klein, R.** - Shareholder, FlowQuant Consultant, Jubilant Life Sciences Limited Shareholder, Jubilant Life Sciences Limited  
**Klotz, E.** - Employee, Siemens AG  
**Kohli, M. D.** - Research Grant, Koninklijke Philips Electronics NV Research Grant, Siemens AG  
**Kolditz, D.** - Employee, CT Imaging GmbH  
**Kripfgans, O. D.** - Research support, General Electric Company Equipment support, General Electric Company  
**Kuhl, C. K.** - Advisory Board Member, Bayer AG  
**Kukreja, K. U.** - Institutional research collaboration, Koninklijke Philips Electronics NV  
**Kunze, H.** - Employee, Siemens AG  
**Kyriakou, Y.** - Employee, Siemens AG

## L

**Langer, J. E.** - Consultant, BioClinica, Inc  
**Larson, S. M.** - Owner, Clinical Silica Technologies Advisory Board, ImaginAb, Inc Advisory Board, Molecular Imaging, Inc Scientific Advisor, Takeda Pharmaceutical Company Limited Advisory Board, Perceptive Informatics, Inc Scientific Advisor, Progenics Pharmaceuticals, Inc  
**Law, E.** - Speakers Bureau, Toshiba Corporation Medical Advisory Board, Bayer AG Medical Advisory Board, Bracco Group Medical Advisory Board, FUJIFILM Holdings Corporation  
**Lee, F. T. JR.** - Stockholder, NeuWave Medical, Inc Patent holder, NeuWave Medical, Inc Board of Directors, NeuWave Medical, Inc Patent holder, Covidien AG Inventor, Covidien AG Royalties, Covidien AG  
**Leiner, T.** - Speakers Bureau, Koninklijke Philips Electronics NV Consultant, Bayer AG Research Grant, Bracco Group  
**Lell, M. M.** - Research Grant, Siemens AG Speakers Bureau, Siemens AG Research Grant, Bayer AG Speakers Bureau, Bayer AG Research Consultant, Bracco Group  
**Levin, D. C.** - Consultant, HealthHelp Board of Directors, Outpatient Imaging Affiliates, LLC  
**Lewandowski, R. J.** - Scientific Advisory Board, Surefire Medical, Inc Consultant, PhaseRx, Inc Advisory Board, Nordion, Inc Advisory Board, Boston Scientific Corporation  
**Li, D. K.** - Researcher, Angiotech Pharmaceuticals, Inc Researcher, Bayer AG Researcher, BioMS Medical Researcher, Johnson & Johnson Researcher, DAIICHI SANKYO Group Researcher, F. Hoffmann-La Roche Ltd Researcher, Merck KGaA Researcher, Schering-Plough Corporation Researcher, Teva Pharmaceutical Industries Ltd Researcher, sanofi-aventis Group Researcher, Transition Therapeutics Inc Consultant, Genzyme Corporation  
**Li, Q.** - Patent agreement, General Electric Company Patent agreement, Hologic, Inc Patent agreement, Riverain Technologies, LLC Patent agreement, MEDIAN Technologies Patent agreement, Mitsubishi Corporation  
**Li, S.** - Employee, General Electric Company  
**Lillholm, M.** - Employee, Biomediq A/S Shareholder, Biomediq A/S  
**Loewe, C.** - Speaker, Bracco Group Speaker, Guerbet SA Speaker, General Electric Company Speaker, Covidien AG Speaker, Bayer AG  
**Lombardi, M.** - Research Grant, Novartis AG Research Grant, Chiesi Farmaceutici SpA Research Grant, Apotex, Inc  
**Lynch, D. A.** - Research support, Siemens AG Scientific Advisor, Perceptive Informatics, Inc Consultant, Actelion Ltd Consultant, InterMune, Inc Consultant, Gilead Sciences, Inc Consultant, F. Hoffmann-La Roche Ltd

## M

**Machac, J.** - Consultant, General Electric Company Research collaboration, Koninklijke Philips Electronics NV Researcher, Lantheus Medical Imaging, Inc  
**Macura, K. J.** - Research Grant, Siemens AG  
**Maidment, A. D.** - Research support, Hologic, Inc Research support, Barco nv Spouse, Employee, Real-Time Radiography, Inc Spouse, Stockholder, Real-Time Radiography, Inc  
**Malaisrie, C.** - Consultant, Edwards Lifesciences Corporation Research Grant, Medtronic, Inc  
**Martin, A.** - Research Grant, MRI Interventions, Inc  
**Matsumoto, S.** - Research Grant, Toshiba Corporation  
**Matthew, S.** - Research funded, Guerbet SA  
**Mayo, J. R.** - Speaker, Siemens AG  
**Mayo-Smith, W. W.** - Royalties, Reed Elsevier Royalties, Cambridge University Press  
**McCarville, M.** - Support, General Electric Company  
**McCullough, C. H.** - Research Grant, Siemens AG  
**McDonald, J. S.** - Research Grant, General Electric Company  
**McMillan, K.** - Institutional research agreement, Siemens AG Research support, Siemens AG  
**McNitt-Gray, M. F.** - Institutional research agreement, Siemens AG Research support, Siemens AG

**Mendel, J. B.** - Advisor, McKesson Corporation  
**Mendelson, E. B.** - Scientific Advisory Board, Hologic, Inc Research support, Siemens AG Speakers Bureau, Siemens AG Medical Advisory Board, Quantason, LLC Consultant, Quantason, LLC Speakers Bureau, SuperSonic Imagine Research support, SuperSonic Imagine Medical Advisory Board, Toshiba Corporation  
**Mews, J.** - Employee, Toshiba Corporation  
**Michaely, H. J.** - Speakers Bureau, Siemens AG Speakers Bureau, Bayer AG Speakers Bureau, Guerbet SA  
**Michel, M. A.** - Author, Amirsys, Inc Co-editor, Amirsys, Inc Consultant, Amirsys, Inc  
**Mitchell, D. G.** - Consultant, CMC Contrast AB  
**Morrison, W. B.** - Consultant, General Electric Company Consultant, AprioMed AB Patent agreement, AprioMed AB  
**Mueller, P. R.** - Consultant, Cook Group Incorporated  
**Mukherjee, P.** - Research Grant, General Electric Company  
**Muradyan, N.** - Employee, iCAD, Inc

## N

**Napel, S.** - Medical Advisory Board, Fovia, Inc Consultant, Carestream Health, Inc Scientific Advisor, Echopixel, Inc  
**Nelson, R. C.** - Consultant, General Electric Company Research support, Nemoto Kyorindo Co, Ltd Research support, Bracco Group Research support, Becton, Dickinson and Company Speakers Bureau, Siemens AG Royalties, Lippincott, Williams & Wilkins  
**Newell, J. D. JR** - Research Consultant, Siemens AG Research Grant, Siemens AG Consultant, WebMD Health Corp Author, Springer Science+Business Media Deutschland GmbH Consultant, VIDA Diagnostics, Inc  
**Nielsen, M.** - Stockholder, Biomediq A/S Research Grant, Nordic Bioscience A/S Research Grant, SYNARC Inc Research Grant, AstraZeneca PLC  
**Nishio, M.** - Research Grant, Toshiba Corporation

## O

**Obara, M.** - Employee, Koninklijke Philips Electronics NV  
**Oelhafen, M.** - Employee, Varian Medical Systems, Inc  
**Ohno, Y.** - Research Grant, Toshiba Corporation Research Grant, Koninklijke Philips Electronics NV Research Grant, Bayer AG Research Grant, DAIICHI SANKYO Group Research Grant, Eisai Co, Ltd Research Grant, Terumo Corporation Research Grant, Covidien AG Research Grant, FUJIFILM Holdings Corporation  
**O'Kane, P. L.** - Research Consultant, NPS Pharmaceuticals Research Consultant, Johnson & Johnson  
**Otake, Y.** - Research support, Siemens AG  
**Overlaet, W.** - Employee, Toshiba Corporation

## P

**Pan, X.** - Research Grant, Koninklijke Philips Electronics NV Research Grant, Toshiba Corporation Consultant, UtopiaCompression Corporation  
**Paysan, P.** - Employee, Varian Medical Systems, Inc  
**Pelizzari, C. A.** - Research Grant, Varian Medical Systems, Inc Scientific Advisory Board, RefleXion Medical Inc  
**Peller, P. J.** - Speakers Bureau, Eli Lilly and Company  
**Pfeiffer, D. E.** - Consultant, Radcal Corporation  
**Phillips, C.** - Stockholder, MedSolutions, Inc  
**Philpotts, L. E.** - Consultant, Hologic, Inc.  
**Pickens, D. R. III** - Stockholder, Johnson & Johnson  
**Poller, W. R.** - Consultant, Devicor Medical Products, Inc  
**Pomper, M. G.** - Co-founder, Cancer Targeting Systems, Inc Royalties, Li-Cor Biosciences Grant, Li-Cor Biosciences Grant, Eli Lilly and Company Royalties, Progenics Pharmaceuticals, Inc Grant, Bind Therapeutics, Inc Royalties, Bind Therapeutics, Inc Grant, Gamma Medical Technologies, LLC Royalties, Gamma Medical Technologies, LLC  
**Pozniak, M. A.** - Stockholder, Novelos Therapeutics, Inc  
**Pyrros, A. T.** - Research Consultant, Document Storage Systems, Inc

## Q

**Qayyum, A.** - Spouse, Employee, Imorgon

## R

**Rana, V.** - Research Grant, Toshiba Corporation  
**Ray, C. E. JR** - Therasphere Advisory Board, Nordion, Inc  
**Remy, J.** - Research Consultant, Siemens AG  
**Remy-Jardin, M. J.** - Research Grant, Siemens AG  
**Rosenthal, D. I.** - Speakers Bureau, ImClone Systems Incorporated Speakers Bureau, Bristol-Myers Squibb Company Speakers Bureau, sanofi-aventis Group Research support, Amgen Inc Research support, MedImmune, Inc  
**Rosenzweig, K. E.** - Consultant, Gerson Lehrman Group, Inc Advisory Board, ViewRay, Inc  
**Rossi, S. E.** - Advisory Board, Koninklijke Philips Electronics NV  
**Roth, C. G.** - Author, Reed Elsevier  
**Ruan, D.** - License agreement, VisionTree Software, Inc  
**Rudin, S.** - Research Grant, Toshiba Corporation  
**Ruehm, S. G.** - Research Grant, Siemens AG  
**Rybicki, F. J. III** - Research Grant, Toshiba Corporation Research Grant, Bracco Group

## S

**Saam, T.** - Research Grant, Diamed Medizintechnik GmbH Research Grant, Bayer AG  
**Sakai, O.** - Royalties, The McGraw-Hill Companies  
**Salem, R.** - Consultant, Bayer AG Consultant, Nordion, Inc Consultant, BioSphere Medical, Inc Advisory Board, Sirtex Medical Ltd Consultant, Merit Medical Systems, Inc  
**Samei, E.** - Research Grant, Siemens AG Research Grant, General Electric Company Research Grant, Carestream Health, Inc  
**Sampson, L. A.** - Research Consultant, NeuWave Medical Inc  
**Schmidt, B.** - Employee, Siemens AG  
**Schoenberg, S. O.** - Institutional research agreement, Siemens AG  
**Schoepf, U.** - Research Grant, Bracco Group Research Grant, General Electric Company Research Consultant, Siemens AG Research Grant, Siemens AG  
**Schroeder, J. D.** - Research Grant, Siemens AG  
**Schuijff, J.** - Employee, Toshiba Corporation  
**Schultz, K.** - Employee, Toshiba Corporation  
**Seiberlich, N.** - Researcher, Siemens AG  
**Serowy, S.** - Consultant, Siemens AG  
**Sheth, S.** - Research Consultant, Star Scientific, Inc  
**Shrestha, R. B.** - Medical Advisory Board, General Electric Company Medical Advisory Board, Nuance Communications, Inc Medical Advisory Board, Toshiba Corporation Editorial Advisory Board, Anderson Publishing, Ltd Advisory Board, KLAS Enterprises LLC  
**Siewerdsen, J. H.** - Research Grant, Siemens AG Consultant, Siemens AG Research Grant, Carestream Health, Inc Royalties, Elekta AB  
**Skalej, M.** - Institutional research collaboration, Siemens AG  
**Slanetz, P. J.** - Consultant, UpToDate, Inc  
**Soulez, G. P.** - Speaker, Bracco Group Speaker, Siemens AG Research Grant, Siemens AG Research Grant, Bracco Group Research Grant, Cook Group Incorporated Research Grant, Object Research Systems Inc  
**Sporring, J.** - Co-founder, DigiCorpus ApS Shareholder, DigiCorpus ApS

**Srinivasan, A.** - Author, Amirsys, Inc  
**Stayman, J. W.** - Research Grant, Varian Medical Systems, Inc  
**Steigner, M. L.** - Speaker, Toshiba Corporation  
**Strother, C. M.** - Research Consultant, Siemens AG Research support, Siemens AG License agreement, Siemens AG  
**Sugihara, N.** - Employee, Toshiba Corporation  
**Sugimura, K.** - Research Grant, Toshiba Corporation Research Grant, Koninklijke Philips Electronics NV Research Grant, Bayer AG Research Grant, Eisai Co, Ltd Research Grant, DAIICHI SANKYO Group  
**Suzuki, K.** - Royalties, General Electric Company Royalties, Hologic, Inc Royalties, AlgoMedica Royalties, MEDIAN Technologies Royalties, Riverain Technologies, LLC Royalties, Toshiba Corporation Royalties, Mitsubishi Corporation  
**Szczykutowicz, T. P.** - Grant, General Electric Company Grant, Siemens AG

## T

**Taouli, B.** - Research Grant, General Electric Company Research Grant, Bayer AG Consultant, Siemens AG Consultant, Bayer AG  
**Tawakol, A.** - Research Consultant, F. Hoffmann-La Roche Ltd Research Consultant, Merck & Co, Inc Research Grant, F. Hoffmann-La Roche Ltd Research Grant, Merck & Co, Inc Research Grant, Bristol-Myers Squibb Company  
**Thurmond, A. S.** - Royalties, Cook Group Incorporated Stockholder, Conceptus Inc  
**Togashi, K.** - Research Grant, Bayer AG Research Grant, DAIICHI SANKYO Group Research Grant, Eisai Co, Ltd Research Grant, FUJIFILM Holdings Corporation Research Grant, Nihon Medi-Physics Co, Ltd Research Grant, Shimadzu Corporation Research Grant, Toshiba Corporation Research Grant, Covidien AG  
**Troubousee, A.** - Researcher, Angiotech Pharmaceuticals, Inc Researcher, Bayer AG Researcher, BioMS Medical Researcher, Johnson & Johnson Researcher, DAIICHI SANKYO Group Researcher, F. Hoffmann-La Roche Ltd Researcher, Merck KGaA Researcher, Schering-Plough Corporation Researcher, Teva Pharmaceutical Industries Ltd Researcher, sanofi-aventis Group Researcher, Transition Therapeutics Inc Consultant, sanofi-aventis Group

## U

**Umutlu, L.** - Consultant, Bayer AG

## V

**Van Cauteren, M.** - Employee, Koninklijke Philips Electronics NV  
**Van Ha, T. G.** - Investigator, C. R. Bard, Inc  
**Viergever, M. A.** - Research Grant, Koninklijke Philips Electronics NV Research Grant, Pie Medical Imaging BV  
**Von Walter, M.** - Employee, Hemoteq AG

## W

**Wacker, F. K.** - Research Grant, Siemens AG Research Grant, Pro Medicus Limited  
**Wakayama, T.** - Employee, General Electric Company  
**Wang, A. S.** - Research support, Siemens AG  
**Wasiak, C.** - Employee, Fraunhofer-Gesellschaft  
**Weber, M.** - Research Grant, Bayer AG Research Grant, Guerbet SA Research Grant, Bracco Group Research Grant, Siemens AG  
**Wendt, G. J.** - Medical Advisory Board, McKesson Corporation Stock Ownership, TeraMedica, Inc Medical Advisory Board, HealthMyne Owner, WITS, LLC  
**Wicklein, J.** - Research collaboration, Siemens AG  
**Willey, B. J.** - Consultant, NeuWave Medical Inc  
**Wintersperger, B. J.** - Speakers Bureau, Bayer AG Speakers Bureau, Siemens AG  
**Woodard, P. K.** - Research support, Siemens AG Meeting travel, Siemens AG Research support, Astellas Group Consultant, Medtronic, Inc Consultant, BIOTRONIK GmbH & Co KGC Consultant, GE Healthcare

## X

**Xing, L.** - Research Grant, Varian Medical Systems, Inc

## Y

**Yamagata, H.** - Employee, Toshiba Corporation  
**Yamashita, Y.** - Consultant, DAIICHI SANKYO Group  
**Yoshikawa, T.** - Research Grant, Toshiba Corporation